Modelling building integrated heating and cooling systems

Weitzmann, Peter

Publication date:
2004

Document Version
Publisher's PDF, also known as Version of record

Peter Weitzmann

Modelling building integrated heating and cooling systems

BYG·DTU

DANMARKS
TEKNISKE
UNIVERSITET

DTU

Rapport
BYG·DTU R-091
2004
ISSN 1601-2917
ISBN 87-7877-155-2

Modelling building integrated heating and cooling systems

PhD thesis

Peter Weitzmann

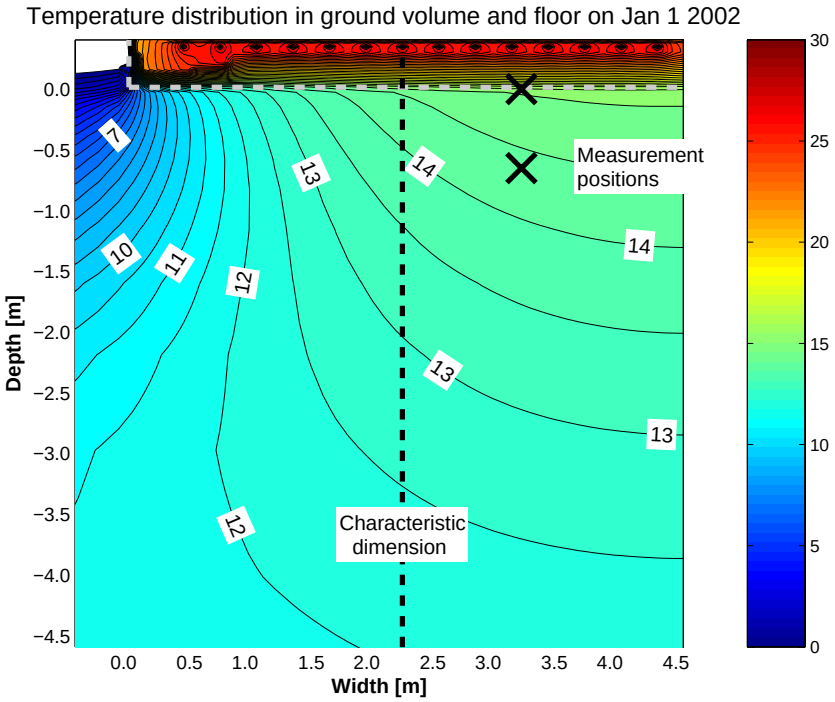

Department of Civil Engineering
DTU-building 118
2800 Kgs. Lyngby
http://www.byg.dtu.dk

2004

Modelling building integrated heating and cooling systems

Department of Civil Engineering
DTU-building 118
2800 Kgs. Lyngby
Denmark

ISBN 87-7877-155-2
ISSN 1601-2917

Preface

This thesis concludes the PhD work entitled *Modelling building integrated heating and cooling systems*. The work has been carried out from February 2001 to July 2004 at the Department of Civil Engineering at the Technical University of Denmark and was financed by a scholarship from the Technical University of Denmark.

The supervisor for the project has been Professor Svend Svendsen also from the Department of Civil Engineering at the Technical University of Denmark

The project is concerned with simulation models of building integrated heating and cooling systems with emphasis on floor heating and thermo active components.

I would like to use this preface to thank Professor Svend Svendsen for many helpful ideas and constructive comments to improve the contents of the thesis.

During the work with this thesis I have had many rewarding discussions with colleagues that have been both on a professional and a sociable basis. Especially I want to mention Jesper Kragh for trying (☺) to use my simulation model as part of a project for investigating energy efficient floor heating systems. He has helped eliminating many bugs and has suggested many improvements to the models.

Further, I would like to thank Peter Roots of Statens Energimyndighet (the Swedish Energy Agency) for supplying me with measurement data for the validation of the ground coupled floor heating model. This work has also resulted in an accepted article which will be published in the journal Building and Environment.

As part of my studies, I spent a three-month period in Gothenburg, Sweden, at Chalmers University of Technology, which was a rewarding period. Here I would like to thank Professor Carl-Eric Hagentoft and all the rest of the staff – especially Angela Sasic Kalagasidis – for accepting me as part of the group.

Finally, and probably most importantly, I would like to thank my wife Annemette for putting up with me even during the final period where I worked for (too) many hours finishing this thesis.

Publications by the author

As part of the work presented here four articles are included in the thesis, three of which have been presented by Peter Weitzmann at conferences while the last has been accepted by Building and Environment for publication. These are attached to this thesis. Three further articles have also been written during the period of the PhD-study. They are however not a core part of the thesis and are not attached to the thesis. Finally, three reports where Peter Weitzmann has participated are mentioned. These are also not part of the thesis.

Articles that are part of this thesis

The following papers are part of this thesis and have been attached at the end of the report. The papers are numbered from 1 to 4.

Paper 1:

Weitzmann P., Sasic Kalagasidis A., Nielsen T. R., Peuhkuri R. and Hagentoft, C-E. (2003): Presentation of the International Building Physics Toolbox for Simulink. In: Building Simulation 2003

Paper 2:

Weitzmann P, Kragh J, Roots P, Svendsen S (accepted for publication): Modelling floor heating systems using a validated two-dimensional ground coupled numerical model. Accepted for publication in Buildings and Environment.

Paper 3:

Weitzmann P (2002): Simulation of temperature in office with building integrated heating and cooling. In: Proceedings of the Sixth Symposium on Building Physics in the Nordic Countries, pp. 897-904.

Paper 4:

Weitzmann P, Holck O, Svendsen S (2003): Numerical analysis of heat storage of solar heat in floor construction. In: ISES Solar World Congress 2003 Solar Energy for a Sustainable Future.

Articles that are not part of this thesis

Weitzmann P, Kragh J and Jensen C F (2002): Numerical Investigation of Floor Heating Systems in Low Energy Houses. In: Proceedings of the Sixth Symposium on Building Physics in the Nordic Countries, pp. 905-912.

Weitzmann P, Svendsen S (submitted): Method for calculating thermal properties of lightweight floor heating panels based on an experimental setup. Submitted to the International Journal of Low Energy and Sustainable Buildings

Reports

Kragh J, Weitzmann P, Svendsen S (2003): Udformning og styring af energirigtige gulvvarmeanlæg (Design and control of energy efficient floor heating systems), BYG·DTU R-063. In Danish.

Weitzmann P, Holck O, Svendsen S (2001): Bygningsintegreret varmelagring af solvarme i terrændæk (Heat Storage of Solar Heat in Floor Construction), BYG·DTU R-006. In Danish.

Hansen J O, Jacobsen T, Weitzmann P (2002): Termoaktive konstruktioner. Fase 1 – forprojekt (Thermo Active Components. Phase 1 – preliminary project), Energistyrelsen, EFP-2001, j.nr. 1213/01-0020. In Danish.

Peter Weitzmann

Lyngby, July 200

Summary

Modelling Building Integrated heating and cooling systems

The purpose of the work which is presented in this thesis is to develop and investigate simulation models for building integrated heating and cooling systems. These models can be used to find the thermal properties of building integrated systems and their influence on the thermal indoor climate and energy consumption in the building. A number of simulation models are developed with different level of detail. The simple models can be used for early estimates in the design phase of a building of the influence of using building integrated heating and cooling systems in buildings, while the models with more details are especially suited for product development and research purposes.

In this thesis two types of building integrated heating and cooling systems are presented and investigated. The first is floor heating, which is the most often used type of heating system in Danish single-family houses. The second is thermo active components – which is a relatively new technology. Thermo active components represents a way of cooling offices by using embedded pipes in the thermal mass of the building – typically in the form of concrete – where cool water is circulated to remove the heat from the concrete and consequently cool the offices in the building. Finally, as an extension to the investigation on floor heating systems, a third type of building integrated system has been included, as an investigation of thermal energy storage of solar energy in a slab-on-grade floor of a single-family house.

Initially, after defining the scientific approach and purpose of the work, a literature evaluation and state of the art review has been completed to establish the basis for the work.

The main element in this project is the development and implementation of simulation models of building integrated heating and cooling systems. For this purpose, two simulation models have been developed; one for floor heating, called FHSim, and one for thermo active components, called TASim. The models are both dynamical simulation models of a room with building integrated heating and/or cooling. The models include heat transfer, heat storage and temperature distribution in the building elements, which include floors, walls, ceiling, windows and elements with building integrated heating and cooling system. The room model includes detailed calculation of the heat transfer, which is split into radiation and convection. Radiation is included both as short wave solar gains on the surfaces and long wave thermal radiation between surfaces based on the view factor between the surfaces. Further, there are models for ventilation, infiltration and venting, as well as models for control of the heating/cooling system and input of weather data. The simulation models FHSim and TASim are for the most parts identical except for the models of the building integrated systems and controls hereof.

The models of the building constructions are based on the numerical Finite Control Volume method. Only heat transfer with constant material properties is included in the models.

The investigation of floor heating systems is the first of the two main parts in the thesis.

Initially, a two-dimensional simulation model of a slab-on-grade floor with floor heating is developed and validated against measurements from a house in Bromölla, Sweden. Here it is found that by using the characteristic dimension of the floor, which is defined as the area divided by half the perimeter, as the width of the model, the numerical model will give results that are in close agreement to three-dimensional measurements. This is the case even for the

very narrow building used for the validation, which is very influenced by three-dimensional conditions. The use of the characteristic dimension to simplify the three-dimensional heat flow problem to a two-dimensional one has previously been demonstrated in the literature only for buildings without floor heating.

Based on the measurements and the validated simulation model of the slab-on-grade floor, the importance of using correct implementation of the floor heating system is demonstrated using both the actually measured temperature and fixed temperatures in the pipe. Here it is shown, that there can easily be large differences in the results using a fixed temperature rather than correct temperatures. This means that in order to find the correct heat loss to the ground from the floor, it is necessary to use a dynamical simulation where the pipe temperature is included and based on the actual energy demand in the room. For these analyses the simulation models introduced in this work are ideal.

The two-dimensional simulation model of the slab-on-grade floor is used for investigating the effect on the energy consumption of improved insulation in floor and foundation. Here it is found that compared to a model without floor heating, the fact that the floor is heated means that the heat loss to the ground will be penalized through higher relative heat loss to the ground in case of poor insulation. In the course of this investigation it is also found that the value of the linear thermal transmittance of the foundation is influenced by the presence of floor heating.

At the same time it is demonstrated that both the insulation under the floor as well as in the foundation is important to minimize the heat loss to the ground.

While being able to accurately model the conditions in a slab-on-grade floor with floor heating, the two-dimensional model is very time-consuming both with respect to defining the geometry of the floor and simulation time. This means that the model is an expert tool which can be used for research purposes and product development of the design of the floor construction. However, it is not a tool which can be used in the design phase, where there are both many unknown factors and perhaps a need for several simulations. A series of simplified models are therefore tested, both one- and two-dimensional finite control volume models and thermal network models using lumped resistances and capacities. Of special interest is that the simplest RC-thermal network model where the linear thermal transmittance of the foundation is included, yield results for both energy consumption and heat loss to the ground that are close to those found by the detailed two-dimensional model. Further, it has been shown that using an electrical inclusion of the floor heating pipe is not sufficient to model hydronic floor heating. Among the reasons is that the electrical implementation is unable to include the temperature of the pipe in the model, which has been shown to impact the energy consumption through different thermal climate in the room.

In the chapter on thermo active components a different approach is used than for the chapter on floor heating. Here emphasis is placed on two measurement setups with the purpose of testing different ways of turning a pre-fabricated hollow core concrete deck into a thermo active component. Two decks are tested. The simplest of these decks is constructed simply by placing the pipe directly in the cavities of the deck, which is tested in a simple setup. This method is of course not as efficient as the second type, where the pipe is integrated in the concrete. However, the cooling capacity is still large enough to cool the office in a consciously designed building or as a supplement to a natural ventilation system.

In the second test setup, two decks are used as floor and ceiling of a room. The purpose of this investigation is, under controlled conditions, to find the cooling capacity under stationary conditions and the temperature variations under dynamic conditions, where the heat load in

the room varies during the day and the flow in the pipe is only turned on during the night. The results clearly demonstrates the possibilities of using pre-fabricated hollow core concrete decks as thermo active components to cool the office, even for heat loads as high as 60-70W/m² during stationary conditions. This should be compared to around 25-30W/m² for the deck with the pipe placed in the cavities.

The stationary cooling capacity is found using different combinations of room air set point temperature and supply temperature to the pipe of the thermo active deck. A linear correlation between the cooling capacity and the temperature difference between fluid temperature and room temperature is found, which means that the cooling capacity coefficient expressed as cooling capacity per area and temperature difference is constant. This was also found for the first simple setup. In the second test setup, the measurements could be used to calculate the cooling capacity of the ceiling and floor surfaces individually – and for this setup it was found that the ceiling surface had a cooling capacity five times larger than for the floor surface.

Besides from the cooling capacity, the thermal conditions in the room with respect to surface (radiant) temperatures and vertical air temperature distribution can be investigated to find the operational conditions in the room with the mainly radiant cooling system.

The dynamic conditions in the room has been demonstrated by using a heat load which is high during the day and low during the night and a flow in the pipes which is only on during the night. Using this setup, the maximum heat load in the room can be found if the room temperature should not surpass the comfort range.

The test setup has been designed in such a way that it can subsequently be used for testing the system in combination with suspended ceilings or even operable ceilings, which can be used to manually control the cooling from the deck, as well as different types of ventilation systems and control strategies of the flow in the pipes.

For both stationary and dynamic conditions, the simulation model TASim has been shown to satisfactorily reproduce the results from the measurements. This means that also the room air model in FHSim has been validated.

The third part of the investigation is the use of thermal energy storage of solar energy in a slab-on-grade floor with two concrete decks, using the lowest deck for energy storage. It is found that even for a house with an already low energy consumption, it is possible to lower this even more through the using the heat storage.

Based on the investigations in this thesis, it is concluded that it is possible to model building integrated heating and cooling systems to find both energy consumption and thermal indoor climate. The implementation of such models in building energy simulation programs will represent an advance towards a more realistic implementation of building integrated heating and cooling systems.

Resume (In Danish)

Modellering af bygningsintegrerede opvarmnings og afkølingssystemer

Formålet med det arbejde, som er præsenteret i denne afhandling er at udvikle og undersøge simuleringsmodeller af bygningsintegrerede opvarmnings- og afkølingssystemer. Sådanne modeller kan benyttes til at finde de termiske egenskaber samt energiforbrug og termisk indeklima i bygninger, hvori de er installeret. I forbindelse med arbejdet er der blevet udviklet et antal simuleringsmodeller med forskelligt detaljeringsniveau. De simpleste modeller kan således benyttes til at finde de termiske egenskaber i en tidlig fase af designet af en ny bygning, mens de mere detaljerede modeller kan bruges til produktudvikling og forskningsformål.

Afhandlingen fokuserer på to typer bygningsintegreret opvarmnings- og afkølingssystemer. Den første type er gulvvarme, som er den mest benyttede form for opvarmning i danske enfamiliehuse. Den anden type er termoaktive konstruktioner – som er en relativt ny teknologi. Termoaktive konstruktioner benyttes til at køle (specielt) kontorer ved at benytte slanger, som er indstøbt i bygningens termiske masse – typisk i form af beton – hvori der kan cirkuleres køligt vand, som kan fjerne varmen fra betonen og herefter også fra rummet. Endelig er der som en udvidelse af undersøgelsen på gulvvarmesystemer også undersøgt en tredje type bygningsintegreret opvarmnings- og afkølingssystem i form af et anlæg til varmelagring af solvarme i terrændækket på et enfamiliehus.

Efter en beskrivelse af den videnskabelige metode og formålet med afhandlingen gennemgås en litteraturundersøgelse og analyse af de bedste løsninger inden for bygningsintegrerede systemer.

Hovedarbejdet i afhandlingen er lagt inden for udviklingen og implementeringen af simuleringsmodeller af bygningsintegrerede opvarmnings- og afkølingssystemer. I forbindelse hermed er der udviklet to beregningsprogrammer; et til gulvvarme kaldet FHSim og et til termoaktive konstruktioner kaldet TASim. Begge modeller er dynamiske simuleringsrutiner af et rum med bygningsintegreret opvarmnings- eller afkøling. Derudover indeholder modellerne varmetransport, varmelagring og temperaturfordeling i bygningselementerne i form af gulve, lofter, vægge, vinduer samt selvfølgelig elementer med bygningsintegrerede systemer. Rummodellen inkluderer detaljeret beregning af varmetransporten og er opdelt i stråling og konvektion. Stråling er inkluderet både som kortbølget solindfald og langbølget varmestråling mellem overfladerne. Sidstnævnte baseret på overfladernes indbyrdes temperaturer og vinkelfaktorer. Derudover er der modeller til ventilation, infiltration og udluftning såvel som vejrdata og styring af varme/køleanlægget. Beregningsmodellerne i FHSim og TASim er for en meget stor dels vedkommende identiske, bortset fra bygningselementerne med den bygningsintegrerede opvarmning og/eller afkøling samt styringen heraf.

Beregningsmodellerne for bygningselementerne er baseret på den numeriske Finite Control Volume metode. Der betragtes kun varmetransport med konstante materialeegenskaber i modellerne.

Den første af to hoveddele af afhandlingen omhandler gulvvarme.

Indledningsvis opbygges en todimensional beregningsmodel af et terrændæk med gulvvarme, som valideres mod målinger fra et hus i Bromölla i Sverige. Herigennem fastslås det, at hvis

den karakteristiske diameter af bygningen, som er defineret som arealet divideret med den halve perimeter af bygningen, benyttes som bredden af det todimensionale udsnit, vil denne model give resultater, som er meget tæt på de målte tredimensionale forhold. Dette gælder også for den meget smalle bygning, som er benyttet til målingerne, som dermed er meget udsat for tredimensionale forhold. Dermed kan den karakteristiske diameter benyttes til at simplificere det tredimensionale varmestrømsproblem til et todimensionalt. Dette er hidtil kun blevet vist i litteraturen at være gyldigt for gulve uden gulvvarme.

Baseret på målinger og den validerede beregningsmodel af terrændæksmodellen belyses vigtigheden af at benytte korrekte dynamiske forhold i gulvvarmeslangen. Dette vises gennem anvendelsen af de faktiske målte data for væsketemperaturen og sammenligne med forskellige faste temperaturer. Herigennem vises det, at der nemt opstår store forskelle i resultaterne mellem den dynamiske implementering og en fast temperatur. Det betyder, at for at finde det rigtige varmetab mod jord fra terrændækket er det nødvendigt at benytte en dynamisk beregningsmodel, hvor forholdene i slangen er baseret på det faktiske aktuelle opvarmningsbehov i rummet. Dermed er den hér opbyggede beregningsmodel ideel.

Den todimensionale terrændæksmodel med gulvvarme benyttes herefter til at bestemme varmeforbrugets afhængighed af forbedret isolering af gulv og fundament. Her findes det, at sammenlignet med et terrændæk uden gulvvarme vil der med gulvvarme være en større relativ forskel ved ændring af isoleringen i terrændækket. Hermed bliver gulve med gulvvarme straffet hårdere rent varmetabsmæssigt for dårlig isolering, end gulve uden gulvvarme. I samme omgang er det også fundet, at linietabsværdien af fundamentet er påvirket af, om der er gulvvarme. Endelig vises det, at forøget isolering i både selve terrændækket og fundamentet er vigtige for at minimere varmetabet mod jord.

Samtidig med at den todimensionale terrændæksmodel kan lave nøjagtige beregninger af forholdene i et gulv med gulvvarme, er modellen dog meget tidskrævende – både at arbejde med i modelopbygning og beregningstid. Det betyder, at modellen mest en dels er et ekspertværktøj, som kan benyttes til forskning og produktudvikling af designet af terrændæk med gulvvarme. Det er dog ikke et værktøj, som kan bruges i designfasen af et byggeri hvor der er mange ukendte faktorer i forbindelse med modelleringen, hvor det måske yderligere er nødvendigt at lave mange beregninger. Derfor udvikles der også en række simplere modeller i form af en- og todimensionale modeller baseret på Finite Control Volume metoden samt termiske netværksmodeller, hvori der benyttes klumpanalyse af varmekapaciteter og varmemodstande. Specielt har det vist sig, at den simpleste model – en termisk netværksmodel hvor linietabsværdien af fundamentet er inkluderet – giver resultater for både energiforbrug til opvarmning og varmetab mod jord, som er tæt på dem, som findes i den detaljerede todimensionale terrændæksmodel. Derudover har det vist sig, at en elektrisk implementering af gulvvarmesystemet ikke tilfredsstillende kan modellere forholdene i et vandbårent gulvvarmeanlæg. Blandt andet er den elektriske model ikke i stand til at inkludere en væsketemperatur, som i beregningerne har vist sig at have betydning for forholdene.

I kapitlet om termoaktive konstruktioner er der benyttet en anden fremgangsmåde end i afsnittet om gulvvarme. Her er hovedvægten lagt på to forsøgsopstillinger, der har til formål at kunne finde de termiske egenskaber for huldækselementer, som benyttes som termoaktive konstruktioner. To forskellige typer huldækselementer benyttes. I den simpleste af de to huldæk er slangen lagt direkte i hulrummene i dækket, hvilket er belyst i den simple forsøgsopstilling. Denne metode er selvfølgelig ikke så effektiv, som en hvor slangen er indstøbt i dækket. Alligevel resulterer designet i en kølekapacitet, som stadig er stor nok til køling i et kontorbyggeri, der er designet med en lav varmelast i rummene eller eventuelt som supplement til en naturligt ventileret bygning.

I den anden forsøgsopstilling benyttes en opstilling med to dæk som danner loft og gulv i et rum. Formålet med denne opstilling er, under kontrollerede forhold, at kunne bestemme kølekapaciteten af dækkene under stationære forhold samt temperaturvariationerne under dynamiske forhold ved variable forhold. Resultaterne viser tydeligt mulighederne for at bruge præfabrikerede dæk som termoaktive konstruktioner til at køle rummet, selv med en varmelast på op til 60-70W/m² under stationære forhold. Dette skal sammenlignes med mellem 25 W/m² til 30W/m² for dækket med løse slanger i hulrummene i huldækket.

Den stationære kølekapacitet er fundet gennem målinger for forskellige kombinationer af fremløbs- og rumtemperaturer. Der findes en lineær sammenhæng mellem kølekapaciteten og temperaturforskellen mellem rum- og middelvæsketemperatur. Det betyder, at kølekapacitetskoefficienten af dækket er konstant. Dette resultat er også blevet fundet for dækket med løse slanger. I forsøgsopstillingen kunne kølekapaciteten bestemmes individuelt for gulv- og loftsoverfladen mod rummet. Her blev det fundet, at loftoverfladen har en kølekapacitet, som er fem gange større end gulvoverfladen.

Bortset fra kølekapaciteten kan de termiske forhold i rummet findes med hensyn til overfladetemperaturer, vertikal temperaturfordeling samt øvrige termiske forhold i rummet der for den største del køles ved stråling.

De dynamiske forhold i rummet er vist i et forsøg, hvor varmelasten i rummet er høj om dagen og lav om natten, mens der kun er tændt for flowet i slangerne i dækket om natten. Herigennem kan den maksimale kølekapacitet findes således, at der undgås problemer med den termiske komfort i løbet af en arbejdsdag.

Opstillingen er designet, så den efterfølgende kan benyttes til målinger af for eksempel nedhængte lofter – måske endda styrbare koncepter, som kan bruges til manuel styring af køleeffekten fra dækket – samt forskellige styringsstrategier, ventilationskoncepter samt opvarmningsforsøg.

I både de stationære og dynamiske forsøg har TASim vist sig at kunne reproducere måledataene på tilfredsstillende vis. Dette gælder dermed også for rummodellen i FHSim.

Den tredje (og mindste) del af afhandlingen er en undersøgelse af varmelagring af solvarme i en terrændækskonstruktion med to betondæk, hvor det nederste dæk benyttes til varmelagringen. Her findes det, at selv i et hus med allerede lavt energiforbrug til opvarmning kan varmelagringen benyttes til at sænke energiforbruget yderligere.

Baseret på undersøgelserne i afhandlingen konkluderes det, at det er muligt at opbygge simuleringsmodeller af bygningsintegrerede opvarmnings- og afkølingssystemer og herigennem finde energiforbrug og termisk indeklima. Implementeringen af sådanne modeller i simuleringsprogrammer af bygningsenergi vil være et skridt mod mere realistiske implementering af bygningsintegrerede systemer.

Contents

1 Introduction

1.1 Background

In recent years, the use of floor heating in domestic buildings has increased substantially and is now used in almost all new single-family houses. The technology has become easier through the use of durable PEX-tubes and due to lower required hating power in a better insulated building envelope. At the same time it is clear that there is a very limited possibility to correctly model the thermal conditions and energy consumption in buildings with building integrated heating such as floor heating.

However, recent reports have pointed to the fact that buildings with floor heating had much higher energy consumption than expected. This has led to a number of investigations to establish the possible reasons for this, including the present one, which is mostly aimed at the creation of simulation models.

Together with the increased use of floor heating in domestic buildings, a new use of the "floor heating technology" has been introduced in central Europe where pipes are integrated into the building core to cool the building. Cooling is often required in modern office buildings since computers, printers and other electronic equipment along with large glass facades results in large heat loads and consequently over-heating. The use of building integrated pipes in the building core is called thermo active constructions. The use of thermo active components can eliminate the need for conventional air conditioning systems which often have very large energy consumptions.

For both floor heating and thermo active components, the same concept is used – the heating and cooling of the room is taking place using a building integrated heating and cooling system. Common for both cooling and heating applications is that the required temperatures in the systems are close to the desired room air temperature – that is low temperature heating and high temperature cooling.

A new directive from the European Union (European Parliament, 2003) has the purpose to increase the energy performance of buildings. The energy performance is a measure of the actual amount of energy "actually consumed or estimated to meet the different needs associated with a standardized use of the building" – as it is stated in the directive. The implementation of this directive is expected to be beneficial for low temperature heating systems and high temperature cooling systems and systems that do not require extensive use of electrical power for circulating air and water.

In Denmark floor heating is used extensively in single family houses where the design is based on many years of hands on experience combined with some scientific investigations. At present, there are almost no experiences with the use of thermo active components. In mainly Germany and Switzerland, thermo active components are used as an alternative to mechanical cooling systems in a number of office buildings.

For both uses of the concept (heating and cooling) a common problem is, that there are only a very limited number of calculation programs and simulation models available for calculating the energy consumption and thermal indoor climate in rooms with building integrated heating and cooling systems.

1.2 Objective

The main objective of this thesis is to develop and implement simulation models of radiant heating and cooling systems that can be used for simulations of the conditions in both

dwellings and offices and to test these models to reveal their thermal behavior and at the same time to discuss the process of implementation and the implications of the use of such models.

The reason for this is the fact knowledge of the use of radiant heating and cooling systems, with respect to both practical use and modelling is fairly limited. This is the case, even though a large amount of work has already been published with both simulation models and measurements. There is therefore a need for further development of models to assist in improving the design of hydronic building integrated heating and cooling systems, while also improving the state of the art knowledge of modelling of these systems.

This improvement of both design and modelling of hydronic heating and cooling systems is the basic driving force behind the work in this thesis. The purpose is to implement simulation models with enough details to be able to use them as tools for product development and also to develop models that are fast enough to be used for optimizations.

Where possible the results in this thesis are based on validated models, and therefore a part of the work is devoted to validation using a test mock-up of a building integrated heating and cooling system for an office and measurements on a house with floor heating.

1.3 Scientific method

In this thesis, computer simulations play a central role in order to be able to assess the thermal behaviour of building integrated heating and cooling systems. It is therefore relevant to make a discussion on the strengths and weaknesses of computer simulations as seen in the light of the work that has been carried out here. In addition to this, a discussion is made to reflect on the use of computer simulations generally – does it, to be provocative, bring out necessary information, or is it simply a waste of time and resources on a problem that could be solved easier and better in another way?

The use of computer simulations in different technical applications has increased immensely since the development of the first computers. An early example is the first lunar landing where the trajectory of the Lander was calculated based on a computer model. It can be concluded, that the simulation was a success – the first man did walk on the Moon, and he did get back in one piece. Today computer simulations are used for weather forecasts, mechanical devices, traffic planning, thermal simulation of houses, and so on. In fact, the usage is limited only by imagination and available computing power.

1.3.1 Basic concept of modelling using computer simulations

The basic concept of computer simulations can be summed up in the following six-point description:

1. The problem is identified. Where are the boundaries of the problem? What should be included into the identification of the problem? Based on this problem identification a system and its boundaries are defined.
2. A model of the problem (or system) is created. This model is based on subsystems and interfaces between these subsystems, which can be formulated in a mathematical model of the initial problem.
3. The model is implemented into a suitable computer programming language. A validation must be carried out. If the results are satisfactory, the model has been validated and can be used within certain limits defined by the area covered by the validation. If the results from this validation are not satisfactory, an analysis must be made to determine the causes of the problem; whether it is in the problem

identification, in the model or in the implementation. Changes must be made according to the findings of this analysis.

4. The implementation of the validated model results in a computer program. This computer program can be used with a given set of boundary conditions and initial conditions to simulate the influence of changing different input parameters.
5. The results from the simulations are analyzed
6. If the results are satisfactory, conclusions can be made. Otherwise changes must be made to the boundary conditions or initial conditions and redo the simulations.

The first three points in the six-point description, is the domain of the development of the program, or rather the implementation of the model of the real system. The next three points is the domain of the use of the program.

The approach used here is called system theory (Wallén, 1996), which is defined as a group of objects that are interacting with each other. System theory is an approach that can be used in a large number of different fields of science. Examples of this could be the solar system, the human temperature control system, economical systems, both closed systems and open systems that interact with the surroundings can be modelled. The strength of system theory is the fact that complex problems can be solved, and the dynamic properties can be analysed.

System theory has been developed along with the development of computers, since even simple models can have immensely complex behaviour that cannot be solved and discovered by simple calculations.

1.3.2 Building energy simulation

Building energy simulations are used to predict the energy consumption in buildings and find parameters for the thermal indoor climate, which is important for persons occupying the building. The results are used in the design of the building where it is required that the building meets different requirements for energy consumption and thermal indoor climate.

A second use of building energy simulation programs is to use the complex modelling of the conditions as part of a product development procedure, where new constructions or systems are tested. Here more details in the product model are needed to be able to compare differences in the design between two versions of the new product.

An example is introduced to explain what is required of a building energy simulation program, here focusing on the heating of a building:

The backbone of a building energy simulation program is to keep track of all energy flows in the model. The negative energy flows (heat losses) are through the building envelope (walls, windows, roof and floor) and through ventilation system, infiltration and venting. On the positive side counts solar heat gain through windows, internal heat gain from persons, lighting and equipment. Finally, a heating system whose purpose is to maintain the temperature at a given set point must also be included. It is obvious, that the actual temperature in a house is represented by a complex interaction between losses and gains, where a large number of variables each contribute to the energy balance. To further complicate this, none of these variables are constant. For instance, the outdoor temperature changes with time. The same is the case for the solar heat gain and internal heat gain. The heating system must keep track of this in order to keep an acceptable temperature in the room while it is attempted to keep the energy bill to a minimum.

In the following part of this chapter, this is referred to as ‘the example’.

In order to gain information about the building before it is built, a computer model can be created where the complex nature of the problem can be included. This will give information about the temperature in the house throughout the year, while also calculating the resulting energy consumption.

Looking at the example it is obvious that many considerations and assumptions must be made from start to conclusion.

An attempt is now made to apply the six-point description above to the example.

At first, a system identification must be made. This is basically what has been done in the description of the example.

In point two of the description a mathematical model of the house should be created. In this model, everything that has a consequence for the energy balance (gains and losses) must be included. In the example this means, that models of walls, windows, ventilation system and so on must be created. Here choices must be made of the level of detail to be used in the model; which assumptions and approximations must be made. In the example, an assumption could be that the infiltration rate is constant, which is not realistic. The choices affect the complexity of the model, which again affects the functionality of the program and influences how the program can be used and for what purposes. A detailed model with many input parameters gives detailed results, but is also tedious to work with. A very detailed model may, in fact, not be required or even wanted.

In point three of the description, the mathematical model of the house is implemented into a computer program. After the initial implementation of the model has been finished, it is necessary to do a validation of the model in order to make sure that the results obtained are realistic. A validation can for instance be performed based on measurements that have been performed under controlled circumstances (boundary conditions). The simulation model should be able to reproduce the measurements if the same boundary conditions are included in the model. Another possibility is to compare the results from similar simulations performed by using other simulation models whose “correctness” has already been established.

Based on the validated simulation program, models of actual houses can be created. (Notice the distinction between the simulation model and the house model). The model of the house will, together with weather data, make up the boundary conditions for the simulation model. Initial conditions (i.e. temperature distribution in walls) are chosen and the model is ready for use. Using this model, simulations can be carried out for different layouts of the house, different insulation thickness and so on. For each simulation different results are obtained. The results can then be compared and analysed.

1.3.3 Considerations on computer simulations

An obvious advantage of simulations is that the basic thermal properties of the house are known prior to the construction. At the same time, it can be seen that results from several simulations with varying parameters, can lead to an improved design of the building.

A secondary advantage of using computer simulations is that they can be used as part of a product development, where the effect of changing a given design can be investigated to improve the product which is under development while the interaction with the rest of the building is included.

In short, the ability to predict the system or product behavior is actually the whole point of performing computer simulations. This means that under a given set of circumstances the design can be tested prior to the actual construction. In the example, the energy consumption

for a house can be found using different insulation thickness in the walls of the building. Knowing the energy consumption and the price of insulation, an optimum insulation thickness can be found by comparing cost and benefit.

Based on this argumentation, a number of other factors must also be considered:

- Which assumptions and simplifications were needed to get a result? And thus:
- Are the results credible?
- Has useful information been gained?
- Can the results be interpreted differently?

The first two questions deal with the credibility of the simulation results. It cannot be stressed enough, that a critical approach must be taken while analyzing the results to get useful information from a series of simulations. This means that common sense should be employed when analysing and interpreting results. See also section 1.3.4 on validation.

Returning to the point of assumptions and simplifications it is important to make sure, that the importance of the assumptions and simplifications are realised. In many cases, assumptions and simplifications can make results invalid, resulting in misinterpretations.

In 'the example' an assumption can be made regarding the air tightness of the building. If more air is infiltrating the building because of leakages, this will result in larger air change rates and consequently larger energy consumption than expected. The tightness of the house is a factor that is hard to estimate accurately, since it is very much dependent on the building process (are the drawings of the house good enough and is the craftsman caretaking enough when building the house?) and therefore the value must be assumed based on prior knowledge of similar houses.

A simplification is that the temperature of the air in the room is the same in the entire room. This is not correct as the air temperature is stratified vertically from floor to roof, and the air is also colder near the outer walls.

In other words – assumptions and simplifications are necessary idealisations that are necessary due to shortcomings in the modelling of the real world.

But when assumptions and simplifications are required, will simulations even be credible and trustworthy? Generally, the shortcomings of the model can to a large extent be circumnavigated, making the simulations credible after all. Further, error estimates can be included, so that the maximum error in a given calculation can be estimated, whereby a figure of the uncertainty of a model is found.

1.3.4 Validation

As mentioned above, a critical approach is needed when analyzing data from a computer simulation. A part of this critical approach is to use a validated model, as it was mentioned in the six-point description in section 1.3.1. But how can a validation of a simulation model be carried out? The following points are a few of the possible approaches, which are taken from the PASSYS project (PASSYS, 1989):

- Theoretical examination of sub systems
- Consistency check of results
- Analytical verification, by comparing calculated results to analytical solutions
- Inter-model comparison of results to calculated results from other models

- Sensitivity analysis
- Empirical validation – comparison of calculations to measured results

As it is obvious from this list, there are numerous ways to "validate" a simulation model, and consequently also numerous ways to claim that a model has been "validated".

In the list, the first point addresses the correctness of the chosen model; do alternative equations give other/better results? The second is aimed at the implementation of the simulation model, where a debugging of the code is needed. The third is aimed at comparing results of subsystems of the model to analytical solutions using the same input. This method is normally limited to special simplified cases where analytical solutions are possible. The inter-model comparison is also limited to special cases. The creation of a new model is often motivated from a need for higher or lower level of detail, where it is tested how much of the model's behavior that is lost or changed by using another model. Therefore, comparing results to existing models often is a good way to validate a model, especially if the model to which it is compared is already accepted as "correct". Notice however, that comparisons to other models can only include parts of the behavior, since new parts cannot be compared to an existing model – otherwise there would be no need to develop a new model. The sensitivity analysis is aimed at checking the results for various inputs to see if certain input parameters (or combinations of input parameters) give unrealistic results. The final point is on comparing simulations to measurements. The comparison to measurements are often the most valuable and most expensive, but also the most difficult, as there are a very large number of parameters that cannot be controlled sufficiently, resulting in uncertainties. This is also the case since good experimental data are actually difficult to obtain. Finally, an experimental validation is also limited to a few cases, since experiments are cannot account for all possible variations.

Above all, the process of validation is often to compare two results that both have uncertainties, and therefore limited in the applicability to the general problem which the model aims to be able to solve.

In total, the discussion of a validation can be seen to, at best, be a correctness check under certain specified conditions that can be controlled to a certain extent. However, it is often possible design comparisons to other models and experimental data in such a way that the validation result can be quite wide in the applicability.

Again, the fact that a model has been validated therefore means that under given circumstances this model can correctly predict the results. In other words, it is still required for the user to use common sense when analyzing simulation results. However, the user can now be certain that the model **can** be used to get correct results under given conditions – it is now up to the user to assess if the model can be used for the conditions that are modelled.

1.3.5 Complexity

The complexity of the model is an important part of the modelling. In other words, how many details should be included in the model and how many parameters should be available for getting the desired results?

As the model is in fact only a model, not all parameters can and shall be included. If the model is used for an initial estimation in the design phase, it will for instance make no sense to be able to define in detail the functionality of the heating system through the use of many different parameters. For instance, instead of a detailed model of the boiler perhaps a simple one including an efficiency term will be more appropriate since a very detailed design will most likely be changed again later. Therefore, at any given phase in the design of a house, there is no need to use too many parameters. In fact the inclusion of too many parameters

might give invalid results if one of them is set to a value that is later changed. Therefore it can often be advantageous to omit a detailed model with many parameters if a simpler model exist that is more appropriate for the design at that stage.

Secondly models can also easily become too detailed without giving more accurate results. If for instance the number of nodal points in a discretized model of a wall is increased the results may not become more accurate if a sufficient number is already used. This only gives longer calculation time. Therefore there is no need to use too detailed models – it will only give longer simulation time and most likely not enhance the results significantly.

In both cases, a main issue in computer simulations is that the user must be aware of the limitations of the model and of the sensitivity of parameters.

1.3.6 Use and misuse of simulation models

Simulation models are, as the name implies, just models of the real world. A model is, almost without exception, not fool proof. To all inputs, there is a certain limit where the model behaves as it is supposed to. If this limit is not respected the model can (and will) give results that are not trustworthy.

Computer simulations are often very complex, and it is therefore important that results are treated with great care to avoid conclusions that are not supported by the model.

Often this is the case when a model is developed for one purpose but used for another – or if a model has been continuously developed from a basic design, where the increased complexity cannot be handled by the initial design. In other cases, the models are simply used outside of the domain where the model behaves physically correct. In any case, the complexity of the model means that the user is unable to realize that the model does not work properly.

This is mentioned to make it clear, that while modelling in most cases results in valid and trustworthy results, it can sometimes be just the opposite.

1.3.7 Technical/scientific modelling

A technical simulation model is based on the use of a mathematically formulated equation system that can be solved using a computer. A computer cannot solve an expression like this: Sum up the heat coming to and from the room. It has to be put in the form of mathematical equations. Both scientifically, and technically based equations obey the same rules. There are, however, differences between scientific and technological modelling.

Where science has the goal of arriving at new knowledge, technology has the goal to make way for new products based on scientific knowledge, which can be produced, sold and used – and be the basis for further development of other technical products. Of course, it goes both ways. One classical example of this is the steam engine, which was developed in England around 1710 by Thomas Newcomen, largely by a practical/technical and non-scientific approach (Nielsen et al., 1995). Later that made way for a completely new field in scientific research called thermodynamics, the field that includes energy and conversion between different forms of energy.

However, it is very rarely the case that such a direct link can be made (Nielsen et al, 1995). Especially since the two fields are so different. More often advances in one field require development in the other, but they are not directly linked.

Returning to ‘the example’, it is very unlikely that a thermal model of a house will make way for new scientific knowledge. But the development of the model and its use may lead to the realization that new technologies must be developed to improve the house. In the example, it

may be found that a different control strategy may be implemented which improves the thermal comfort in the house and at the same time lowers the energy consumption. Therefore a new control unit with this type of control strategy included can be developed. However, this is a technological progress, not a scientific one.

To sum up: If the simulations are used simply to calculate the energy consumption in a building, it is simply a "technical calculation". If the simulations for instance lead to the development of a new and inventive control strategy, it is "technical development". And, if the new control strategy further gives the realization that a new type of control theory can be developed, it might be called "science". However, the aim of the simulation model was probably never to give way to a new control theory, so the "science" took place in the developer of the model's head – not in the model.

On the other hand, modelling is a valuable tool for developing basic understanding of very complex systems, for instance a meteorological model. Here modelling is a necessity in order to gain new knowledge, and therefore it must be considered science. Using computer modelling in this case actually represents a completely new type of science.

Therefore:

- Does a computer model give new and valuable information, or could this information be obtained more easily in other ways?

Yes, a computer model can, if designed properly, give valuable information – information that could not be obtained otherwise. In other cases, models can only tell us what we already knew. This has, however, nothing to do with the model, only the user.

1.3.8 Accumulation of knowledge

An issue in technical as well as scientific applications is the accumulation of knowledge. Accumulation of knowledge can occur when a given problem has been examined – and possibly even solved. Through a documentation of the work, knowledge can be passed on. In science and technology, this is normally done through publication of the results.

This type of publication increases the level of knowledge in a given field – at least if knowledge is defined as the amount of information available in that field. However, information and knowledge is not the same. Information only has value if at the same time the recipient of the information has a certain amount of knowledge in advance. This is, and has always been, a problem for scientist and engineers (and everybody else). This point is not stressed further here but mentioned for completeness.

When it comes to computer modelling, yet another problem arises. This problem is the possibility to reuse already existing models and only add new parts as required by the problem at hand. For instance an engineer wants to implement a floor heating system to an existing building energy simulation program. So instead of having to start all over by creating a new model that must be implemented, tested and developed to include floor heating, an existing model, which only lacks floor heating, could be used. Now, only the floor heating subsystem and the interaction with the rest of the model needs to be developed (and validated).

This problem can be formulated in the following questions:

- How can new models be directly based on existing models
- At the same time as knowledge can be maintained and developed?

One in theory simple answer to this is standardization. In practise, it is almost impossible!

Standardization is here defined as the need for a common platform for the development of new models, so that new models can be used by other engineers/scientists working in the same field. The use of standards is already widely used for definitions of technical terms, i.e. what do we mean when a specific word is used. Taking the example of floor heating mentioned above, the way standardization could be used, would be to have a definition of the interface between the floor model (with floor heating) and the rest of the model of the house. This means, that a newly developed floor model should simply be "plugged" into an existing building energy simulation model.

Of course, other factors must be included in the discussion of accumulation of knowledge. For instance, how should the validation of a model be carried out, and what kind of documentation is needed.

1.3.9 What is a good simulation model?

In this section, the use of computer simulations for technical purposes has been discussed with respect to the basic concept of creating a model of a system followed by implementation, validation and calculation.

It is initially pointed out, that computer modelling of technical systems gives huge opportunities for better design. First of all, the behaviour of a system (building) can be known already before it has been built. Secondly, the model can easily calculate what will happen if given parameters are changed. This way, the system can be optimized without producing and testing many prototypes. If the product for instance is a building (or a space shuttle for that matter), huge amounts of money can be saved, if changes to the product can be simulated in a computer model, instead of tested on a real product.

A computer model of a system is called system theory, and represents a fairly new approach in scientific and technical work. The strength of this type of approach is that complex systems can be modelled, so that the properties and dynamic behaviour of the system can be extracted from the model. It is also worth mentioning that the approach can be used in a number of different fields of scientific and technical work.

However, computer models of technical systems have different drawbacks, and these are also discussed here. Among these is the need to simplify the model since the total complexity of the real world cannot be included in a model – since it is just a model. Also, assumptions are needed to be able to do the simulations. This raises the question of the credibility of the model, which can be established by validating the model based on known data and using common sense when analyzing the results from the model.

This is followed by a discussion of the required complexity of modelling. It is established, that models should not include more information than required to give the needed results. If a model is too complex, it can lead to misinterpretation.

A question, which is not easily answered, is whether a model is science. A main point in this is the use of the model. If it is a technical model of for instance a house, it will rarely become scientific unless it can be used to find new basic properties of the system. Whereas a scientific model of the green house effect by definition is scientific, since the use of system theory is the only way to gain information about the extremely complex system that the earth's atmosphere is. In both cases however, the computer model is only a calculator, while the system model is where the system is defined. The basic properties of the system will be revealed in the calculations.

Finally it is discussed how knowledge can be accumulated in modelling. A means of doing this is through standardization.

To sum all this up, one final question can be answered:

- What is a good simulation model?

It is simply a model that does what is required from it. It should be able to answer the questions that the engineer or scientist asks while providing easy access for interpreting the results. Finally it should also give information that could not otherwise be obtained by simpler methods.

1.4 Organization of thesis

A brief overview is given in this section.

In **Chapter 1** the basis for the work in this thesis is presented along with considerations of the scientific method which has been used.

Chapter 2 is a short introduction to the different types of building integrated heating and cooling systems that are used for the analyses.

A literature evaluation and state of the art review is described in **Chapter 3**, for both research and products

The numerical models which are used in this thesis are described in **Chapter 4**. This chapter describes the contents of the models while **Appendix A** contains the detailed description of the actual modelling techniques. **Paper 1** is attached to the thesis as part of Chapter 4.

The first main chapter in the thesis is **Chapter 5**, which deals with floor heating. **Paper 2** is attached to the thesis as part of Chapter 5.

Chapter 6 is the second main chapter, where thermo active components are investigated. **Paper 3** is attached to the thesis as part of Chapter 6.

A special type of floor heating using heat storage of solar energy is described in the last main chapter, **Chapter 7**. **Paper 4** is attached to the thesis as part of Chapter 7.

Finally **Chapter 8** contains the conclusion and recommendations for further work, before **Chapter 9** and **Chapter 10** where the references and nomenclature are given.

2 Building integrated heating and cooling

This chapter contains a very brief general overview of building integrated heating and cooling systems with applications and types. The chapter also serves as the demarcation of the work, which is presented in the thesis.

2.1 Conceptual description

Building integrated heating and cooling represents a way to heat or cool the building by utilizing the building structure itself. In short, building integrated heating and cooling systems has pipes, ducts or electrical cables embedded in the building structure. By circulating water, air or electrical current in ducts, pipes or cables in the building structure, the building surfaces can be used to heat or cool the building (in case of electrical cables only heating is possible). The large surface area used for the heating/cooling has the advantage, that relatively small temperature differences between the heating/cooling medium and desired room temperature are required. In other words, the systems enable low temperature heating and high temperature cooling, which means that a very wide range of heating and cooling sources can be used.

Building integrated heating and cooling systems have a slow reaction time compared to other types of heating and cooling, since the system is typically placed in a concrete layer inside the building structure away from the room which it is heating or cooling. This means that the change in the conditions is slow as the large thermal mass in the concrete has to be heated or cooled before the conditions in the room changes due to the heating or cooling. This is an important fact, which has a number of possibilities and limitations that are very relevant for the use of building integrated heating and cooling systems. On one hand, the long reaction time means it takes long time to change the temperature in the room by changing the state of the system, but conversely, the small temperature differences between the system and the room means that even small changes in the room temperature will have a large influence on the heating/cooling in the room from the surfaces where the energy is supplied to or removed from the room.

The fact that large surface areas are used means that building integrated heating and cooling systems are mainly radiant in the way energy exchange between surface and room. Normally over 50% of the heat transfer from the surface to the surroundings is through radiation.

2.1.1 Floor heating systems

The best known application of building integrated heating is floor heating, which is today widely used in the domestic sector in especially the Nordic countries (Radisch, 2001; Olesen, 2002; Roots, 2002). This is due to considerations of thermal comfort as well as aesthetic appearance. Floor heating can be used both as the only heating system in a house and in conjunction with conventional heating by radiator panels. Of course the surface used for the heating is not restricted to floors, both walls and ceiling can be used. These systems are, however, rarely used.

Floor heating also has a few other applications, which are not directly addressed in this work. However, they should be mentioned for reasons of completeness. Large indoor sports facilities and warehouses with large room height can also be heated by floor heating. So instead of needing to heat up the air, which will inevitably rise to the top of the room, where it is not interesting seen from a thermal comfort point of view, the surface closest to the people

in the room is heated instead. This gives both higher thermal comfort and lower energy consumption.

2.1.2 Thermo active components

In recent years, a new use of embedded pipes in the building structure has been introduced (Meierhans, 1996; Meierhans, 1993; Olesen, 2000); namely the so-called thermo active structure or component. A thermo active component is a deck floor with embedded pipes in multi-storey buildings. Thermo active components are mainly used in office buildings, where they are mostly used to cool the buildings. The thermal mass of the concrete means that the cooling capacity can be "stored" in the thermo active component during the night time and cool the building during the day time, because the surface temperature will continuously be below the room temperature as a result of the stored cooling capacity. Therefore, the energy does not need to be removed from the building at the same rate as it is produced. This means that an air-conditioning system can be avoided, and therefore it is only required to ventilate to ensure sufficient supply of fresh air in the room. In the winter time when there is a (typically) small heating demand, the same embedded pipes can also be used to heat the building.

2.1.3 Thermal energy storage in floor construction

A special case of floor heating which is investigated separately in this thesis is the use of heat storage of solar energy in the floor construction of single-family houses. This use of solar energy is cheap, as the extra cost of installation when it is part of solar domestic hot water system is small. Therefore this represents an interesting option to lower the energy consumption for heating in buildings at little extra cost.

The research field of Thermal Energy Storage is very large and has many advanced features such as phase change materials and complex control systems. Here only a very cheap possible use is investigated, which is a natural extension to the work carried out on floor heating systems.

2.2 Discussion on novelty

One may (rightly) argue that using the building envelope to heat rooms in a building is not in any way a novel discovery. Already around 100 B.C (Olesen, 2002), and in the Roman Empire (Bansal and Shail, 1999), hypocaust heating was used. 'Hypocaust heating' means a "heating apparatus placed under the building it proposes to heat" (Forbes, 1958).

In Olesen (2002), it is stated that modern day floor heating was invented around 70 years ago, but due to the need for high temperature levels in the floor construction because of the poor insulation standard of buildings, floor heating got a bad reputation.

However, two things have made floor heating (and now also thermo active components) technically possible; namely the increasingly well insulated building envelope, which has lowered the required temperature level in the floor construction considerably, and the introduction of plastic pipes, which are durable and easy to work with compared to cupper or steel pipes.

Today floor heating is widely used in domestic buildings and in office buildings thermo active components may get accepted as an economically feasible technology with positive implications on thermal comfort and energy consumption.

However, the possibility to predict both thermal comfort and energy consumption is very limited, as there are no – or at best, only a few tools available for designing and dimensioning floor heating and thermo active components.

One final and very important point that needs discussion is the implementation of the EU-directive 2002/91/EC on Energy Performance of Buildings (European Parliament, 2003). With this directive the energy requirements in the national building regulations in the European Union will become based on the 'amount of energy actually consumed' as it is stated in the directive. This should be implemented on national level by Jan 2006; with a possibility for a three year extension period if required by special considerations on a national basis. In practise, this directive is expected to make the use of air-conditioning in buildings too energy consuming and therefore in practise impossible to use. For office buildings this means that building designers need to focus on other technologies to avoid overheating in hot summer periods, as for instance thermo active building components. Therefore, this new development calls for increased research and development in alternative technologies to air conditioning systems.

2.3 Demarcation of this work

The purpose of this thesis is to present, implement and compare modelling techniques of the heat flows, temperatures and thermal indoor climate for building integrated heating and cooling systems and to discuss possibilities and shortcomings of the different models presented. Where possible, measurements will be used to assess the validity of the simulation models to ensure correct behaviour for both steady state and dynamic modelling.

The models will be used to for simulations of different relevant problems illustrating the use of the model and the results from these simulations will be presented and discussed.

Three types of building integrated heating and cooling will be considered; floor heating, thermo active components and thermal energy storage of solar energy in floor constructions.

The work will only consider waterborne (hydronic) systems.

The work is focused on the demand side of the heating/cooling system and the room that it is heating or cooling. The work will not include analyses on the supply side of the heating system, such as boilers, district heating units or "free coolers", though a few considerations will be presented on the effectiveness of such systems. The only exception from this is an investigation of a thermal energy storage charged by solar energy

3 Literature evaluation and State of the Art review

This chapter investigates and discusses the current state of the art for building integrated heating and cooling systems as the background for the work presented here. The investigation includes journal and conference papers as well as reports and books and information from manufacturers. Of course the review and background is in no way comprehensive for any of the fields addressed here.

Initially, sections common to floor heating and thermo active components are described before sections dedicated to the two main areas are described individually. Finally two sections describe heat storage in floor constructions and simulation programs available for modelling hydronic radiant heating and cooling systems.

3.1 Standards and building code requirements

A number of standards and building code requirements address floor heating and thermo active components. These standards are mainly aimed at floor heating systems, but many of the requirements are equally applicable to building integrated heating and cooling systems in a broader sense than just floor heating.

Traditionally the heating system has not been included in (Danish) building codes. However, recent discoveries have indicated that special care must be taken for floor heating systems to avoid large extra energy consumption through the ground and foundation. The Danish Building Code 1995 (Boligministeriet, 1995) and the Danish Building Code 1998 (Boligministeriet, 1998) give limits for allowed energy use for heating in buildings. The two are identical except that the 1995 version covers large buildings while the 1998 version covers smaller buildings. Floor heating is mentioned in supplements from 2001 setting maximum U- and ψ-values of floor construction and foundation that are lower than for houses without floor heating. This extra requirement for floor heating is based on the expected higher energy consumption.

As mentioned in Chapter 2 the EU-directive on Energy Performance of Buildings (European Parliament, 2003) will form the basis for future national building codes in the European Union. In the directive, the energy performance is defined as the actual energy consumption of the building. Or more popularly: The amount of fossil fuel that has been “tapped” from outside the building. Because of the low temperature capabilities of radiant heating and cooling systems, it is expected that this directive will be beneficial for these types of systems.

DS418 (DS, 2002) with the title “Calculation of heat loss from buildings” sets the background for finding the energy consumption in Danish buildings. Heated floors are included by setting a larger dimensioning heat loss to the ground as the temperature in the plane of the floor heating pipes should be used. In the dimensioning case, this value is set to 30°C, or 10K over the dimensioning room temperature.

EN 832 (CEN, 1998b) with the title “Thermal Performance of Buildings – Calculation of Energy Use for Heating – Residential Buildings”, handles the required energy to heat residential a building. EN ISO 13790 (CEN, 2004) with the title “Thermal Performance of Buildings – Calculation of Energy Use for Space Heating” expands the use of EN 832 to all types of buildings and not just residential buildings. In both methods are given to find the energy required to heat the building based on an energy balance of gains and losses. The heating system is included through an extra heat loss term. However, floor heating is not mentioned specifically.

The dimensioning and design of floor heating systems is treated in the standard EN1264 (CEN, 1997) with the title: Floor Heating – Systems and Components. It is divided into three parts. The first part deals with definitions and symbols, the second part with determination of the thermal output while the third part gives dimensioning diagrams. The heat flow density, or thermal output, is given by the following power-law expression:

$$q = B \cdot \prod_i \left(a_i^{m_i}\right) \cdot \Delta\theta_H \qquad \textbf{(3.1)}$$

That is, the heat flow density is given by a system dependent coefficient, *B*, multiplied by a power product of system factors, *a*, each with a power coefficient, *m*, multiplied by the logarithmic temperature difference between heating medium and room air. The coefficients, which are based on finite element calculations, can be found in tables in the standard. One of these system factors can be found experimentally, can be utilized to take other factors that are not tabulated into account.

The standard only deals with steady state conditions and only with the thermal conditions in the floor construction itself.

The standard is not applicable to lightweight floor heating systems. Only heavy systems where the pipe is placed in, or immediately next to, a concrete layer are considered in the three types of floor heating system that are included in the standard.

Lightweight floor heating has been included in the Nordtest VVS127 standard (Nordtest, 2001). This standard is an addition to EN1264. There are, however, large differences in the way Nordtest VVS127 determines the thermal output of the floor heating system. Instead of system factors, the standard uses thermal resistances in a thermal network. Again, typical values of the system parameters can be found as tabulated values. However, more emphasis is put in the description of a procedure for an experimental setup, as there are more unknown factors included in a lightweight floor heating system than in a heavy system.

EN ISO 13370 (CEN, 1998c), with the title ‘Thermal Performance of Buildings – Heat Transfer via the Ground – Calculation Methods’, defines calculation methods for heat loss to the ground. The calculation of the heat loss to the ground is complex since many parameters need to be considered in a two- (or ideally three-) dimensional calculation of floor construction foundation and surrounding ground volume. The method presents a set of equations for the calculation of the U-value of the total floor construction including foundation. It is also described how numerical procedures can be used instead. In the realization that the method should also be applicable to building energy simulation programs, the method describes a way to include the 2D or 3D heat loss to the ground and at the same time keep simulation time short by using two calculations. The first finds average steady-state heat loss to the ground in a detailed calculation including floor construction, foundation and ground volume. The second is the dynamic part, which can be used in the building energy simulation program. Here it is sufficient to use a simple 1D model with one meter of ground below the floor construction. The lower boundary condition is adiabatic, so the ground volume is only included to add seasonal variation. Floor heating is mentioned in an informative annex. In the calculations of the heat loss to the ground, the average temperature in the plane of the heating pipes must be used instead of the room temperature.

There are at present no standards directed at thermo active components. However, a more generally applicable replacement of EN1264 and Nordtest VVS127 is currently underway, which includes both heating and cooling and using internal building surfaces (walls, floor and ceiling), for both heavy floor heating systems, lightweight floor heating systems and thermo

active components (Olesen et al, 2003). Here Part 1 of the upcoming standard is presented. The characterisation can use the power function presented in EN 1264 (CEN, 1997) for heavy systems, the equivalent thermal resistance method presented in Nordtest VVS 127 (Nordtest, 2001) for lightweight systems, and finally a general thermal resistance model (Koschenz and Lehmann, 2000) for thermo active components and capillary systems[1]. This standard can therefore be used to determine the heating and cooling capacity of embedded hydronic heating and cooling systems in general.

Generally the standard introduces surface heat transfer coefficients for the heating and cooling through floor, ceiling and walls. The values are shown below:

$$\begin{aligned} &\text{Floor heating and ceiling cooling: } q = 8.92 \cdot \left(T_{sur} - T_{room}\right)^{0.1} \text{ W/m² K} \\ &\text{Wall heating and wall cooling: } q = 8 \text{ W/m² K} \\ &\text{Ceiling heating: } q = 6 \text{ W/m² K} \\ &\text{Floor cooling: } q = 7 \text{ W/m² K} \end{aligned} \tag{3.2}$$

As it can be seen the coefficients are given constant values except for floor heating and ceiling cooling.

In all cases this new standard proposal only covers steady-state conditions.

3.2 Thermal comfort and indoor climate

Probably the main reason for the popularity of floor heating in modern houses is based on the fact that the radiant heat supply to the room is considered comfortable by the occupants. The use of radiant cooling is assumed to have the same positive effect on the thermal sensation. However, no published works seems to have established this.

A few more advantages can be mentioned:

- The vertical temperature distribution in rooms heated with different heating systems has been investigated (Caluwaerts et al, 1980) with the result that there is only a small vertical temperature difference from bottom to top in the room.
- Because the main part of the heat exchange in the building is through radiation, there will be less convective forces and thereby less air movement in buildings with radiant heating and cooling. This lower rate of air movement will generally cause less dissatisfaction for occupants.

Two factors are important for the thermal comfort when the building is heated or cooled from the surfaces; firstly the general operative temperature in the zone and secondly the surface temperatures.

3.2.1 General thermal comfort

Thermal comfort is treated in both international and Danish standards in ISO 7730 (ISO, 1994), CR 1752 (CEN, 1998a) and DS 474 (DS, 1993).

The general thermal comfort is based on the combination of room air temperature, radiant temperatures from the surfaces, relative humidity, air velocity and level of activity of the

[1] Capillary systems are systems with very small pipe diameters normally placed close to the surface. These are not treated in this thesis.

occupants in the room. The operative temperature is typically calculated as the mean value of the room air temperature and the mean radiant temperature. Finally, the thermal comfort parameter called the Predicted Mean Vote (PMV) (Fanger, 1970) is the overall index for general thermal comfort based on a seven point voting scale. The Predicted Percentage of Dissatisfied (PPD) can be found based on the PMV-value.

In CR 1752 (CEN, 1998a) three levels of thermal comfort have been defined. That is, Class A corresponds to less than 6% dissatisfied, Class B to 10% and Class C to 15%, shown in Table 3.1. In all cases the requirements result in a range of allowed internal temperature. This range is important as the thermo active components cannot maintain a fixed temperature, but rather keep it within a temperature range. Therefore the allowed temperature range introduced in the standards must be used in the considerations when using building integrated heating and cooling.

Table 3.1 Thermal comfort classes defined in CR 1752 (CENa, 1998).

Class	PPD	Temperature range, Winter 1.0 clo, 1.2 met	Temperature range, Summer 0.5 clo, 1.2 met
A	< 6%	21-23°C (22.0±1.0)	23.5-25.5°C (24.5±1.0)
B	< 10%	20-24°C (22.0±2.0)	23-26°C (24.5±1.5)
C	<15	19-25°C (22.0±3.0)	22-27°C (24.5±2.5)

In special conditions, periods with temperatures outside of the allowed range may be permitted. An example of this can be found in DS 474 (DS, 1993), where 100 hours per year are allowed with temperatures above 26°C and 25 hours above 27°C. A different approach is to calculate the number of degree hours above the allowed maximum temperature (De Carli and Olesen, 2001). Finally it should be noticed that national standards might use other conditions.

3.2.2 Surface temperatures

The recommended maximum temperatures are given in Table 3.2.

Table 3.2 Recommended maximum and minimum temperatures on surfaces with embedded pipes. Based on Olesen et al. (2003).

	Maximum temperature	Minimum temperature
Floor – peripheral zone	35°C	19°C
Floor – occupied zone	29°C	19°C
Wall	40°C (not higher to avoid burns on bare skin)	Limited by dew-point temperature (valid for pipe temperature)
Ceiling	Should not be set higher than to give a radiant asymmetry of less than 5 K	Limited by dew-point temperature (valid for pipe temperature)

The floor surface temperature must be held within certain limits to ensure thermal comfort. These limits are given by different practical and physical requirements. A floor surface temperature of around 24-30°C gives a minimum percentage of dissatisfied for standing people with bare feet depending on floor covering materials (Olesen, 1975).It was also found that sedentary persons preferred 1 K higher temperatures. Further, people with socks have the same thermal preferences as people with bare feet, also concerning floor covering materials. These results have been based on short period (up to ten minutes) measurements. For longer term influence, people with shoes with soles thicker than approximately 5mm found that the floor covering material did not influence the results. The temperature should be in the interval of 20°C and 26°C for standing persons and approximately 2K higher for sedentary persons.

To reflect these findings, EN 1264 (CEN, 1997) sets a maximum floor surface temperature in occupied areas is set to 29°C (35°C in peripheral areas). However, if a wooden floor is used as the floor covering material, normally a maximum floor surface temperature of 27°C is allowed to ensure the durability of the wooden floor.

For heating from the ceiling the percentage of dissatisfied rises steeply with the surface temperature, for walls the level is dictated by the avoidance of burns on bare skin if the wall is touched.

For cooling the temperatures are dictated by the dew point temperature and thermal comfort criteria. Notice that to avoid condensation anywhere in the construction, the lowest temperature (the supply temperature) should always be above the dew point.

Another problem that needs to be addressed is to avoid cold drafts from windows during cold periods. The traditional way to avoid this is to use radiators placed immediately below the windows. With floor heating this is not possible. However, an experimental setup to measure the convection from a cold window in a room with floor heating concluded that floor heating was efficient towards minimising thermal discomfort due to downdrafts from windows (Peng and Peterson, 1995). Another investigation with highly insulating windows (Rueegg et al, 2001) concludes, "Generally speaking, our measurements show, that buildings with window sills and highly insulated windows (glazing and frames) need no heating appliances under the window or other means to compensate cold air down draughts." Therefore no special attention needs to be placed on extra peripheral heating under windows in case of floor heating, unless the windows have a high U-value or are unusually tall.

3.2.3 Vertical air temperature difference

The vertical air temperature difference between ankles and head level is also of interest, since especially for thermo active components, the floor surface is colder than the room air. EN ISO 7730 (ISO, 1994) defines the percentage of dissatisfied for this vertical air temperature difference. A temperature difference of less than 2K will give less than 2% dissatisfied, while 4K difference will result in less than 5% dissatisfied.

3.2.4 Air quality

The effect of radiant heating and cooling system on the non-thermal part of the indoor climate has also been investigated.

The effect on house-dust mites has been reported (De Boer, 2003). In this Dutch investigation, it is found that houses with surface heating (floor heating) generally have less house-dust mites than houses with radiator heating. However, houses with floor heating could nonetheless easily sustain populations of mites. Another investigation has shown that the use of floor heating gives less airborne particles as it is assumed that there is less air movement, and therefore less irritation of the mucous membranes. (Eijdems et al, no year). This is also expected to be the case for buildings cooled by thermo active components where there is also less air movement in the room.

The fact that a mechanical air conditioning system can be avoided means that the level of sick building syndrome symptoms is expected to drop, as the air conditioning system is often the cause of these symptoms due to poor maintenance or faulty operation.

3.3 Modes of heat transfer in room

As found above in section 3.1, Eq. (3.2) shows that the heat transfer coefficient varies with the thermal conditions in the room and on the surfaces, especially for floor heating and ceiling cooling.

Generally speaking, floor heating is a mainly radiant heat source where over half the heat from the floor is supplied by radiation to the room (i.e. Hanibuchi and Hokoi, 1998). This can also be seen from the fact that since the radiative heat transfer coefficient is approximately 5.5W/m²K in rooms under "normal" conditions, and the total value is between 9 and 11W/m²K (see Eq. (3.2)) the radiative part is larger than half the total heat exchange. In Koschenz and Lehmann (2000) the radiative part is found to be approximately 80% when the temperature difference between floor surface and room air is 1K and around 65% with a 4K difference.

3.3.1 Radiant heat transfer coefficient

The larger part of the heat transfer from the heated or cooled surface is through radiation as it was found above. Radiation is a well-described physical phenomenon, which can be calculated by equations that can be found in many books on heat transfer (Mills, 1992; Incropera and DeWitt, 1996). While complicated because the equations are quite complex, it is however possible to create an analytical tool for this.

3.3.2 Convective heat transfer coefficient

Contrary to the radiant heat transfer, the convective heat transfer depends on a long list of factors, which cannot satisfactorily be included in an analytical investigation. Therefore the convective heat transfer coefficient has traditionally been investigated through the use of experiments or – more recently – through Computational Fluid Dynamics models. In the literature a large number of investigations on the convective heat transfer coefficient have been published. This has led to many correlations of both free (also called natural) and forced convection. Free convection is influenced by surface geometry and thermal boundary conditions while forced convection is driven by e.g. a ventilator or an open window. Typically the convective heat transfer in a room is governed by both types of convection. Examples of correlations of both free and forced convection can be found in the literature (Dascalaki et al, 1994; Awbi, 1991; Wallentén, 2001), where many different methods, assumptions and limitations are imposed to establish the correlations.

3.4 Floor heating systems

Historically, floor heating has been used in both the ancient Roman Empire (Bansal and Shail, 1999) and in Korea around 100 B.C. (Olesen, 2002). Here, hot gasses from fire places or furnaces were distributed in subfloor air channels, thereby heating the floor and consequently also the room above. This type of heating is also called 'hypocaust' (Bansal and Shail, 1999). In modern times the first known use of floor heating was in the US in the 1930's (Olesen, 2002). At least two problems impeded the use of floor heating at this point; (i) the use of steel or copper pipes as the heat distribution system gave a short life expectancy due to corrosion and (ii) the large heat loss from the poorly insulated buildings, meant that the floor surface temperature was unacceptably high. In the 1970's a shift in technology towards plastic pipes without leakages, along with better insulated building envelopes, has led the way towards the introduction of floor heating in modern day houses.

Today, after the turn of the millennium, floor heating is widely used in new residential houses. In detached single-family houses, it is by far the preferred heating system, with a large market share. This is especially the case in Germany, Switzerland, Austria and the Nordic countries (Olesen, 2002; Radisch, 2001).

3.4.1 Applications

In this section the basic construction of floor heating systems will be described with respect to different types, building elements and suitable types of buildings. This is just a very brief introduction to describe the current state of floor heating systems and is in no way comprehensive. More thorough descriptions are available in books and on the homepages of the manufacturers of floor heating systems.

Normally, an on/off type control is used in Danish systems.

The pipes used in the floor heating system are typically made of PEX, which is cross-linked polyethylene, optionally equipped with an oxygen diffusion barrier. It is obviously very important that there are no hidden joints. Typically, pipes with an external diameter of between 15 and 20mm are used. A pipe of 20mm, with an internal diameter of 16mm will have a maximum length of the floor heating pipe of approximately 100-120m due to the pressure drop in the pipe. A smaller pipe diameter gives a higher pressure drop in the pipe and thus a shorter possible pipe length.

The floor heating pipes are normally laid out with a pipe distance of 300mm. In special cases, the pipes can be placed closer under windows if there is risk of cold drafts, which is however rare due to the much improved thermal insulation of new windows. See also section 3.2.2.

When comparing the different types of floor heating systems, a central parameter is the time constant, which is a measure of how fast the floor reacts to changes in the supply temperature.

The response for a unit step change in a first order system (linear system) is defined as shown in Eq. (3.3):

$$y(t) = 1 - e^{-\frac{t}{\tau}} \tag{3.3}$$

Inserting the time constant, τ, into Eq. (3.3) therefore yields:

$$y(\tau) = 1 - e^{-1} = 0.632 \tag{3.4}$$

Consequently, the time constant is the time it takes for a step change to reach 63.2 % of the final value when the unit step change is applied as input. This value can be used to easily characterise and compare different floor heating systems with different setups.

Notice, that in order to get a meaningful definition of the time constant, it is required that a lumped analysis can be used. The Biot number, Eq. (3.5), can be used to establish whether or not a lumped analysis can be used (Hagentoft, 2001).

$$Bi = \frac{L_c}{d} \le 0.2 \text{ where } L_c = 2\frac{V_{material}}{A_{surface}} \text{ and } d = \frac{\lambda_{material}}{h_{surface}}$$

or

$$Bi = \frac{h_{surface} \cdot L_c}{\lambda_{material}} \le 0.2 \tag{3.5}$$

The Biot number is the ratio of the internal heat transfer resistance to the external heat transfer resistance (Mills, 1992). The limiting criterion of 0.2 will ensure that all the material will have nearly the same temperature, and therefore can be assumed lumped. This requirement is met by floor heating systems, while this is typically not the case for thermo active components where the concrete has a larger volume to surface ratio.

Heavy floor heating system

Heavy floor heating is the most often used type of floor heating. The word "heavy" means that the floor heating pipe is placed in a concrete layer. Figure 3.1 shows an example of a heavy floor heating system.

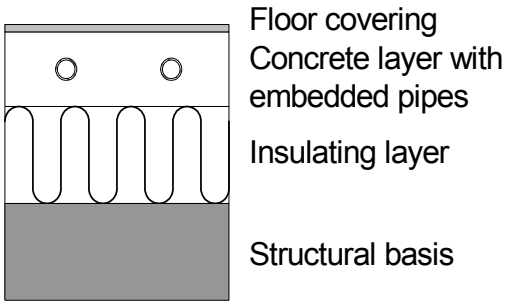

Figure 3.1 Heavy floor heating system.

The floor covering material can be chosen freely as tiles, linoleum or wooden floor with combinations of carpets that can cover the entire surface or parts of it. It is clear however, that a less thermally insulating floor covering gives faster reaction time and lower requirements for the fluid temperature in the floor heating pipes.

The time constant varies from around three hours for a floor with tiles to around five to six hours with wooden floor when measured on the floor surface. The value is lowest if no carpets and a relatively thin wooden floor is used (Weitzmann and Jensen, 2000).

Light floor heating system

Light floor heating systems refer to systems in which the pipes are not embedded in a layer of concrete. This means that the system has a faster response to changes in the supply temperature. Here the time constant is in the range of 30 minutes to two hours, again depending on the resistance and density of the floor covering material. Light systems cannot normally be used together with tiles.

Figure 3.2 shows two different types of light floor heating systems. In the light systems a metallic heat transfer plate is normally used to distribute the heat from the pipe to the entire floor area as the insulation or wooden materials, which are otherwise used in the construction, prevent a good distribution of the heat across the surface. This heat transfer plate is typically made of aluminium. Some systems exist that do not use heat transfer plates, however this will lower the possible heat supply from pipe to room.

Many different types of light floor heating systems are available with combinations of the use of heat transfer plates, wood and insulation – Figure 3.2 shows two of these types, while Figure 3.3 shows a picture of the system with heat transfer plates

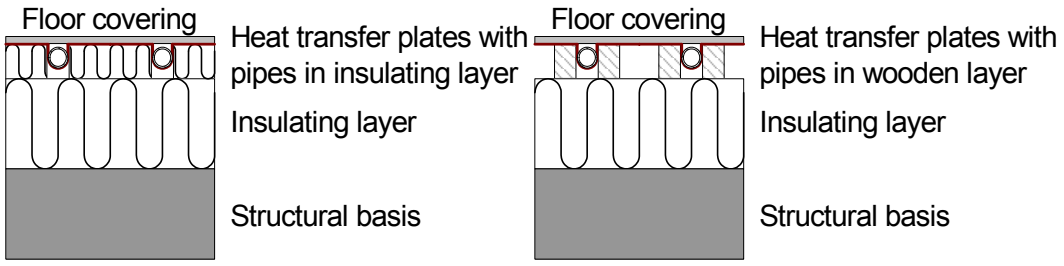

Figure 3.2 Light floor heating system with heat transfer plates (left) and in wooden layer (right).

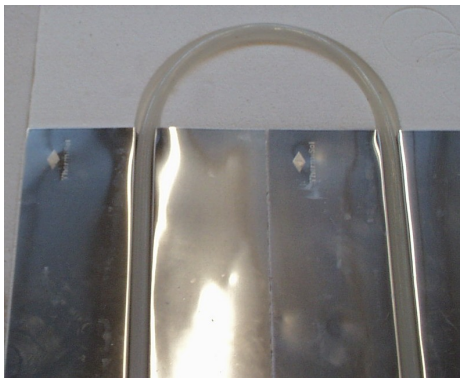

Figure 3.3 Picture of light floor heating system with heat transfer plates.

Retrofit

Both heavy and light floor heating types can be used for retrofit solutions, which can be placed directly on top of the existing floor construction. Common to these is that they can be installed with very low building height between 25-35 mm, as they use smaller pipes.

Electrical

One final type of floor heating system will be briefly mentioned: Electrical floor heating systems. In an electrical floor heating system, an electrical cable or mat is placed in the floor construction. The resistance in the cable/mat ensures an even distribution of the supplied heat. Electrical floor heating can also be used for retrofit solutions.

3.4.2 Characterisation of parameters in the floor construction

In this section the main parameters to characterise the heat loss from the floor construction are mentioned. Two different procedures are considered; one based on EN ISO 10211-1 and DS418 and one based on EN ISO 13370. The two methods differ in both the methodology of the calculation procedures and in the definition of the parameters.

Procedure based on EN ISO 10211-1 and DS418

The approach is based on ISO 10211-1 (CEN, 1994), where the basis for calculating the heat flow is divided into three different parts; surface, linear assemblies and corners in a U-value, a ψ-value and a χ-value.

Thermal transmittance (U-value)

The U-value of the floor construction without floor heating can be calculated from the following equation:

$$U_{floor} = \frac{1}{\sum_i \frac{x_i}{\lambda_i} + R_{si} + R_{ground}} \quad \textbf{(3.6)}$$

The ground thermal resistance is a measure of the resistance from the lower side of the floor construction to the "ground", or to undisturbed conditions with a fixed temperature. Strictly speaking the thermal resistance is not physically correct as it is assumed that the heat is transferred to the ground, which is considered a heat sink with infinite thermal mass. In reality the ground temperature is not constant, as it is influenced by both indoor and outdoor conditions.

Linear thermal transmittance (ψ-value)

The ψ-value of the foundation is calculated based on the description in Danish Standard 418 (DS, 2002). The two-dimensional heat flow is calculated using a numerical model of the construction including the surrounding area near the foundation – that is the floor construction and outer wall. This two-dimensional heat flow is then compared to the one-dimensional heat flows through floor and outer wall. The extra heat flow, which cannot be attributed to the one-dimensional heat flows, must consequently be the two-dimensional contribution from the foundation.

In spite of the simple description of the calculation procedure, the value of the linear thermal transmittance is in fact difficult to determine, because of the transient behaviour of the heat loss from the building through the floor which therefore requires the use of a transient calculation based on yearly variations of the outdoor climate.

χ-value

The corner thermal transmittance can equivalently to the linear thermal transmittance be found in a three-dimensional simulation model. Here both the one- and two-dimensional contributions to the total heat loss must be subtracted from the total heat flow before finding the χ-value. This is not elaborated further here.

Procedure based on EN ISO 13370

An alternative method based on EN ISO 13370 can also be applied. In this standard, the data can be characterised by a U_0-value (basic thermal transmittance), a U-value incorporating the entire heat flow between the indoor and outdoor environment and, L_s, which is a steady-state thermal coupling coefficient. Both U and L_s have correction terms for the foundation, which can be found from numerical models.

EN ISO 13370 contains a method for finding the average heat loss from the floor construction by adding the steady-state thermal coupling coefficient multiplied by the average temperature difference between interior and exterior and two correction terms including seasonal variations.

In an upcoming revision of EN ISO13370, four ways of calculating the heat transfer to the ground are given, where (1) is a full three-dimensional simulation giving the ground heat loss directly, (2) is a two-dimensional model using the characteristic dimension of the floor which will be defined in section 3.4.6, while (3) and (4) can be found from Eq. (3.7) as:

$$(U \cdot A)_{ground,tot} = U \cdot A + P \cdot \psi \quad \textbf{(3.7)}$$

The value of the linear thermal transmittance can either be calculated by a using a numerical method or by tabulated values based on e.g. national tables.

With floor heating

The methods above have no inclusion of floor heating in the calculation procedures. A practical approach is to use higher floor temperature to account for the fact that the floor is warmer in order to heat the building, when finding the heat loss through the ground. At the same time, only the thermal resistance from the level of the floor heating pipe and down should be considered.

However, it is obvious that especially the size of the linear thermal transmittance is influenced by the fact that the floor is heated, as there will be a much larger temperature difference than for buildings heated by other means than floor heating. In EN ISO 13370 this fact is included by using the average temperature at the pipe level instead of the room air temperature for the calculations of the heat loss. No method exists in DS418

3.4.3 Energy consumption

Several studies have focused on the energy consumption of houses with floor heating. As it will be shown, there are large discrepancies in the results from measured field data, laboratory tests and theoretical considerations.

Floor heating has been used in Danish houses to some extent for the past many years, and towards the end of the 1990'ies, floor heating was introduced as the main heating system in new Danish detached single-family houses on a large scale. A few years later, around 2000, the Danish District Heating Union (Danske Fjernvarmeværkers Forening) reported unexpectedly high energy consumption in these new houses with floor heating systems (VVS Danvak, 1999). This led to an investigation by Radisch (2001), comparing energy consumption in houses with and without floor heating. Here 34% higher energy consumption is reported when comparing newly built houses with floor heating to older houses with radiator heating. While it was established that the higher value could be assigned to a number of factors such as larger rooms, larger windows and changed user habits, the presence of floor heating was still found to increase the energy consumption by about 10%. A Swedish investigation from 1997 (Harrysson, 1997), concludes that floor heating led to an energy consumption that was at least 30% higher, compared to radiator heating. These two investigations therefore agree in their findings. Notice however, that Roots (2002) finds that a more reasonable conclusion in Harrysson (1997) would be that the results *indicate* that floor heating leads to higher energy consumption than radiator heating, since many other factors also contribute to the higher energy consumption.

This finding has of course been examined further because of the very surprising results. Therefore a second Danish investigation has been carried out on houses built between 2000 and 2002 based on field studies, questionnaires and theoretical considerations (Olsen and Christiansen, 2004). This investigation has not found the same difference in the heating demands. In fact, the energy consumption in houses with and without floor heating could not be distinguished. This indicates that a better design and construction of buildings with floor heating has been implemented in these newer buildings.

In a comparative study using a laboratory mock-up, Olesen (1994) has reported an extra energy consumption of less than 5% between all different heating systems under dynamic conditions. The mock-up was created as an office room with one outer wall with a window. The room was placed in a conditioned space with the same temperature as the room itself. A

similar result has been found in a German investigation, where a method for comparing different types of heating systems has been developed (Bauer, 1998).

In two theoretical studies (Roots and Hagentoft, 2002a; Hagentoft and Roots, 2001) an extra consumption of between 2% to 15% over radiator heating was found using a simple numerical simulation model incorporating a performance factor to account for the fact that the heat is not supplied to the room directly, but indirectly through the building construction.

Contrary to these investigations all showing larger or similar energy consumption using floor heating, manufacturers often claim that lower energy consumption can be expected. The argument is that since floor heating heats the room by radiation, a lower room air temperature is needed to maintain the same level of thermal comfort because the operative temperature will be larger at the same air temperature.

The ability for floor heating systems to use low temperatures is also pointed out to be a large advantage to the connected energy system (Boerstra et al, 2000), as the low temperatures mean that only a small amount of exergy is used. Exergy is defined as the "usable" energy from a given heat source. Therefore, more energy can be extracted from a given heat source as temperature close to the desired room temperature can be used, which is not the case for radiator heating.

3.4.4 Limiting criteria for practical use of floor heating

The maximum output of a floor heating system is limited by the heat exchange coefficient from surface to room and the maximum possible temperature difference from floor surface to room. The heat exchange coefficient is approximately 9-11W/m² K and the maximum possible temperature difference is around 7-9 K in a room which is heated to 20°C. The maximum heating capacity is therefore up to 100W/m² (175W/m² in peripheral areas where the maximum temperature difference between surface and room air is 15 K). This value is independent of floor covering material as the equation only considers the heat flux from surface to room. For wooden floors this value is only 60-70W/m² due to the lower maximum floor surface temperature.

In practise such high heat loads are not recommended, since this will make the floor heating system impossible to control. The relatively small heat exchange coefficient means that a large area must be available to supply enough heat to the room. Therefore, houses must have a large surface area that can be used for floor heating and must not have too large heating demand.

3.4.5 Thermal performance – modelling and testing

As previously mentioned, modern floor heating can be dated back to 1930's in the US (Olesen, 2002). In this period there is an understanding that insulation towards the ground and (especially) in the foundation is important to minimize the heat loss to the ground and that the thermal resistance between the floor heating plane and the room is important.

In recent years, Olesen (1994) undertakes an experimental investigation of the dynamic conditions of floor heating systems compared to radiator heating systems. Both heavy and light floor heating systems are included in the investigation. It is found that for a well insulated room, an acceptable thermal indoor climate can easily be maintained. A minor deviation of less than 5% in the energy consumption between all three systems is reported. In another experimental study (Sanchez-Romero and Alavedra-Ribot, 1996), different investigations show that the concrete thickness and conductivity as well as the placement of the pipe in the concrete are important for the reaction time and heat transfer rate.

Modelling requirements

To model floor heating systems correctly, the following requirements must be met:

- Detailed radiation exchange between internal surfaces (Achermann and Zweifel, 2003)
- Inclusion of distribution of solar radiation on internal surfaces (Athienitis and Chen, 2000)
- Inclusion of water loop if hydronic systems are modelled (Achermann and Zweifel, 2003)
- Control systems (See below in this section under 'Control strategies')
- Ground volume (See below in 3.4.6)

The difference between electrical and hydronic inclusion of the floor heating system has not been investigated in detail. However, it is a fact that hydronic systems cannot be as easily controlled as electrical systems. This approach of using electrical instead of hydronic inclusion of the pipe hence does not include the complex dynamics of hydronic floor heating system.

In an IEA Task 22 Report (Achermann and Zweifel, 2003), a method for validation of numerical simulation programs of radiant heating and cooling systems has been developed. Five different modelling tools are compared with respect to the "correctness" of the different programs. It is found, that the different programs give reasonable results, even if detailed calculations of the internal surface radiation exchange have not been included.

The basis for the above-mentioned IEA Task 22 report is the so-called BESTEST procedure (Judkoff and Neymark, 1995) which states procedures for testing building energy simulation programs. A special case of this is called RADTEST and states different procedures for the inclusion of radiant heating and cooling systems in building energy simulation programs (Achermann and Zweifel, 2003).

An example of how floor heating can be modelled in a simple way using a building energy simulation program has been described in Rose and Svendsen (2002), where the required power to heat the room was applied directly to the floor surface. While giving more realistic indoor thermal conditions, the thermal mass of the concrete layer and the hydronic system is not included. Up to date building energy simulation programs now have the possibility to apply the heat inside the construction, but generally floor heating is not easily included in building energy simulation tools. This of course comes from a need to make the models simple and fast, which is not always possible since it often requires many inputs (pipe placement, pipe spacing, supply temperature, internal resistances and perhaps more), while the numerical requirements of stability and low simulation time must also be met.

Dimensioning

Besides from the dimensioning described in EN1264 (CEN, 1997) and Nordtest VVS127 (Nordtest, 2001), both of which have been described in section 3.1, a number of papers have focused on dimensioning floor heating systems.

An alternative approach to characterise heavy floor heating systems has been shown in Comini and Nonino (1994). Instead of the approach used in EN1264 employing a power product of system factors, thermal resistances are used to characterise different types of floor heating systems as in Nordtest VVS127. This approach has been tested against measurements and finite element calculations.

Design tools for optimally design new and retrofit buildings with floor heating have also been presented (Kilkis and Coley, 1995; Kilkis and Sapci, 1995).

Modelling experiences

In Chen and Athienitis (1998), the effect of different floor covering materials is investigated. Here it was found that the floor covering had a major impact on temperature levels, reaction time and energy consumption. In all three cases the situation is worse with the introduction of a thick carpet in the room. This conclusion is also supported by another investigation (Seta et al, 1993), which explores different carpets on heated floors. It is found that thickness and thermal conductivity of the carpet is important for the heat flow; the higher the heat conductivity and the thinner the carpet the better. In Athienitis and Chen (2000), the authors investigated the dynamical performance of floor heating systems exposed to solar radiation. Common for both of these investigations is the use of an electrical floor heating system, which does not include the dynamical effect of the water in the floor heating pipes.

Ho et al. (1995) investigates the dynamical behaviour using experiments and numerical validation using a 2D model of the floor construction without foundation and ground volume. It is found, that both steady state heat flux and dynamic response of the system are reproducible by using this approach. A 2D model of a solar slab-on-grade floor heating system has also been investigated (Youcef, 1991). Here a solar collector is heating the floor heating system. A model of floor construction and foundation is used to find temperatures and heat flows in the ground. Good agreement is found between measured and simulated temperatures. However, the heat fluxes tend to be underestimated. This early work shows that it is possible to model the very complex dynamical combination of a flat plate solar collector and floor heating system in interaction with room and ground.

The effect of the thermal mass of the floor construction with respect to utilization of passive solar heat gains has been investigated (Athienitis, 1997). Generally it is found that the combination of passive solar energy and floor heating efficiently uses the solar gains to lower the energy consumption. A concrete slab of 10cm does not use the solar gains more efficiently than one of 5cm, while the 10cm slab resulted in higher temperature fluctuations than the 5cm slab.

Different types of floor heating systems have been compared (Weitzmann et al, 2002). In this investigation heavy and lightweight systems are compared with respect to the energy consumption. It is found that the use of the lightweight system in rooms with wooden floor coverings lead to 5% lower energy consumption than with heavy systems.

The dynamical behaviour of floor heating has been investigated by Fort in two pieces of work (Fort, 1989; Fort, 1993). Here experimental investigations are carried out to help design a dynamical simulation model. The models have coarse grid due to the limited computer power available at that time. It is found that both the floor and the walls influence the time constant of the room, and that the wall structure is more important than the type of floor heating system. The investigation finds that floor heating has the ability to be “self”-controlling, because of the low temperature differences in the room. This means that if for instance a heat source (e.g. solar radiation) is suddenly introduced in the room, the heat flux from the floor surface to the room will stop or even reverse, as the room temperature quickly rises above the floor temperature. Consequently, the lower the floor temperature the better the better the self-control of the floor heating system will be utilised. This model has, along with further development for hypocaust (and airborne) floor heating, been the basis for type 160 (Fort, 1999) used in TRNSYS.

An extra comment should be made to the term “self control”: Self control is the ability of the heating system to stop supplying heat to the room when the room temperature rises for instance due to solar heat gains. For a system to be self controlling, the temperatures in the

system must be low. A simple example can be used to illustrate this; if the floor surface temperature is 23°C and the room temperature is 20°C, the heat transfer will be 29W/m² (where the heat transfer coefficient is based on equation (3.2)). If the temperature in the room is raised to 21°C the heat transfer drops to 19W/m² - or 35%. Similarly a rise to 22°C will lower the heat transfer to 9W/m² - or 69%. Conversely, if a radiator has a surface temperature of 45°C, a 1 K change in the room temperature will not affect the heat transfer to nearly that extent.

This self control is a main advantage of floor heating systems used in houses with small energy demand, as the low over-temperature in the floor construction ensures that when there are solar gains, the heating system stops almost immediately to supply heat to the room.

Control strategies

The effect of different control strategies and control types has also been investigated in numerous publications. Here only a few are mentioned of a very large amount available.

Still in Fort (1989), different control strategies are tested and compared. It is found that choosing different control strategies dramatically changes the energy consumption. However, no general conclusions are made as to which control system is the optimal.

For an electrical floor heating system it is shown that proportional control performs better than an on/off control while an on/off control gives temperature cycling and risk of overheating (Athienitis and Chen, 1993). Further in the same source, a night setback contributed to energy savings, but the price was a 100% increase in peak heat load on cold days when the system was turned on in the morning.

IEA Annex 37 – concept of exergy

An important concept for systems such as the radiant heating and cooling systems is the concept of exergy. This has been investigated in IEA Annex 37 (http://www.vtt.fi/rte/projects/annex37/) with the title “Low Exergy Systems for Heating and Cooling of Buildings”. While energy cannot be used as it is stated by the second law of thermodynamics, exergy is popularly speaking the part of the energy which can be used. The concept of exergy has been described in Shukuya and Hammache (2002). The advantage concerning radiant heating and cooling systems is that they can use low temperatures for heating and high temperatures for cooling. This makes building integrated heating and cooling systems low exergy systems. This means that a heat sink at a given temperature can be more efficiently used to heat or cool the building. In practice this also means that heat sources which are close to the desired room temperature can be used.

Literature review reports

Finally for completeness, two excellent reports containing literature reviews of floor heating systems and their applications should be mentioned. (Persson, 2000; Roots, 2002). In both of these, a number of papers and reports, which are not described here, have been reviewed.

3.4.6 Ground coupling

So far the referred work has, with a few exceptions, focused on the heat transfer to the room from a plane in the floor where the heating system is placed. If even considered, a very simple model for the heat transfer to the ground is assumed. E.g. in EN1264 (CEN, 1997), the heat loss to the ground is simply assumed to be 10% of the heat supply to the room above. In typical building energy simulation programs a fixed temperature and ground thermal

resistance is defined. Therefore, the dynamical behaviour of the ground heat loss is not very well known for single-family houses with floor heating. Especially the influence of the foundation must be better investigated. This is of interest since the importance of ground coupling and foundation is expected to be greater when floor heating is used. This is also the case since the ground heat loss is becoming increasingly more important as the above ground parts of the building are getting still better insulated (Claesson et al., 1991). The effect of heat transfer to the ground through the floor construction and foundation is the subject of another research field called earth- or ground-coupling (Deru et al., 2003; Adjali et al., 2000a; Thomas et al., 1996; Davies et al., 1995; Anderson, 1991; Hagentoft, 1988), which deals with the heat loss through the floor construction to the ground. This subject has proven difficult, as it requires a large number of parameters to be included in the calculation models.

The following considerations must be made with respect to ground coupling calculations:

- Numerical procedure: A 2D or 3D model quickly becomes complex and time demanding for simulations. Therefore simulation models are most likely unusable for practical purposes (Deru et al., 2003). However, using ground-coupling normally requires multidimensional analyses. The importance of using 2D or 3D analysis has been investigated in a case without floor heating (Davies et al., 1995). Here it is reported that using a 1D rather than a 2D or 3D model gives a difference in the energy flow of 22% between the 2D and 3D simulations and 41% between the 1D and 3D simulation models. So obviously the inclusion of foundation has a large effect on the results from the simulations.
- Ground properties: A lot of factors influence the thermal properties of the ground volume (Janssen et. al, 2002a; Janssen et. al, 2002b; Farouki, 1986). Temperature, amount of rain, moisture content and composition and type of ground material all affect the heat transfer and temperature level in the ground volume. I.e. the heat transfer coefficient of soil varies by a factor 10 depending on moisture levels and composition (Janssen et al, 2002a).
- Boundary conditions: Again a number of factors are important. Air and sky temperatures, ground surface covering, precipitation, snow covering, solar radiation and wind (Deru et al., 2003).
- The actual geometry of the floor construction and foundation also has a large influence on the conditions in the ground volume and consequently also the heat loss to the ground.
- Such factors as other buildings and vegetation also have an impact on the conditions.

The implications of these points are discussed in the following sections.

Multidimensional analyses

As mentioned above it has been found that using one-, two- or three-dimensional models for calculating the heat loss to the ground gives very different results. In other studies investigating the difference between one-, two-, and three-dimensional analyses (Adjali et al., 2000b; Anderson, 1991; Hagentoft, 1988), it is generally found that ground heat loss is a three-dimensional process. Anderson (1991) finds that by introducing a characteristic dimension of the floor defined as the floor area divided by half the exposed perimeter instead of the width of the building, the three-dimensional problem can be simplified to a two-dimension one. This means that a square building will have a characteristic dimension equal to half the side length and an infinitely long building will have a characteristic length of the width of the floor. A typical Danish single-family house is around 8 m wide times 16 m long, which corresponds to a characteristic dimension of 5.3 m.

Notice that while the characteristic dimension has proven useful for reducing a three-dimensional situation to a two-dimensional one, this has not been tested for floors with floor heating.

Adjali et al. (2000b) shows that large floors can be considered two-dimensional but near corners a three-dimensional calculation is needed to accurately account for the heat flows.

An investigation of the influence of the ratio of the floor surface area (A) to the perimeter (P) on the heat loss to the ground is presented (Bahnfleth and Pedersen, 1990). The work aims at producing a design procedure for estimating the total heat loss from the building during a whole year. Here it is assumed that the total heat flow can be approximated by adding two terms; a constant term and a fluctuating term. Building sizes of 12 x12 m to 60 x 60 m are examined. It is found that the fluctuating heat loss is proportional to $(A/P)^{-d}$. The factor, d, is a factor which depends on soil properties, insulation and climate. The annual average heat loss can be found from $q = c \cdot (A/P)^{-d}$. This means that the heat loss from the building can be found by only taking the area and perimeter into account, while neglecting the influence from the corners of the building.

A standard for calculating the heat loss to the ground has also been established in EN ISO13370 (CEN, 1998c), where the width of the floor construction is required to be at least as large as the characteristic dimension. The basis for heat losses through building components has been described in EN ISO10211.1 (CEN, 1994) and EN ISO10211.2 (CEN, 1995). Here the total heat loss can be summed by one-, two- and three-dimensional contributions. For a floor construction this corresponds to the slab, the foundation and the corners of the building. In Delasante (1991) and Hagentoft (1988) it is found that the heat loss through the slab and foundation must be found by transient analysis while the heat loss through the corners can be found from steady state analysis.

Adjali et al (2000b) investigates a heated ground floor slab in a large building structure by comparing measurements and numerical modelling using three-dimensional modelling. It is concluded that, while good results are obtained when comparing the results of the simulation to the measurements, the calculation speed is not acceptable. Youcef (1991) examines a two-dimensional model of a slab-on-grade floor with solar heated floor compared to measurements. Good agreement was found between measured and simulated values, though for a relatively short measurement period. However, the investigation was performed for a slab that was only insulated at the edge of the building, which is not the case in modern buildings in Northern latitudes.

To ensure undisturbed conditions from the “far-field” of the model it is recommended in EN ISO 13370 that the ground volume should be extended to a minimum of 2.5 times the characteristic dimension of the building downward and outward from the floor construction, where adiabatic boundaries are assumed to the sides and below. The width of the floor construction should be at least 0.5 times the characteristic dimension. By making sure that these minimum requirements for the dimensions are used for the simulation model, it will be sufficient to perform two-dimensional simulations and omitting the influence of the corners. While this is true for the analysis of heat transfer for the entire building, this approach is of course not applicable to assess the risk of moisture damage, because the temperature in the corner of the buildings will naturally become lower than it is along the edge.

Boundary conditions

The outside boundary condition depends, among others, on the incident radiation, snow, wind, evaporation and rain (Janssen et al, 2004; Deru et al, 2003; Adjali et al, 200b;

Hagentoft, 1988). A comparison of using very detailed boundary conditions including all of the factors above and simple convective conditions has been investigated (Janssen et al, 2004). Here it is found that while the average temperature during the year is the same for the two different models, the amplitude of the temperature in the ground volume, especially close to the ground surface, will be very different, with much larger amplitudes in the detailed models. The temperature amplitude will be larger down into the ground volume for the coupled model than for the uncoupled model. However, the difference in the amplitude quickly decreases with increased depth.

Another investigation (Bahnfleth and Pedersen, 1990) has looked at the evaporation from the ground surface, which can vary depending on the moisture conditions in ground and air. This is especially important in dry and hot climates, but not a factor in temperate climates.

Towards the bottom of the ground volume either an adiabatic boundary or a fixed temperature from the groundwater level can be used. Typically, the differences between the two are small since the heat flow to the bottom will be small in case of a fixed temperature (Janssen, 2002).

To the sides of the ground volume, adiabatic boundary conditions are used.

Effect of coupling heat and moisture transfer

Janssen et al (2002) performs a theoretical study of a fully coupled simulation model considering heat transfer, moisture and boundary conditions. It is concluded, that a fully coupled model does give significantly different results than a model with constant material properties. However, it is also acknowledged that considering the uncertainties in material properties, the simplification of not using a fully coupled model can be justified. This point is further elaborated in a later work by the same authors (Janssen et al., 2004), where it is found that a model without coupling between heat and moisture underestimates the heat loss from the construction by around 15%. However, this difference decreases with increased insulation thickness. The comparison is made for a basement construction – if instead a slab-on-grade floor is used – the difference is also smaller. Therefore, a better insulation standard decreases the need for using coupled models.

Moisture in the concrete slab

Especially concerning floor heating, there is a concern that moisture migration into the floor construction can occur when the heating system is turned off in the spring. This moisture migration can occur if the ground volume is warmer than the concrete slab. A Swedish investigation (Roots and Sandberg, 2001) did not find any general risks of “reverse” diffusion. Mineral wool gave higher moisture content in the concrete slab than expanded polystyrene (EPS), but in all cases the average direction of the diffusion was downwards, indicating a drying out of the slab. However, under different climatic conditions or ground compositions investigations may be required to minimize risks of moisture migration.

Ground coupling and building energy simulation programs

A ground-coupled model has also been attached to a building energy simulation program (Deru et al., 2003). The three-dimensional model created here was compared to other building energy simulation programs to investigate the accuracy of the models. The investigation aims at improving the existing ground-coupling models used in building energy simulation programs. It is found that the models yield a large variation in heating loads, which are both larger and smaller than the result found using the three-dimensional ground-coupled model. The comparison is based on the BESTEST procedure. It is concluded that the ground-coupling used in the simple cases has the correct order of magnitude. It is acknowledged that

the three-dimensional models are difficult and time consuming, but the calculations can be used to find correction factors for implementations into simpler programs.

Modelling approach

Different approaches can be used to model the heat flow in the ground volume. The most detailed (and time consuming) approaches are achieved by using numerical models based on finite element, finite difference or finite control volume methods. Once the method is implemented, it is simple to create an accurate geometric model with detailed boundary conditions and consequent parametric analysis. Other methods for solving the linear systems (which heat transfer in the ground with constant material properties represents) using eigenvalues or response factor methods (Lefebvre, 1997; Davies et al., 2001; Pan and Pal, 1995; Hsieh and Hwang, 1989; Ménézo et al, 2002) are used to reduce the simulation time considerably compared to numerical implementations. The reduction in simulation time is achieved as they are based on (semi)-analytical methods, which require approximating the actual geometry either by finding the eigenvalues or response factors using a numerical pre-processing, which often requires simplifications that are not needed for numerical methods. These models are normally steady-state or periodic stationary.

3.4.7 Conclusion on literature review on floor heating

In this literature review the present state of knowledge concerning modelling of mainly hydronic floor heating has been described.

The literature survey has found that the ground heat loss from buildings with floor heating has only been scarcely investigated. The dynamical behavior of the floor heating systems has also not been investigated in detail with respect to finding the heat loss to the ground in the literature. To correctly finding the dynamical behavior, it is necessary to couple the model of the floor with the floor heating system to a room model with dynamical heat loads and energy demands. There is therefore a need for developing detailed models of floor constructions with floor heating, where such factors as insulation thickness and level of insulation in the foundation can be investigated in dynamical calculations to find the heat loss to the ground in a model where the interaction with the rest of the building is also included.

At the same time, the difference between simulation models of floors with floor heating with different level of detail has not been investigated. In fact, there is a large discrepancy between the results and implementation between the often very detailed models used in the presented literature and the models used in the energy simulation programs that are often very simple. However, this difference has not been investigated in similar setups. Therefore there is a need to compare detailed and simple models.

3.5 Thermo active cooling systems

Where floor heating systems are generally used in domestic buildings, thermo active cooling systems are mainly used in office buildings where there is typically a need to cool the building. Where floor heating systems have been subject to many investigations, the newer concept of thermo active components has been described more scarcely.

Notice that much of the description from the previous section on floor heating also applies to thermo active components.

In the late 1970s and throughout the 1980s, Sweden and Denmark made experiments with systems called TermoDeck (Strängbetong, 1987; Andersson and Isfält, 1978) and Termoton (Byberg et al, 1989) both with air circulation in hollow concrete decks. The concept being that

the ventilation air was first circulated through the thermal mass of the concrete before ventilating the room. In the summer time the building can be cooled by cool night air, thereby enabling storage in the concrete deck of the excess heat during the daytime. During winter periods excess heat from the daytime will be stored in the construction and re-emitted to the room during the night. Here the system will also ensure that the ventilation air to the building will be preheated before entering the offices. In both systems good results with low energy consumption were achieved in test buildings. These concepts gave promising results, with large energy savings especially for heating. However, today these systems are not used to a large extent in office buildings. Perhaps a reason is a focus on heating, which is not the main issue in today's office buildings due to higher heat load coming from computers and increased glazed area. Another reason could be the fact that it requires a large amount of electric power to run the ventilation of the air in the system. Finally, cleaning the air ducts has proven difficult. The TermoDeck system has been investigated further (Barton et al., 2002), but again with focus on heating.

In 1986 a new energy law was passed in Zurich, Switzerland which required energy conservation to be taken into account when erecting new buildings while only allowing compressor cooling in special cases (Meierhans, 1993). The problem as it is stated here is that the peak load in the cooling system is at the same time as the outdoor temperature is at the highest. As for airborne systems, the concrete mass of the building can be used to shift the time when cooling is needed and the time when the cooling is available to not coincide. This paper contains the first description of an office building where the thermal mass in the building is used to actively cool the rooms by pipes embedded in the concrete slabs between the storeys of the building. It is also shown that the system works very well to cool the building even during very hot days and periods. Thermo active components have been investigated in many later works; a few are mentioned here (De Carli and Olesen, 2002; Meierhans and Olesen, 2002; Meierhans, 1996). These papers include descriptions of actual buildings and measurements of their thermal behaviour and energy use.

3.5.1 Applications

Thermo active components are thermally heavy building components with embedded pipes for circulation of water or ducts for circulation of air. The systems can be embedded in walls, ceilings, floors or in floors betweens storeys in multi-storey buildings. The main focus in this thesis is embedded pipes in floors in multi-storey buildings. The components used in thermo active components are very much the same as for floor heating systems and the same basic considerations as for floor heating still apply with respect to thermal properties, layout of the pipes, controllability and building materials.

The actual thermal properties of the constructions are decided by such parameters as the vertical distance of the pipes to the surfaces, pipe distance, floor and ceiling covering, layout of pipes/ducts and flow.

Airborne systems

Airborne systems use cavities in the concrete to circulate air to heat or cool the thermal mass of the concrete. The system has been used mainly in office buildings in the 1980's, but still today they are used. The circulated air is often used also as supply air to the room, as it will have a comfortable temperature once it has passed through the concrete core, regardless if it is being used to heat or cool the concrete.

Figure 3.4 shows an example of a thermo active deck where the cavities in the hollow deck can be used for circulation of the ventilation air. Notice, that the decks must be constructed in

such a way that the cavities are connected to get air through the floor construction and to create a large surface between the air flow and the concrete core.

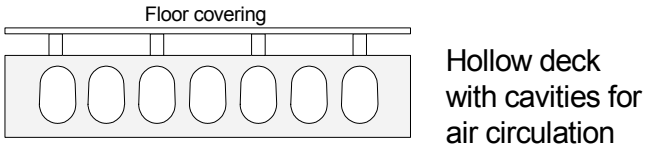

Figure 3.4 Floor with cavities used for circulation of (ventilation) air

In situ constructed systems

Figure 3.5 shows the type of thermo active component which is typically used in buildings in Central Europe where the system is installed. The pipes are normally placed in the lower half of the deck towards the ceiling surface. Between the concrete and the floor surface there might be a layer of insulation to ensure that the heat flows in the construction will be directed downwards and prevent noise distribution between the storeys. The vertical placement of the pipes is ensured by fixating to or hanging from the reinforcement in the deck.

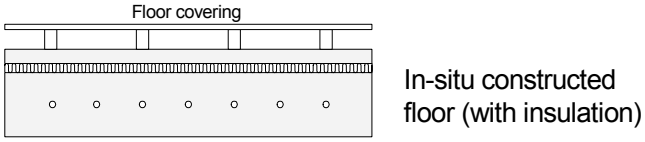

Figure 3.5 In-situ constructed thermo active component, here shown with an insulation layer

Prefabricated hollow deck concrete elements

Figure 3.6 shows a prefabricated hollow deck floor with embedded pipes. This type is based on the Danish building tradition of using prefabricated hollow deck floors. The pipes are placed fairly close to the ceiling surface as they, because of the fabrication process, must be fitted below the cavities.

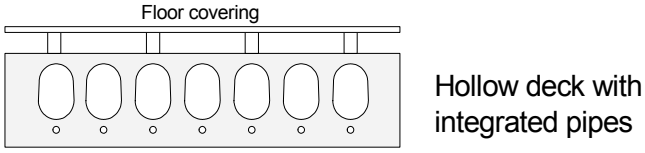

Figure 3.6 Prefabricated hollow deck thermo active component with embedded pipes

This system is investigated further in this thesis with measurements in a test setup, which will be described in Chapter 6, where a more thorough description of the deck will also be presented.

Other types

As indicated above, there are a lot of different applications of thermo active components. They can, besides from being installed between storeys, also be placed in ceilings, floors and walls. Different types can be combined in the same thermo active component, i.e. air and hydronic systems, or a building can be equipped with i.e. ceiling and wall cooling.

3.5.2 Functionality

Heat transfer between room and thermo active component

Like floor heating, thermo active components have a large radiative part in the heat transfer between surface and room, which can be seen by comparing the radiative and convective

transfer coefficients. For radiation this value is approximately 5.5W/m² K in rooms under "normal" cooling conditions, while the convective coefficient is between 3 and 5.5W/m² K. Therefore the radiative part is larger than half the total heat exchange.

The larger part of the heat transfer from the rooms above and below the deck to the concrete core will, for cooling, be through the ceiling surface. The distribution is found to be 2/3 through the ceiling and 1/3 through the floor (Koschenz and Lehmann, 2000). Another report (Hansen et al., 2002) finds that 85% of the heat transfer is through the ceiling surface. As it can be seen, the actual distribution depends greatly on the actual configuration of the deck construction with respect to floor covering and i.e. acoustic ceilings.

Dynamic behavior

The dynamic behavior has been investigated by various authors (Meierhans, 1993; Olesen, 2000). A main result from these investigations is the realisation that the room temperature is not going to be stable during the day but will rise from morning to evening.

This has been illustrated very well by a simple example (Olesen, 2000). Here the entire building (room and thermal mass) is in thermal equilibrium 20°C at the start of a working day. During the next 12 hours the room is supplied with a heat load of 90W/m². After 12 hours the heat load is set to 0W/m². Without any cooling, the room air temperature rises to around 28°C and the operative temperature 26°C during the working day. The next morning the temperature in the building has risen to about 21.5°C. This is the case for both room air and concrete slab. If instead cooling in the concrete slab is activated using a water temperature of 20°C, the room air and operative temperatures will still rise to a level which is almost as high. However, during the night, the building will be cooled to 20°C again. Further, if cooling in the slab is only activated during the night time, the result will be almost the same as with 24 hours operation.

The following points can be summed up from this simple example:

- Buildings with thermo active components cannot be expected to keep a fixed temperature. Rather it will drift during the day.
- Thermo active components can be used to keep the building cool during warm periods where the entire building is cooled down during the day to avoid a progressive heating of the building core from day to day, which will eventually lead to unacceptable temperatures.
- Applying cooling only during the night time gives almost the same result as continuous operation. This is because there will be a larger temperature difference between the fluid in the pipe and the concrete, and therefore a larger heat transfer between deck and fluid.
- The temperature of the cooling water can be close to desired room temperature.
- A very important final point can also be seen from this. As the system, due to the thermal mass, can cool the building during all 24 hours of the day, the cooling system does not have to be designed to cool equivalent to the maximum heat load in the room. Instead it is sufficient to have a system that can meet the average heat load during the day. This will lead to much smaller cooling machines. Another advantage, in areas with lower prices of electricity during the night, is that the main need for electricity for the pumps can be shifted to the night, resulting in lower electricity costs.

Ventilation

Using thermo active components effectively reduces the requirements of the ventilation system. This means that there is only a need to supply fresh air with much lower air change rates than what is needed by mechanical cooling systems, since these require recirculation. If extra cooling is required, the inlet air can be cooled slightly to provide this extra cooling during peak loads.

Night cooling

An alternative to using building integrated cooling system, and still avoid the use of mechanical ventilation systems, is to use night cooling of the building by using cool outside air directly in the room by opening of windows in the building. This method is used in climates where the night temperature rarely exceeds 15°C-16°C, which is the case for the Danish climate. Two independent investigations of British office buildings (Olsen and Chen, 2003; Kolokotroni and Aronis, 1999) both find considerable saving potentials for night cooling of the building. This therefore represents a simple way to cool the building by flushing it with cool outside air during the night time, which will cool the thermal mass of the building in the same way as the building integrated systems. In both cases, it is also found that it is necessary to have access to the thermal mass of the building, which is also the case for building integrated systems, as it will be described below. Normally, night cooling is a control strategy which is imposed in naturally ventilated buildings. An obvious drawback to night ventilation is that in many buildings opening the windows during the night is not possible due to risk of burglaries.

No references have been found in the literature comparing the cooling capacity of these systems.

3.5.3 Thermal properties – modelling and measurements

Probably the first paper describing the use of embedded pipes in office buildings for heating and cooling the building was Meierhans (1993). Two buildings were described; an office building in Horgen, Switzerland and an art museum in Bregenz, Austria. Results in the form of measurements and simulations are presented only for the office building. It is shown here that the system is able to keep the temperature at an acceptable temperature even during very hot outdoor conditions.

The fact that this paper showed that it was possible to build office buildings with thermo active components led the way to an interest in this technology.

Measurements

The building presented in Meierhans (1993) has also been subject to measurements on the thermal behaviour (Meierhans, 1996), where three identical rooms in the building were tested. The first with a high internal heat load of 52.5W/m², ventilation through operable windows and no cooling, the second with the same heat load, mechanical ventilation and cooling from the concrete core, and the third with a heat load of 17.5W/m², mechanical ventilation and cooling from the concrete core. It is shown that even during very hot outdoor temperatures (up to 35°C) the temperature can normally be kept below the upper comfort temperature using cooling from the concrete core.

A very thorough investigation of field measurements in four buildings has been conducted and presented (De Carli and Olesen, 2002). These four buildings are equipped with combinations of radiant heating and cooling panels embedded in walls, ceilings, floors and

between storeys. A general conclusion is that the buildings can easily maintain temperatures below 26°C for nearly all of the working hours and never goes above 27°C even for outdoor temperatures exceeding 30°C, which is very satisfying. Further, the temperature increase during the day is reported for the four buildings. Generally, the increase is less than 5K for three of the buildings and for the fourth the increase is less than 6K for 95% of the time. If Class B from Table 3.1 is to be followed, the increase should be less than 4K during the working hours, while assuming the temperature in the morning is 20°C (lower comfort temperature). This is met in two of the buildings for nearly all the working days, while in the other two buildings this is the case for 75% and 85% of the working days. Again this result is acceptable, but it clearly illustrates the difficulty in maintaining the temperature in the ranges defined by CR 1752 (CEN, 1998a) if less than 10% dissatisfied are allowed. Actually, the fact that the temperature range must be fully used can be seen since low temperatures in the buildings are reported as problems in the morning hours of the day as the building core may be cooled too much during the night. It is however stated that no evaluation of the thermal comfort has been carried out, so it is not clear whether these low temperatures will cause thermal discomfort. It should be stressed that there are no problems maintaining comfortable temperatures in all the buildings for a very large fraction of the time even with high outdoor temperatures. Unfortunately, the supply temperatures to the thermo active constructions in the buildings are not described in detail. A final point to this is that apparently most of the measurements have been performed before fine tuning the control system and therefore the systems can be expected to perform better after this fine tuning has been completed.

The German Fraunhofter Institut für Bauphysik are presently in the design process of a VERU test facility[2] for energetic and indoor climate tests to test under real weather conditions. This is a full-size house where the functionality of different energy saving building components can be investigated under controlled conditions. Among others, thermo active components will be tested in this setup. No results are yet available; however such results will be interesting, especially concerning verification of simulation models.

Another full-size test facility has been built in Zentrum für Umweltbewusstes Bauen in Kassel, Germany[3]. This facility is equipped with thermo active components. Measurements from this setup have been used by Schmidt (2004) as part of a PhD thesis. This will be described in details in the next section.

Modelling

Similarly to floor heating systems, the models described in the literature have different approaches and levels of details. As far as the interaction with the rooms above and below the thermo active component the same requirements exist. These have been discussed in section 3.4.5 under ‘Modelling requirements’.

Here the different approaches to modelling of thermo active component will be discussed. Only dynamical models are considered. The modelling can be either through analytical solutions, thermal networks (RC-networks with resistance-capacitance), finite difference schemes or finite element schemes in one, two or three dimensions or as equivalent networks. Here only a few are mentioned.

An example of the use of RC-networks can be found in Stetiu (1998). The method uses a two-dimensional thermal network with a grid of 3x5 or 5x5 points and the pipe as another point.

[2] See www.bauphysik.de/veru for further information.
[3] See www.zub-kassel.de for further information

The model includes detailed radiation exchange between inner surfaces in the room model and has an implementation of the water pipe with fluid temperature instead of adding or removing heat through a heat flux term.

In Koschenz and Lehmann (2000) a different approach is used for the modelling. Here the heat transfer is reduced to three equivalent resistances in a thermal network model, one between the lower surface and the concrete core, one between the upper surface and the concrete core, and one between the pipe and the concrete core. The equivalent resistances are found from a complex set of equations, which among others includes pipe material resistance and heat transfer coefficient from fluid to pipe surface. Especially the cooling of the fluid in the length direction of the pipe is given special attention. The implementation of the model is compared to simulations using a finite element model. The TABS model –for Thermoactive Bauteilsysteme – is included in Type 56 of TRNSYS 15 (Beckman, 2000).

A single paper presenting a three-dimensional implementation of a ceiling with embedded pipes has been published (Antonopoulos and Tzivanidis, 1997). Using this method has been found to give more accurate results than using one- or two-dimensional models. However, it is also recognized that this implementation is very complex and time consuming.

Two theses from 2004 (Weber, 2004; Schmidt, 2004) focus on the energy performance in buildings and low exergy design. The concept of exergy has been described above in connection to IEA Annex 37 on page 29. Special attention is placed on thermally activated building components – or thermo active components as they are called in this thesis. The reason for the focus on thermo active components is that they due to their low temperature heating and high temperature cooling have low exergy use. Obviously, since e.g. the temperature for cooling can be as high as perhaps 18°C, it can use a source at say 10 °C more efficiently than if 13 °C is required. Therefore, building integrated heating and cooling systems have been found to be a step towards lower energy and exergy consumption. Both theses are based on using simplified thermal network models for the modelling of the thermal conditions in the buildings. E.g. Weber (2004) uses different RC thermal network models that are verified against FEM solutions of the same problem. The models that are introduced are a further development of the work described above (Koschenz and Lehmann, 2000). The aim is to check the validity of the models for different operating conditions.

The parameters in the RC thermal network models are optimized based on frequency domain analysis based on simulations in a FEM model of the problem. See for instance Paper VI in Weber (2004). This so-called ω-RC method, where ω indicates that the frequency is included, is based on an accurate solution in the FEM mode to find the parameters used by the RC model, which can then be used – within certain limits especially concerning geometry – for fast solution of the problem. Therefore using this approach, it is possible to do multiple simulations of different parameters within certain limits defined by the geometry, which makes it ideal for inclusion in building energy simulations such as the TABS model used in TRNSYS. However, for a model where the detailed geometry is important (and often changed) for instance as part of a product development, a numerical model is preferable since the conversion from numerical model to thermal network model is not needed.

Control and control strategies

Controlling the temperature in buildings with thermo active components is difficult since the thermal mass in the concrete core is so large. As described previously it is not possible to control the temperature to a fixed set point, but rather keep the temperature within an interval. Further, it is also not possible to have individual temperature control in single rooms in the building. In practice, the building is divided into a few zones, for instance a zone for each of

the facades in the building (i.e. Olesen, 2002). Due to the small temperature differences, the system will have a large degree of self control, which means that even small changes in the temperature of the room will give large changes in the heat fluxes between the heated or cooled surface and the room. One very important limit in the systems is the lowest allowed supply temperature to the system. This is equal to the dew point temperature in order to avoid condensation, which therefore limits the cooling power of the system. However, if a mechanical ventilation system is available, the dew point temperature can be controlled by dehumidification of the inlet air. A point often mentioned in the literature is the fact that the system needs fine tuning after the building during the first year(s) of operation. This is again due to the close interaction between the large thermal mass and the room air and the long time constants in the system.

In the list below a few examples of controls and control strategies that have been described in the literature are mentioned (Meierhans, 1993; Meierhans, 1996; Olesen, 2002):

- 24 hours operation with a constant supply temperature
- Control of the average temperature to a constant value
- System on during the night and off during the day
- Shorter on/off periods during the day (intermittent operation)
- The pump is stopped when the temperature is 22°C ± 1°C
- Control of the supply or average water temperature based on the outside temperature
- Off during weekends
- Other means of controlling the temperature in the rooms are naturally also used, i.e. activating solar shading systems to lower the solar income.

Large differences in the energy demand for both heating, cooling and pump power can be observed for the different control strategies.

3.5.4 Limitations

One very obvious limitation to building integrated heating and cooling systems, especially those using the ceiling surface to interact with the room, is the fact that while the thermo active construction needs free concrete surfaces to efficiently cool the room, the need for noise control dictates acoustic ceilings which are thermally insulating. The need for acoustic ceilings is large in open plan offices, which are the types of offices that are normally built today. However, there are no descriptions in literature of how to solve acoustic problems. Often it is stated that since there is no lowered ceiling, the acoustics must be solved otherwise.

Another limitation is that the type of work performed in the buildings can prevent the use of thermo active constructions; For instance if stable temperatures are required or if the building has very high heat loads. In these cases, an air conditioning system is required.

Limitations to the cooling capacity can be determined by the minimum allowed supply temperature to the room, which is given by the dew-point temperature and the fact that the building surfaces should not be cooled to such a temperature that it will cause thermal discomfort. Assuming that the heat transfer coefficient for cooling is around 11W/m² K from the ceiling surface and the lowest surface temperature is 17°C, a cooling capacity of 99W/m² is available if the room temperature is 26°C. The cooling through the floor surface is not included here, but it will further increase the cooling capacity, but at the same time limit the capacity as the floor surface temperature is limited to 19°C. However, the value of 99W/m²

requires that the thermal mass of the thermo active construction is cooled down to a low temperature, which in practise means that the system cannot be controlled. Instead it is recommended that the heat load in the room should be less than 50W/m² (Olesen, 2001).

During the winter period the thermo active constructions can also be used for heating. However, as the systems are designed for cooling, the main part of the heating will be through the ceiling surface as the floor surface will have a floor covering with a large resistance (as it will be used for cabling and other installations). For heating through the ceiling surface, the heat transfer coefficient is around 6W/m² K and the maximum allowed surface temperature is around 27°C for comfort reasons. This will give a heating capacity of 42W/m². Again a somewhat lower limit is recommended; in this case no more than 20-30W/m² (Olesen, 2001).

3.5.5 Conclusion on literature review of thermo active components

Thermo active components represent a novel way to get cooling in office buildings if air conditioning is not an option or simply not wanted. Because of the large thermal mass, designers must abandon the idea of being able to accurately control the temperature in the building. Instead the designer has to use different means to control the temperature in a desired range of temperatures.

Compared to investigations on floor heating systems, thermo active components have been scrutinized for a much shorter period of time. Yet, as the physical processes are very much alike those found in floor heating systems, thermo active components can be seen simply as a natural extension to those used in floor heating systems, perhaps even with the simplification that the complex ground heat loss is not a factor that needs to be taken into account. And like floor heating, there are only a few possibilities in existing commercially available simulation programs to include thermo active components. However, this will probably change in the near future, as the interest in floor heating and thermo active components is still expected to rise.

Typically, thermo active components are made in buildings where the concrete is cast in-situ. The Danish building tradition normally uses pre-cast hollow deck concrete elements. Therefore it needs to be proven that pre-cast elements can also be used for thermo active purposes. This will be done through the use of experimental setup, which will be used for measuring the actual cooling capacity of the pre-cast concrete deck. Besides from being used directly for finding the cooling capacity, the measurements in this experimental setup will also be used for validation of the simulation model of the thermo active component and room model.

3.6 Thermal energy storage in floor construction

A special case of floor heating is the use of thermal energy storage in the floor construction of a single-family house, which is investigated to test whether the concrete in the floor construction can be used to store energy from solar panels in a house, which is also equipped with floor heating.

This is based on:

- Lower energy consumption is a direct goal of the EU directive on the energy performance of buildings (European Parliament, 2003). Thermal energy storage of active solar heating system will result in increased energy savings in buildings, which is important to comply with the Kyoto Protocol.
- The normal practise of decreasing the energy consumption by increasing insulation thickness, using low energy windows and heat recovery units in the ventilation system is

only economically viable to a certain point. Especially for the outer walls simply using more insulation is becoming difficult and expensive, resulting in architectonic and economic problems. Architectonic because of the appearance of the thick walls and economic because the increased wall thickness requires a more expensive type of foundation. Therefore just adding extra insulation to the building envelope may not be the cheapest way to reduce the heating demand. (Munch-Andersen et al., 2000).

- If a solar domestic hot water system is installed in a house, it will be relatively cheap to install extra capacity in the system which can be used for heating purposes.
- The thermal mass in the floor construction represents a cheap way to store energy with an integrated heating system.

Using solar energy to lower the energy consumption in houses can be both passive and active. Passive systems simply use the solar energy that is transmitted through windows. This greatly impacts the energy performance (Nielsen et al, 2001). In active systems the energy from a solar collector is used directly in the heating system or by storing the heat in the building construction, thereby indirectly heating the building. This heat storage can be with or without the use of phase change materials, as reported in Lee et al. (2000).

3.7 Integrated heating and cooling in building energy simulations

The previous sections have described investigations on building integrated heating and cooling systems based on a mix of measurements and simulations. For these investigations different kinds of simulation programs based on numerical or analytical models have been used. However, most of the models that have been based on "homemade" programs specifically designed for the actual analysis, which is incidentally also the case in the work in this thesis.

In the sections 3.4.5 and 3.5.3 requirements of simulation models have been described for floor heating and thermo active components respectively. These include among others the ability to model the mainly radiant behavior of the system and a correct implementation of the pipe.

In this section the possibilities of modelling building integrated hydronic heating and cooling systems in commercial simulation programs will be described to give a brief overview of the availability of such models.

Notice that this section is kept very brief due to the fact that there is a continuous and quick development of the simulation models, which means that the contents of this section will be quickly outdated. Further, only a few programs are mentioned here, also a consequence of this development.

3.7.1 Implementations

A number of simulation commercially available programs exist in which it is possible to simulate floor heating and thermo active components.

The implementations used for building integrated system are often very simple with an "electrical" inclusion of the heating/cooling system, where a heat flux rather than a temperature is used as the pipe. This approach is used in ESP-r[4] in the current version of the

[4] See http://www.esru.strath.ac.uk/ for further information

program and BSIM2002[5]. Concerning ESP-r, a new model is in the test phase, where a hydronic system is included.

As previously mentioned, TRNSYS, which is a modular simulation program has models for both floor heating systems and thermo active components. Type 56 is a model of thermo active components called TABS (Koschenz and Lehmann, 2000). This is a semi-analytical simulation model where the pipe with fluid is implemented to give correct conditions in the construction. Type 160 (Fort, 1999) contains a model based on a finite difference implementation of a floor heating system which can also be used for thermo active components. In the model, only few nodal points can be used. Both types model the fluid temperature correctly.

A very promising building energy simulation program, which can also be used to model building integrated systems, is EnergyPlus[6]. A few examples are given in papers on implementation of low temperature radiant systems (Strand and Pedersen, 2002). However, at the time of this thesis there is no user interfaces available, so the program is very much an expert tool. This can of course change quickly with the introduction of a well-designed user interface.

3.7.2 Conclusion on the use of simulation approaches

Typical simulation models are either expert tools, as the ones described in the sections above, or as described in this section fairly simple models typically with electrical inclusion of the system

[5] See http://www.dbur.dk/english/publishing/software/bsim/index.htm for further information
[6] See http://www.eere.energy.gov/buildings/energyplus/ for further information

4 Modelling building integrated heating and cooling

This chapter describes the simulation programs used in this thesis. A thorough description of the numerical models used in the thesis can be found in Appendix A. Therefore, this chapter only outlines the implemented models, the possibilities of the use of the models as well as the implications of using them for the analyses in the thesis.

4.1 General introduction to simulation programs

4.1.1 Objectives

The objective of developing and implementing the simulation models described here is to be able to model building integrated radiant heating/cooling systems, which can be used for both dwellings and offices. In Chapter 3 it was found that there is a need to create and further develop simulation models for building integrated heating and cooling systems. Or more accurately; many models have been created and analysed with many significant results, which have been documented in literature. However, there is still a need for further development and analysis before these models can be used in general building energy simulation programs. Among the required investigations, is a need to compare different levels of detail in the modelling of the floor heating system, with respect to the following points:

1. Accuracy of the models; how does the simple model perform compared to a more detailed model? Which parameters are important for a good result?
2. User requirements; what should the model be used for? A simple model may be more adequate early in the design phase of a building than a detailed model, where many of the required input parameters are unknown.
3. User friendliness; no more parameters than necessary should be required as inputs
4. Simulation time; important in the modelling process since a too detailed model can have unacceptably long simulation time.

With respect to these four points, it is important to realize what the model should be used for and based on this choose the correct level of detail. For instance, a model intended for consultants and i.e. optimization calculations must have a short simulation time, while complex and slow multidimensional models, often with a simulation time of hours, can be used for design and product development of floor heating systems.

Essentially, the choice of level of detail in the model is a trade-off between accuracy and simulation time. However, using a too detailed model may lead to results that are correct for the actual setup but which will not be valid if even small changes to the design are made. That is, there is no need to use a very detailed model if few details in the final design are decided.

The programs that have been developed for this thesis are called FHSim for Floor Heating Simulation and TASim for Thermo Active Simulation. FHSim was initially developed as part of a master's thesis (Weitzmann and Jensen, 2000) where the use and functionality of the program was shown and validated by comparing the results to the commercially available simulation program BSim2000. The program used a model of the floor with floor heating with only few details. In this context, the program has been expanded with the development of new models for the floor and floor heating system. The program is built of modules of the main building elements, room air zone and weather data to give the total program. TASim has been developed based on the same basic platform as FHSim with respect to implementation, numerical procedure and use of the model.

Finally, one more program is mentioned. This is called the International Building Physics Toolbox (IBPT), which has been developed in cooperation with Chalmers University of Technology and the Section of Building Physics and Services at the Technical University of Denmark. The program is a common platform for modelling building physics problems using a programming language with a graphical user interface. IBPT is also a modular program that has been developed to be a simple way to creating complex models through an extensive reuse of programming code. The purpose of this has been to demonstrate a different approach to creating simulation programs using open source code and downloading through the internet. In exchange for the use, newly developed modules can be returned to the "editors" of the webpage and included in future versions of the program.

4.1.2 Programming elements

As stated above, the programs used in this work are modular. The modules and their implementation are briefly mentioned in this section, with a detailed description in Appendix A including the system of equations used in the models.

Dynamic simulation models of building integrated heating and cooling systems should include:

- Dynamical implementation of temperature and heat flows in the constructions. This means that the model must include heat storage in order to include the effect of the time lag.
- Multidimensional models are required in order to correctly include the temperature distribution.
- Detailed radiation exchange between internal surfaces
- Inclusion of distribution of solar radiation on internal surfaces
- Inclusion of pipes if hydronic systems are modelled
- Control systems
- Ground volume, preferably in two or three dimensions (only applicable for floor heating, not for thermo active components)

Based on this list of requirements, FHSim and TASim have been designed to consist of the elements, which have been described in Table 4.1.

Table 4.1 Modules in the simulation programs FHSim and TASim

Module	Description
Building integrated heating and cooling systems	The models of building integrated heating and cooling systems used in the analyses are based on different level of detail and different implementation of the heating/cooling coil. Generally two different modelling types have been used: - Finite control volume (FCV) method, and - Thermal network based on a resistance/capacitance (RC) model. The implementation of the FCV models is either one- or two-dimensional with "many" nodal points, whereas the RC models are models with only a few nodes, where the heat capacity of the construction is lumped.

Module	Description
	The models are in all cases dynamic. The boundary conditions towards the room reflect the requirement of including radiant heat transfer, since this is the main heat transfer from the construction. Therefore, the boundary conditions treat convection and radiation separately. The different models used are described in detail in Chapter 5 for floor heating systems and Chapter 6 for thermo active components.
Building elements (i.e. walls, ceilings, inner walls, floors, etc.)	The models of the building elements excluding building integrated heating and cooling systems are one-dimensional implementations of the FCV method. The boundary conditions are combined with both radiation (long and short wave) and convection. The following should be noticed for the models. - The ceiling can face either outdoor conditions or another room. - The inner walls are assumed to have an adiabatic boundary condition in the middle of the wall. - The walls are facing outside conditions.
Windows including solar gains	The window model is split into a transparent and an opaque part corresponding to glazing and frame. In the glazing model the transmission and absorption of the solar radiation is based on the incident angle. The heat transfer is modelled by a finite control volume model with four nodal points; one in each glass layer and one on each of the external surfaces. Here, the heat balance is influenced by the absorbed solar radiation in each of the glass layers. A dynamic lumped model is used. The frame is also a dynamic lumped model with four nodal points, two internally in the frame and two surface nodes. Solar shading is possible by introducing a reduction factor of the solar gain, which can be controlled by the heat flux on the external surface.
Room model	The room model is a single node air volume with convective heat exchange with the surrounding surfaces. The air node also has heat gains from the convective parts of the internal sources and incoming solar gains. The solar gains are assumed to have a convective part coming from the part of the radiation which is absorbed by surfaces with low thermal capacity like for instance furniture which is therefore directly transferred to the room air by convection. Further, the room model includes radiation exchange between internal surfaces based on view factors between the surfaces. The surfaces also receive solar radiation. The distribution of the solar gains to the surfaces is distributed evenly on the surfaces with the same heat flow density (W/m²) on all surfaces. The ceiling surface does not receive

Module	Description
	any solar radiation. In the room model, the room air temperature is calculated based on the energy balance of the convective gains and losses. The room air is assumed to be at a steady-state condition in each time-step, thereby finding the equilibrium temperature for the room air temperature. This means that the heat storing capability of the room air and furniture is excluded from the model.
Ventilation	A simple balanced mechanical system with or without heat recovery is used. The effectiveness of the heat recovery unit is based on the temperature efficiency.
Infiltration	The infiltration rate is constant and equal to the exfiltration rate.
Venting	The windows can be opened to avoid overheating by giving a larger air change rate with the surrounding temperature. A method is used with a variable air change rate to ensure that the room air temperature is kept below the maximum set point value. A maximum allowed air change rate due to venting is included in the model. Therefore, if this maximum rate is exceeded or if the outdoor temperature is higher than room air temperature, the room air temperature will rise above the allowed maximum value.
Control systems and strategies	Generally an on/off type control system with a dead band is used. This is based on the fact that the thermally heavy constructions will not (or only to a small degree) benefit from more advanced controls. Different control strategies of the supply temperature have been investigated.
Thermal comfort	Thermal comfort including mean radiant temperature, operative temperature, PMV and PPD, and radiation asymmetry.
Weather data	Weather data based on the Danish Design Reference Year – or for validation purposes; based on measured data. The weather data based on the design reference year are hourly data for outdoor temperature, sky temperature, air velocity and direct and diffuse solar radiation.

In section 4.2 and 4.3 the programs FHSim and TASim are described with respect to the context in which they are used.

The following general limitations have been used in the programming, some of which have already been mentioned in Table 4.1:

- Constant material properties. This means that the influence of moisture and temperature on the material properties have been omitted in the analysis. This is mainly important for the ground model with floor heating. The effect of neglecting the coupling is discussed in Chapter 3.

- Only one room air node has been included for the air in the room model, which means that it is not possible to model the vertical temperature distribution in the room. This is however expected to be small for a room with heated/cooled surfaces since there is less air movement due to convection.
- Equilibrium room air temperature calculated each time step. Therefore the storage capacity of the room air and furniture is neglected. This means that the room temperature will change instantly with solar gains and ventilated outside air and therefore the damping on the temperature fluctuations from the heat capacity is not included.
- Only one zone in the model. Therefore the influence on multiple rooms with individual heating circuits and set points cannot be included.
- Fairly simple inclusion of the air handling in the model with respect to infiltration, ventilation and venting.

In other words, the programs used in this work are modular with models for walls (including solar radiation), ceiling, floor, ventilation, room, and weather data. The single zone room model includes detailed calculation of radiation exchange between internal surfaces based on view factors, which is important when modelling floor heating, as the room is heated mainly by radiation. Walls, ceiling, floor and windows are modelled using a finite control volume method with an implicit solution scheme. Except for the two-dimensional floor construction, the models are one-dimensional. The ventilation system is a simple balanced system optionally with heat recovery. As input, measured data or weather data from a design reference year can be used.

4.1.3 Implementation of programs

Both FHSim and TASim have been developed in Matlab Release 13 (Mathworks, 2002). Matlab has the great advantage that it is simple to implement simulation models since many functions are predefined, especially concerning handling of matrices and plotting of results. This is a major advantage over for instance C/C++, where neither matrix handling nor graphs are an integral part of the program. The simulation time is expected to be slightly longer than if a lower level programming language is used. However, the implementation time is much shorter using Matlab, which therefore makes it an ideal tool for research where the code is often changed.

4.2 FHSim (Floor Heating Simulation)

FHSim has been designed for simulations of the energy consumption and thermal conditions in a room with floor heating. The focus of FHSim is to find the energy consumption and thermal conditions during the entire heating season in dwellings.

Figure 4.1 shows the elements used in FHSim to simulate the conditions in a house with floor heating, based on the description above of the elements in the program. The figure shows the floor model including foundation and ground volume.

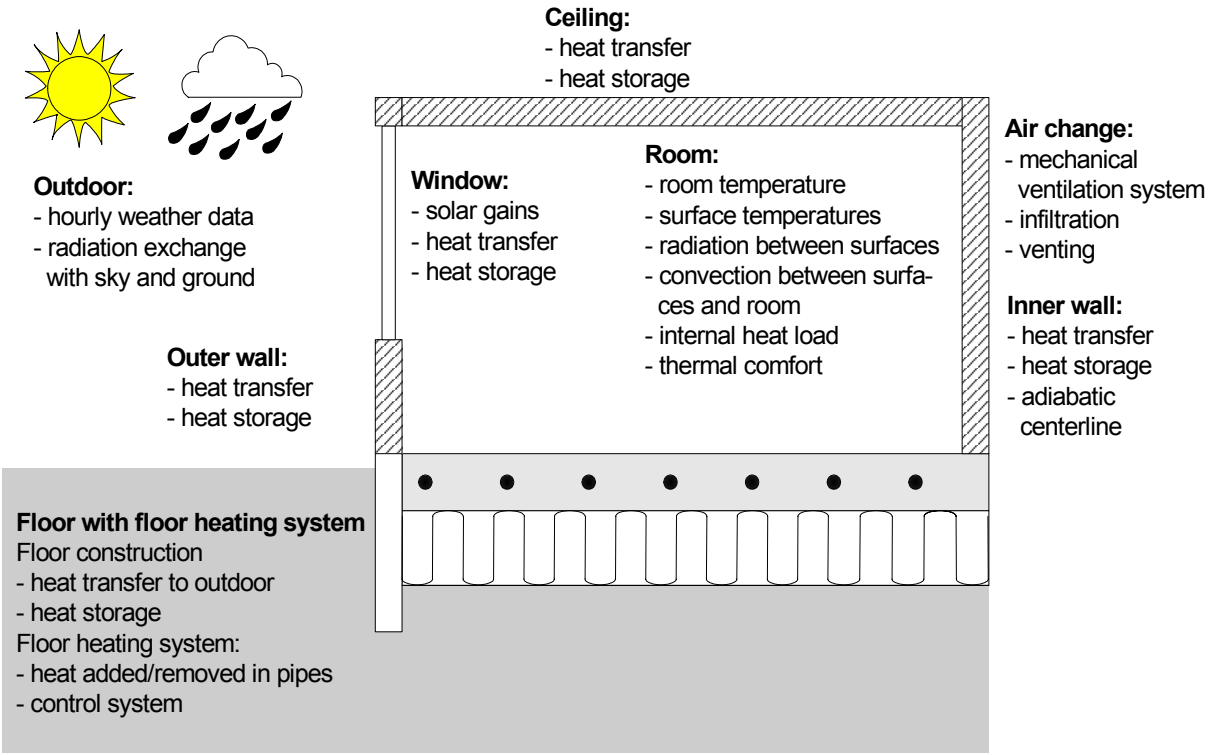

Figure 4.1 Elements used in FHSim for the dynamic simulations

4.2.1 User interface

Generally, both FHSim and TASim are "expert tools" with only one user; namely the developer. Therefore, the user interface is very simple or non-existing and typically changes to the inputs must be made directly in the source code.

However, an example of a graphical user interface, which has been developed for FHSim, is presented in this section.

A general limitation to graphical user interfaces is that they are very time consuming to develop, and consequently that changes made to the simulation model are cumbersome to include in the user interface. Therefore, this example graphical user interface is shown as an appetizer showing how the simulation program can be made available to a larger group of users. The program currently needs Matlab to run. However, it is possible to create a stand alone application based on the current implementation, which can be used on computers where Matlab has not been installed.

In the following a few main windows from the user interface has been shown to give an idea about the possibilities of an interface used in the simulation program.

Figure 4.2 shows the main window of FHSim.

Figure 4.2 Main window in FHSim showing the available main functions in the menu

Here the main functions of the programs can be accessed. These include:

- File: Loading and saving building model
- Building: Definition of geometry, building elements, windows, ventilation systems and floor with floor heating system
- Comfort data: Data for calculating the thermal comfort
- Solar calculation: Algorithms to find the solar radiation on surfaces and definition of shades
- Simulation: Definition of simulation period and main simulation window
- Results: Post-processing with graphical representation of the simulation results
- About: Data of the implementation and contact information.

A few of the most important windows for input and results are shown in the following.

Figure 4.3 shows the window for defining the dimensions in the room model.

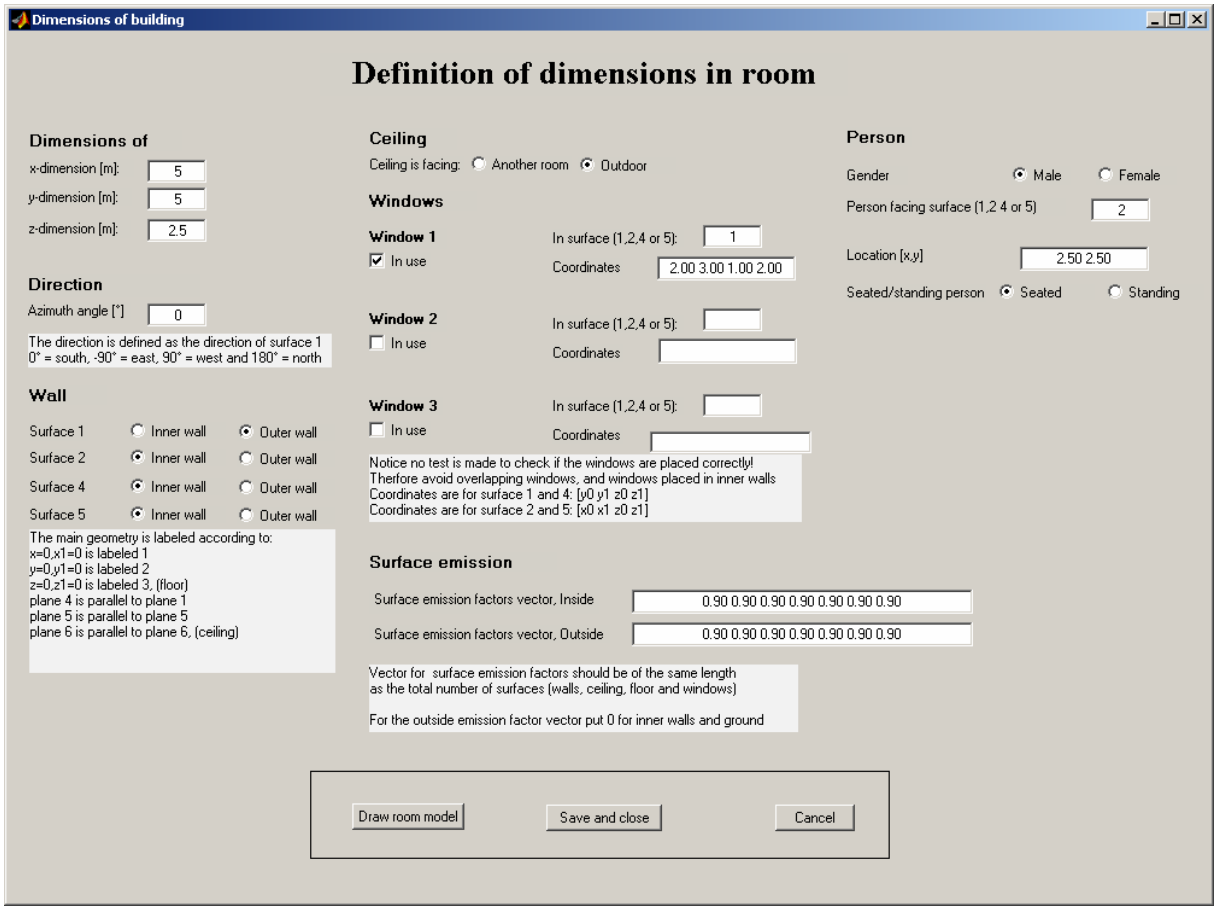

Figure 4.3 Definition of the dimensions of the room zone which is used in FHSim

In this window, the size of the room and orientation, wall types, ceiling inclusion, number of windows and their position, emission factors of inside and outside surfaces and gender and position for a person in the room. The data in this window is therefore the required input for calculating the main geometrical data for the room; number of surfaces, wall and window areas, volume, view factors and data required for finding view factors of surfaces and the person in the room.

The room model, based on the geometry defined in Figure 4.3 can be drawn by pressing the ‘Draw room model’ button. This is shown in Figure 4.4 for the data given in Figure 4.3.

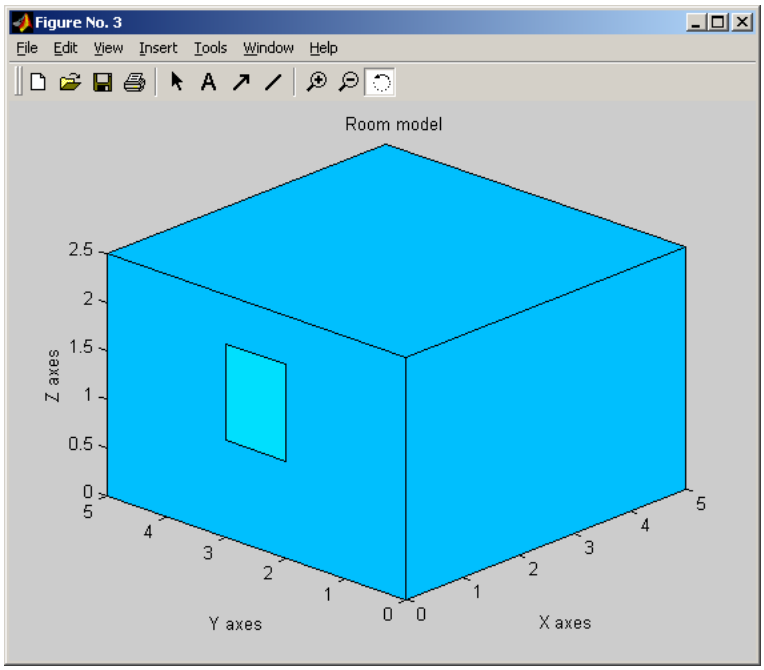

Figure 4.4 Graphical presentation of the room model

Figure 4.5 shows the definition window for the floor with floor heating system.

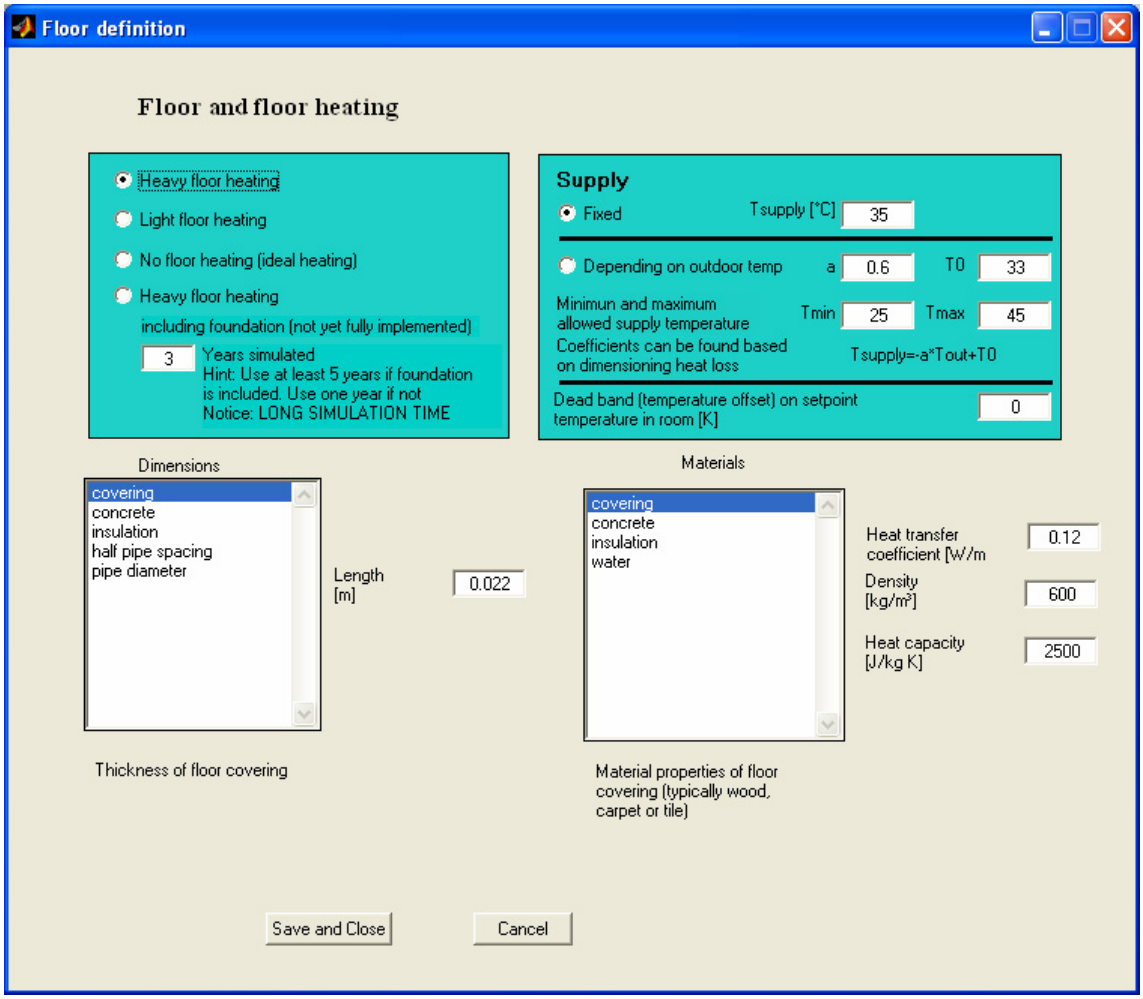

Figure 4.5 Definition of the floor and floor heating system with type of floor heating system to be modelled, dimensions and supply temperature.

In Figure 4.5 the type of floor heating system can be defined. In the upper left corner, four types of floors can be chosen; heavy and light floor heating based on two-dimensional models of a section around a pipe, a floor without floor heating and finally a two-dimensional model of the floor construction including both floor heating pipes, foundation and ground volume. In the bottom half of the window, dimensions and materials for the pre-defined floor heating types can be changed. In the upper right corner, properties of the supply temperature to the floor heating pipe can be defined.

Finally, Figure 4.6 shows the results window.

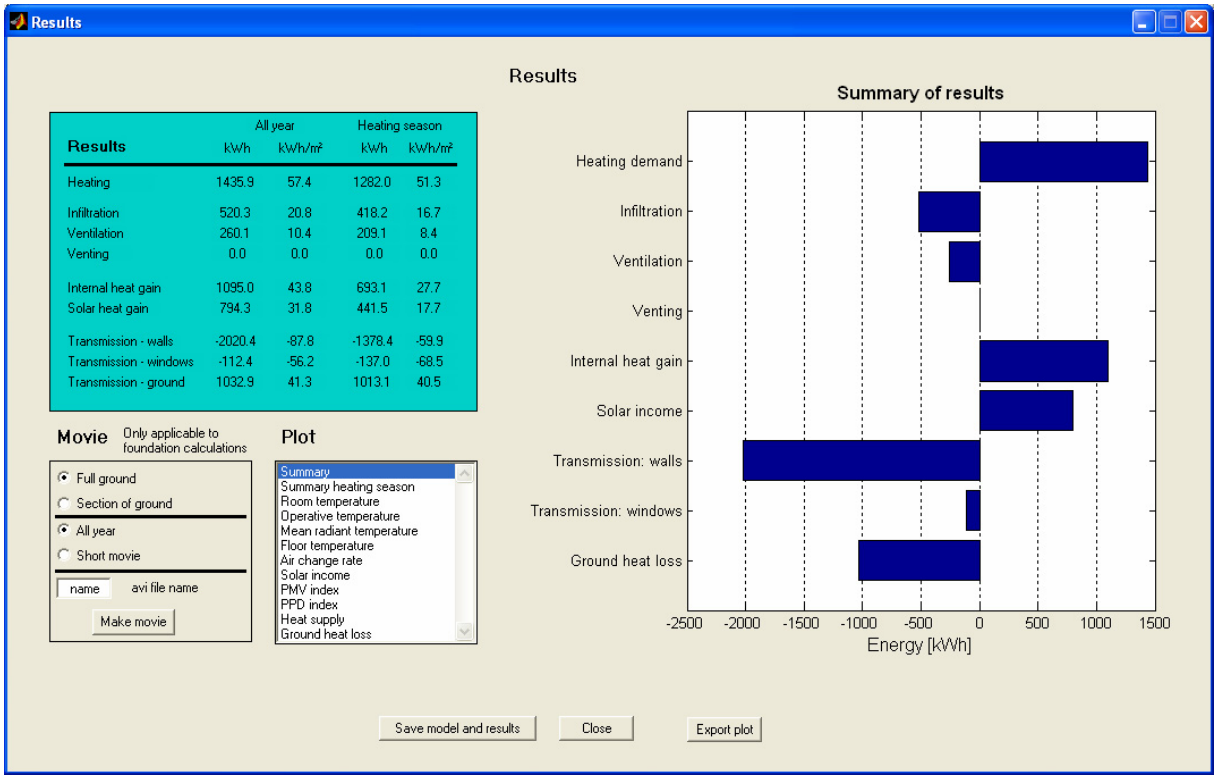

Figure 4.6 Result window showing a bar graph of the summary of the results of the main heat flows in the model as well as a tabular overview

The upper left of the result window shows a main overview of the simulation results for the main heat flows in the model. The same data are shown in the graph on the right side of the window. In the plot menu, different plots can be chosen, including different temperatures (room air, operative, and floor surface), monthly heating, ground heat loss and more. The plots can be exported and inserted in reports. Finally in the lower left corner of the window, the results can be used to create a movie-file of the temperature distribution during the entire year or for a short period of a few days. This is only active if the model results are shown for the two-dimensional simulation model of the floor construction with ground volume and foundation.

4.3 TASim (Thermo Active Simulation)

The second program, which has been developed, is called TASim for Thermo Active Simulation. This program is directed towards multi-storey office buildings where the decks between the storeys can be used to heat or cool the building using building integrated pipes.

TASim focuses more on the temperature in the room during hot summer days and the short term (daily) variations in the conditions as opposed to FHSim where the focus is on the entire heating season. This of course comes from the fact that in office buildings the temperature in

the offices is regulated with respect to maximum allowed temperatures and therefore the model generally uses shorter time steps than FHSim.

Figure 4.7 shows the elements used by TASim to simulate the conditions in an office equipped with a thermo active deck.

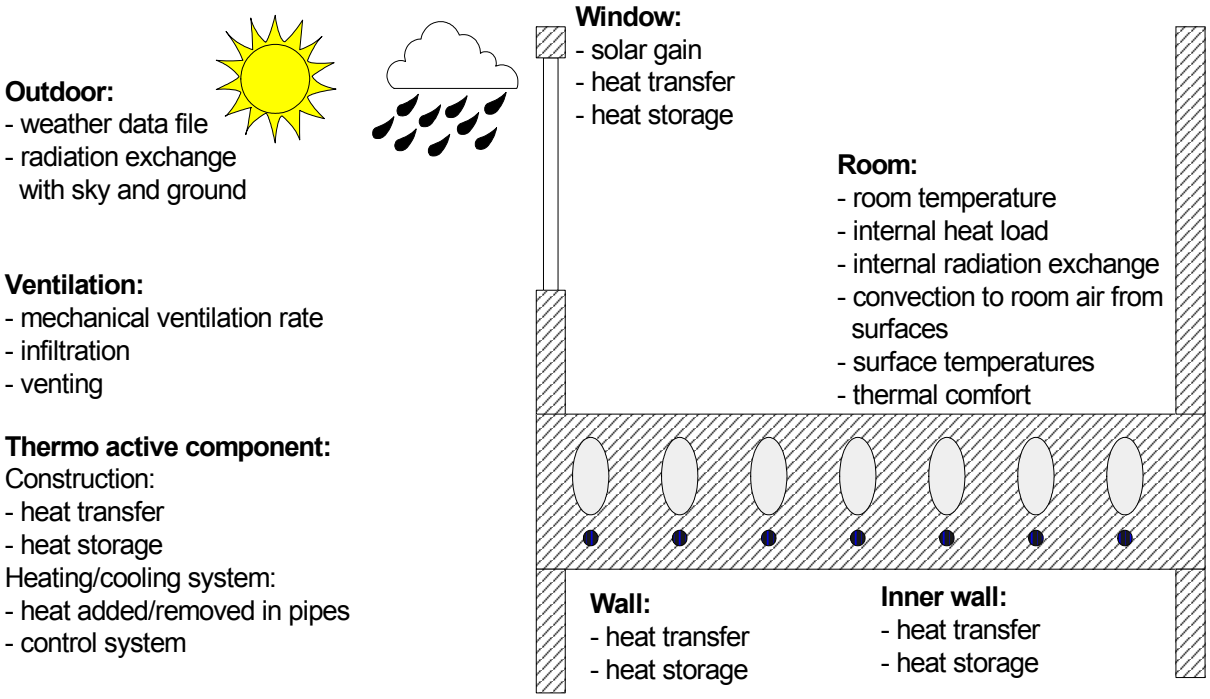

Figure 4.7 Elements used in TASim for the dynamic simulations

4.4 International Building Physics Toolbox

Where FHSim and TASim are both programs that are difficult to use since there is no well developed user interface, a third program has been developed as part of this work. The International Building Physics Toolbox (IBPT) has been developed in cooperation between Chalmers University of Technology and the Technical University of Denmark.

The description in this section is a short introduction to the toolbox, which has been attached as Paper 1 with the title: *Presentation of the International Building Physics Toolbox for Simulink* (Weitzmann et al, 2003a). This paper describes the toolbox and shows the design and examples of using the toolbox. A basic overview of the contents of the paper concerning the implementation of the toolbox is described in this section.

The program and models is freely available as open source code from www.ibpt.org.

The purpose has been to create a simple yet advanced platform for modelling building physics problems. The toolbox consists of models for the elements in a model of a building, which can be combined to create a model of a zone for simulation of temperatures and energy flows. The program includes models for constructions, thermal zones, systems, helpers such as weather data and gains. The idea is that novel building elements can be tested in the program together with already developed models, so that there is no need to start from scratch when developing simulation models. I.e. thermo active components could be modelled, simply by using the building elements from the toolbox along with the new developed model of the thermo active component. Therefore it is only needed to build the thermo active component in the simulation program while the rest can be taken directly from the toolbox. This approach will make it easier to implement and model novel building elements.

Based on the graphical programming language used in Simulink the program is very easy to use even for programming novices, which makes it ideal for teaching purposes. At the same time, a large number of different modelling techniques can be used, such as:

– Thermal networks implemented directly in Simulink using the standard blocks in the program.
– State space models of the equation systems.
– Models written as S-functions using either C++ or Matlab-code.
– Finite element models which can be created for instance in Femlab and imported into Simulink.

The advantage is that there is no need to consider how to solve the equation system, as Simulink itself sets up the solver and solves the problem using built in state of the art solvers.

The toolbox is based on the definition of a number of communication arrays, which ensures that the blocks created by different users can exchange data, since this format is common and unique. Therefore for instance, the output array from a wall model will have its surface temperature in the first position, which the developer of a room air model can base his or her model on.

The main window of IBPT is shown in Figure 4.8, where the main groups of modelling elements in the program library is shown; constructions, zones, systems, helpers and gains. In these groups the blocks used for the modelling can be found.

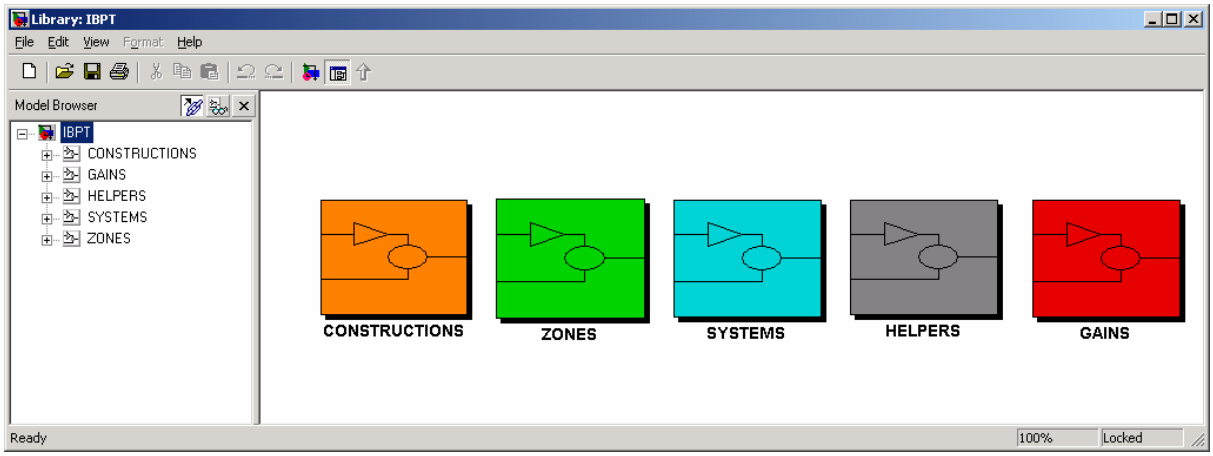

Figure 4.8 Main window of the International Building Physics Toolbox.

Based on the blocks from the library, an example file is shown below in Figure 4.9, which is a simple model of a room with one outer wall, one window, floor with floor heating, one inner wall, ventilation and internal gains. In the upper left corner of the model, the weather data are read into the model as a block whose data is available throughout the model. The communication arrays are shown by arrows. For example, the block called ‘thermal zone’ has an output array called ‘zone array’, containing the actual values for among others room air temperature, which is read by most of the blocks as an input.

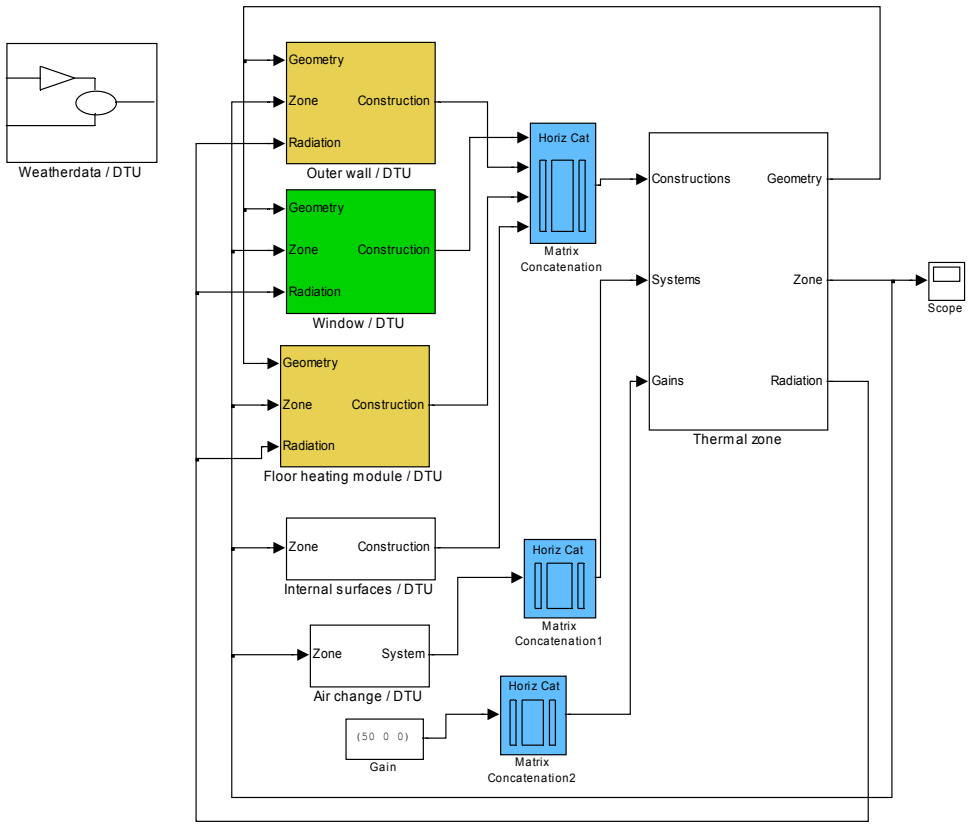

Figure 4.9 Main simulation model used in IBPT to model a simple room with floor heating.

A look "under the hood" of the block with the floor with floor heating reveals the model internally in the block. This is shown in Figure 4.10. The main part is the block called 'fhmodule', which contains the numerical model of the floor with floor heating system is modelled using a so-called S-function. The S-function represents one of the many ways of creating models in Simulink. The other parts of the floor heating block are taking care of the input and output of arrays, control system and calculation of the pipe temperature.

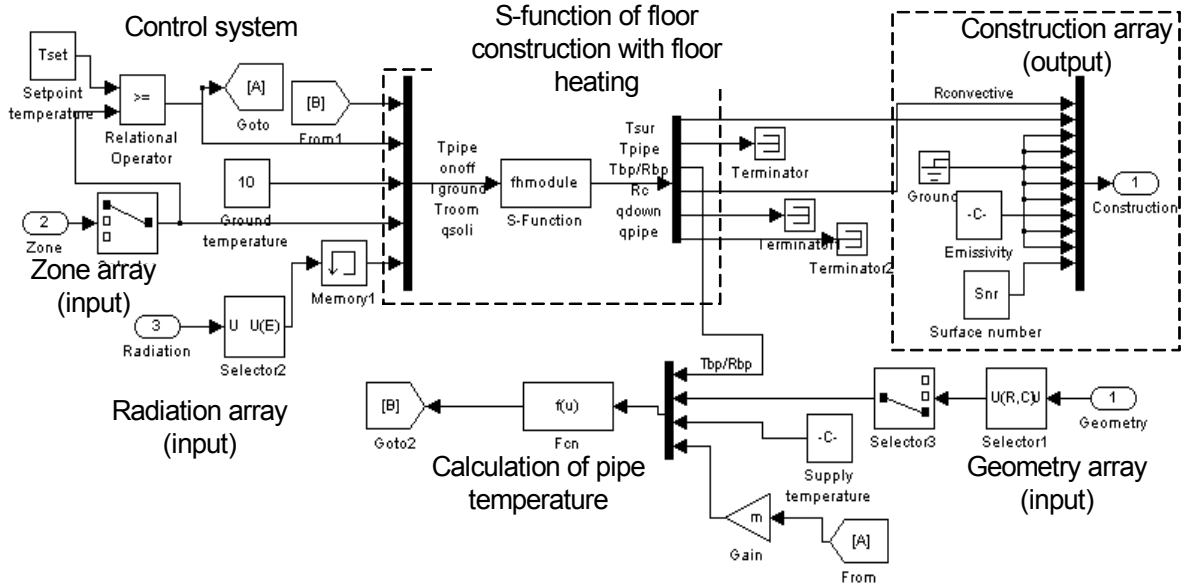

Figure 4.10 Floor heating block. The numerical model of the floor heating system is placed in the S-function called 'fhmodule', placed centrally the block.

A central point in developing models using IBPT is that as long as the basic rules of the order of the data in the data exchange arrays between the blocks is obeyed, the block can communicate with the other blocks in the models. For instance, the floor heating block outputs a construction array, which can be read by the thermal zone block. At the same time, the actual model used in the blocks can be made of any kind of modelling, complex or simple based on built-in functions or custom made. So internally in the blocks, the data flow can be chosen freely as long as the output arrays are composed to comply with the definition used in the main model in the toolbox.

4.5 Summing up

In this chapter two simulation programs called FHSim and TASim have been presented. The programs have been implemented to be able to model building integrated heating and cooling systems. The programs are the basis for the analyses in this thesis.

The models are implemented in Matlab, which is a powerful programming language with many built-in features for matrix manipulation and graphical representation of results. The programs are “expert tools” that are difficult to use since there is no user interface and all changes to the program must be made directly in the source code or by changing program variables with (typically) nonsensical names. Since this is very difficult for all other users than the developer(s), an example of a user interface to make the model more generally available is also presented.

Finally a third modelling tool called the International Building Physics Toolbox for Simulink is also presented as a way to make advanced modelling of building physics problems more available is presented. This method is based on a set of pre-defined communication arrays and a set of basic models for building energy simulation.

5 Floor heating

In this chapter, the modelling of floor heating systems has been described based on the simulation program FHSim, which has been described in Chapter 4. The aim of the chapter is to investigate implementations with different levels of detail in the model.

The chapter has been divided into three parts:

1. Validation of the two-dimensional ground coupled model of a floor with integrated floor heating system.
2. Detailed analyses of ground coupled floor heating, where the influence of different parameters are compared
3. Comparison of the level of details in the simulation models.

The basic properties of floor heating have been described in connection to the literature review in Chapter 3. Here it was found that while several models exist for the simulation of the conditions in a floor heating system, these models can still be improved before being introduced in building energy simulation programs or as expert tools for the use of product development in the design of floor constructions with floor heating.

Therefore, in the first part the two-dimensional ground coupled model is validated against measurements to ensure that the modelling is credible. Here it will, among others, be shown that a two-dimensional model can fully account for the conditions by introducing the characteristic dimension of the floor construction.

The second part is used to investigate the conditions when the model of the floor with floor heating is coupled to the ground volume, to find the influence of changing U-value and ψ-value of floor and foundation respectively, as well as the characteristic dimension and supply temperature to the floor heating system. This section will also show that in order to calculate the heat loss to the ground correctly, the floor must be coupled to a room model to include the dynamical conditions. Therefore, in order to model floor heating systems correctly, both for finding the temperature, energy consumption and heat loss to the ground, a coupled model with heating system and room model must be used. FHSim contains such a model.

The results in this part are directly aimed at product development, since very detailed models of the floor are used, which means that many different parameters can be used for “tuning” the design.

Parts of the results from these first two sections have been described in Paper 2 with the title: *Modelling floor heating systems using a validated two-dimensional ground coupled numerical model* (Weitzmann et al, not yet published). The main results from this paper are briefly described and discussed in the sections.

The third part is aimed at comparing simpler models of the floor with floor heating to the detailed two-dimensional model. The reason is that the detailed model is too complex and time-consuming to use for most practical purposes. Therefore, a series of simple models will be implemented to investigate their individual properties and compare them to the detailed model. The approach is – like for the second part – to compare models that are otherwise identical. Thereby, a direct comparison of the importance of the level of detail in the simulation models can be made, and therefore the importance of including or excluding certain details in the modelling process can be found. Firstly, this is aimed at the fact that including building integrated heating and cooling systems in simulation models requires a large number of inputs, such as pipe dimensions, pipe distance, control strategy and a

generally more complex geometry. A lot of this information is typically not available at the time of the simulations as these are often part of the design process which means that many parameters can be changed before the building is actually erected. Therefore it is relevant to know what parameters can be safely omitted and also for the important parameters how much the results change if this is changed. Secondly, certain details of the simulation model itself may be omitted and still get the same results. Combining these two points, this means that the most important factors can be included in the simulation models, while the not so important factors can be excluded – resulting in simpler simulation models, where the actual requirements of the simulation can be taken into account when choosing the model.

5.1 Validation of ground coupled floor heating model

A problem normally arising when validating a simulation model using measurements is to account for the simplifications that have been introduced during the modelling process. One such simplification is to model three-dimensional conditions, using only a two- or one-dimensional model. A wooden house built by the Swedish contractor LB Hus in Bromölla, Sweden, which is equipped with floor heating (Roots, 2001; Roots and Hagentoft, 2002b; Roots and Hagentoft, 2002c) has been used for the validation.

The validation of the ground coupled floor heating model is described in Paper 2, which means that in this section only the main results will be given.

5.1.1 Ground coupled floor heating

Figure 5.1 shows the two-dimensional model of the floor construction. The numerical procedure has been described in detail in Appendix A. It includes floor construction, foundation and ground volume.

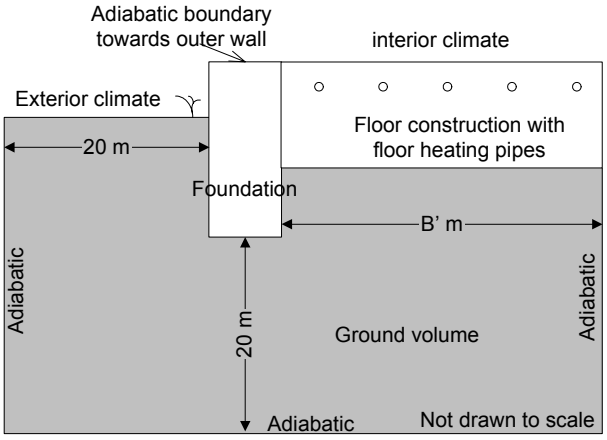

Figure 5.1 Two-dimensional section of the floor construction and ground volume.

The boundary conditions are adiabatic to the sides, bottom, and towards the outer wall. Indoor climate is applied above the floor construction while exterior climate is applied on the ground surface and the foundation. To ensure an undisturbed temperature field at the edge of the model, 20 meters of ground downwards and to the side have been used.

The width of the floor from foundation to the central part of the floor has been chosen such that the model can include the effects of corners by using the characteristic dimension of the floor. The characteristic dimension has been defined in Chapter 3, as the area of the building divided by half the perimeter.

5.1.2 Description of house and measurements

The house in Bromölla is a typical Swedish timber frame single-family house placed in the south eastern part of Sweden. The house is well insulated with low energy requirement for heating. A detailed description of the house and the measurements can be found in Roots (2001), from which data have been kindly offered for the present analysis.

The measurements are taken in the centerline of the living room of the house, which is appended to the house at a 90 degree angle from the main body of the house as shown in Figure 5.2.

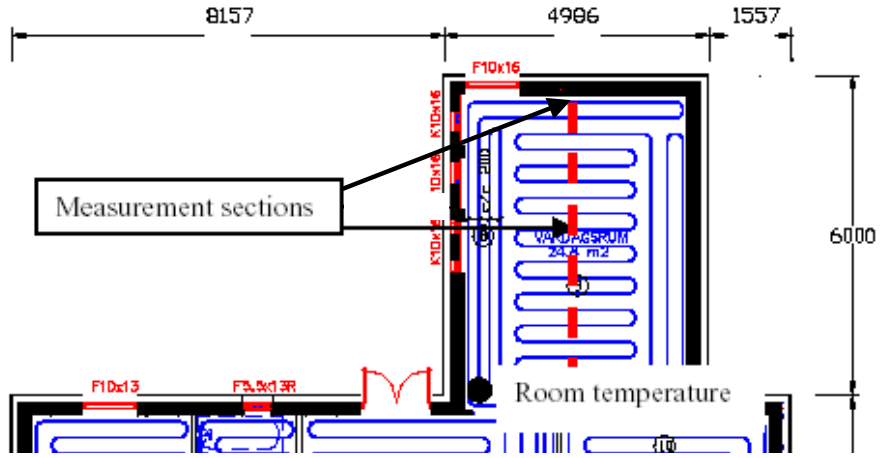

Figure 5.2 Partial floor plan of the house in Bromölla. The measurements are carried out in the appendix to the main house.

The measurements are of temperatures in the floor construction, ground volume, and foundation while the heat flows are measured between the floor and ground volume. The measurement positions of temperature and heat flows are shown in Figure 5.3.

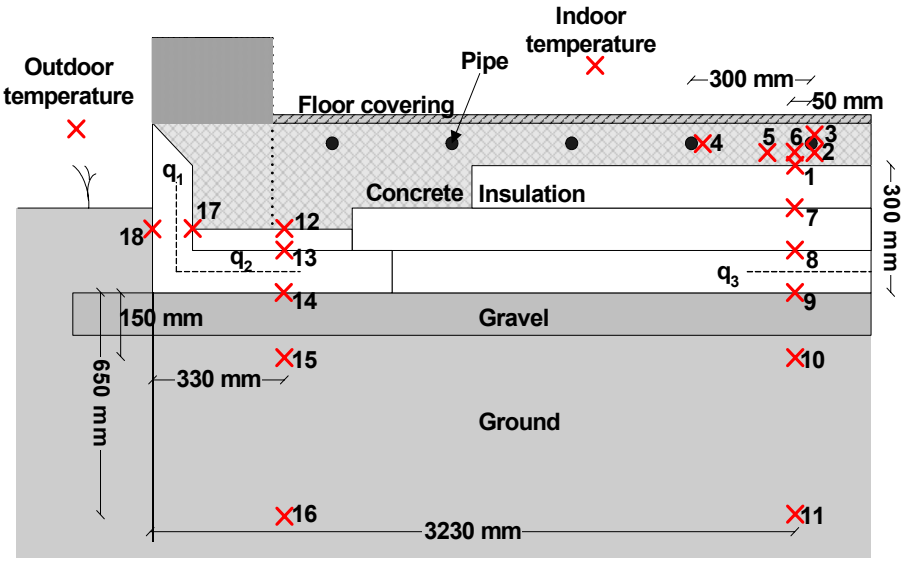

Figure 5.3 Vertical view of foundation and floor construction of the house in Bromölla, Sweden. Measurement of temperatures is marked with x'es, and the measurement of heat flows is denoted by dotted lines. Notice the figure is not drawn to scale.

The measurement data only makes it possible to validate the model of the floor construction with ground included. This is due to the fact that the conditions for the house concerning solar heat load, internal heat load, and set point temperature are not detailed enough to be used as input for the simulation model used in FHSim.

5.1.3 Validation results

Comparison of heat flows

Figure 5.4 shows the heat loss to the ground through the entire slab on grade floor. As it can be seen, there is a very good agreement between measured and simulated values, with a difference between measured and simulated heat loss is less than 2%, which is very satisfactory.

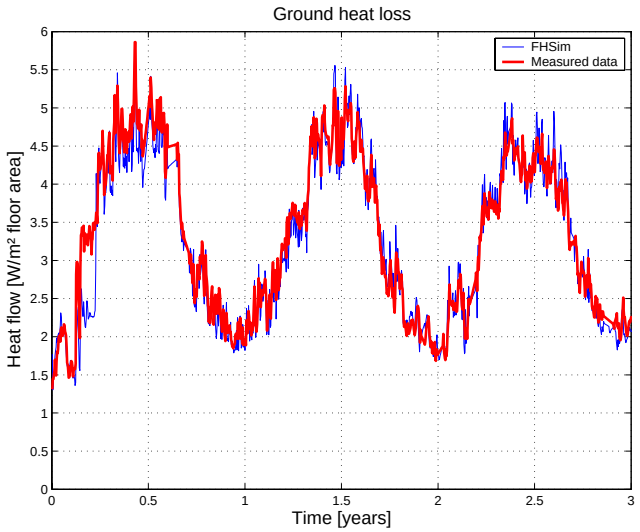

Figure 5.4 Total heat loss through the entire slab to the ground shown as the heat flow inW/m² of internal floor area.

Comparison of temperatures

Figure 5.5 shows the temperature distribution in the floor construction and ground volume near the floor. As it can be seen, the isotherms are fairly one-dimensional from the position of the characteristic dimension and further into the construction. This model is shown to assess the temperature distribution in the ground volume further into the construction than the width of the characteristic dimension. In the simulations above a model with a width equal to the characteristic dimension has been used.

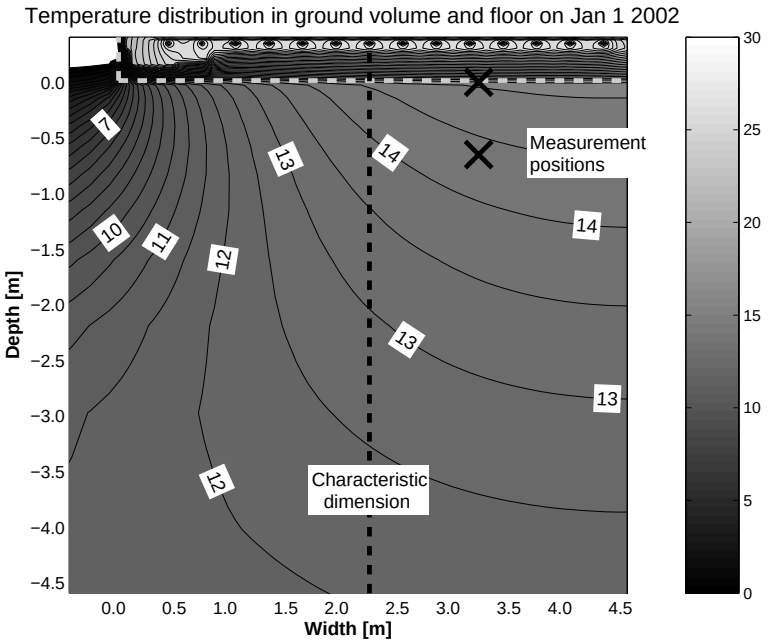

Figure 5.5 Simulated temperature distribution in ground volume The outline of the floor construction is shown with the dotted grey line. The figure also shows the characteristic dimension. The isotherms are shown for each 0.5 K.

To show the conditions in the floor construction itself, Figure 5.6 shows the foundation and first 1.5m of the floor construction. Notice especially that the conditions for the two outermost pipes are different from the following ones due to the position near the foundation.

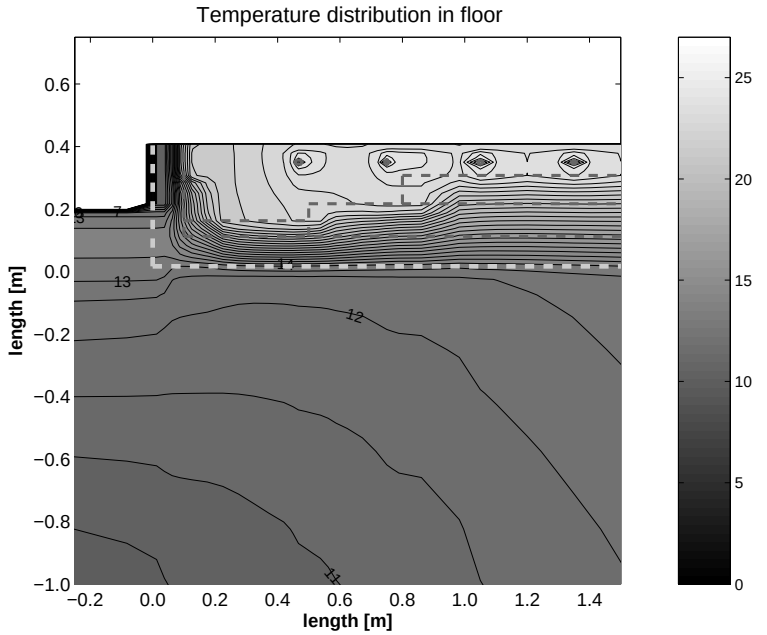

Figure 5.6 Simulated temperature distribution in deck

Figure 5.7 shows a comparison of the measured temperature in point 9 and 11 and the simulated temperatures in the position of the characteristic dimension, using the model which is only as wide as the characteristic dimension. This comparison is possible because the isotherms are nearly one-dimensional from the point of the characteristic dimension as Figure 5.5 shows. Again close agreement between the measured and simulated data can be observed.

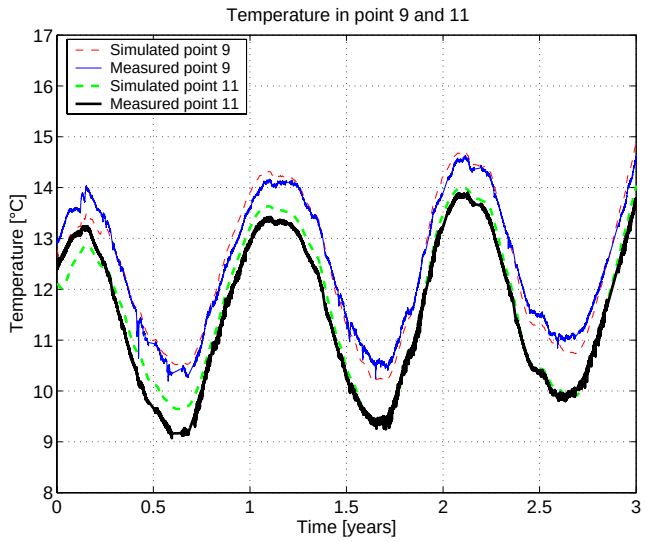

Figure 5.7 Comparison of temperature in the ground volume under the central part of the floor construction in measurement points 9 and 11. The time 0 years corresponds to Aug. 20 1999

A similar observation can be made for the points under the foundation.

5.1.4 Conclusion

Based on the comparison of the measured and simulated heat flows and temperatures, the main conclusion for this validation is that the simulation model of a ground coupled floor with floor heating is fully able to predict the conditions for both heat flows and temperatures.

A very important spin-off from the validation is that the use of the characteristic dimension as the width of the section of the floor construction can be used to eliminate the need for calculations. However, it has not been used for heated floors, as is the case here. Especially the fact that the corners of the floor are heated can be expected to give different conditions than for a model without floor heating, which means that the corners will have larger influence on the heat loss than if the floor is not heated. Nevertheless, it has been shown here that the use of the characteristic dimension is also valid for heated floors. This in spite of the fact that the building used for the validation was both small and narrow, which means that it has been heavily influenced by three-dimensional conditions.

In total, it is concluded that the model can be used for the work presented here.

Finally, the validation in this section has only focused on the heat transfer and temperatures in the floor construction and ground volume. This means that room model is not actually part of this validation. However, in Chapter 6, the room model is validated based on measurements in an experimental setup on thermo active components, but since the room model is the same in both conditions, this validation will be general for both models.

5.2 Energy efficiency of ground coupled floor heating

In this section focus is turned to the two-dimensional simulation model with the purpose of investigating the influence from the floor heating system especially on the heat loss through the foundation and ground volume.

As it has been found previously in Chapter 3 and section 5.1, the heat loss to the ground is a three-dimensional process, which can be simplified to a two-dimensional process by introducing the characteristic dimension as the width of the floor construction.

In this section the influence of floor heating has been investigated in order to find the influence on the ground heat loss and energy consumption for different levels of insulation in the floor construction and foundation. This is very relevant with respect to using the model for product development of the floor construction and floor heating system.

The investigation is aimed at detailed modelling of the floor construction.

A central point in this section is that the results are found using the dynamical simulation program FHSim. This means that the conditions in the floor construction are correctly modelled with respect to the temperature in the concrete deck. This will be shown to impact the results from the simulations considerably.

5.2.1 Simulation model

A simple reference room for the parametrical analysis has been created. Because of the influence of the orientation of the room, two simulations are carried out with a south/west and a north/east orientation. An average of the energy consumption for the two orientations is used for the comparison of the results. The difference in the energy consumption is typically 20%. The room has two outer walls with a 4m² window in each. The floor area is 6m · 6m = 36m². The inputs to the room model are shown in Table 5.1 and Table 5.2.

Table 5.1 Physical dimensions and U-values of walls, ceiling and windows.

Parameter	Area [m²]	U-value [W/m²K]
Outer walls	22	0,18
Window	8	1,50
Inner walls	32	-
Roof	36	0,12
Floor	36	0,12

Table 5.2 Input data, set points and ventilation rates.

Parameter	Value
Ventilation & Infiltration	0,5 h^{-1} + 0,1h^{-1}
Internal heat load	5W/m²
Control strategy of heating supply	On/Off
Supply temperature	40ºC
Set point temperature	21ºC
Weather data (Danish design reference year)	DRY

Figure 5.8 shows the slab on ground floor, which is a sandwich construction with two concrete decks around the insulation layer. The floor heating system is placed in the upper concrete deck, with a pipe distance of 300mm. The floor covering is a 20mm wooden floor. The house is well insulated. As weather data, the Danish design reference year (DRY) has been used.

It has been chosen not to include a heat recovery unit on the ventilation system. This is a de-facto requirement for energy efficient houses, but here it has been omitted to see the effects of changing the parameters more clearly. The simulations have been allowed to run for several years to ensure periodic stationary results of the heat flows and temperature distribution in the ground volume.

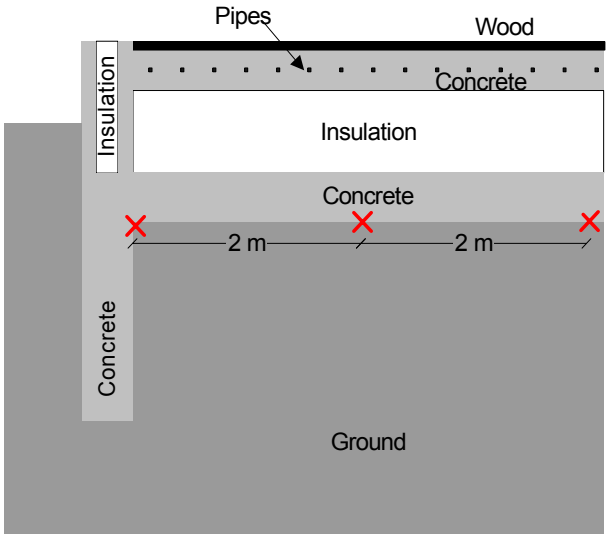

Figure 5.8 The simulation model of foundation and floor construction. The pipe distance is 300mm. Not drawn to scale.

A series of investigations are undertaken to investigate different parameters. The detailed two-dimensional model has been included in FHSim, with the coupling to the room model, has been used for the following investigations:

- Finding the linear thermal transmittance of a floor with floor heating and comparing it to similar calculations where heating is supplied directly in the room
- The influence of the characteristic dimension on the energy consumption
- Finding the temperature under the floor construction and in the ground volume
- The influence of linear thermal transmittance and thermal transmittance on the energy consumption and heat loss to the ground
- The influence of the supply temperature and set point temperature on the energy consumption

Initially, however, the measurements from section 5.1 are used to test the dynamical inclusion of the temperature in the floor heating system by comparing simulation results with two constant pipe temperatures to the measurement data. Since dynamical conditions of the floor heating system can only be included by an integrated model with both room model and floor heating system, this investigation will show whether it is necessary to use an integrated model to find the heat loss to the ground.

5.2.2 Need for dynamic calculations

While this section uses the floor model shown in Figure 5.8, this section returns briefly to the floor model used for the validation.

Figure 5.5 and Figure 5.6 illustrates the importance of correct geometrical implementation of the floor heating pipes as it can be seen that the temperature distribution around the pipes close to the foundation are different from those in the central part of the construction. However, another issue is to compare the measured data to a calculation where a constant pipe temperature is used, as it is typically prescribed in for instance EN ISO 13370. for heat loss calculations to the ground

However, the average temperature is difficult to estimate. Therefore, two simulations using constant temperatures have been undertaken: One using the measured average pipe

temperature of 24.8°C during the three-year period and one using 30°C. The latter value represents a conservative estimate. Figure 5.9 shows the calculated ground heat loss for two simulations compared to the measurement data, which is equivalent to Figure 5.4, where measured and simulated conditions were compared using constant pipe temperature.

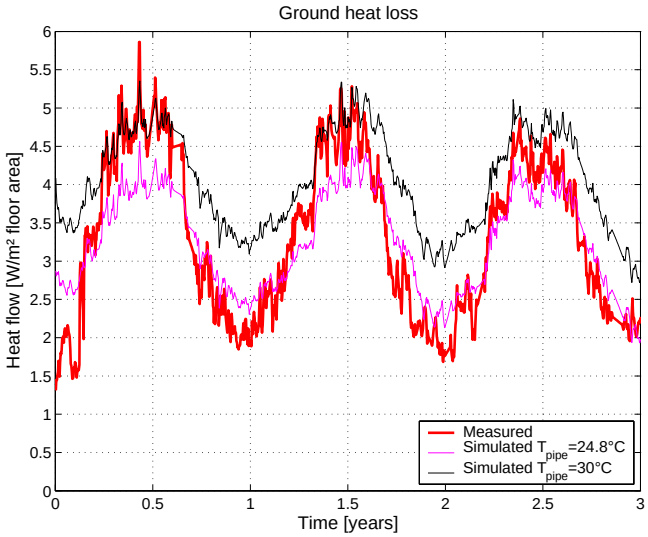

Figure 5.9 Ground heat loss using a constant pipe temperature as input in the simulation model, using the average temperature during the measurement period and 30°C shown together with the measured heat loss.

As it can be seen, both overestimate the heat loss during the summer periods (with low heat loss). In average a pipe temperature of 24.8°C leads to an underestimation of the heat loss of 2% while an average pipe temperature of 30°C finds a 23% higher heat loss.

The calculation with a constant temperature of 30°C shows the need for an accurate estimate of the average pipe temperature. However, an accurate estimate is difficult to find since many parameters influence this value.

The fact that the dynamical implementation both finds the most accurate value (See Figure 5.4) and does not need to estimate the average temperature illustrates the advantage of using dynamical models.

Therefore, a dynamical inclusion including both ground coupled floor heating and room model is necessary since a correct dynamical implementation of the floor heating system also means that a correct control of the floor heating system must be included.

5.2.3 Linear thermal transmittance when floor heating is present

The calculation procedure used in Denmark for calculating the linear thermal transmittance is based on the description in DS418 (DS, 2002), which is briefly described here:

The method is based on a two-dimensional section as shown in Figure 5.8. During the simulations a constant indoor temperature of 20°C should be used along with the following outdoor temperature

$$T_{out} = 8.0 + 8.5 \cdot \sin\left(2 \cdot \pi \frac{M-4}{12}\right) \quad \textbf{(5.1)}$$

This formula has been fitted to the average Danish weather conditions. The average outdoor temperature during the heating season, $\overline{T}_{out}$, from September to May is 5.54°C. *M* is the time of the year given in months (i.e. 3.5 is the middle of March).

The thermal resistance is 0.04m²K/W for the outdoor conditions and 0.13m²K/W for the inner wall and 0.17m²K/W for the floor. The heat conductivity of the ground should be 2.0W/mK, and the heat capacity should be 2000kJ/m³K unless more accurate values exist.

The model of the floor construction is simulated with these input data until yearly periodic stationary conditions have been achieved. The temperature in the so-called reference point, T_{ref}, which is placed just under the insulation at the length, *w*, from the inside of the foundation should be recorded along with the two-dimensional heat flows from the internal climate to the construction, q_{tot}. The length *w* should be 4 m.

The one-dimensional heat loss through the floor construction is calculated from the average recorded reference point temperature during the heating season, $\overline{T}_{ref}$, and the one-dimensional U-value of the floor from the inside to the position reference point.

$$\overline{q}_{1D,floor} = w \cdot U_{floor} \cdot \left(T_{room} - \overline{T}_{ref}\right) \quad \textbf{(5.2)}$$

The linear thermal transmittance, $\psi_{foundation}$, can then be calculated as

$$\psi_{foundation} = \frac{\left(\overline{q}_{tot} - \overline{q}_{1D,floor}\right)}{T_{room} - \overline{T}_{out}} \quad \textbf{(5.3)}$$

In the procedure as it has been described in DS418 it the one-dimensional heat flow through the outer wall, $\overline{q}_{1D,wall}$, must also be subtracted. The procedure has been designed to give a conservative estimate of the ψ-value. Notice that the procedure also includes the heat loss through the outer wall. This has been omitted in this work; however this simplification is not expected to influence the results to a large degree since the outer wall typically does not alter the isotherms in the floor construction considerably.

It is clear that this procedure cannot be directly used to find the linear thermal transmittance for a model with floor heating, since (1) the heat flow through the floor surface is used to find the heat loss to the ground. In the floor heating model, the heat flow through the floor surface will be in the opposite direction. Additionally, (2) a fixed room temperature is assumed without a heating source. Using a floor heating system, the room temperature depends on the pipe temperature and therefore a colder outdoor temperature requires a higher floor surface temperature.

The first can be solved by finding the heat loss through the outside of the construction instead of through the floor surface. The second is more difficult. Here it has been chosen to use the concrete temperature instead of the room temperature as the inside boundary condition. However, it has previously in this work been found that a dynamic simulation of the temperature is needed to find correct heat loss to the ground. Therefore, the calculation has been based on actual dynamical modelling in FHSim based on the Danish Design Reference Year and not Equation (5.1).

At the same time it must be noticed that the purpose of this investigation is not to find a conservative estimate of the linear thermal transmittance, as is the case in the DS418 (DS, 2002). If this was wanted a “high” concrete or pipe temperature could be used instead.

The same equation system can be used if the following are complied with:

- The room temperature must be replaced by the average concrete temperature during the heating season, $\overline{T}_{conc}$
- The average heat loss, $\overline{q}_{tot}$, from the floor construction must be found from the "outside" of the floor heating pipes
- The one-dimensional heat loss in the floor construction must be calculated from the concrete layer to the reference point and consequently also the U-value between these two points
- The Danish Design Reference year is used in a dynamic simulation using a room with correct heating demand

Three different insulation thicknesses are used in the floor construction, 150mm, 250mm and 350mm, corresponding to the U-values of 0.17W/m²K, 0.12W/m²K and 0.09W/m²K. Two different levels of the energy consumption have been used. This has been achieved by using models with and without heat recovery unit on the ventilation air. The model without heat recovery unit has an energy consumption of around 80kWh/m² and the model with has an energy consumption of around 40kWh/m². These are referred to as "high" and "low".

The linear thermal transmittance has been calculated, using the method described in DS418 and using the adapted method both with and without floor heating. In total three methods and two levels of energy consumption are used.

Table 5.3 shows the data used for the calculation of the linear thermal transmittance using the model without heat recovery unit (high energy consumption) and a U-value of 0.12W/m²K. For each, the data used in Eq. (5.1) to (5.3) are shown.

Table 5.3 Main data for calculating the ψ-value for the model with a U-value of 0.12W/m²K and "high" energy consumption. The heat flows have been shown for the floor width of 4 meters. Notice, that the first row shows the concrete temperature for the dynamic model with floor heating, the average room temperature for the dynamic model without floor heating and the fixed room temperature for the method according to DS418 (DS, 2002).

Parameter	Method		
	Dynamic with floor heating	Dynamic without floor heating	According to DS418 (no floor heating)
$\overline{T}_{conc} / \overline{T}_{room} / T_{room}$	26.7°C	21.4°C	20.0°C
$\overline{q}_{tot}$	11.70 W/m	7.45 W/m	6.61 W/m
$\overline{q}_{1D,floor}$	8.48 W/m	5.61 W/m	4.81 W/m
$\overline{T}_{ref}$	13.5°C	12.0°C	9.6°C
$\overline{T}_{out}$	3.7°C	3.7°C	5.5°C
U_{floor}	0.156W/m² K	0.146W/m² K	0.146W/m² K
$\psi_{foundation}$	0.141 W/m K	0.104 W/m K	0.130 W/m K

Notice that the heat flows are larger for the model with floor heating which, is of course due to the heating of the concrete deck.

Similarly to the data shown in Table 5.3, Figure 5.10 shows the calculated ψ-values based on the simulation data for each of these parameter variations.

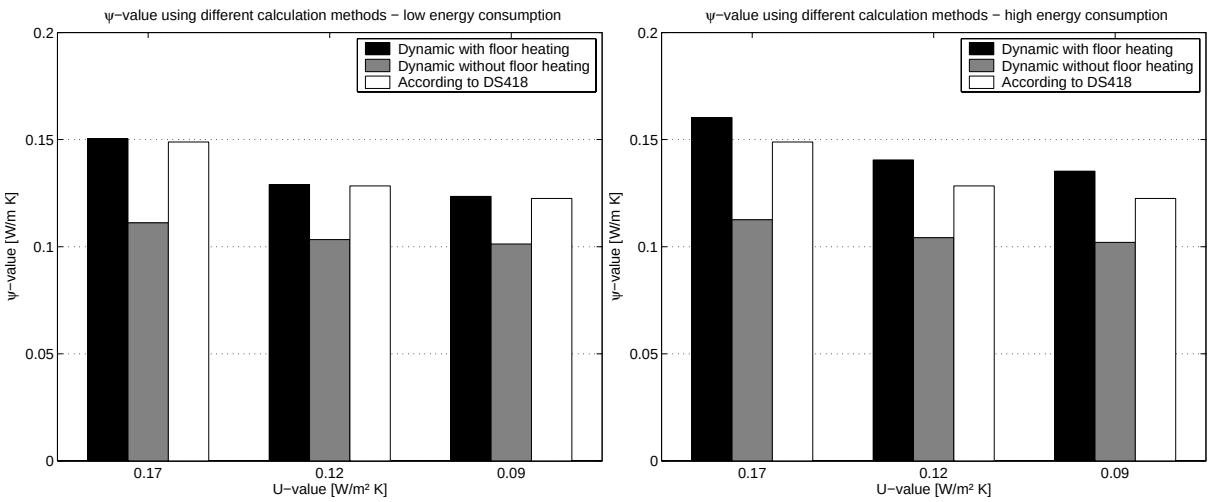

Figure 5.10 ψ-value of floor construction using different calculation methods. Left figure shows a model with "high" energy consumption, while the right figure shows a model with "low" energy consumption. The U-value refers to the three insulation thicknesses used in the simulations

It can be seen for all calculations that:

- The ψ-value calculated by the DS418 method is conservative when compared to the dynamic calculation without floor heating included by giving higher values than for the calculation without floor heating.
- The ψ-value calculated by the DS418 method is **not** conservative when compared to the dynamic calculation with floor heating included by **not** giving higher values than for the calculation with floor heating.
- When the ψ-value is calculated dynamically, using floor heating, the value depends on the energy consumption in the room, which is not the case when floor heating is not included, as this value is almost constant. With floor heating the difference is between 6% and 10% between the high and low energy case relative to the low energy case, while the difference is around 1% without. The data based on the DS418 method is the same in both cases.
- The dynamically calculated ψ-value with floor heating is nearly the same as according to DS418 when the energy consumption in the room is low, while it is around 7% to 10% higher for the model with high energy consumption.
- The calculation method in DS418 is therefore not completely suitable for finding the linear thermal transmittance using floor heating.
- The ψ-value depends on the U-value of the floor construction. This is a result of the way the model has been implemented and is due to the fact that the heat flow has a longer distance from the heated concrete deck to the outside condition.

In this work no effort has been made to create an alternative method to get a conservative estimate of the linear thermal transmittance of the foundation using heated floors. However, these results indicate that such a method should be considered.

5.2.4 Characteristic dimension

As it was found during the validation, the characteristic dimension of the floor heating system influences the heat loss from the floor construction as well as the total energy consumption, due to the influence from the foundation and three-dimensional conditions. In this examination the energy consumption and ground heat loss have been calculated as a function

of the characteristic dimension of the room. However, the same room size is used for all simulations, which will not be the case if the characteristic dimension of the building changes. Therefore the results should be considered valid for a room in a building with the given characteristic dimension.

Figure 5.11 shows the ground heat loss and energy consumption for the model with 250mm of insulation with and without floor heating for the high and low energy consuming models.

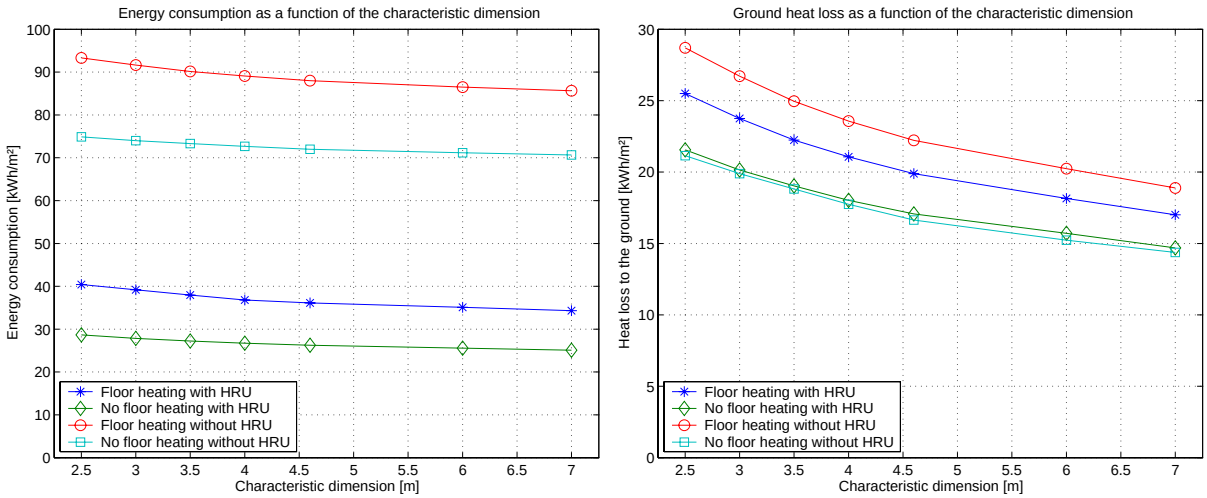

Figure 5.11 Energy consumption and ground heat loss as a function of the characteristic dimension of the floor in the 2D model. 'HRU' means heat recovery unit on the ventilation air, where the model with 'hru' has low energy consumption, while the model without has high energy consumption.

In all cases, the larger the characteristic dimension, the smaller the heat loss to the ground and the smaller the energy consumption. This corresponds to the larger the building, the smaller the energy consumption for each square meter of building. However, the larger the characteristic dimension, the smaller the decrease. The same is the case for the heat loss to the ground.

Another observation is that the models with floor heating have a larger increase in the energy consumption than the models without. The relative increase in energy consumption compared to a characteristic dimension of 7 meters is for both the model with high and low energy consumption largest for the model with floor heating. This is a natural consequence of the fact that the concrete slab is heated. Therefore, the floor with floor heating is penalized heavier for small characteristic dimensions than buildings heated by other means.

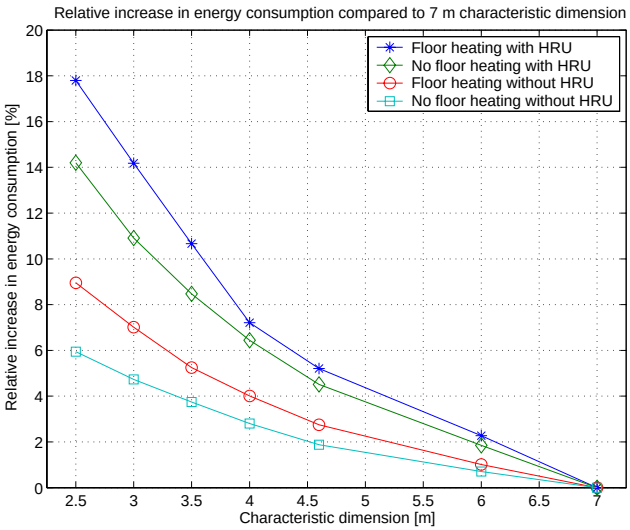

Figure 5.12 Relative increase in energy consumption as function of the characteristic dimension. The data are relative to a characteristic dimension of 7 m.

In total, the characteristic dimension is important when assessing the heat loss from the ground and also the total energy consumption.

5.2.5 Temperature under slab-on-grade floor

The influence of the floor construction and foundation can be seen from Figure 5.13, where the temperature distribution in the ground volume is shown for four different days during the year: Jan. 1, Apr. 1, July 1, and October 1. The floor construction is shown with the dotted grey line. The figure shows 5 meter in the horizontal direction away from the foundation and 8 meters below the ground volume, which is the reason for the isotherms not being perpendicular to the figure boundary at the sides away from the floor construction. As described above in 5.1.1, a total of 20 x 20 m was used for the calculation domain. Generally it can be seen that the temperature distribution in the ground volume is influenced by both house and surroundings. The influence from the floor construction can be seen to extend far into the ground volume. With this investigation in mind, however, it is interesting to notice, that the temperature directly under the insulation is far from constant, neither from foundation to the central part of the building, nor during the year, as there are large differences in the temperature distribution. One interesting aspect is that the temperature under the house is highest during the heating season (October and January) and coldest during the summer period (April and July). Notice also, that the presence of the foundation is very evident in the figures, as the isotherms are almost vertical from the foundation and down into the ground volume during the periods where the floor is heated.

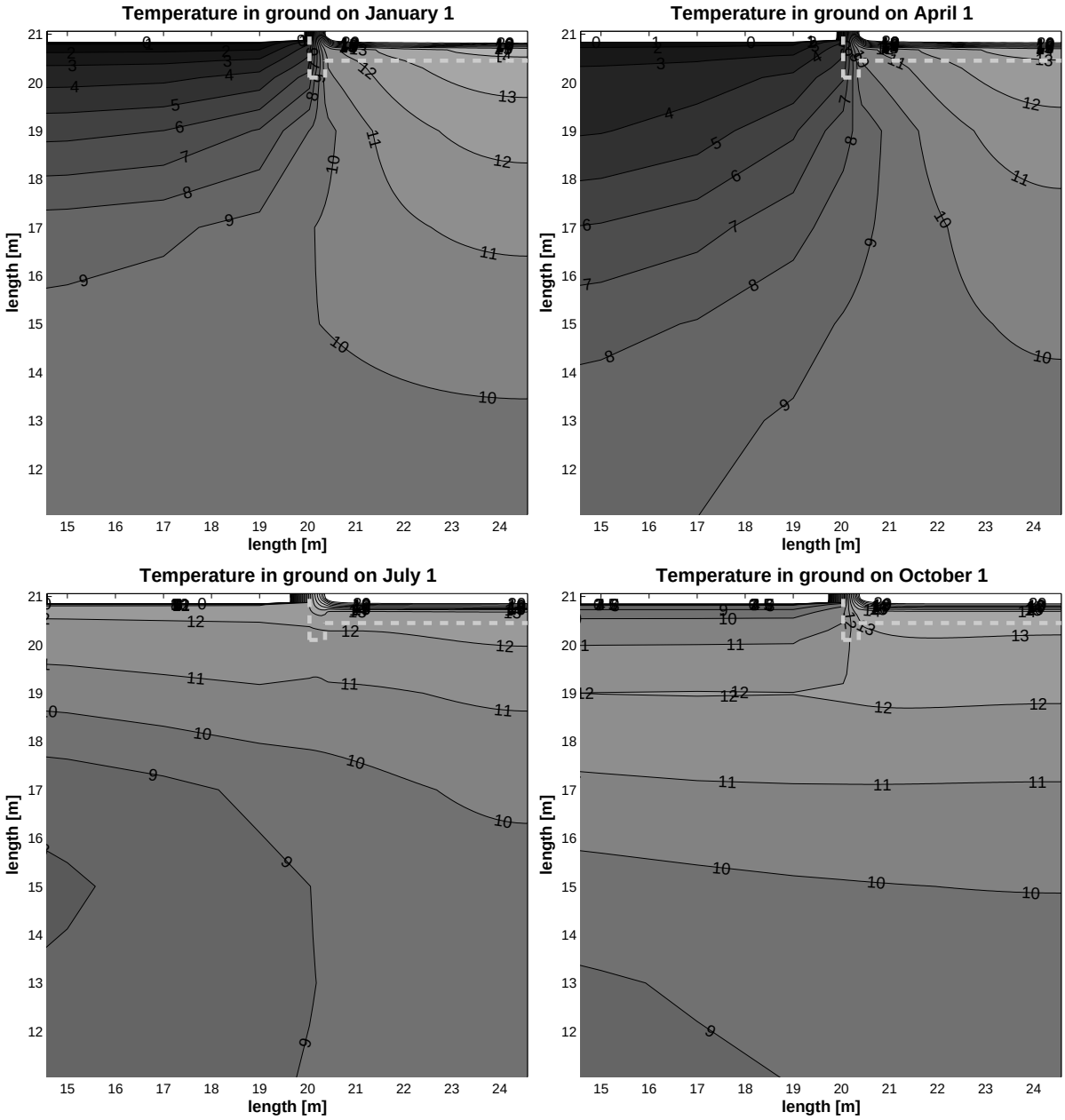

Figure 5.13 Temperature distribution in ground volume on Jan 1, April 1, July 1, and October 1. The temperature for the isotherms are shown with black figures. The ground volume has been shown approximately 5m from the foundation in the horizontal direction and 8m from the floor construction in the vertical direction. An insulation thickness of 250mm and a linear thermal transmittance of 0.11W/mK are used. The floor construction and foundation of the house is shown by the grey outline in the top right corner of the figures. Temperatures below 0°C and above 20°C are not shown.

Figure 5.14 shows the temperature in three points directly under the insulation layer. The first point is immediately inside the foundation, the other two points are placed 2 m, and 4 m from the foundation, as shown in Figure 5.8. The response to the outside temperature is faster directly inside the foundation than further into the construction and the amplitude is smaller.

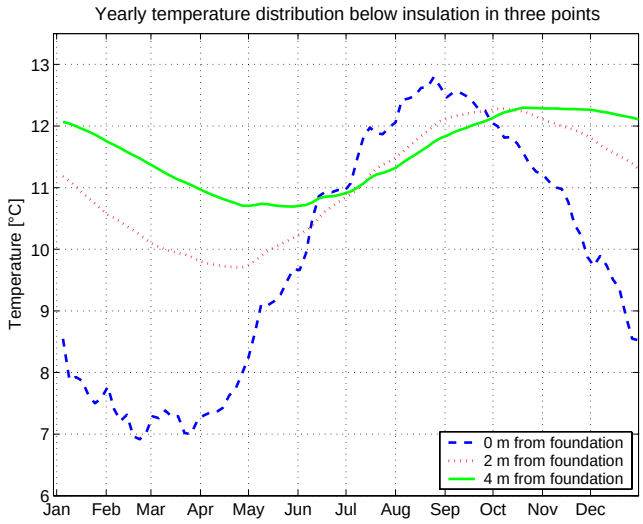

Figure 5.14 Yearly temperature distribution in three points directly under the insulation.

To find the influence of the floor heating system in the ground volume, the temperature difference between a house with and without floor heating in the ground volume has been found by simulations. In the house without floor heating, the same simulation model is used, but the floor heating system is never turned on. Instead, the room is heated directly in the thermal zone. This difference is shown in Figure 5.15 for the same three points as in Figure 5.14. There is only a small difference in the temperature under the insulation layer of up to 0.5K. The difference becomes larger further into the construction. Further down in the ground volume, this temperature difference will become smaller. Therefore, there is only a small influence from the floor heating system on the temperature distribution in the ground volume with an insulation thickness of 250mm, as is the case here. Notice also, that the temperature is always higher in the ground volume when using floor heating, even during the summer period. This comes from the storage of heat in the ground volume.

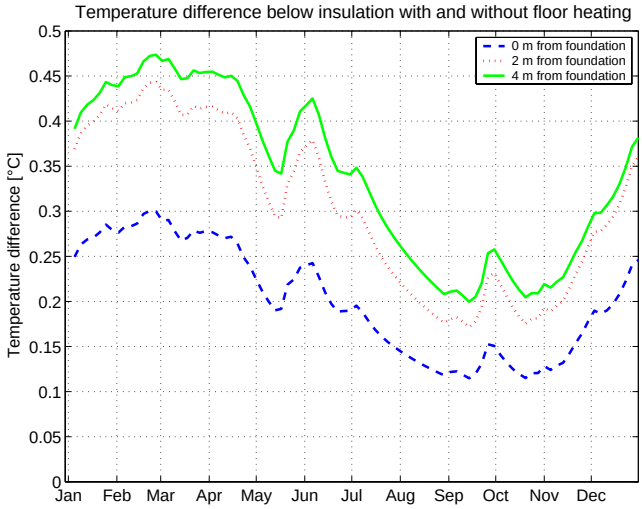

Figure 5.15 Temperature difference in ground volume between a house with and without floor heating. A positive value means that the temperature is higher with floor heating than without floor heating.

5.2.6 Influence from U- and ψ-value

Energy consumption in room

The higher floor temperature compared to other heating systems increases the heat loss to the ground. Figure 5.16 shows the yearly energy consumption as a function of the linear thermal transmittance coefficient, $\psi_{foundation}$, calculated as described in Chapter 3, while Figure 5.17 shows the energy consumption as function of the U-value of the floor construction.

In both cases, a linear correlation between energy consumption and linear thermal transmittance or U-value can be observed, both influencing significantly on the energy consumption. The lines are almost parallel, indicating that regardless of insulation thickness, the same relative saving in the energy consumption can be expected when improving the foundation and that increasing the insulation thickness will provide energy savings. Especially for the foundation, the results show that this construction detail should be given more attention in the design of new houses with floor heating, regardless of the insulation thickness in the floor. In this example, the energy consumption is the same for a $\psi_{foundation}$-value of 0.3W/mK and 350mm of insulation as $\psi_{foundation}$-value of 0.1W/mK with 100mm insulation.

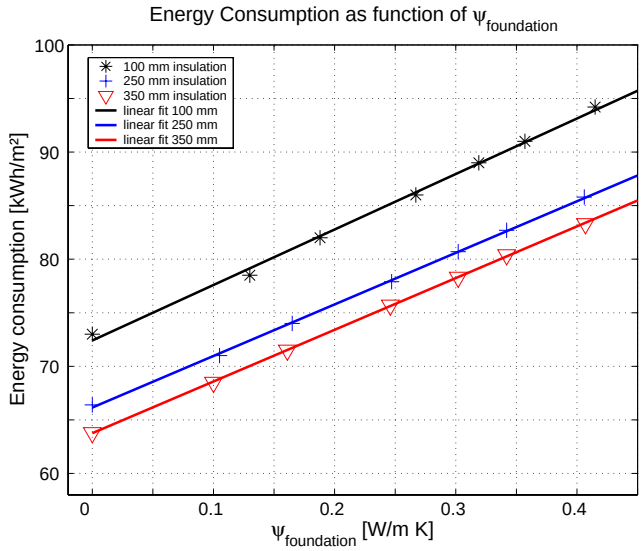

Figure 5.16 Annual energy consumption as a function of the linear thermal transmission coefficient.

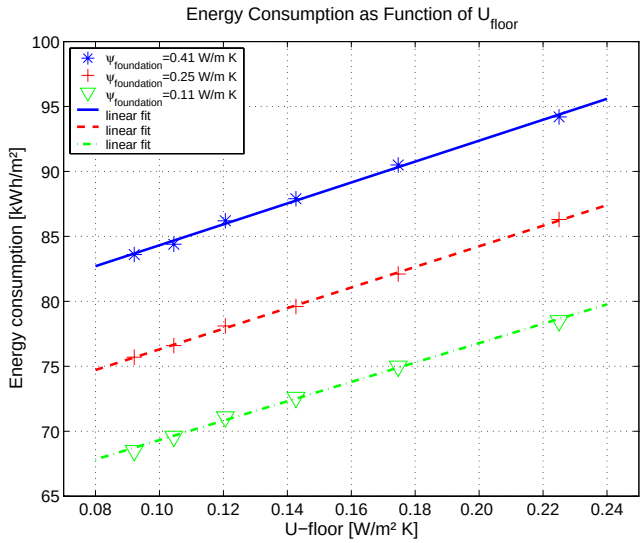

Figure 5.17 Annual energy consumption as function of U-value of the floor construction.

Heat loss to the ground

Where the previous section has focused on the energy consumption, this section considers only the heat loss to the ground through the slab-on-grade floor. Figure 5.18 shows the ground heat loss with and without floor heating for different U-values for the entire year and for the heating season only (September to May). In order to compensate for the larger heat loss caused by the floor heating, extra insulation can be used. For instance a U-value of 0.2W/m²K can be seen to result in a heat loss to the ground of around 11kWh/m² during the heating season. In order to get the same heat loss in a house with floor heating, the U-value of the floor constructions must be reduced to around 0.11W/m² K. This is equal to an extra insulation thickness of app. 150mm. If the same heat loss for the entire year is used, the U-value should only be lowered to 0.14W/m² K, corresponding to only 75mm corresponding to a ground heat loss of 20kWh/m².

An interesting observation is that the difference in the heat loss to the ground between the models with and without floor heating is increasing with increasing U-value. This means that for smaller insulation thickness, the heated floor will be "penalized" more for the poorer level of insulation than if the floor which is not heated. This result complies with the previously found data for the characteristic dimension and for the ψ-value, where a heated floor has a higher relative influence from changes in the input parameters.

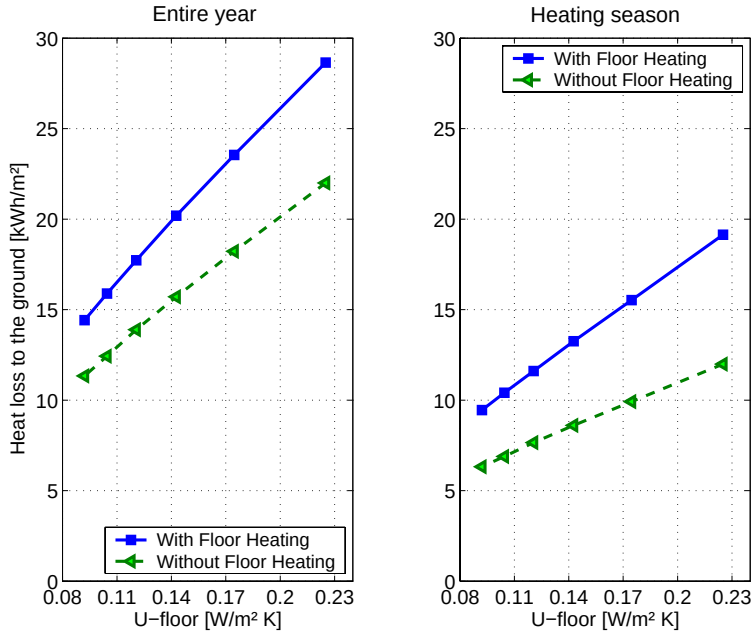

Figure 5.18 Heat loss to the ground for the entire year (left) and for the heating season (right) as function of the U-value of the floor construction with and without floor heating. A ψ-value of the foundation of 0.11 W/m K has been used.

5.2.7 Control system

Supply temperature to the floor heating system

The supply temperature has previously been found to influence the energy consumption (Weitzmann et al., 2002). In new houses, it is only necessary to use low supply temperature to maintain the room temperature between 20°C and 22 ºC. However, to avoid complaints from the customers on too low room temperatures, the floor heating system is often installed with a high supply temperature (45 ºC). Lowering the supply temperature will result in a more even temperature level in the concrete layer and therefore less chance of overheating and thus also

less chance of wasting energy. Table 5.4 shows the energy consumption for different supply temperatures.

Table 5.4 Energy consumption in room as function of the supply temperature to the room. The energy consumption is shown both inkWh/m² and as a percentage of the maximum value.

Tsupply [° C]	30	35	40	45	Variable
Energy consumption [kWh/m²]	73.5	76.3	77.1	77.8	69.4
Energy consumption [% of maximal value]	94%	98%	99%	100%	89%

Using 35°C to 45°C has almost no influence on the results, but using 30°C gives a reduction of 5% compared to 45°C. This relatively small difference comes from the fact, that the average concrete temperature is almost the same in the two cases – the higher temperature simply means that the system is turned on less often. Finally, using a variable supply temperature lowers the energy consumption even more. The variable supply temperature is a function of the outdoor temperature and the heat loss from the room. This control type will be described in detail below; see Table 5.11 and Figure 5.30.

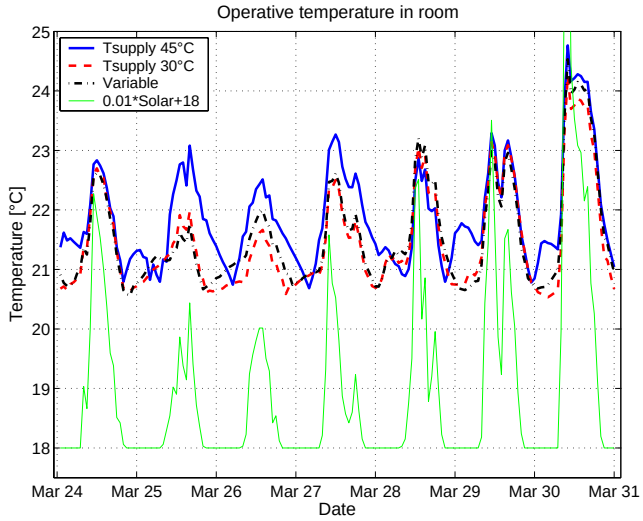

Figure 5.19 Operative temperature in the room using a supply temperature of 35ºC and 45ºC. The solar gains to the room have been multiplied by 0.01 after which the value 18 has been added to make it fit on the figure. A period of one week is shown.

Figure 5.19 compares the operative temperature in the middle of the north/east room using supply temperatures of 30 ºC and 45 ºC and the variable supply temperature. In addition, the solar gains are shown. The operative temperature in the room is generally higher using the highest supply temperature, especially during periods with solar gains. This can be explained by the fact that less heat is stored in the concrete layer using lower supply temperature. Therefore, the temperature will not rise as much. This is most evident during day 2-4 in the figure. During day 5-7 the operative temperature curves have almost identical peak values, due to the large solar gains, which will inevitably lead to a large rise in the temperature regardless of the temperature in the concrete deck. The variable supply temperature and the low supply temperature of 30°C have almost the same values during the period, but with lower energy consumption.

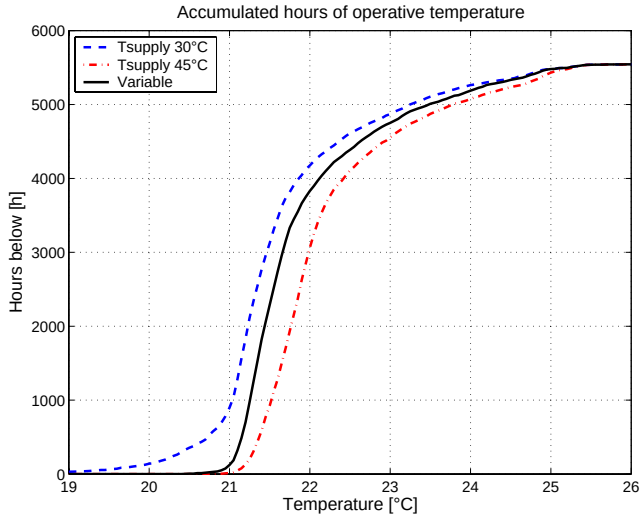

Figure 5.20 Accumulated hours with operative temperature below a given value. Data are shown for four different supply temperatures in the heating season (approximately 5500 hours).

Figure 5.20 shows the accumulated hours of the operative temperature using variable and fixed supply temperatures of 30°C and 45°C. As it can be seen, using 30°C will give many hours with cool temperatures below 21°C, which is the simulated set point temperature. However, using 45°C gives many hours with higher temperatures especially in the interval between 21°C and 23°C. This increases both energy consumption as well as the risk of thermal discomfort. The variable supply temperature gives almost no hours with temperatures below 21°C, but still manages to keep the room free from too warm temperatures. Therefore, the value and type of the supply temperature is important both with respect to the temperature in the room, but also as shown in Table 5.4 to save energy.

Set point temperature

The set point of the room will also influence the energy consumption in the room. Using four different set point temperatures ranging from 20°C to 23°C in increments of 1K and the model with and without heat recovery unit on the ventilation system give the results shown in Figure 5.21.

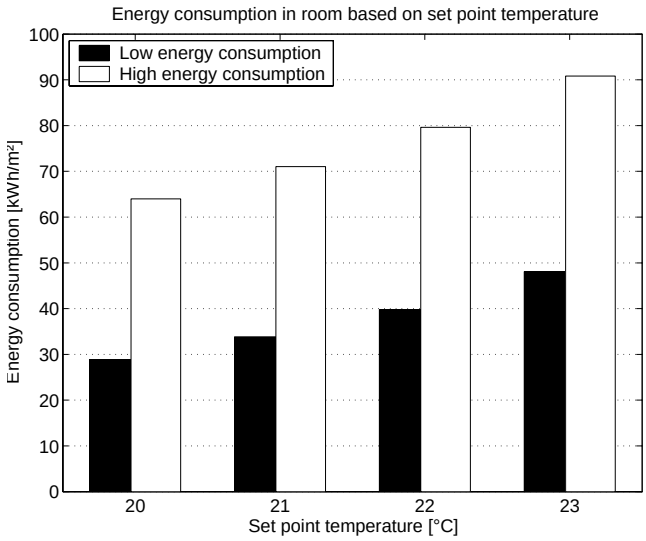

Figure 5.21 Energy consumption for different set point temperatures and model with high and low energy consumption.

As expected, the energy consumption increases with increasing set point temperature. For the model with high energy consumption, the energy consumption rises by an average of 11%, while it is 16% for the model with high energy consumption.

5.2.8 Discussion

In this section detailed analyses have been carried out to find the properties of floor heating using a detailed two-dimensional floor model coupled to the ground. Where Section 5.1 found that a two-dimensional simulation model is adequate for modelling the ground heat loss by introducing the characteristic dimension, this section has shown the need for correct dynamical implementation of the floor heating system in the floor construction. Therefore, in order to find the influence from the floor heating system on the energy consumption and heat loss to the ground, it is necessary to include correct dynamical conditions in the simulations with respect to the heating of the room. This means that the modelling of floors with floor heating needs to be coupled to a room model to correctly include both the heat loss to the ground and the energy consumption of the room. Therefore FHSim represents a good tool for these analyses, as the above mentioned influences are included in the program.

Linear thermal transmittance

The influence of floor heating on the linear thermal transmittance (ψ-value) has been investigated. A method based on DS418 has been used as basis for the calculations. To include floor heating in the calculation, it is necessary to take into account the fact that the floor is heated. Therefore the concrete core temperature is used instead of the room temperature. This temperature is not constant and depends on the heating demand in the room and will therefore influence the ψ-value.

Here it is found that the existing method without floor heating will not give a conservative estimate of the ψ-value, which means that a new method must be developed in which floor heating is included. Such a method has not been investigated further in the frame of this work. Obviously it should include the increased temperature in the deck, but this increase depends on the rest of the building. Therefore the actual influence of the deck temperature must be investigated further to (hopefully) find a simple correlation between the room temperature and the deck temperature, and the deck temperature and the psi-value.

Characteristic dimension

Different values of the characteristic dimension of the floor construction have been used in a series of simulations to find the influence on energy consumption and heat loss to the ground. As expected it was found that the smaller the characteristic dimension, the larger the energy consumption and heat loss to the ground. It was also found, equivalently to the investigation on the linear thermal transmittance, that when the floor is heated the influence of this increase is larger than when the floor is not heated. This further strengthens the suggestion that since corners in the building are heated, there will be an extra heat loss from the corners.

Energy consumption and heat loss to the ground

The influence of the level of insulation in floor construction and foundation has been investigated. For both, a linear correlation between the energy consumption and the U-value/ψ-value has been found. Therefore decreasing energy consumption can be expected improving either one of them or through a combination. Additionally, it is shown that buildings with floor heating are more heavily “penalized” on the heat loss to the ground for poorer insulation than buildings without floor heating. This proves that setting maximum

allowed values for **both** the U- and ψ-value, as in the Danish Building Code, is a correct approach.

Since the heat loss to the ground has been shown to be larger when floor heating is used, an obvious investigation – to which end FHSim can be used – is to find the necessary improvement of the U- and/or ψ-value to ensure that the heat loss to the ground is not larger than for an unheated floor. Conversely, the model can be used to establish the level of insulation required by future versions of the national building codes.

Supply temperature

Finally it has been found that energy consumption and heat loss to the ground are both influenced by the supply temperature to the floor heating system. Therefore it is also important to use as low supply temperature as possible to lower the energy consumption. This result has previously been found in the literature as described in Chapter 3. However, none of these investigations have included the influence of the ground coupling and foundation. Therefore this result can be seen to extend the validity of the previously found results, and in addition the influence of the foundation can be directly included in the results.

Do notice that the results from this investigation do not arrive at the same operative temperature for the different supply temperatures, and therefore the lower resulting energy consumption from using lower supply temperature will also inevitably give a lower average temperature in the room. The lower average temperature can be a result of either too low temperatures, which will occur if the supply temperature simply cannot heat the room sufficiently, or it can be a result of less stored heat in the floor construction, which means that the room will not be overheated as the floor will stop emitting heat to the room when the room temperature is higher than floor surface temperature. Therefore a comparison of the energy consumption for different supply temperatures must include an assessment of the "type" of deviation to the desired temperature that causes the difference in the energy consumption. In this work this assessment has been presented in a graphical comparison of the duration curve of the temperature in the room showing the number of hours below a given temperature. Using this curve, two different supply temperatures can be compared to check if lower energy consumption is in fact an energy saving with fewer hours of too high temperature and not just caused by too low temperatures.

Combining the results

Combining the results from the investigation of the characteristic dimension and U- and ψ-value as well as the supply temperature to the floor heating system shows that finding the energy consumption and heat loss to the ground is a complex problem where all parameters influence the results. These results can be used for further development of the design of floor heating systems and floor constructions in which floor heating is used.

Since these results have been found for just one room size, they cannot simply be considered generally applicable, as they will also depend on the dimensioning heat loss and other parameters such as window areas and orientation, ventilation systems and strategies and more. However, all of these points can be addressed by analyses in FHSim, which has proven a powerful tool for this kind of investigations.

The results are based on buildings with energy consumption for heating between 40kWh/m² and 100kWh/m². An interesting further analysis would be to investigate buildings with even lower energy consumption, which would have a very large degree of self control. Therefore a control system would probably not be needed – the system will by itself maintain a

comfortable temperature if a constant supply temperature is upheld – perhaps with a simple strategy where the system is on during the day and off during the night. This would decrease the price of the floor heating system and enable a system with very little power output at a very low supply temperature.

A noteworthy result in this investigation is that for both the linear thermal transmittance, the characteristic dimension and the thermal transmittance, the fact that the floor is heated imposes a "penalty" on the energy consumption and heat loss to the ground. This shows that if a floor is heated, a better design is needed to avoid extra heat losses.

5.2.9 Conclusion

In this section, the validated floor model with an integrated heating system has been analysed in combination with the room model in FHSim. The purpose of the investigations has been to find the influence and importance of using a ground coupled model with respect to energy consumption of the entire model and heat loss to the ground.

Calculations have shown that in order to correctly find heat loss to the ground, it is necessary to model the dynamical conditions in the floor heating pipes. This in turn requires the coupling of the floor to a room model. For such analyses, FHSim is an ideal tool.

However, FHSim is a time consuming expert tool and it is therefore best suited for e.g. product development and research work, while it is too cumbersome for designing actual buildings.

The correct dynamical implementation also means that the calculation of the linear thermal transmittance needs to take the floor heating system into account. A method based on the Danish method described in DS418 (DS, 2002) for the calculation is sketched. However this will need further work before a general method can be proposed.

The calculations of energy consumption and heat loss to the ground have shown a large dependence of both U- and ψ-value as well as the characteristic dimension. In all three cases, the floor heating means that the absolute and relative values for the heat loss to the ground and energy consumption are larger for changes in the design than without floor heating.

5.3 Comparison of level of detail in simulation models

When performing building energy simulations a problem that will always arise is the level of detail needed for sufficiently accurate results for temperatures and energy consumption. A large number of considerations must be made with respect to the modelling. This is of course also the case for floor heating systems. Especially the inclusion of the floor heating pipe can be troublesome. The pipe can be included in different ways, either by a simple heat flux term or as a very complex inclusion of the pipe with fluid flow in the hydronic system coupled to a boiler. As the temperature in the pipe is not the same in the floor construction from supply to return, this must also be considered.

The simulation models of the floor with floor heating, can range anywhere from a simple resistance-capacitance thermal network with just a few nodal points to a three-dimensional finite difference, finite control volume or finite element model with thousands of nodal points. At the same time different level of detail can be included; these include ground coupling, inclusion of the pipe, "advancedness" of the boundary conditions and geometrical details.

In all cases it is important to consider the purpose. If the purpose is to make a preliminary assessment at an early stage in the design process, a simple model will be adequate, whereas a

much more detailed model is required if the influence of the floor heating system on the heat loss to the ground and through the foundation is needed.

In this investigation a number of simulation models with different level of modelling detail will be compared, using the simulation model in FHSim where the rest of the simulation model will be held constant. By only changing the floor model, the results from the calculations are directly comparable, since all other parameters and procedures are exactly the same. Therefore the influence on both energy consumption and heat loss to the ground can be found for the different models and consequently the results from the modelling types and techniques can be quantified and described.

5.3.1 Types

In this section the, different types of models are shown. As the numerical implementation of the models is fairly straightforward, this will not be elaborated further here. The boundary conditions are described separately in section 5.3.2.

Common for the simulation models are (except for the RC thermal network), that they are based on a Finite Control Volume (FCV) method for calculating heat flows and temperature distribution. The modelling approach has been described in detail in Appendix A.

This investigation only covers heavy floor heating systems.

Floor model to be simulated

The floor construction used in the modelling is shown in Figure 5.22. A double deck floor with the insulation layer between the decks is used for the modelling. The floor heating system is placed in the upper deck. The floor covering is made of a wooden parquet floor.

All floor models with different levels of detail presented below will model this floor construction with as many details as possible in that particular model. A common simplification for the 1D- and "1.5D"-models compared to the actual physical model is the omission of the lower concrete layer, which will not have a significant influence on the results, since the material properties of the concrete layer are close to those of the ground volume.

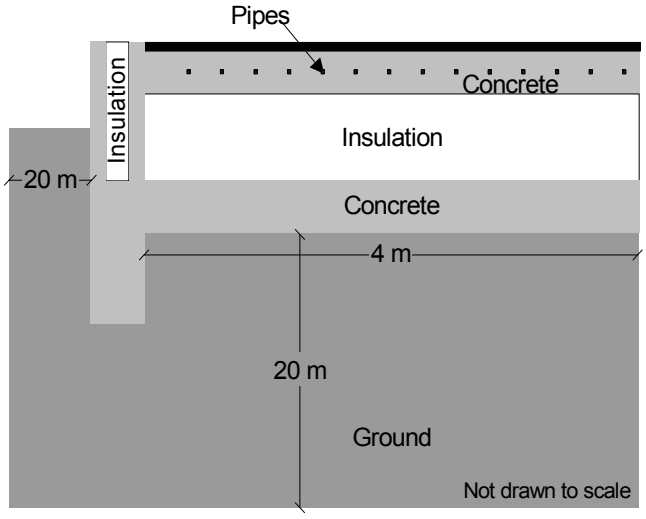

Figure 5.22 Floor construction used for the simulation models.

In the following sections, sketches of the different models used in the comparison are shown. In all cases, data for the construction can be found in Table 5.5 on page 86.

The conditions in the model are considered to be the average values for the entire floor construction, unless otherwise noted. Therefore in the hydronic models the temperature of the fluid in the pipe is calculated as the mean temperature of supply and return, which is calculated based on the flow rate and the temperature in the concrete next to the pipe.

1D model of electrical floor heating

The electrical model shown in Figure 5.23 has a 1D mesh definition. Floor heating is included as a supply of an energy flux directly in one of the nodal points in the concrete layer of the model. This approach is similar to that used in typical building energy simulation programs.

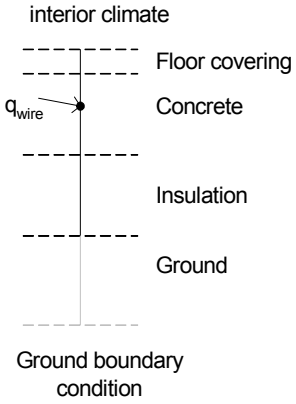

Figure 5.23 1D model with electrical implementation of the pipe.

1D model with pipe

Figure 5.24 shows the 1D model with the floor heating pipe using a FCV model. The pipe has been included as an extra nodal point which can interact with one of the nodal points in the 1D mesh. A thermal resistance is included between the pipe and the concrete. This resistance is difficult to accurately define and will be subject to an investigation later in the chapter.

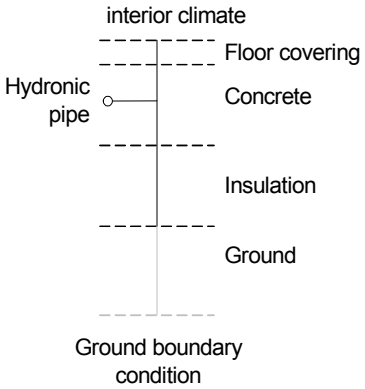

Figure 5.24 1D model with pipe included.

"1.5D" (2D section around pipe)

The 1.5D model has its name from the fact that it is a 2D model of the thermal conditions immediately around one pipe. All lines of symmetry have been used to make the section as small as possible, which is shown in Figure 5.25. "1.5D" therefore refers to the fact that the model is not a full 2D model of the floor, foundation and ground volume, but that it still has more detail than the 1D model.

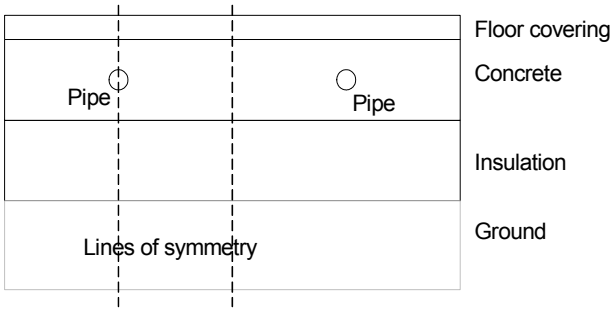

Figure 5.25 1.5D section showing the lines of symmetry.

The simulation model, which is implemented in FHSim, is shown in Figure 5.26. As for the 1D model with pipe, a thermal resistance between pipe and concrete can be defined. Here the purpose is to model the thermal resistance of the pipe itself and the internal convective resistance and not between the fluid and the average concrete conditions as for the 1D model.

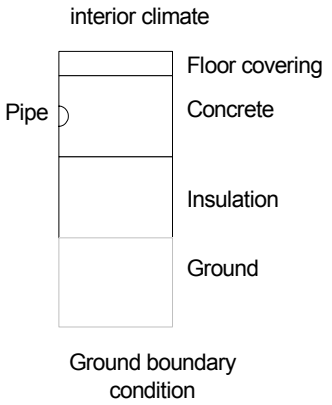

Figure 5.26 1.5D model with pipe included.

Serial "1.5D" models

The serial 1.5D model, shown in Figure 5.27, is a serial coupling of the 1.5D model. That is the outlet temperature in the pipe from the first section or element is used as input to the next. This is to compensate for the fact that the cooling in the pipe can result in different thermal conditions close to the inlet compared to the outlet. The surface temperature towards the room is found as the average of the surface temperatures in each of the sections, which is used for the calculation of the radiation heat exchange with the other surfaces in the room. For the calculation of the convective heat exchange with the room air, the individual surface temperature is used.

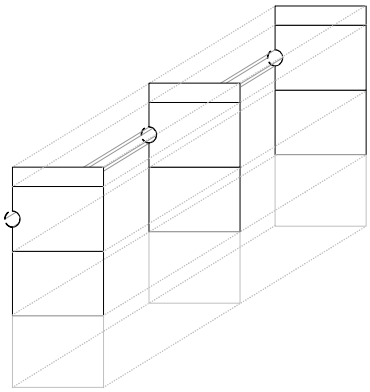

Figure 5.27 Serial coupling of the 1.5D model – here shown with three serial coupled 1.5D models or sections.

RC-thermal network model

In the RC-model resistances and thermal capacities are lumped together to simplify the modelling as much as possible, which is shown in Figure 5.28. Compared to the other models, this model uses fixed convective surface resistances to simplify the model even further.

As input, values for the thermal resistances and thermal capacities are based on simple assumptions of the resistances and capacities based on geometrical data. Therefore, each of the lumped thermal resistances are calculated as the sum of the thermal resistance of each layer, while the thermal capacities are based on the cross sectional area of the floor construction. However, as this initial estimation based simply on geometry is probably not very accurate, special attention must be paid to the values of the resistances and capacities. Especially the thermal resistance between the pipe and the upper node and the thermal capacity of the three nodes must be chosen carefully. This is also investigated below, where the properties have been fitted based on calculations using the 1.5D model.

The inclusion of the foundation is based on EN ISO 10211 (CEN, 1994; CEN, 1995), where the heat flow from a given construction can be split into three components; one-, two- and three-dimensional for areas, linear and point heat losses. In this model the one- and two-dimensional heat flow is considered as the heat loss to the ground is the one-dimensional part and the heat loss to the foundation is considered two-dimensional part. The length of the two-dimensional heat loss is taken as the length of the foundation towards the outside condition.

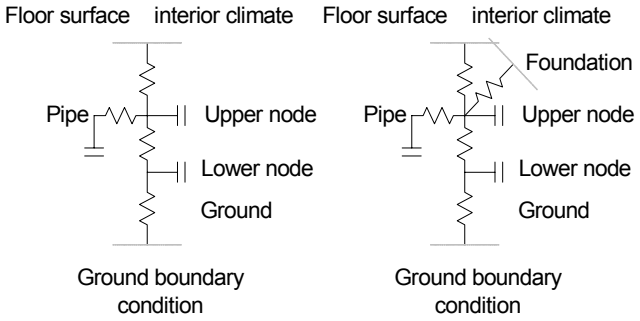

Figure 5.28 Simple RC-model with and without influence from foundation.

2D ground coupled model

The ground coupled model is shown in Figure 5.29. This model is the most detailed in this comparison. The model is identical to the model used in section 5.2.

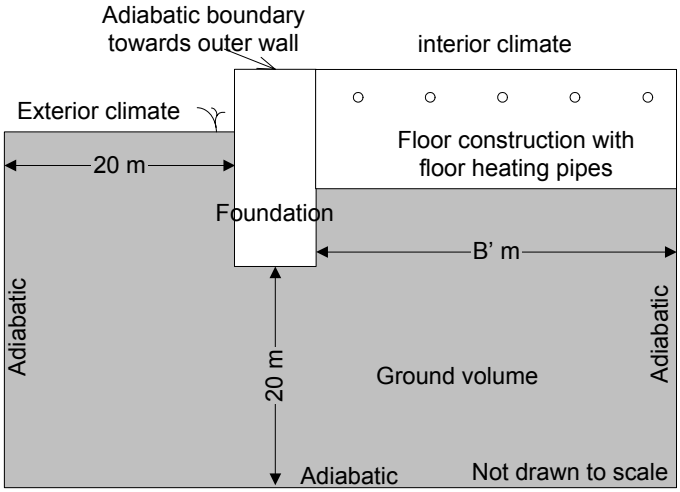

Figure 5.29 2D ground coupled model showing the dimensions and boundary conditions.

The model of the 2D ground coupled floor construction is also used to calculate the conditions in a model without floor heating.

5.3.2 Boundary conditions

Five different types of boundary conditions towards the ground are applied to the floor models are shown in Table 5.5. The different boundary conditions are included to test the influence on the heat flow to the ground.

Table 5.5 Boundary conditions towards the ground and/or foundation used in the simulation models presented here.

Boundary condition name	Boundary condition number	Linear thermal transmittance of foundation	Ground temperature	Thermal resistance	Ground heat loss
Simple	1	-	10	1.5	As found in model
1 m ground volume	2	-	10	1.0	As found in model
EN ISO13370	3	As described in EN ISO13370	Adiabatic	Adiabatic	Found from the fixed part of the heat loss
Full 2D model	4	As described in DS 418	Dynamic based on the outdoor temperature	Dynamic based on the outdoor temperature	As found in the model
Foundation included	5	Uses the same value as for type 4	10	1.5	As found in the model

The simplest boundary condition has a ground temperature of 10°C and a ground thermal resistance of 1.5m²K/W, as defined in DS418. To include the dynamic properties of the ground volume directly below the floor construction, a second version has a 1m ground volume below the floor construction. The ground temperature is still set to 10°C, but the ground thermal resistance is lowered to 1.0 m²K/W to correct for the extra insulation introduced by the ground volume.

The foundation and ground volume is included in the procedure based on EN ISO13370. Here a detailed calculation of the average heat loss to the ground is performed, and this value is held constant during the entire simulation period of one year. The dynamic part is included by using the floor model with 1m ground volume, but with an adiabatic boundary condition towards the ground. The constant heat loss from the floor construction (the average value found from the two-dimensional calculation) is included in the dynamic simulation model as a negative heat flux from the heat balance for the room air.

In the two-dimensional model, the boundary condition towards the ground actually does not exist. Instead the outdoor temperature is applied to the ground surface, while the bottom and sides of the ground volume are assumed adiabatic. Finally the influence of the foundation can be included in the RC thermal network model by adding an extra term to the equation system. This extra term is added as a resistance on the concrete layer with the floor heating system.

5.3.3 Comparison of models

Table 5.6 shows the definition of the simulation models used in the model comparison. A total of 17 models will be compared. The models are grouped with three models for each of the types 1D electrical, 1D pipe, 1.5D pipe, RC and serial 1.5D. These three models differ in the boundary conditions towards the ground, based on boundary condition type 1, 2 and 3, as

defined in Table 5.5. However, for the RC thermal network models, the type 2 boundary condition has been replaced by type 5 where the ψ-value of the foundation is included instead of 1m of ground volume. The sets of three model numbers will be referred to as 'groups' in the following. In total these variations will enable a comparison of the boundary conditions in the simulation models. Finally the two 2D models with ground volume and foundation with and without floor heating are included to bring the total up to 17 models.

Table 5.6 Model comparison of the 17 simulation models, based on the five simulation models presented above with different boundary conditions towards the ground as described in Table 5.5.

Model-number	Type	Floor heating type	Ground boundary condition implementation	Ground boundary condition number	Nodal points	Convective surface resistance
1	1D electrical	electrical	none	1	9	variable
2	1D electrical	electrical	1 m	2	14	variable
3	1D electrical	electrical	according to EN ISO13370	3	14	variable
4	1D pipe	pipe	none	1	10	variable
5	1D pipe	pipe	1 m	2	15	variable
6	1D pipe	pipe	according to EN ISO13370	3	15	variable
7	"1.5D"	pipe	none	1	112	variable
8	"1.5D"	pipe	1 m	2	147	variable
9	"1.5D"	pipe	according to EN ISO13370	3	147	variable
10	2D with ground volume	pipe	full 2D	4	3328	variable
11	2D with ground volume	no floor heating	full 2D	4	3328	variable
12	RC	pipe	none	1	5	fixed
13	RC	pipe	with ψ-value	5	5	fixed
14	RC	pipe	according to EN ISO13370	3	5	fixed
15	Serial "1.5D"	pipe	none	1	5 x 112	variable
16	Serial "1.5D"	pipe	1 m	2	5 x 147	variable
17	Serial "1.5D"	pipe	according to EN ISO13370	3	5 x 147	variable

In the table, the number of nodal points used for the different types are also shown as well as the internal convective boundary condition towards the room air. With the exception of the RC thermal network models, these are variable based on a correlation of the actual temperature difference between room air and surface temperature.

Simulation time step

All simulations have used a time step of 1800 seconds or 30 minutes. A few simulations have been carried out using other time steps to investigate the influence from this parameter. This will be clearly pointed out where relevant.

Control system

As far as possible, the same control algorithm is used for all models. However, as different parameters are controlled (power or supply temperature depending on the inclusion of the pipe), it is not possible to use the same control for all simulation models. Nevertheless, in all cases an on-off type control with a dead band is used.

5.3.4 Simulation model

The 17 models have each been used in a room with the data shown in Table 5.7 and Table 5.8. Two different models have been investigated with the only difference being the fact that one model has a heat recovery unit on the ventilation system while the second does not. These two variations will be referred to as 'without heat recovery unit' or 'model with high energy consumption' for the first variation, while the second will be referred to as 'with heat recovery unit' or 'model with low energy consumption'. In the figures, heat recovery unit will be abbreviated by 'hru'.

Table 5.7 Areas and U-values of walls, windows, floor and ceiling.

Property	U-value	Area
Floor area	-	30 m²
Window 1	1.44W/m² K	4 m²
Window 2	1.45W/m² K	2.5 m²
Outer walls	0.18W/m² K	20.9 m²
Inner walls	-	27.5 m²
Ceiling	0.10W/m² K	30 m²
Floor	See Table 5.9 and Table 5.10	30 m²

Table 5.8 Air handling in the models, where the difference is that one has a heat recovery unit on the ventilation air while the second does not.

Air handling	Air change rate	Ventilation type
Ventilation	0.5 ACH	Heat recovery unit efficiency 0.8 ('hru') Heat recovery unit efficiency 0 ('no hru')
Infiltration	0.1 ACH	
Venting	up to 4 ACH when Troom>26°C	

Table 5.9 shows the material properties and physical dimensions of the floor construction.

Table 5.9 Material properties of floor construction.

Material	Heat conductivity	Density	Specific heat	Thickness
Insulation	0.039W/mK	50kg/m³	850J/kgK	0.15/0.25/0.35m
Concrete	1.6W/mK	2300kg/m³	900J/kgK	0.10m
Floor covering (wood)	0.17W/mK	600kg/m³	2500J/kgK	0.022m
Ground (where applicable)	2.0W/mK	2000kg/m³	1000J/kgK	-

As indicated in Table 5.9 all simulations have been performed with three different insulation thicknesses. For each of the three insulation thicknesses the thermal transmittance of the floor construction (U-value) and the linear thermal transmittance of the foundation (ψ-value) have been calculated based on the description in section 5.2.3. This is shown in Table 5.10.

Table 5.10 U-value and linear thermal transmittance in the floor models.

Insulation thickness in floor construction [mm]	Linear thermal transmittance of foundation [W/mK]	U-value [W/m²K]
150	0.15	0.17
250	0.13	0.12
350	0.12	0.09

For comparison, the allowed maximum value of the U-value in the current Danish building regulation is 0.15W/m²K, while the allowed linear thermal transmittance should not exceed 0.20W/mK. Therefore these values represent constructions that meet the current requirements but also future constructions.

Three different supply temperatures have also been tested in the simulations. These are 35°C, 45°C and a variable supply temperature based on the outdoor temperature, where a lower temperature is used when the outdoor temperature rises, as can be seen in Table 5.11.

The maximum output of in the electrical floor heating system is 80W/m² when the system is turned on. However, if the floor surface temperature is above 27°C the system will be turned off as a precaution.

Table 5.11 Supply temperatures in models for the implementations using a pipe and maximum heat flux from "electrical" implementation of the system. All values shown for the system when it is turned on.

Type of supply temperature	Without heat recovery unit	With heat recovery unit
Constant	35°C	35°C
Constant	45°C	45°C
Variable	$-0.54 \cdot T_{out} + 33.6$ °C	$-0.33 \cdot T_{out} + 30.2$ °C
Electrical	80W/m²	80W/m²

Two fix points are used to find the variable supply temperature as a linear function of the outdoor temperature. The high fix point is defined as the required supply temperature when the outdoor temperature is -12°C to uphold a room temperature of 21°C; the second is simply a supply temperature of 25°C when the outdoor temperature is 16°C. This is shown in Figure 5.30. To give an idea about the actual supply temperatures used in the system, the duration curve for the accumulated hours of temperatures below a given outdoor temperature in the Danish Design Reference Year. As an example, the supply temperature will only be above 32°C for around 300 hours a year corresponding to an outdoor temperature of –5°C, assuming the system is turned on.

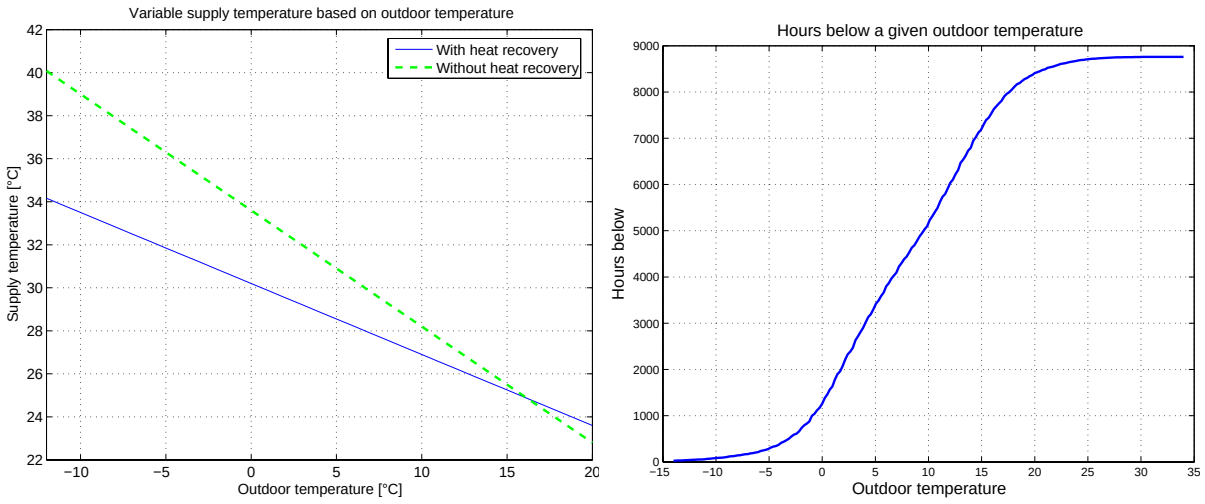

Figure 5.30 Variable supply temperature based on outdoor temperature to the left and the accumulated hours of temperature below a given temperature to the right based on the Danish Design Reference Year.

Floor heating control

In all simulations a temperature set point of 21°C on the room air temperature has been used in the simulations with a dead band on the temperature control of 0.25 K. This means that the

temperature will not be turned on before the temperature drops below 20.75°C and not turned off before reaching 21.25°C. During the summer period from May 13 until September 24 the system is never turned on.

5.3.5 General comparison of models

The comparison starts by a general overview of the results from the simulations with focus on the energy consumption. In the following sections, the differences are analysed further to find both the differences in the models but also to generally analyse floor heating systems and numerical modelling of floor heating systems.

Energy flows

Figure 5.31 shows the energy flows in the simulation model for one of the simulation models with heat recovery unit. The passive gains are solar gain and the internal heat gain while the "heat to pipes" represents the heat used to heat the building through the floor heating system. The losses are split into transmission losses through walls and ceiling, windows and ground; while ventilation, infiltration and venting represent the airborne heat losses. The values are shown for the heating season, which in the Danish Design Reference Year is defined to be from September 24 to May 13.

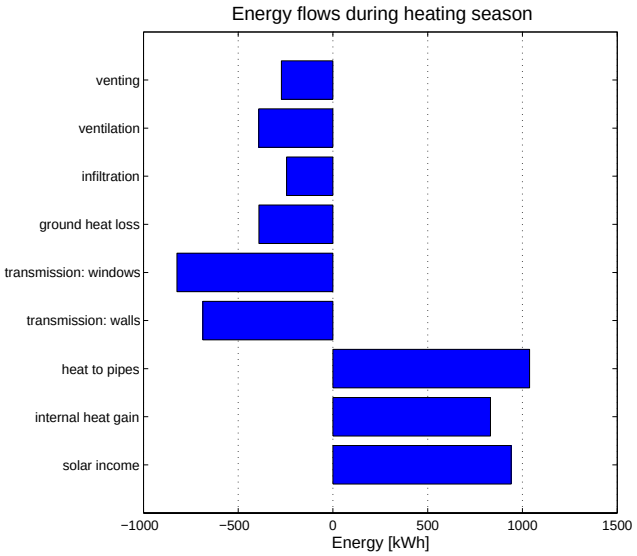

Figure 5.31 Energy flows in model shown for the 2D model with heat recovery unit on the ventilation.

Energy consumption and heat loss to the ground

Figure 5.32 and Figure 5.33 show the energy consumption for the seventeen different variations of the floor model with the three different insulation thicknesses. A supply temperature of 35°C is used in the floor heating pipes. The first figure shows the results for the model without heat recovery unit which has the largest energy consumption while the second figure shows the results with heat recovery unit on the ventilation air.

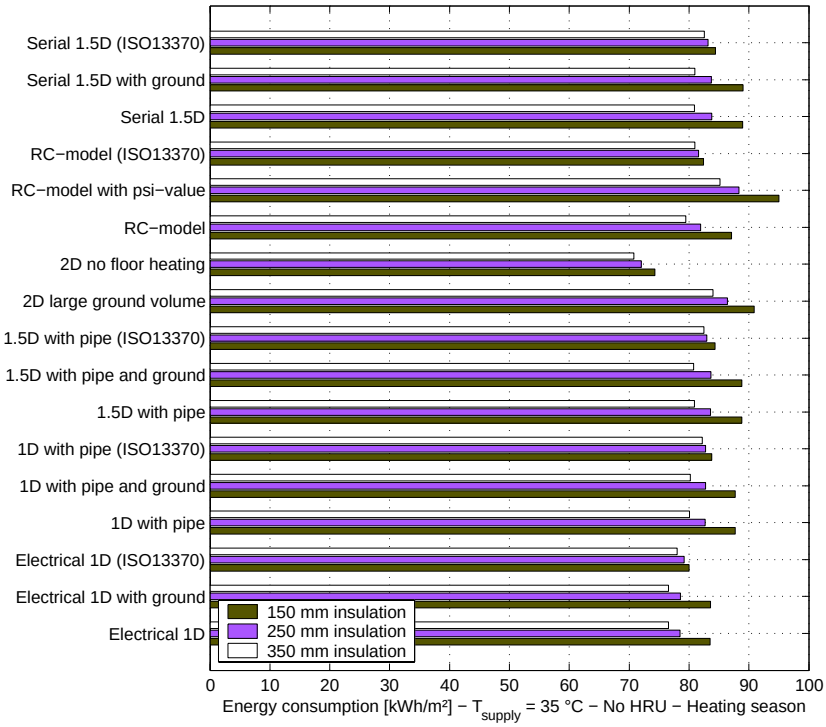

Figure 5.32 Simulated energy consumption using the different simulation models without heat recovery unit on the ventilation system.

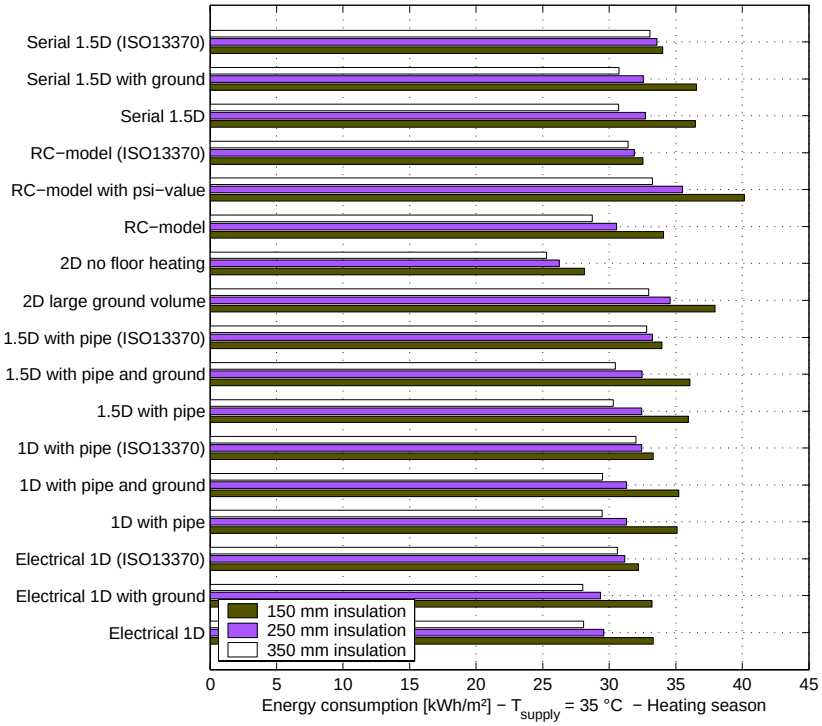

Figure 5.33 Simulated energy consumption using the different simulation models with heat recovery unit on the ventilation system.

The energy consumption is around 80kWh/m² for the model without heat recovery unit, while it is around 30kWh/m²-35kWh/m² for the model with heat recovery unit. The results are most uniform for the high energy consumption regardless of model type and insulation thickness. For the model with low energy consumption the differences are larger relative to the total energy consumption.

The smallest energy consumption in both figures are for the ground coupled 2D model without floor heating, where the heat is supplied directly in the room air zone, which will give a lower energy consumption as the temperature in the room is controlled perfectly to the set point temperature. The lowest values with floor heating are found in the models with the electrical inclusion of the floor heating system. This is due to the fact that electrical floor heating has faster reaction time than using hydronic systems. Also notice, that the basic RC-model has lower energy consumption than the other models. The highest energy consumption is found in the 2D model with large ground volume and in the RC-model with the linear thermal transmittance included. This is a natural consequence of the inclusion of the foundation in these two models. The models based on ISO13370 have smaller energy consumption than these two models, even though they also have the foundation and ground volume included.

The energy consumption found in the 1D and 1.5D models is almost the same when comparing the three different models from each group. The serial 1.5D models can also be seen to give almost the same results as the 1.5D model which only uses a single model.

The difference in the energy consumption when the insulation thickness is changed is also shown in the figures. As expected, all models have smaller energy consumption when the insulation thickness is increased, but the rate of decrease is very different in the models. All models based on EN ISO13370 have small differences in the energy consumption with the different insulation thickness compared to the other models in the same group. This is also the case with the 2D model without floor heating. As opposed to this, the difference for the 2D model with floor heating and the RC-model is much larger when the insulation thickness is changed. This is especially the case when going from 150mm insulation to 250mm insulation with low energy consumption.

It can also be noticed that comparing the results in the models for the different insulation thicknesses gives very different results. As an example the 2D model with floor heating and the RC-model with linear thermal transmittance can be compared in Figure 5.33. For an insulation thickness of 350mm the energy consumption is almost the same for both, while the results are very much different for 150mm insulation thickness.

Looking at the different insulation thicknesses in Table 5.12 individually – the average, maximum and minimum values of the simulated energy consumption for the models with floor heating – very large differences can be found. For the model without heat recovery, the difference is almost 11-15kWh/m². For the model with heat recovery it is more stable around 6-8kWh/m².

Table 5.12 Average, maximum and minimum value of the energy consumption in the 16 different floor construction models with floor heating.

	Insulation thickness [mm]	Average [kWh/m²]	Maximum [kWh/m²]	Minimum [kWh/m²]
Without heat recovery	150	86.8	95.0	80.0
	250	82.8	88.4	78.5
	350	80.8	85.5	76.6
With heat recovery	150	35.2	40.2	32.2
	250	32.3	36.2	29.3
	350	30.8	34.4	28.0

In Figure 5.34 and Figure 5.35, only the heat loss to the ground is shown. Here the differences are more obvious than for the total energy consumption. It especially becomes obvious how the insulation thickness influences the heat loss to the ground.

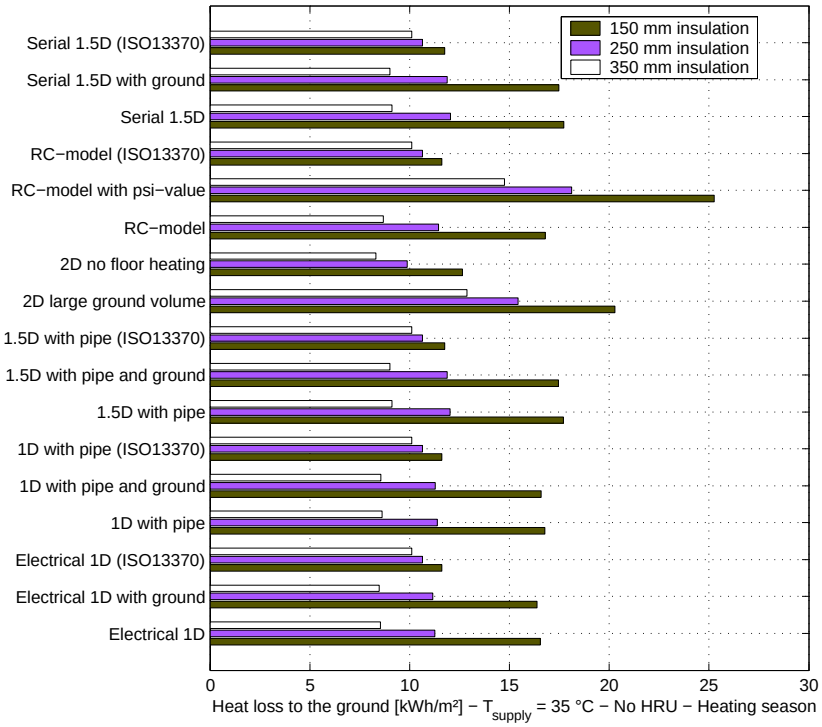

Figure 5.34 Simulated heat loss to the ground using the different models for models without heat recovery unit on the ventilation system.

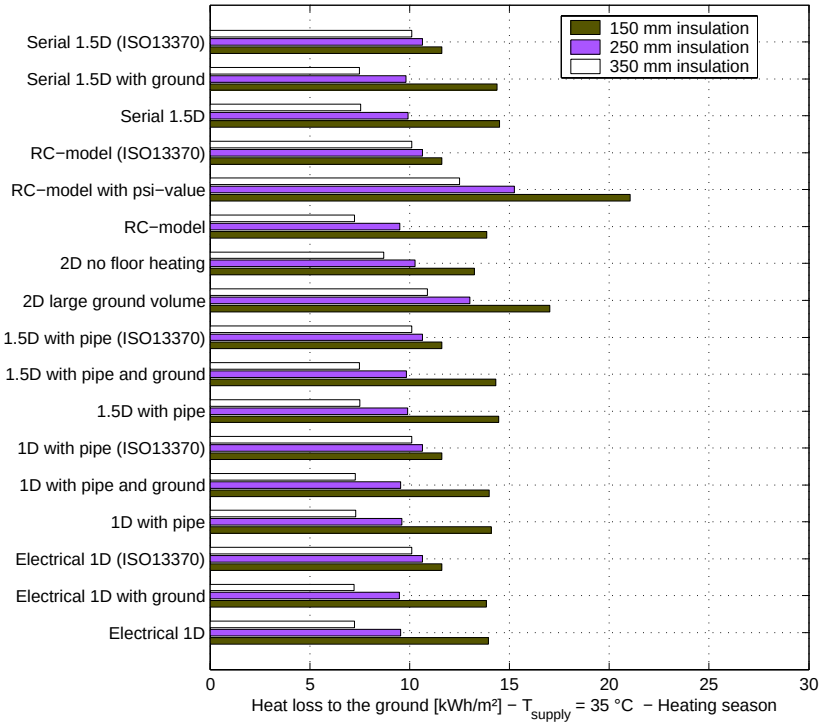

Figure 5.35 Simulated heat loss to the ground using the different models for models with heat recovery unit on the ventilation system.

The heat loss to the ground for the models without foundation and ground volume is lower than the models where this is included. Generally the differences between the models are smaller for larger insulation thicknesses. Models based on EN ISO 13370 again have smaller difference between the heat losses for different insulation thicknesses.

Comparing the 2D models with and without floor heating, it can be seen that floor heating have larger heat loss to the ground, which is as expected since the floor temperature is higher. Generally the heat loss to the ground in the model without floor heating is around 85% of the heat loss with floor heating in the model with low energy consumption, while it is around 75% for the model with high energy consumption. This means that that since the floor is not heated as much for the low energy consumption as it is for the high energy consumption, the relative difference in the ground heat loss is also smaller for the house with low energy. At the same time it has been found that the relative difference is independent of the supply temperature to the floor heating system. This is not shown in the figures.

It is noticed, that even though the total heat loss is more than twice as large for the model without heat recovery unit on the ventilation system, the heat loss to the ground is almost the same, differing by less than 10% in most cases. For the models based on ISO13370, the heat loss to the ground is the same both for the model with high and low energy consumption, since the average concrete temperature is not calculated separately in the two models.

Similar to Table 5.12, Table 5.13 shows the average, minimum and maximum values of the ground heat loss for the models with floor heating. Especially for the small insulation thickness it is obvious that the models have large differences, where the minimum value is only about half of the maximum value.

Table 5.13 Average, maximum and minimum value of the heat loss to the ground in the 16 different floor construction models with floor heating.

	Insulation thickness [mm]	Average [kWh/m²]	Maximum [kWh/m²]	Minimum [kWh/m²]
Without heat recovery	150	24.2	35.8	18.3
	250	18.2	25.7	16.7
	350	15.0	20.9	13.2
With heat recovery	150	22.1	31.6	18.3
	250	16.8	22.9	15.4
	350	14.0	18.6	11.8

Finally, the ratio of the heat loss to the ground to the total energy consumption has been calculated for the models. This value is 10% to 20% for the model with large energy consumption, while the corresponding values are 25% and 50% for the model with low energy consumption; largest for the model with the low energy consumption. A heat loss of up to 50% through the ground and foundation of the total energy consumption in new buildings with low energy demand is comparable to findings in other works as described in Chapter 3.

Dynamic response for the different models

The response is compared through the time constant. In this case, the flow is turned on from a steady state situation where the room is at 21°C and the ground is at 10°C. The pipe temperature is set to 35°C. The time constant – which has been defined in Chapter 3 as the time it takes for a step change to reach $1-e^{-1}$ 63.2% of the final value when the unit step change is applied as input – is almost the same in all cases ranging from 4 to 5 hours, with the RC-model being the fastest and the serial models being slowest of the models with pipe implementation. The electrical implementation has a slower reaction time because the heat output from the "pipe" is constant once it has been turned on. This is not the case in the hydronic models, where the maximum heat output peaks right after the flow has been turned on and drops towards a steady-state value hereafter. It should be noticed that the time constant very much depends on the value of the thermal resistance between fluid and concrete. However, this value is very difficult to estimate. In fact, by changing the value from a "low"

to a “high” value, the time constant for the 1D model changes from 3.5 to 5 hours. However, the energy consumption only changes by about 4% in a yearly calculation. Because of the lack of a better value, the value in the 1D model is set to 0.1m²K/W between the pipe and concrete. The thermal resistance between pipe and concrete deck is therefore important for finding the time constant, while it is not important with respect to the energy consumption.

Figure 5.36 shows the operative temperature for all models. One curve stands out; namely the one representing the model without floor heating. Because of the lower radiant temperature, the operative temperature is lower than for the models with floor heating. Generally the temperature can be controlled to above 21°C, which is the set point temperature for the room air temperature. The models have nearly the same peaks during periods with solar gains, differing by less than 1 K. Without solar gains during an entire 24 hour period, as is the case between approximately hour 1475 and 1500, the models have different temperature courses.

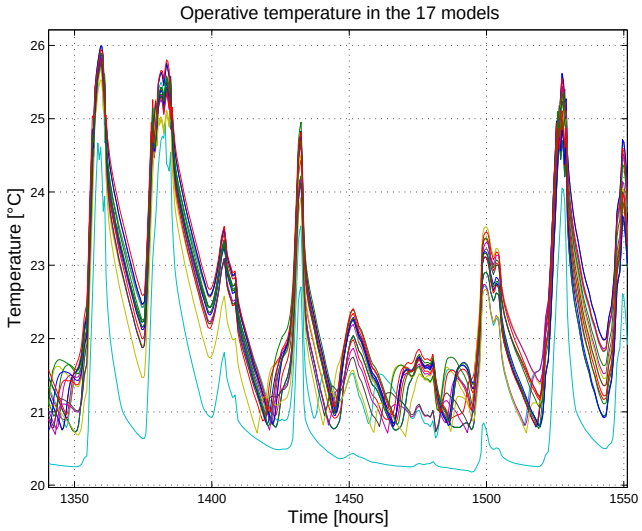

Figure 5.36 Operative temperature in the 17 simulation models. It is not indicated which temperature profile belongs to which model, as it would not be possible to make distinctions between them.

During the summer period, the temperature profiles are almost identical, regardless of type, indicating that when the heating system is turned off the models have almost the same behaviour, which is shown in Figure 5.37.

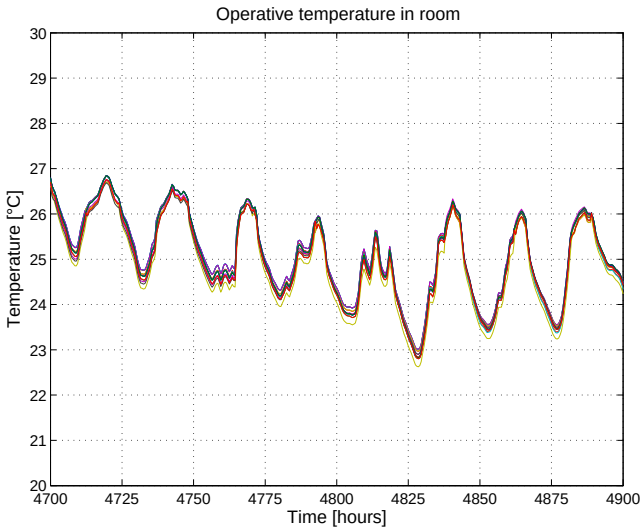

Figure 5.37 Operative temperature during summer period.

Supply temperature

Figure 5.38 and Figure 5.39 show the energy consumption with 250mm insulation for three different supply temperatures, 35°C, 45°C and variable, as shown in Figure 5.30. The models with electrical floor heating and the 2D model without floor heating have the same energy consumption regardless of the supply temperature, as this parameter is not used as input. In almost all cases, the energy consumption is lowest for the variable supply temperature and highest with 45°C. This is as expected and in accordance with the description in Chapter 3.

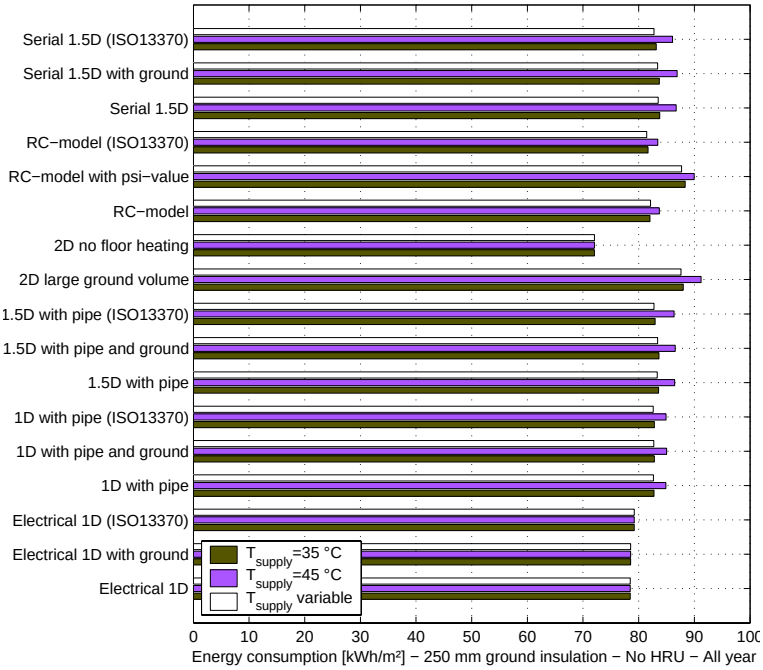

Figure 5.38 Simulated energy consumption for the different floor models with different supply temperatures – here shown for 250mm insulation without heat recovery on the ventilation air.

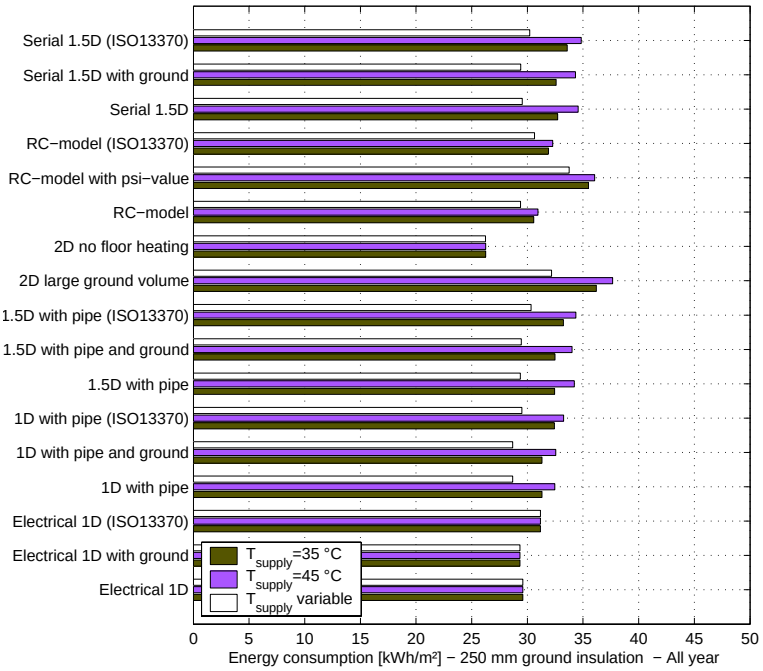

Figure 5.39 Simulated energy consumption for the different floor models with different supply temperatures – here shown for 250mm insulation with heat recovery on the ventilation air.

A very relevant discussion when comparing the calculated energy consumption with different supply temperatures is that the thermal comfort has **not** been the same. Therefore, a model with larger energy consumption will have higher average temperatures. However, this will not necessarily lead to a higher level of thermal comfort, as the higher temperature is a consequence of more inaccurate control of the indoor temperature. To assess the thermal comfort, a duration curve or temperature distribution curve during the heating season can be used. Figure 5.40 shows this curve for model type 7 using three different supply temperatures; 35°C, 45°C and variable. The curve shows the number of hours during the heating season below a given operative temperature. For instance, there are approximately 2000 hours during the heating season when the operative temperature has been 22°C or less for the case with 45°C supply temperature in the right figure. The figures show the temperature distribution during the heating season from Sep. 24 to May 13, approximately 5500 hours.

The left figure shows the model with high energy consumption, while the right figure shows the model with low energy consumption. In all cases, there are very few hours with temperatures below 20°C or even 21°C, which is satisfactory seen from a thermal comfort point of view. However, especially for the right figure, it is obvious that the supply temperature has a large impact on the distribution of the operative temperature during the heating season, as there is a large difference between the number of hours below 22°C with 2000 hours with 45°C supply temperature and just over 3000 hours with the variable supply temperature. This means that there are many hours with too high temperatures for 45°C supply temperature. As it can be seen in Figure 5.39, the difference in energy consumption from the variable supply temperature to 45°C is approximately 10%.

The right figure shows a more even distribution of the operative temperature in the room, which can also be seen in Figure 5.38, as the models differ less in the energy consumption, though with a larger value for 45°C than for the other two. Therefore the results for a building with low energy consumption are more influenced by a high supply temperature.

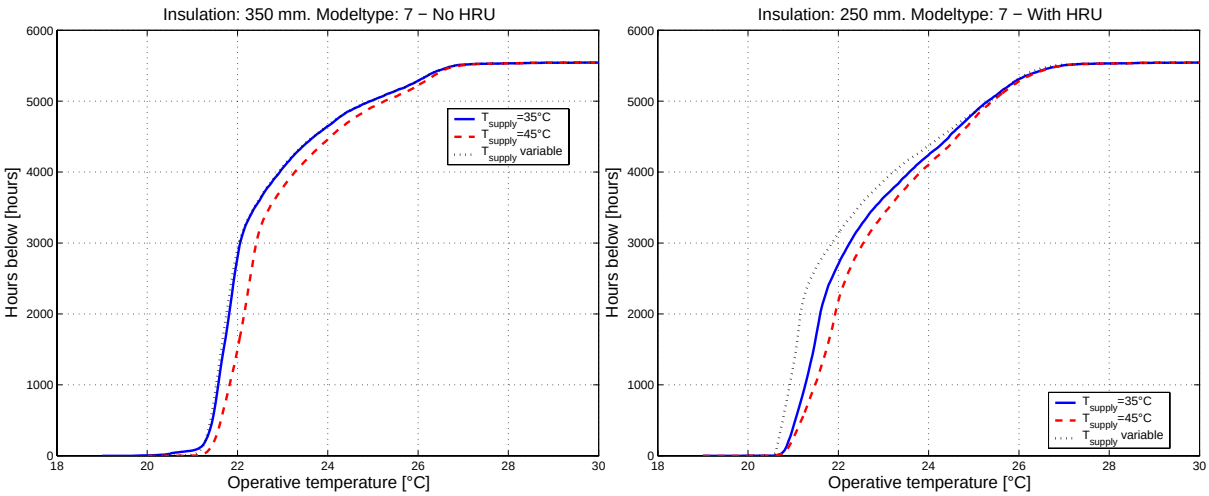

Figure 5.40 Operative temperature distribution curves for three different supply temperatures, based on the 1.5D model without ground volume. The data with high energy consumption are shown to the left.

If the curves are compared for the two models, notice that the model with low energy consumption (the right figure) has a sharper curve around 21°C than for the model with high energy consumption. This indicates that the control is more efficient, as there are basically no hours with low temperature. Further, the heating system can easily supply sufficient heat to ensure that the set point temperature can be upheld. For the model without heat recovery unit there are around 100 hours with temperatures below 21°C for the variable and 35°C supply

temperature. The upper part of the distribution curves (above 24°C) shows almost the same behaviour for both high and low energy consumption, a consequence of the fact that for high temperatures the solar gains almost exclusively decide the temperature in the room.

Room temperatures with and without floor heating

The temperatures in the room are very different comparing the model with and without floor heating. Figure 5.41 shows three different supply temperatures (35°C, 45°C and variable) along with the model without floor heating. The set point temperature is an air temperature of 21°C. The most obvious difference is the floor surface temperature, which is much lower for the model without floor heating. Here the lowest temperature is 19.5°C compared to 21°C for the models with floor heating. Notice that 19°C is still above the lower comfort limit for floors as described in Chapter 3. It can also be seen how large the influence from the lower floor surface temperature is on the mean radiant temperature, as the number of hours below any temperature is considerably larger than when floor heating is present.

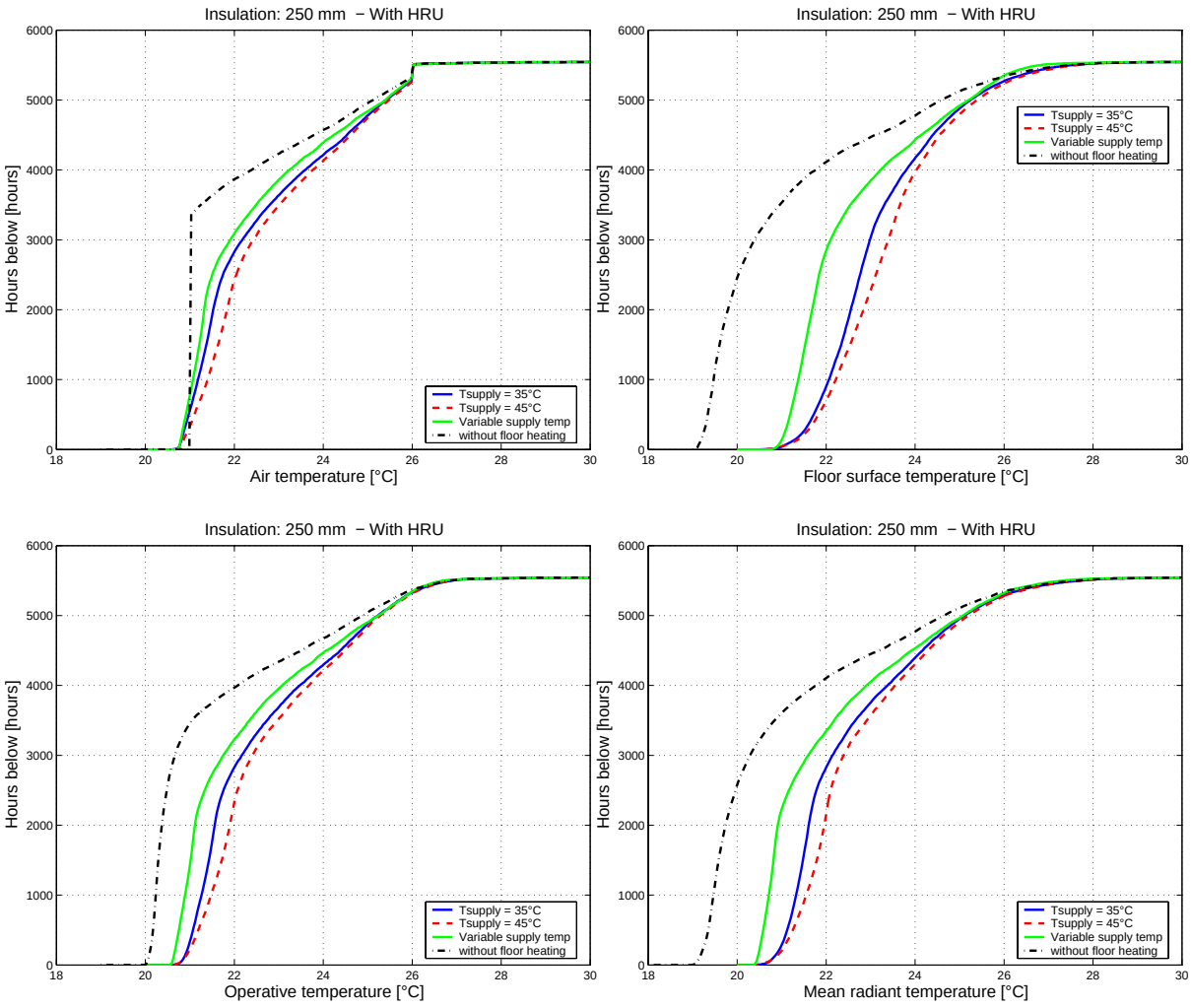

Figure 5.41 Comparison of temperature distribution of air, floor surface, operative and mean radiant temperature for model type 10 and 11 with and without floor heating respectively

The function of the heat supply to the model without floor heating can be seen in the upper left part of Figure 5.41 for the air temperature where there is a straight line at 21°C with 0 hours below this limit.

The maximum room air temperature is 26°C is achieved by increasing the ventilation rate to ensure that the temperature reaches 26°C.

It is very important to notice that this comparison to an "ideal" heating system is not realistic, because of the way the heating is supplied to the room – namely by a perfect control which ensures that the room air temperature is always precisely 21°C when heating is required. Such a heating system would need to have an infinitely fast reaction time, which is of course not possible. A heating system with radiations placed under the windows on the outer walls will also not be able to control the temperature accurately at the desired set point and will due to its higher temperature also give a higher heat loss through the outer wall and window. Comparisons of different heating systems have been carried out in papers and reports, mentioned in Chapter 3. Here it is only important to notice that model type 10 with "ideal" heating is **not** possible.

Simulation time

The simulation time for the program execution is shown in Figure 5.42. The 2D models are by far the most time consuming. The 1D and RC models are approximately 10 times faster, while the 1.5D models are about 7 times faster and the serial 1.5D model is around 5 times faster. The simulation time in FHSim for the 2D model is approximately 45 minutes on a 3.4 GHz Pentium 4 processor for one year of simulation. The fastest models have a simulation time of approximately 5 minutes. Notice also that the 2D models typically require five years or more of simulation before the conditions in the ground volume are periodic stationary, which further means that a long extra simulation time is needed for these models.

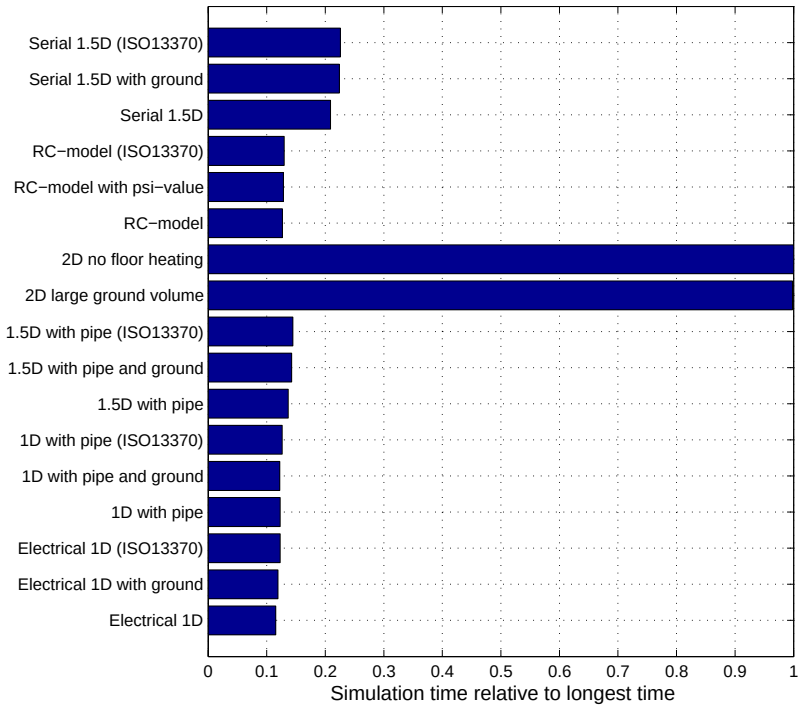

Figure 5.42 Relative simulation time for entire simulation program. The longest simulation time is approximately 45 minutes.

Figure 5.43 shows the simulation time for the models relative to the 2D model (type 10), for the floor model only. The rest of the simulation program has not been included. Notice, that data is shown in a logarithmic scale because of the large differences in the simulation time. The simulation time varies by a factor of over 100 between the fastest RC thermal network models (type 12-14) to the 2D models (10-11). The 1D models (type 1-6) have almost the

same simulation time, while the 1.5D models (type 7-9) are 6 to 7 times slower. The serial models (type 15-17) with five serial coupled 1.5D models are around 5 times slower than the 1.5D models.

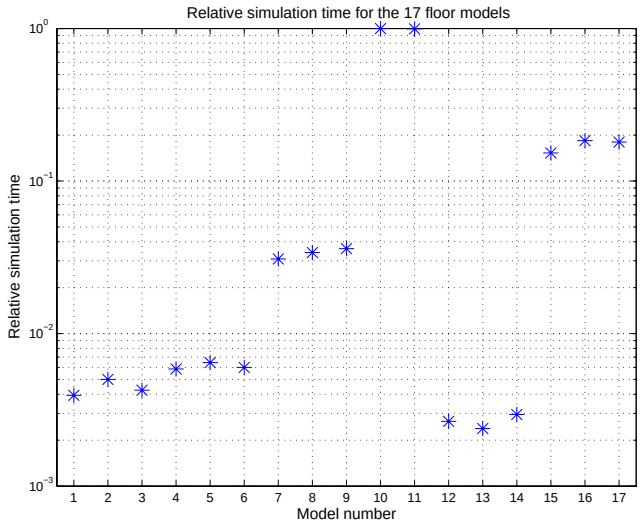

Figure 5.43 Relative simulation time shown in a logarithmic scale for the floor model only.

Notice, that the relative differences are smaller when the entire program is included than for just the floor model. This is due to the fact that the rest of the simulation model is identical in all cases.

5.3.6 Individual comparison of models

This section compares differences caused by the model definition.

Electrical or pipe inclusion of floor heating pipe

A common simplification when modelling floor heating is to use an “electrical” inclusion of the floor heating system where a heat flux is supplied in the floor construction instead of using a floor heating pipe with a fluid with a given temperature. For this comparison, the two 1D models with electrical and pipe and the 1.5D model with pipe are compared.

Figure 5.44 shows the duration curves for these three models. The figure shows that the two models with hydronic inclusion of the floor heating system show almost the same behavior, while the electrical model tends to have lower temperatures during the heating season. At the same time, it can be noticed that there are only very small differences between the temperature distribution for the 1D and 1.5D models with pipe included.

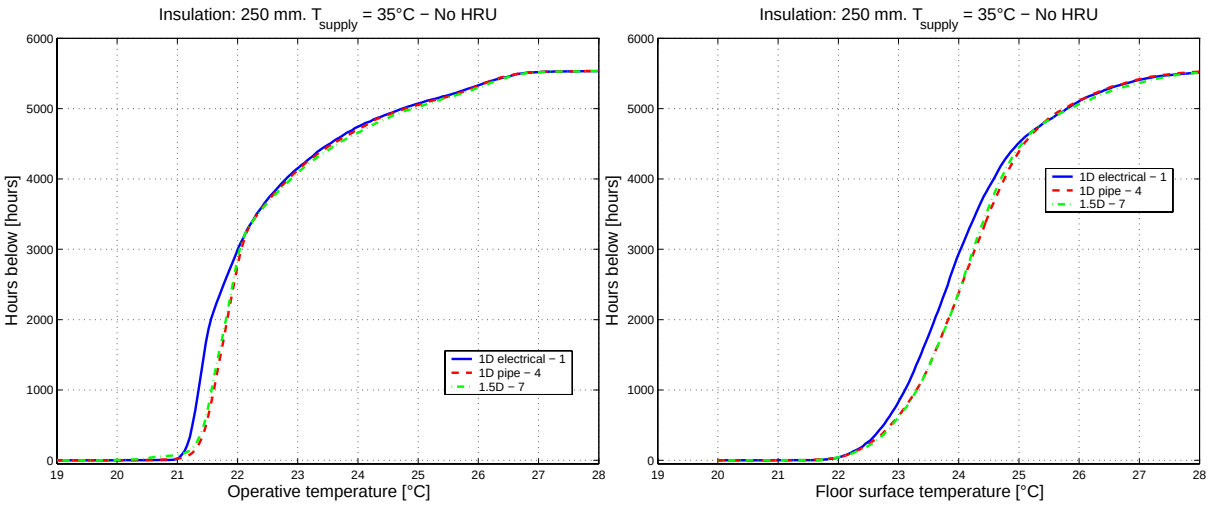

Figure 5.44 Comparison of 1D model with electrical inclusion of pipe, 1D with hydronic inclusion and 1.5D model. The numbers in the legend refer to the model number as defined in Table 5.6.

The more efficient control of the floor heating system can also be seen in Table 5.14 where the energy consumption and the heat loss to the ground are compared for the models with and without heat recovery unit for three insulation thicknesses. In all cases, the 1D electrical models have lower energy consumption and heat loss to the ground. The energy consumption is typically around 5% lower than the 1D/1.5D model with pipe. The heat loss to the ground is mainly influenced by the temperature of the concrete deck, as this will almost always be the highest temperature in the floor construction. This means that the average concrete temperature is lower for the model with electrical floor heating, which indicates a more efficient control.

Table 5.14 Comparison of total energy consumption and heat loss to the ground during the heating season using the 1D (type 1) electrical, 1D pipe (type 4) and 1.5D pipe (type 7) models.

Energy consumption	Insulation thickness	1D electrical [kWh/m²]		1D pipe [kWh/m²]		1.5D pipe [kWh/m²]	
		Total	Ground	Total	Ground	Total	Ground
With HRU	150mm	33.3	14.0	35.1	14.1	36.0	14.5
	250mm	29.6	9.5	31.3	9.6	32.4	9.9
	350mm	28.1	7.2	29.5	7.3	30.3	7.5
Without HRU	150mm	83.6	16.6	87.7	16.8	88.8	17.7
	250mm	78.5	11.3	82.7	11.4	83.6	12.0
	350mm	76.6	8.5	80.1	8.6	80.9	9.1

Another difference is that the peak value of the heat supply to the room is limited by the allowed maximum peak value, where the maximum heat supply from the pipe is given by the actual temperature difference between pipe and surrounding concrete. This difference is shown in Figure 5.45 where the heat flow from the pipe for the two different implementations is shown.

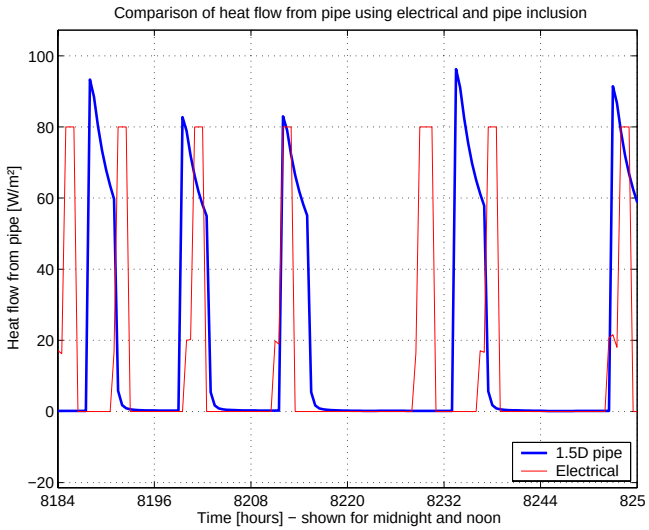

Figure 5.45 Heat supply from floor heating system using electrical and 1.5D pipe inclusion of the pipe.

The heat flow using the 1.5D pipe inclusion has different peak values depending on the actual conditions, while this is not the case for the electrical type. In addition, the electrical system maintains a constant heat flow to the floor during the period when there is a heating demand, the pipe inclusion starts with a peak value which drops during the period when it is turned on because the surrounding concrete is heated from the pipe. Finally, when the heating system is turned off, the heat flow from the electrical system immediately returns to zero, where the pipe inclusion requires some time before the temperature of the fluid in the pipe has dropped to that of the surrounding concrete.

The change in the energy consumption changes with the maximum heat output, has been tested with four different values; 80W/m² (standard simulation value), 100W/m², 120W/m² and 140W/m². The model without heat recovery unit and 250mm of insulation is used. The results are shown in Table 5.15.

Table 5.15 Comparison of energy consumption using different value of the maximum allowed heat output from the 1D electrical inclusion of the pipe (model type 1) and for reference the 1.5D model with pipe (model type 7).

	max 80W/m² [kWh/m²]	max 100W/m² [kWh/m²]	max 120W/m² [kWh/m²]	max 140W/m² [kWh/m²]	1.5D pipe [kWh/m²]
Total	78.5	78.7	78.6	79.2	83.6
Ground	17.3	17.4	17.5	17.6	18.0

As it can be seen, there is very little difference in the energy consumption for the models ranging between 80 and 140W/m². Compared to the 1.5D model with pipe all electrical models – regardless of maximum heat output – have lower energy consumption than the 1.5D model with pipe.

As it can be seen in Figure 5.45 the maximum heat flow is fairly close to that which is found in the 1.5D model with a 35°C supply temperature and can therefore be seen to correspond to this supply temperature. If instead the maximum heat flow is raised to 200W/m², this will correspond to a supply temperature of 45°C. By raising the maximum heat flow to 200W/m², the energy consumption and ground heat loss will change to 82.4kWh/m² and 17.7 kWh/m² compared to 86.5kWh/m² and 18.3kWh/m² for the 1.5D model. Again the values are smaller than for the 1.5D model. Like the comparison of 80W/m² to 35°C supply temperature and 200W/m² to 45°C, both results in a 5% underestimation of the energy consumption.

Therefore, using different maximum heat supply from the electrical model shows that this can to some extent be used to model the supply temperature, since a larger maximum value results in higher energy consumption.

Ground volume in 1.5D model

Two different types of inclusion of the ground volume are compared in this section. They are the models with no ground volume and a thermal resistance to a fixed ground temperature and the model with 1 m of ground volume and a fixed (but smaller) thermal resistance to the same fixed ground temperature. This corresponds to boundary condition 1 and 2 in Table 5.5. Figure 5.46 shows the duration curves of operative and floor surface temperature, while Table 5.16 shows the heat loss to the ground for the models.

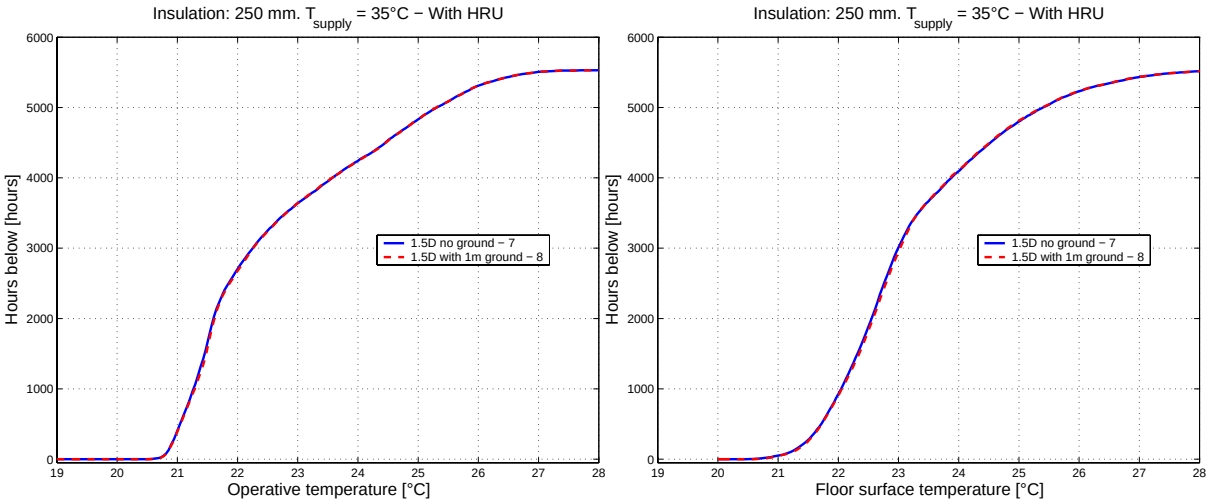

Figure 5.46 Comparison of different inclusion of ground volume with no ground volume and with 1 m ground volume. Data shown for model with low energy consumption.

As it can be seen from these figures, both the temperature distribution and the heat loss to the ground are almost identical. It can therefore be seen that the inclusion of a 1 m ground volume in the simulation model does not alter the results in any significant way.

Table 5.16 Comparison of heat loss to the ground during the heating season found using a model with no ground volume (type 7) and with 1 meter ground volume (type 8) and their difference relative to the model with no ground volume.

Energy consumption	Insulation thickness	No ground [kWh/m²]	1m ground [kWh/m²]	Difference [%]
With HRU	150mm	14.5	14.3	0.9
	250mm	9.9	9.8	0.7
	350mm	7.5	7.5	0.4
Without HRU	150mm	17.7	17.5	1.4
	250mm	12.0	11.9	1.2
	350mm	9.1	9.0	1.2

Based on these findings, there are virtually no differences in the results when a 1 m ground volume is included below the insulation layer. This is also the case for the energy consumption, which is not shown here.

Serial 1.5D models

The influence of serial coupling of the 1.5D model has been investigated by comparing models using a different number of sections. In this case, 1, 2, 3, 5 and 10 sections for the

30m² floor area, corresponding to 30, 15, 10, 6 and 3m² of floor area per section. Notice, that models with one and five sections are the same as presented above as model type 9-11 and 15-17.

Figure 5.47 shows the energy consumption for the serial 1.5D models with 1, 2, 3, 5 and 10 subdivisions, respectively without ground volume, with 1 m of ground volume and according to ISO13370. Data are shown for 250mm insulation with low energy consumption. The right figure shows the ground heat loss, which is almost the same for all cases regardless of the number of subdivisions, with slightly higher values for ISO13770. The same is the case for the energy consumption in the room.

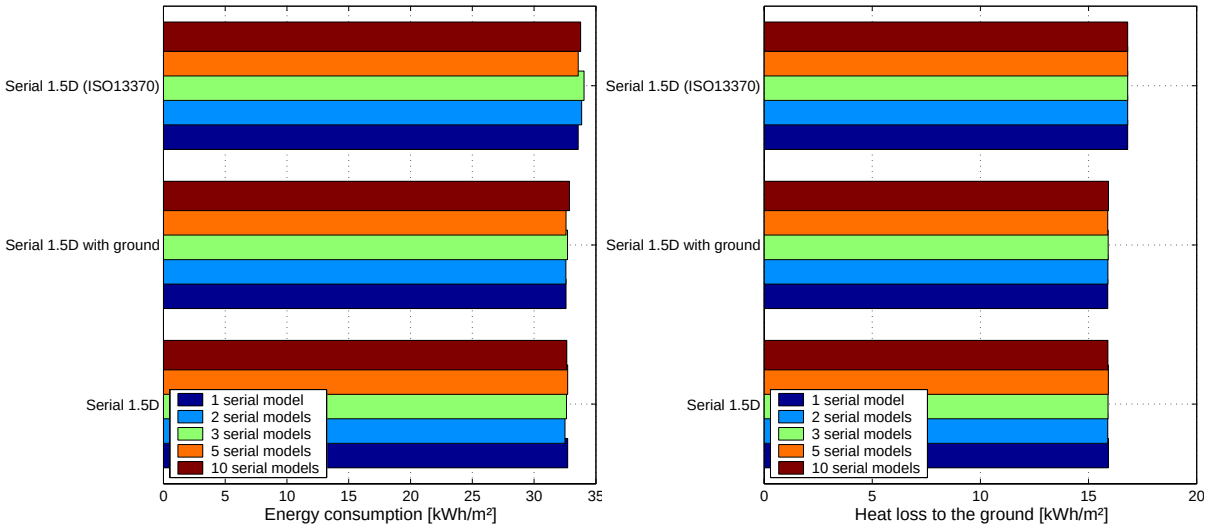

Figure 5.47 Energy consumption and heat loss to the ground.

Figure 5.48 shows the pipe temperature during a two-day period with one on/off cycle pr. day, comparing a single model with a serial model with 10 sections. The figure shows that the pipe temperature in the single model is close to an average of the 10 section model. The 10 section model does however give more detailed information on the thermal properties. For instance, it can be seen that the largest temperature difference in the pipe is through the first sections and smallest through the last ones.

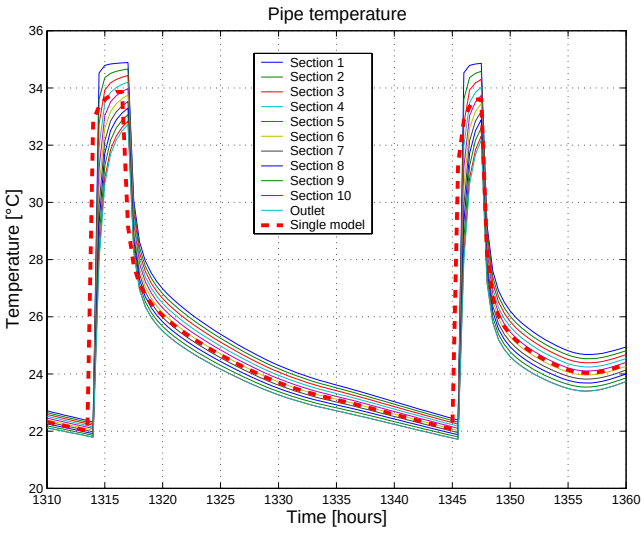

Figure 5.48 Pipe temperature through the serial models comparing a model with ten serial sections to a model with just one section.

To further elaborate on the return temperature for a different number of sections, Figure 5.49 shows the outlet temperature comparing the models with 2, 3 and 10 sections. The models have very similar outlet temperatures both during periods when the flow is turned on and during periods without flow in the pipe. Therefore as shown in Figure 5.48 and Figure 5.49, the different models can satisfactorily predict the outlet temperature of the fluid in the pipe.

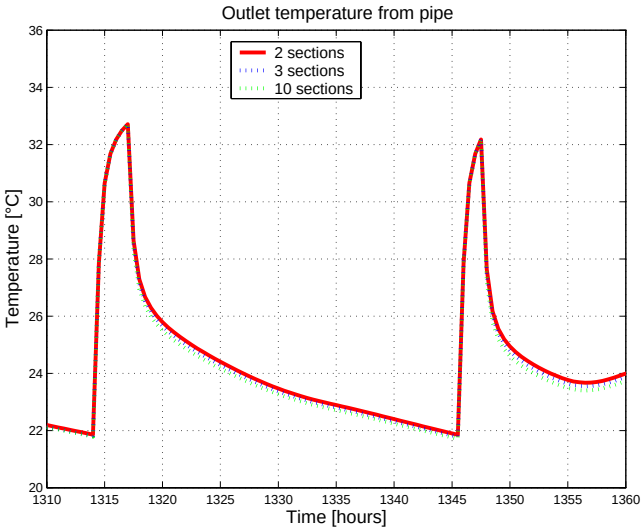

Figure 5.49 Return temperature as a function of the number of elements.

The left side of Figure 5.50 shows the operative temperatures for the models with 1, 2, 3, 5 and 10 sections for a period of one week. During periods dominated by solar gains as seen in the first two days, the temperature in the room is the same. During periods without solar gains, the temperature can be seen to vary considerably. In this case, the three-section model (coincidentally) has a fairly different temperature profile compared the rest of the models. This shows that the models have different reaction time to the turning on or off the pipe. This can be seen in the right figure, where the time constant has been compared. The comparison finds that the time constant is around half an hour faster for the model with only one section compared to the models with two or more sections, which on the other hand are almost identical. This is due to the fact that the floor is heated more slowly in the last sections, since the first section will be heated before the following sections.

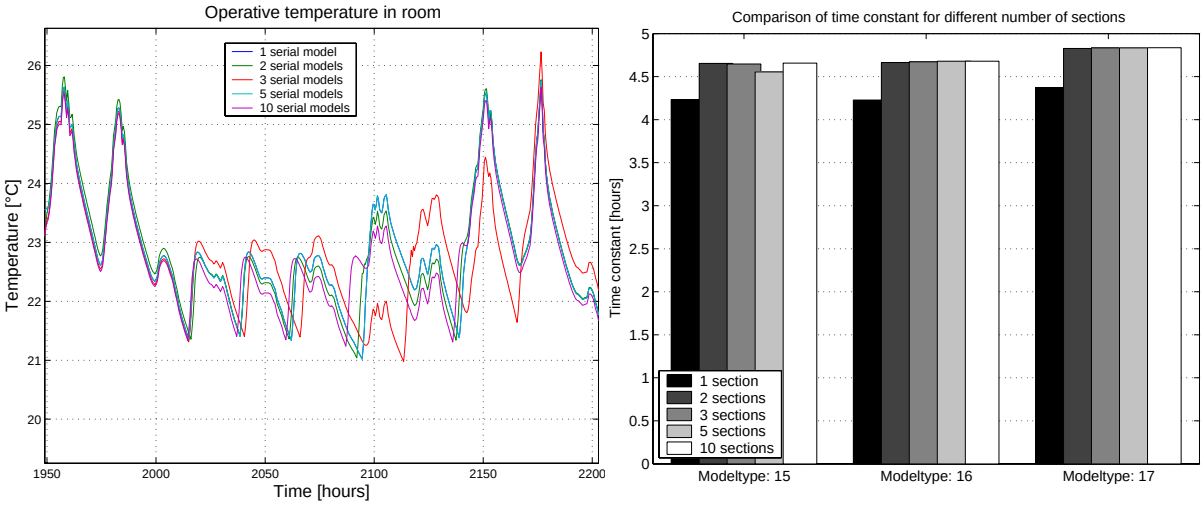

Figure 5.50 Dynamic properties for serial models with different number of sections. The left temperature profiles for a week are shown for type 15; the right figure shows the time constant for types 15, 16 and 17.

The operative and floor surface temperature in the models with different numbers of sections have been compared with respect to the number of hours below a given temperature (Figure 5.51). The models can be seen to be almost alike regardless of the number of sections used, which is the case for both floor surface and operative temperature.

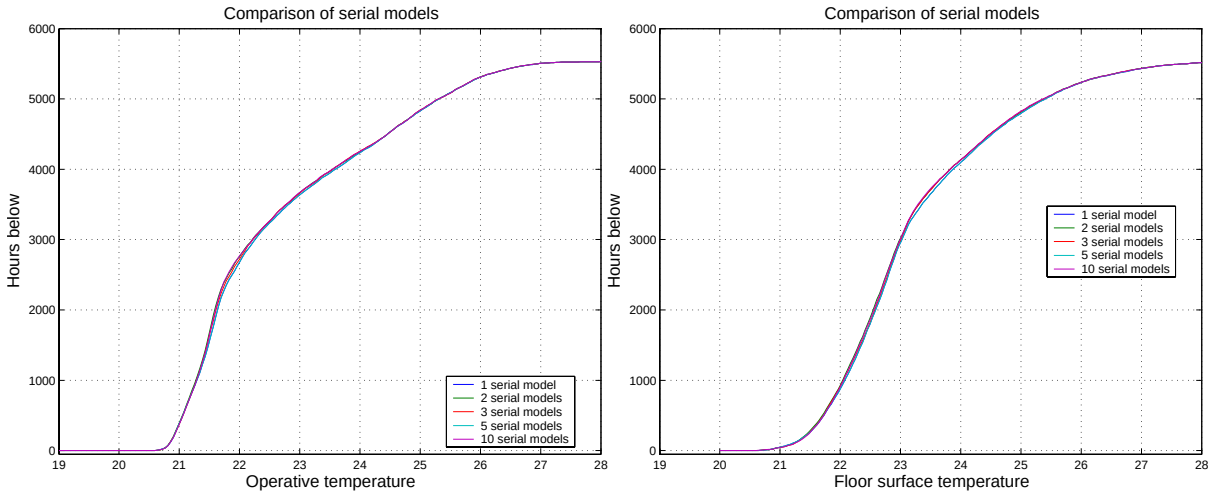

Figure 5.51 Comparison of hours below a given temperature for the serial 1.5D models with 1, 2, 3, 5 and 10 sections. The left figure shows the operative temperature while the right figure shows the floor surface temperature.

RC thermal network compared to 1.5D model

The RC thermal network represents the simplest model with hydronic floor heating. The model consists of only 3 nodal points with heat capacity and two surface nodes, which are simple heat balance equations. In the model, the parameters used for thermal resistances and heat capacities are based on purely geometrical considerations. However, this approach may be too simplified, since it is well-known that thermal network models are very influenced by the parameters. Therefore a simple optimisation of the parameters in the thermal network model is also included and compared.

This optimisation will be based the Matlab Optimisation Toolbox using Nelder and Mead's simplex method (Nelder and Mead, 1965). As reference for the optimisation a data set is calculated using the 1.5D model, which therefore in this context is considered to be "correct".

Figure 5.52 shows the equivalent thermal network of the RC-model with the resistances and heat capacities involved in the model. Four parameters are important. These are the two resistances R_1 and R_{pipe} and the two heat capacities C_1 and C_{pipe}. The lower heat capacity, C_2, has been shown in the previous section on ground volume not to have any impact on the properties of the model. The sum of the two thermal resistances, R_2 and R_3, must equal the thermal resistance of the concrete below the concrete deck. The five temperatures are also shown in the figure.

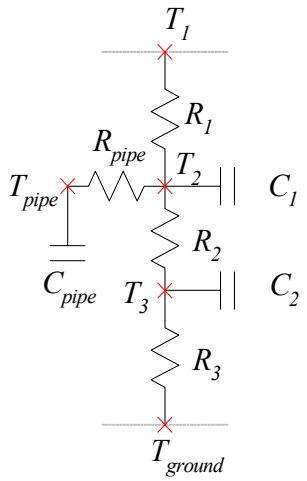

Figure 5.52 RC thermal network showing thermal resistances, heat capacities and temperature nodes.

In the optimisation procedure a sinusoidal temperature of the pipe temperature, T_{pipe}, is applied and simulated in the 1.5D model. The heat flow from the pipe is recorded. Using this value, the parameters R_{pipe}, R_1 and C_1 are fitted to give the same heat flow from the pipe as recorded in the 1.5D model.

The basis of the optimisation is to solve the over determined systems of non-linear equations, where the purpose is to minimize the difference between the 1.5D model and the RC model.

A slightly more detailed description of the data fitting problem is presented in Appendix A[7]

Table 5.17 Parameters in the optimised and non-optimised RC-thermal network model.

Parameter	Non-optimised initial value	Optimised
R_{pipe},	0.1m²K/W	0.08m²K/W
R_1	0.23m²K/W	0.104m²K/W
C_1	240 kJ/kg K	150 J/kg K
C_{pipe}	4.0 kJ/kg K	2.8 kJ/kg K

The value of R_1 and C_1 have been calculated as the thermal resistance from the middle of the concrete layer to the room through the floor construction and the thermal heat capacity of the concrete core surrounding one floor heating pipe respectively. There are large differences in the optimised and non-optimised values. The fact that the optimised value of C_1 is much smaller than the non-optimised is that not all the concrete in the construction is used as effective thermal capacity. The smaller thermal resistance in the optimised model between the concrete and floor surface is most likely due to the assumption that the heat is first transferred to the concrete and after that to the floor surface, while at least parts of the heat flow passes directly from the pipe to the surface. The initial guess of the resistance between pipe and concrete has been fitted "by hand" in a steady-state calculation to give the same heat flow from the pipe using the non-optimised values. Figure 5.53 shows the 1.5D model compared to the optimised and non-optimised parameters. The 1.5D model and non-optimised initial guess values have been shown for the entire period before periodic stationary conditions have been established, while the optimised value is only shown for the periodic stationary conditions. As it can be seen, there is fairly good agreement for the initial guess, while the optimised model gives an almost perfect fit.

[7] The optimisation procedure has been developed in cooperation with Frank Pedersen, who is a fellow PhD student at the Department of Civil Engineering at DTU. The results from this small investigation will be expanded in greater detail in a future effort to develop simple models, for the early design phase of buildings.

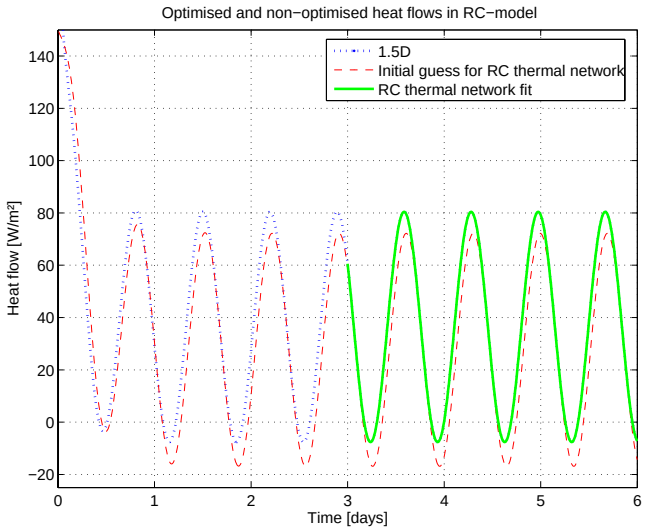

Figure 5.53 Optimisation of parameters used in RC-model. The results using fitted parameters are shown from app. $2.6*10^5$ seconds.

The final parameter for the heat capacity of the fluid in the pipe, C_{pipe}, cannot be fitted here as the pipe temperature is an input, and as such has an infinite thermal capacity. Instead the flow in the system is turned off from a steady condition, where the temperature in the pipe will drop to the level of the concrete.

Table 5.18 shows the energy consumption for the model with 250mm insulation and high and low energy consumption.

Table 5.18 Comparison of total energy consumption and heat loss to the ground during the heating season using the RC model (type 12) with non-optimised and optimised parameters compared to the 1.5D pipe (type 7) model.

Energy consumption	Insulation thickness	Non optimised RC [kWh/m²]		Optimised RC [kWh/m²]		1.5D pipe [kWh/m²]	
		Total	Ground	Total	Ground	Total	Ground
With HRU	250mm	30.5	9.5	28.6	9.1	32.4	9.9
Without HRU	250mm	82.1	11.5	79.1	10.2	83.6	12.0

For both the model with and without heat recovery unit the same trend can be seen, as both heat loss to the ground and energy consumption are lower for the RC thermal network, which is the case for both the optimised and non-optimised thermal network. This indicates that the thermal network tends to overestimate temperatures and, consequently, underestimate the energy consumption. In the optimised RC-model, the energy consumption is found to be 12% lower than compared to the 1.5D model. Comparing the optimised to the non-optimised values of the RC thermal network model shows that the energy consumption differs by 6% for the low energy model.

Time step in RC-thermal network model

One possible reason for the lower energy consumption in the RC-thermal network than in the 1.5D model is that the RC-thermal network is more influenced by the time step. Therefore this has been tested in the optimised RC-thermal network for four different time steps; 1 hour, 30 minutes, 15 minutes and 10 minutes. The model with low energy consumption and 250mm of insulation has been used for the test.

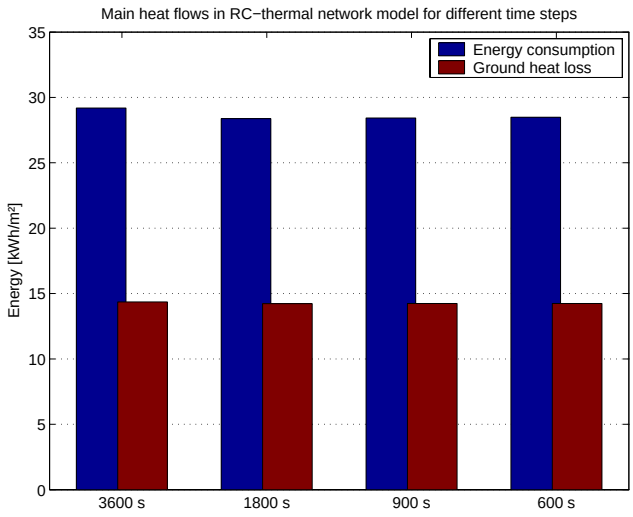

Figure 5.54 Influence of time step on RC-thermal network model (type 12) using the optimised parameter values found in Table 5.18. Data shown for energy consumption and ground heat loss.

As it can be seen, the energy consumption and ground heat loss are both influenced by the different time steps used. The difference between the model with a one-hour time step and the 10-minute time step is 2.5% on the energy consumption and 0.9% on the ground heat loss.

This means that the differences are not large enough to account for the difference found in the section above. Similar observations can be made for the other model types.

Temperature under floor construction

The temperature in the ground volume is, as shown in Figure 5.13, neither constant in time nor in the spatial domain. The same goes for the temperature below the floor construction shown in Figure 5.14, which depends on both the distance from the foundation and the time of the year and whether or not the floor is heated. Therefore, it is relevant to compare the ground temperature for the different models for any noteworthy differences with respect to floor heating and the level of detail in the modelling.

The simulation models with different level of detail are compared. Figure 5.55 shows the temperature directly under the insulation in the seventeen models. The model with low energy consumption and 250mm insulation has been used.

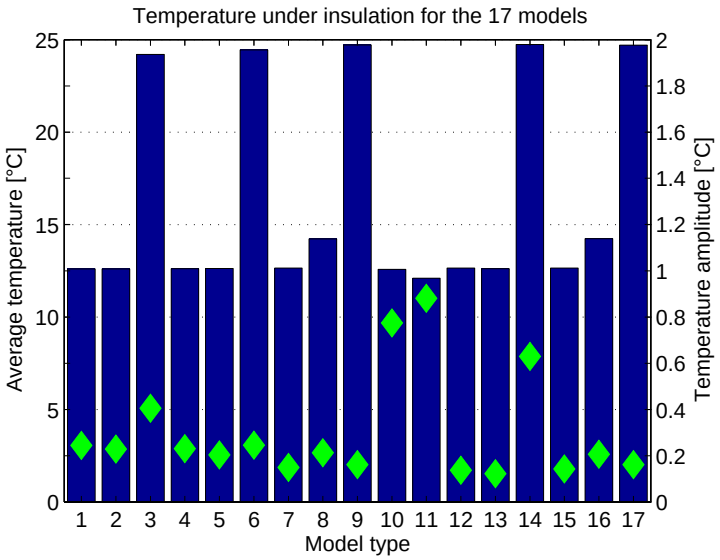

Figure 5.55 Average temperature and yearly amplitude under insulation for the different models for models with low energy consumption. The average temperature is shown as bars, while the amplitude are shown with diamonds.

Generally, the model types based on EN ISO 13370 (number 3, 6, 9 14, and 17) stands out from the rest, as the average temperature here is around 25°C, since the bottom boundary condition is adiabatic, which means that the entire floor construction is heated to the average temperature of the floor heating pipe. This fact will be discussed further below in a succeeding section. The other models have almost the same average temperature just under the insulation, which is around 12°C. This means that the boundary condition of 10°C and a thermal resistance of 1.5m²K/W, which is applied in this analysis, have temperatures that are comparable to those found in the two-dimensional simulation model. This means that this boundary condition can be used for the 1D and 1.5D models to calculate the heat loss to the ground. This is of course only the case as long as the influence of the foundation is neglected.

Generally, the simplified models predict a smaller amplitude of the temperature under the insulation layer compared to the detailed two-dimensional models (type 10 and 11). This is a result of the fixed temperature applied in the simple boundary conditions.

Finally notice from Figure 5.55 that the boundary condition of 10°C and 1.5m²K/W – which is used in the model numbers 1, 4, 7, 12 and 15 – is also applicable to floor heating, for a well insulated floor.

The 2D models are compared to investigate the temperatures using different levels of insulation and energy consumption. Figure 5.56 shows the average temperature under the floor construction from just inside the foundation and until the reference point.

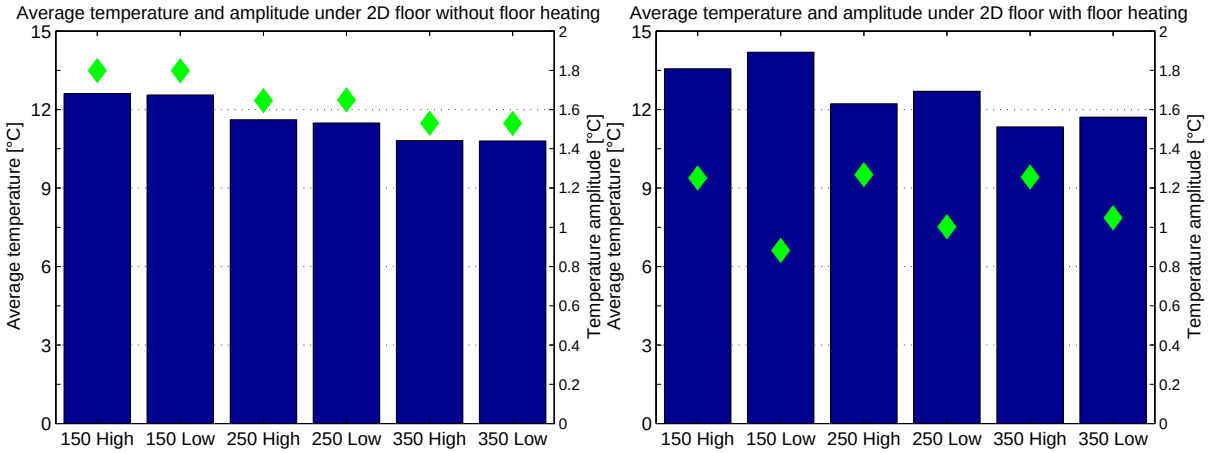

Figure 5.56 Yearly average temperature and amplitude directly under the insulation for three different insulation thicknesses 150mm, 250mm and 350mm insulation with high and low energy consumption. The left figure shows results without floor heating and the right figure shows results for model with floor heating. The average temperature is shown as bars, while the amplitude are shown with diamonds.

Initially, comparing the models with and without floor heating it can be seen that the average temperature under the floor construction is higher with floor heating, while the amplitude is smaller. The difference is generally larger for the models with the lowest insulation thickness. For the models without floor heating the temperatures and amplitudes are the same regardless of the energy consumption in the models. The only deciding factor is the insulation thickness. This is not the case with floor heating where the energy consumption influences both temperature and amplitude. Conversely for the model with floor heating, where different energy consumption will lead to different average temperature in the concrete layer and therefore also different heat loss to the ground.

Two results can be extracted from this. (1) The average temperature depends on both energy consumption and insulation thickness for the model with floor heating, while it only depends on the insulation thickness when floor heating is not used and (2) the temperature under the insulation is more uniform during the year when floor heating is present as the amplitude is smaller, while however, the amplitude depends on the energy consumption.

The minimum temperature under the floor construction is during the months of March through May and the maximum is during the late summer.

EN ISO13370 type models compared to 2D model

A comparison is made between the 1.5D model and the 2D ground coupled model to find the differences in the results. Table 5.19 shows a comparison of the energy consumption based on EN ISO13370 and on the 2D model. The average heat loss to ground has been added into the simulation model as a convective negative heat flux in the room air for the model based on EN ISO 13370.

As it was shown in 5.1 for the validation of the floor model, the heat loss to the ground is influenced by the average concrete temperature and room temperature. The calculation of the average heat loss to the ground using the EN ISO 13370 standard has been based on a pipe temperature of 35°C and an average room temperature of 23°C. The room temperature is the average value during the heating season of a simulation in the 2D model, while the pipe temperature of 35°C is higher than the average value of the fluid temperature but equal to the supply temperature.

The models with large energy consumption differ by up to 10% and 7% for the model with low energy consumption. The values for the heat loss to the ground are 32% and 42%, respectively, largest for the models with the smallest insulation thickness. The difference in total energy consumption with 250mm and 350mm is very small, differing by less than 5%.

Table 5.19 Comparison of the ISO13370 (type 9) relative difference of the 2D model (type 10) of energy consumption and heat loss to the ground during the heating season.

Energy consumption	Insulation thickness	ISO13370 [kWh/m²]		2D [kWh/m²]		Difference [%]	
		Total	Ground	Total	Ground	Total	Ground
With HRU	150mm	34.0	11.6	38.0	17.0	-10.5	-31.8
	250mm	33.2	10.6	34.6	13.0	-3.9	-18.3
	350mm	32.8	10.1	33.0	10.9	-0.5	-7.2
Without HRU	150mm	84.4	11.8	90.9	20.3	-7.2	-42.0
	250mm	82.9	10.6	86.4	15.4	-4.0	-31.1
	350mm	82.5	10.1	94.0	12.9	-1.8	-21.4

One possible reason for this large difference in the heat loss to the ground is the temperatures in the floor construction and ground volume below. Due to the adiabatic boundary condition below the ground volume, the average temperature of the floor construction is higher than for the models with a boundary condition with a temperature of 10°C (see also Figure 5.55).

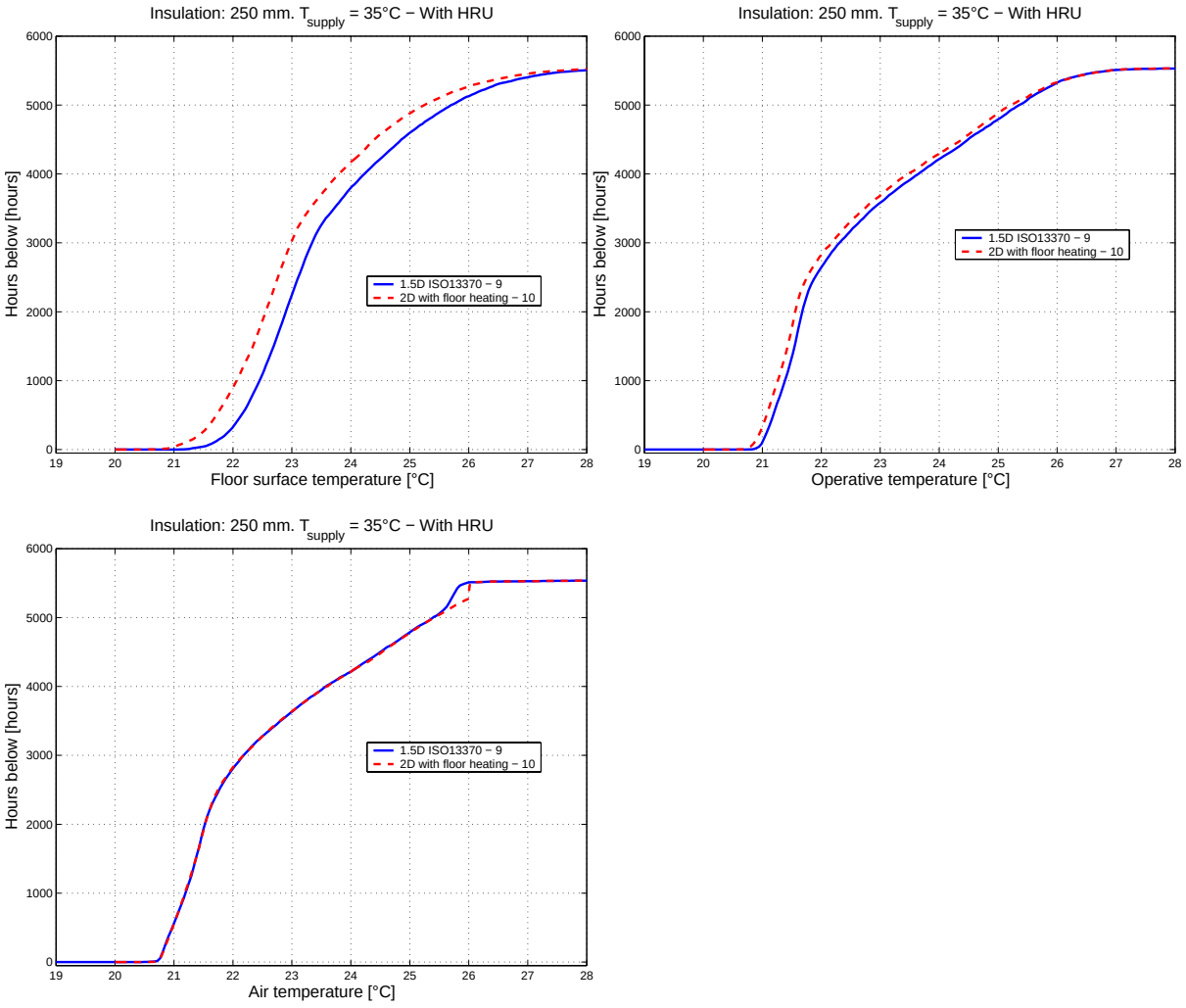

Figure 5.57 Comparison of the 1.5D model based on EN ISO13370 and the 2D model showing hours below a given floor surface, operative and air temperature.

This means that the room can be more easily heated because the floor is already warmer than for the models with heat loss. This can also be seen from the upper left of the figures in Figure 5.57 where the floor surface temperature is generally higher even though the energy consumption is lower. In addition to this, the operative temperature is actually also higher.

2D model compared to RC-model with ψ-value

The two models where the linear thermal transmittance is directly included are the 2D model and the RC thermal network model with the ψ-value. The two models are very different as one of them is very detailed with correct physical representation of the actual building structure, while the other simply uses the linear thermal transmittance as an input value, which must consequently be found outside the model.

Figure 5.58 shows the duration curves of operative and floor surface temperature for the model without heat recovery, while Table 5.20 shows the total energy consumption and heat loss to the ground during the heating season.

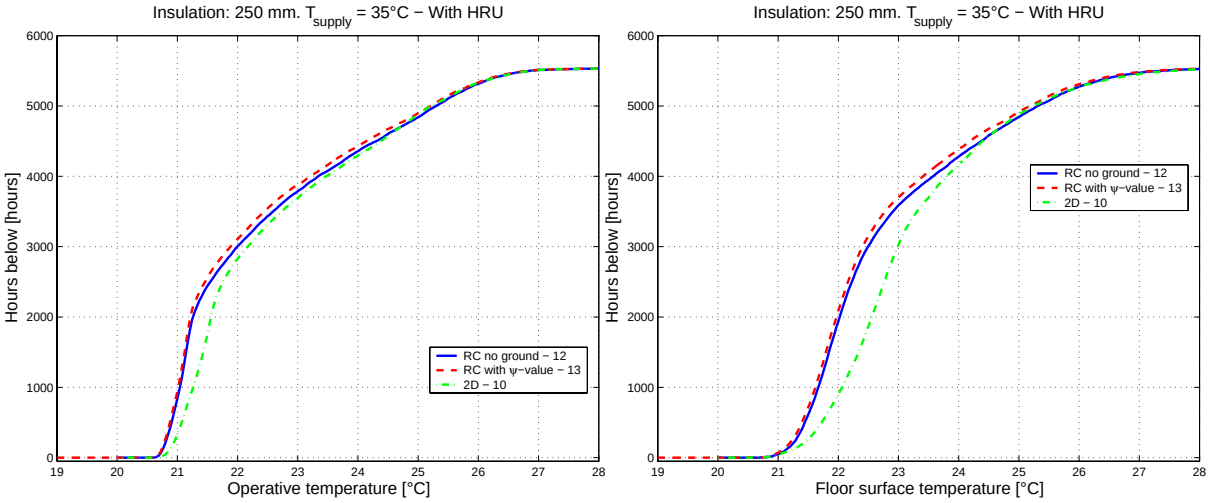

Figure 5.58 Comparison of RC-model and 2D model. Data shown for the model with low energy consumption

Figure 5.58 shows the number of hours below a given temperature for the two RC thermal network models with and without ψ-value included compared to the 2D model. For both the models with high and low energy consumption, the RC-models predicts higher temperatures than in the 2D model. In all cases there are very few hours with too low temperatures.

Table 5.20 Comparison of heat loss to the ground during the heating season found for the RC model with ψ-value (type 13), 2D model (type 10) and difference relative to the 2D model.

Energy consumption	Insulation thickness	RC model with ψ-value [kWh/m²]		2D model [kWh/m²]		Difference [%]	
		Total	Ground	Total	Ground	Total	Ground
With HRU	150mm	40.2	21.1	40.2	17.0	-0.2	19.4
	250mm	35.5	15.2	36.2	13.0	-1.2	17.0
	350mm	33.2	12.5	34.4	10.9	-3.4	14.7
Without HRU	150mm	93.2	25.3	95.0	20.3	-1.9	24.6
	250mm	88.0	18.1	88.4	15.4	-0.4	17.5
	350mm	85.5	14.8	85.3	12.9	-0.3	14.7

Looking at the energy consumption and ground heat loss in Table 5.20, notice that while the energy consumption between the two models differs only very slightly – in all cases less than 4%, the differences in the ground heat loss are in all cases between 15% and 25%. In all cases

the ground heat loss is largest in the RC model while the energy consumption is largest in all cases.

There are many reasons for the differences in the heat loss to the ground. As it was found above on page 70, both heat loss to the ground and energy consumption are influenced by the characteristic dimension for the 2D model and the combination of ψ-value and U-value. Finally, it has been found in 5.2.3 that the ψ-value also depends on floor heating. These differences are not analysed further here, but it is noticed that the RC-thermal network is able to find almost the same energy consumption as the far more detailed 2D model.

5.3.7 Summing up and discussion of modelling results

In this section the results from 5.3.5 and 5.3.6 will be compared and discussed.

In the investigation seventeen different model types with different implementation have been compared. Included in the investigation are also different boundary conditions, supply temperatures and insulation in the floor construction.

The comparison has been made for two versions of a room which differ in the energy consumption. One has an energy consumption of around 30-35kWh/m² and one with approximately 80-85kWh/m². The room model has been tested with three different levels of insulation in the floor construction; 150mm, 250mm and 350mm. This gives a range of U-values from slightly below the present Danish standard, to a future insulation level.

The purpose has been to compare the different modelling techniques and find the differences, which make them more or less useful for simulations of floor heating systems. This is possible by using the simulation model in FHSim, which except for the floor model is identical regardless of floor model.

For reasons of simplicity a very basic on/off heating strategy of the floor heating system is used.

General results

Initially it can be concluded that the different models result in large differences for both energy consumption, heat loss to the ground and temperatures. These differences are solely based on the different implementation of the floor and floor heating system, as the rest of the models are identical. The discrepancies are quite large especially for the heat loss to the ground which differs by nearly a factor two for the smallest insulation thickness. Fortunately this difference is not as large when more insulation is used. For the energy consumption, the difference is of course smaller since all other parts of the model are the same. Still however, the difference is almost 25% in the worst case.

Another not so obvious result – which has been shown before in the literature – is that the energy consumption depends on the supply temperature to the floor heating system. The reason is that the higher supply temperature generally results in higher average room temperature since the concrete will be heated to a higher temperature level before the system is turned off, once the set point temperature has been reached. This is due to the fact that the time constant is the same regardless of the supply temperature and therefore more heat will be supplied from the pipe during the same time with higher supply temperature. This larger amount of stored heat will contribute to heating the room also when this is not needed during periods with solar gains. This extra heating from both solar gains and surplus heat from the pipe will consequently not only be used to keep the desired temperature, but also to overheat the room. Therefore there is a point in using as low a supply temperature as possible to heat the room to avoid overheating. Another reason for using lower supply temperature is to lower

the unwanted heat losses in the heat distribution system – this point has not been included in these investigations.

In this work the detailed two-dimensional simulation model has been taken as the reference to the other models – since this model has been validated in first the section of this chapter. Therefore it can be said, that most of the simplified models cannot be used to model floor heating, as they give results with large discrepancies compared to the detailed model. In fact, only the simple thermal network model with the linear thermal transmittance included is able to reproduce the results from the much more complex two-dimensional model. However, the simplified models are (as the name implies) much easier to implement and use in building energy simulation programs, where they in any case will represent an improvement over models where the floor heating cannot be included. At the same time, it can also be seen that even though the results for the heat loss to the ground differ by a factor of two, the difference for the total energy consumption is much smaller. In total, this means that the simplified models can be used to model the influence from the floor heating system, though this discrepancy must be kept in mind when analysing the results.

In addition, the results have shown that the difference between detailed and simple models becomes smaller with increased insulation – both for the relative and absolute values, which is based on the fact that the increased level of insulation means that influence from the ground becomes smaller. Therefore the need for a detailed model may actually decrease with further improvements of the insulation standard, but this is still in the distant future.

Simple models with foundation compared to detailed two-dimensional model

Two simplified methods including the influence of the foundation and ground coupling have been tested and compared to the validated two-dimensional model.

The first is based on EN ISO 13370, which uses a detailed steady-state model to find the average heat loss and a simple dynamical model without heat loss to the ground in the procedure. While simplifying the dynamic modelling considerably, the fact that no heat is lost through the floor means that the entire floor is heated to the average fluid temperature. The method is therefore not useful for floor heating systems. In addition, the steady-state calculation proved to underestimate the heat loss to the ground compared to the dynamic two-dimensional model, especially for the model with the largest heat loss to the ground, while the model with lowest heat loss was close to the two-dimensional model.

This model can therefore not be recommended for floor heating modelling.

The second model is a very simple RC thermal network model based on lumped heat capacities and thermal resistances. Here the influence of the foundation has been included by an extra heat flow term from the concrete deck to the surroundings. The model is fast because it only has four nodal points, and consequently only four differential equations. Yet the results are close to the two-dimensional model results –especially the total energy consumption while the ground heat loss is overestimated. The reason comes from the fact that RC thermal network models tend to underestimate the energy consumption and overestimate the temperatures especially in the room. The reasons for this difference have not been satisfactorily explained.

In total, though, the thermal network is very useful as an early estimate of the energy consumption in the design process and can be used to model floor heating systems in a context where fast simulations are needed.

A drawback to the RC thermal network model, as well as the one based on EN ISO 13370, is that it is necessary to create a two-dimensional simulation model to find the heat loss from the

building or the linear thermal transmittance of the foundation. This can probably to a large extent be avoided by using tabulated values for typical construction details. Such tabulated values are becoming more common in the building industry with the increasing demands for detailed characterisation of their products.

However, the inclusion of the linear thermal transmittance of the foundation in the RC-thermal network requires a "correct" value. As discussed in section 5.2.8 the linear thermal transmittance requires a detailed dynamical two-dimensional simulation – which the introduction of the thermal network was meant to replace.

Finally for the thermal network models, results have shown that the parameters for thermal resistances and heat storage capacities can be fitted from measurement data or based on more complex data to give better estimates of the parameters. Unfortunately though, this has proven to give unexpected results for the energy consumption and heat loss to the ground – which has not been satisfactorily explained. Nevertheless, the simple method is so versatile in the inclusion of for instance the linear thermal transmittance, and gives such promising results that it is absolutely useful for inclusion in optimisation procedures where the heating system is suddenly included in the model – which has not previously been the case. As an example the simple method given in EN 832 (CEN, 1998b) or EN ISO 13790 (CEN, 2004) do not include the heating system. Therefore, the RC-method opens for building integrated heating and cooling system to be included in simplified methods.

Simple implementations

Besides from the thermal network model, three other models have been developed. The most detailed of these is a two-dimensional section around a pipe, called a 1.5D model here. The two remaining models are one-dimensional; one models a pipe system and the other is an electrical analogy where a heat flux is used in the model instead of a fluid with a given temperature.

The main advantage of the 1.5D model compared to the one-dimensional model is that it can correctly model the conditions around the floor heating pipe and therefore does not need to include a resistance from the pipe to the concrete. This resistance is fictive – as the concrete temperature is not defined in a single point to which the resistance is "ending" – which makes it is difficult to estimate. However, this parameter is not important for the calculated energy consumption, only for the reaction time of the floor construction. The thermal resistance between pipe and concrete can be fitted by comparing to measurements or more detailed simulations. Therefore, a one-dimensional model can be fitted to be as good as a 1.5D model. However this fit is not straight-forward and again a more sophisticated model or measurements is required. None of which are normally available. Generally speaking though, the 1D and 1.5D models essentially give the same results, which have been obtained without using fitted values for the thermal resistance. Nevertheless, the 1.5D model does have the advantage that it can be used to calculate the influence of for instance the pipe spacing and pipe diameter which the 1D model cannot.

The 1.5D model has also been used to test whether the inclusion of a 1 meter ground volume below the insulation would change the dynamical (seasonal) behavior of the heat loss to the ground. It was found that this did not in any significant way change the results, and therefore it cannot be recommended to use the ground volume to improve the results. This also shows that there is no need to include the lower concrete layer from the reference model in the simple models. Consequently, the conditions below the insulation layer will not influence the conditions above the insulation layer with respect to both short and long term dynamic conditions and temperatures in the deck and room.

Electrical inclusion of pipe

A main point in this investigation has been to compare a one-dimensional model using an electrical inclusion of the heat supply from the floor heating system. The electrical inclusion is typically used in the present state of the art of building energy simulation programs. This has been compared to a hydronic model where the pipe with a given temperature is included to supply heat through a thermal resistance between pipe and concrete. It has been shown that the electrical model has lower energy consumption than the models with a pipe inclusion. The differences have been shown to especially come from two factors, where (1) the heat flow from the pipe starts by an initial peak followed by a decay in the heat flow, as the concrete is heated resulting in a smaller temperature difference. Compared to this the electrical inclusion has a constant heat supply which does not change. The second reason (2) is that once the electrical system is turned off the heat flow is zero, which is not the case for the pipe inclusion where the higher temperature of the pipe results in a heat flow from the pipe even after the system has been turned off.

A remark on the use of the electrical inclusion is that by changing the maximum heat supply from the "pipe" can emulate different pipe temperatures and give the same basic properties of higher energy consumption with higher supply temperature. However, because the actual supply from a pipe with a given temperature depends on the temperature of the surrounding concrete and the flow in the pipe, the electrical inclusion of the pipe will not give an exact supply temperature.

Serial 1.5D models

In the RC, 1D and 1.5D models one section is assumed to cover the entire floor surface, thereby modelling the average conditions of the entire floor surface. However in reality the fluid in the pipe is cooled from supply to return. A simple average value may not be enough – especially if the flow is small or if the heating demand in the room is large. Therefore a serial coupling of the 1.5D models was introduced, where the outlet from one section was used as supply to the next. It was shown, that no major differences could be detected in the results, at least for the cases studied here. Of special relevance is that all models were able to predict the same outlet temperature, which is important when the supply side of the heating system is coupled to the system.

Control system

A final remark can be made to the control system, which in this work has been based on a simple on/off control. The heavy floor heating system which is the basis for this investigation has proven to rely on simply needing "one shot" of hot water a day, whose duration is based on the outdoor temperature and level of solar gains to the room. Therefore, a discussion can be made on the need for using an advanced control system with wireless transmitters in each room, if in fact a much simpler outdoor temperature sensor can decide how much heating is needed in a room. This has not been investigated here, but if this is the case, the installation cost of the floor heating system can be reduced considerably.

5.3.8 Conclusion

In this section, models with different levels of detail of a floor with integrated floor heating system have been investigated, with the purpose of being able to find the general difference between simple and complex models. The approach has been to use the same room model in FHSim and only change the floor model.

The models generally give results that are very different for both heat loss to the ground and for energy consumption of the room. The models where foundation has been included gave higher values than those without foundation. This result is as expected. However, the differences shows that the foundation is an important factor for the heat loss to the ground especially for well insulated buildings and therefore this single factor should be included.

For the simple models, an important result is that the use of electrical implementation of hydronic floor heating results in too low energy consumption and heat loss to the ground compared to models with a pipe inclusion of the floor heating. The difference is around 10% in the cases investigated here. However, the model is simpler to implement than models with hydronic inclusion of the pipe and requires very few inputs and can therefore be recommended for simple estimates.

Another simple model is the RC-thermal network which only has three nodal points and therefore results in short simulation time. The model is also versatile as the influence of the linear thermal transmittance can easily be included in the simulations. Using this model, the results are very close to those from the far more detailed two-dimensional simulation model, which has been investigated in previous sections. This model will be ideal for e.g. estimating energy consumption at an early phase in the design phase, where only few parameters are known.

The two-dimensional model is the most detailed model with the most nodal points. Therefore it is both the most accurate and most time consuming with respect to both model design and simulation time. Nevertheless, the model is by far the best for e.g. product development and detailed analyses.

5.4 Conclusion

This section is a conclusion on the entire investigation on modelling of floor heating systems. Discussions of the individual sections have been included in the sections.

The following results have been achieved:

- As basis for the results, the simulation program FHSim has been used. The program has proven useful for modelling floor heating systems by coupling the floor with floor heating to the room model where the room temperature is calculated. Thereby, dynamical calculations of the conditions in the floor heating system are possible.
- The two-dimensional model has been validated against measurements from a small and narrow building showing that the required simulation could be simplified from a three- to a two- dimensional analysis by introducing the characteristic dimension of the floor as the width of the model. This has previously been shown only for buildings without floor heating. It is also shown that the smaller the characteristic dimension, the higher the relative extra heat loss compared to a model without floor heating.
- It is important to use a dynamical simulation coupling the detailed floor model to a room model for finding the correct heat loss to the ground. Therefore a dynamical inclusion of the temperature in the pipe of the floor heating system cannot only be used to correctly model the temperature and thermal comfort in the room and energy consumption – it is also important for correctly finding the heat loss to the ground.
- The heat loss from the floor construction and foundation is larger in a building with floor heating compared to a building heated by other means and especially the linear thermal transmittance has a large impact. Additionally, it is shown that a poorly insulated

foundation is more critical for a house with floor heating than one which is heated by other means.

- A calculation of the linear thermal transmittance including floor heating based on dynamical simulations has been compared to standard methods. This dynamical calculation resulted in larger ψ-values, which means that the standard method does not give a conservative estimate for floors with floor heating as it is supposed to. Moreover, the dynamically calculated ψ-values also depends on the energy consumption in the house. An interesting investigation would consequently be to establish a calculation procedure for the linear thermal transmittance where floor heating is included.
- A higher supply temperature to the floor heating system resulted in higher energy consumption. However, here it must be noticed that the larger energy consumption led to higher temperatures in the room above the set point temperature – a result of inefficient control.
- The last section investigates different modelling techniques, both simple models with only a few nodal points and a detailed two-dimensional model. Generally a comparison to the two-dimensional model showed that all other models had lower energy consumption and heat loss to the ground. One reason for this is that the influence of the foundation is typically not included, which in this chapter has been found to be important.
- The simulation time in the different models range from a few seconds to half an hour for one year of simulation – a relative difference of approximately 1:100.
- A simple thermal network model can include the linear thermal resistance as an extra heat loss term from the concrete deck. This method is by far the simplest, yet it has results that are close to those found using the detailed two-dimensional model.
- An electrical inclusion of the floor heating pipe has shown to underestimate both energy consumption and heat loss to the ground compared to models with a hydronic implementation of the pipe due to more efficient control and a system that can be turned off immediately. Further, the method cannot model a given supply temperature. The system is therefore not particularly useful for hydronic floor heating.
- Using a serial coupling of several identical simple models to include the cooling in the length direction of the pipe has proven not to be needed – at least not with the heat losses that are used in the models. A single model has proven able to also finding the return temperature from the pipe.
- The inclusion of extra ground volume below the floor construction in one-dimensional models to include the dynamics of the ground volume does not influence the results.
- The method supplied in EN ISO 13370 where the heat loss is split into a stationary and a dynamic part is not useful for models with floor heating since the adiabatic ground boundary condition means that the floor is always heated and the functionality of the floor heating is therefore not going to be realistic

6 Thermo active components

The thermo active system has so far mainly been used in buildings where the deck has been in-situ cast, which is the typical building tradition in the Central European countries where the system was first introduced. In the Danish building tradition buildings are most often based on pre-fabricated building elements. Therefore, one aim of this work is to investigate pre-fabricated decks where the thermo active components are integrated already in the production. In section 6.1 the use of pre-fabricated decks designed as thermo active components is described.

In section 6.2 a simple way of integrating thermo active capabilities in an existing pre-fabricated deck will be investigated using a simple test setup. The activation of the deck is achieved through placing a pipe directly in the air cavities in the deck. However, the heat transfer in the cavities is not as effective as pipes integrated in the concrete and at the same time difficult to predict by simulations. Nevertheless if such a setup should prove to have a cooling capacity, which is large enough to cool the building, it would be a very simple way to make a thermo active component.

Thermo active components based on pre-fabricated hollow core decks is tested in section 6.3 in a large test mock-up. The measurements will be used to find the maximum cooling capacity of the decks and to validate the simulation model used by TASim.

Finally, in section 6.4 a simulation study using TASim will be presented.

6.1 Construction types

In this investigation only thermo active components placed in the floors in multi-storey buildings will be considered. Two types will be described both based on a pre-fabricated concrete deck.

A main concern for the implementation of thermo active components in the Danish building tradition is that it should be possible to integrate into the pre-fabricated deck. This should be done in a simple way, to prevent the production from becoming excessively more difficult and expensive. The price is not investigated in the work in this thesis.

6.1.1 Hollow deck with integrated pipes

The pre-fabricated hollow deck is, as mentioned in the previous section, used to a large extent in the Danish building industry. Therefore, if Danish buildings should use thermo active components, it will most likely be in the form of pre-fabricated hollow decks.

This type of deck has been used in the test mock-up, which is presented below in section 6.3 and will be the basis for the main part of this chapter.

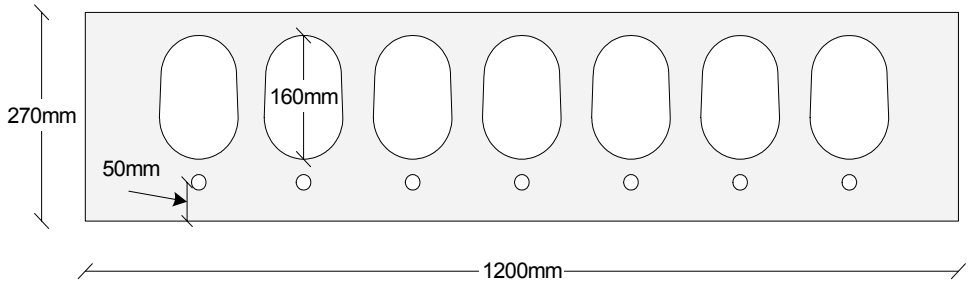

Figure 6.1 Hollow deck with integrated pipes showing the main dimensions of the deck.

To make the deck thermo active, the height of the standard version of the deck has been increased by 50mm to make room for the integrated pipe. A few of the practical considerations concerning hollow floor decks with integrated pipes based on a regular deck will be described.

Assessment of heat transfer

This section the heat transfer from a thermo active deck with integrated pipes will be assessed to establish the basic properties of this type of deck construction. The purpose is to find the thermal properties for different layout of the deck using steady-state calculations.

Generally, Heat2 (Blomberg, 2000; Blomberg, 1996) is used for the simulations.

Unless otherwise noted, the boundary conditions have been chosen to be 26°C and thermal surface resistance of 0.17m²K/W for the floor and 0.1m²K/W for the ceiling. A pipe temperature of 15°C is used. Notice that while the calculations of the heat transfer in the deck itself are detailed, the boundary conditions are simplified to constant values.

The geometry of the deck is shown in Figure 6.1. The size of the deck is assumed constant; however, the pipe diameter, cavity dimension and vertical position of the pipe are changed.

Pipe diameter

Table 6.1 shows the total heat flow from the room to the deck by changing the pipe dimension. As it can be seen, changing the pipe diameter has little impact. Therefore it is more important to consider that a smaller pipe diameter gives a larger pressure drop in the pipe, which consequently requires larger electricity consumption for running the pumps.

Table 6.1 Total heat flow from room to pipe for different values of the pipe diameter. The pipe dimension is given as the aa x bb, where aa is the external diameter and bb is the thickness of the plastic pipe. Therefore a 25 x 2.5mm pipe has an internal diameter of 20mm

Pipe dimension [mm]	Total heat flux [W]
25 x 2,5	89.4
20 x 2	87.0
16 x 2	83.9

Cavity dimension

The effect the cavity dimension is investigated in Table 6.2. The smaller of the two has the same cross sectional area as the standard deck, which is assumed to be the largest possible value to ensure the mechanical properties of the deck. In the calculations, the cavity has been simplified to a rectangular area. It can be seen that by decreasing the cross sectional area of the cavity by 20% the heat flow is only changed by around 2%. Therefore the cavity only has very little influence on the cooling capacity – a natural consequence of the fact that the heat transfer between room and pipe is mainly through the lower surface of the deck, which is not influenced by the conditions above the pipe.

Table 6.2 Total heat flow from room to pipe for different cavity dimensions

Cavity dimension [mm]	Total heat flux [W]
100x160	103.0
80x160	105.0

Vertical position

The vertical position of the pipe is dominated by two conditions, which have opposite importance. Firstly, the higher in the deck the pipe is placed the smaller the heat flow, but secondly, the better the use of the thermal mass in the concrete deck and consequent possibility to even the load during the day, since a larger part of the deck is activated. Another advantage of a position as far from the surface as possible is that the risk of accidentally drilling into the pipe from the ceiling is reduced.

The vertical position of the pipe is changed with the centerline 30mm to 60mm above the ceiling surface. Two situations are calculated; one with no floor covering and one with a floor covering in the form of a wooden floor with a thermal resistance of 0.32m²K/W. The results are shown in Figure 6.2.

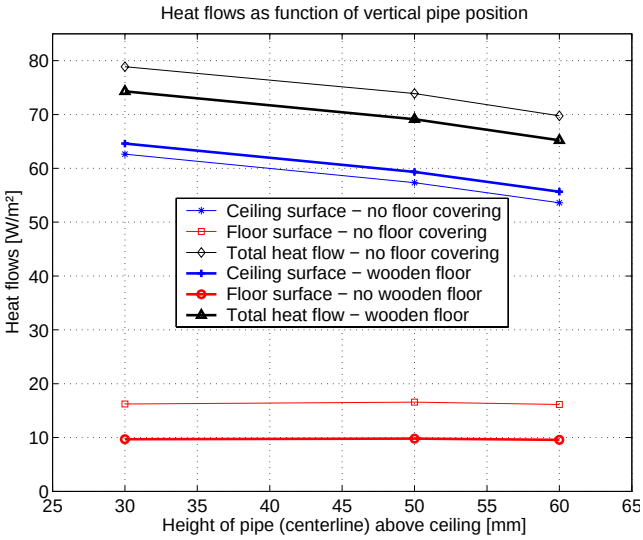

Figure 6.2 Steady-state heat flows in the deck construction for different vertical position of the pipe. The heat flows in the deck with floor covering is shown with the thicker line. The room temperature is 26°C and the fluid temperature is 15°C.

The heat flux through the floor surface is almost constant, while the heat flow through the ceiling surface and the total heat flow decrease with higher vertical position. For both the total heat flow and through the floor surface, the model without floor covering has the highest heat flow. This is not the case for the heat flow through the ceiling, which is actually higher with the floor covering, since the deck will be colder when the deck is insulated on the top side, resulting in lower surface temperature on the ceiling surface.

The heat flow is larger when the pipe is placed closer to the deck. The decrease in the total heat flow is around 12% in both situations when the pipe is moved from 30mm to 60mm above the ceiling surface.

The dynamical behavior is tested by finding the time constant for the different vertical positions of the pipe. The time constant has been defined in section 3.41. Figure 6.3 shows the heat flow through the surfaces. In the figure, the room temperature is changed from 21°C to 26°C with a fluid temperature in the pipe of 15°C. The deck is in a steady state condition before changing the room air temperature. It can be seen that the reaction time in the heat flux across the surfaces of the deck results in the same thermal behavior.

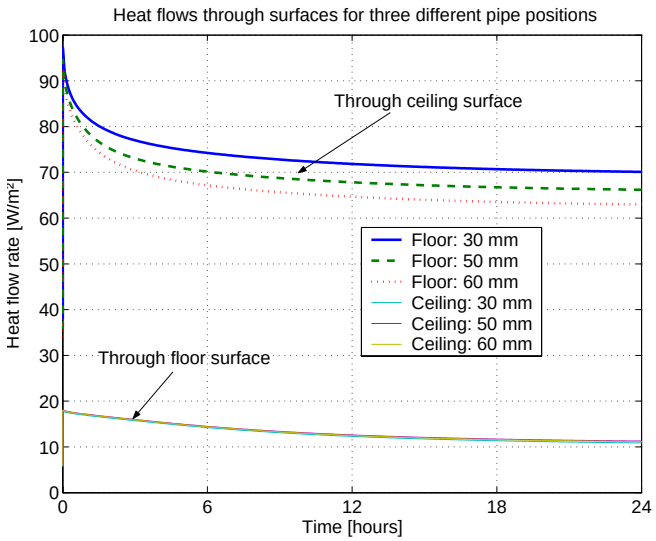

Figure 6.3 Heat flow through surfaces for different vertical position of the pipe

Conversely for Figure 6.4, where the heat flow from the deck to the pipe is shown. Here the model with the pipe placed closest to the surface has a steeper curve for the increase in the heat flow, and therefore also a shorter time constant.

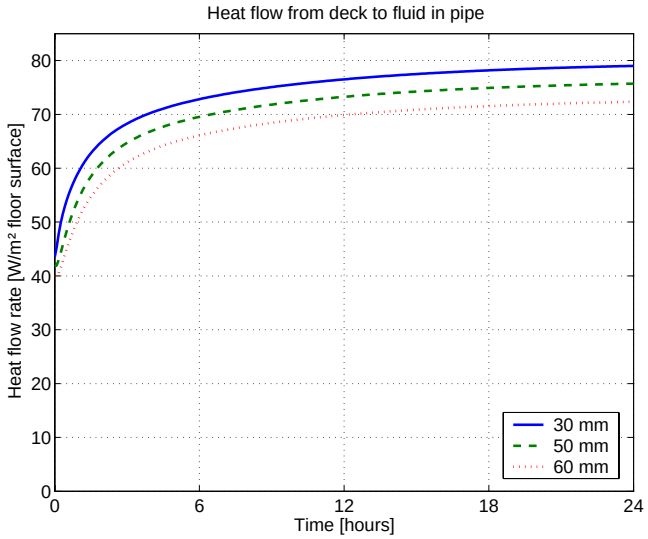

Figure 6.4 Heat flow from deck to pipe for different vertical position of the pipe, shown in W/m² floor surface

The time constants for the heat flows in the deck as found in Figure 6.3 and Figure 6.4 are shown in Table 6.3.

Table 6.3 Time constant for the heat flow in the deck construction as found by the calculation shown in Figure 6.3 and Figure 6.4

Time constant for vertical position of pipe	Through floor [hours]	Through ceiling [hours]	Through pipe surface [hours]
30mm	9.0	1.7	2.3
50mm	8.5	1.7	2.7
60mm	8.5	1.8	3.0

As expected, the results show that the time constant is largest for the floor surface, because of the large thermal mass of the concrete above the pipe and lowest for the ceiling surface. Also

the time constant is largest through the floor surface for the pipe position furthest away from the surface. This is also the case for the ceiling surface. However, here the time constant is much smaller due to the proximity to the ceiling surface compared to the floor surface. For the heat flow from deck to pipe, the values are larger than for the ceiling surface, but smaller than for the floor surface.

Preliminary conclusion

Based on these investigations a few preliminary conclusions can be made for the hollow deck with integrated pipes:

- The pipe diameter does not have any significant influence on the cooling capacity. Hence, the pipe diameter can be chosen based on considerations of pressure drop and installation costs
- The cavity size has little influence on the cooling capacity. Hence, the size of the cavity can be chosen based on considerations of static properties and load bearing capabilities and low weight of the deck.
- For the vertical distance of the pipe from the ceiling surface it is more difficult to find a simple conclusion on the best position. Two opposite properties exist. The first is the maximum heat transfer (cooling capacity), which is larger the closer the pipe is to the ceiling surface. However, the time lag between the time when the heat is absorbed by the deck until it is removed by the pipe is shorter. This means that one of the main advantages of the thermo active component, namely the ability to store heat in the deck is decreased by placing the pipe close to the surface.

6.1.2 Hollow deck with pipe in cavity (PIC)

The use of pre-fabricated hollow decks is typical in the Danish building industry. A simple and cheap way to include thermo active capabilities in the deck is to place the pipe directly in the cavities of the standard deck construction. The solution has the advantage that it can use a standard hollow deck.

This solution is called PIC for Pipe In Cavity and is shown in Figure 6.5. Obviously the heat transfer between the pipe and the concrete will be poorer since the pipe is placed in the air cavity and must rely on radiation and convection. This will limit the cooling capacity of the system. However, compared to the type with integrated pipes, the position of the pipe closer to the middle of the deck may give better use of the thermal capacity.

A simple test has been performed to find the cooling capacity. This is described in section 6.2. Another reason is that simulations of the cooling capacity have been very inconclusive, which means that it is necessary to use a test setup to find the cooling capacity.

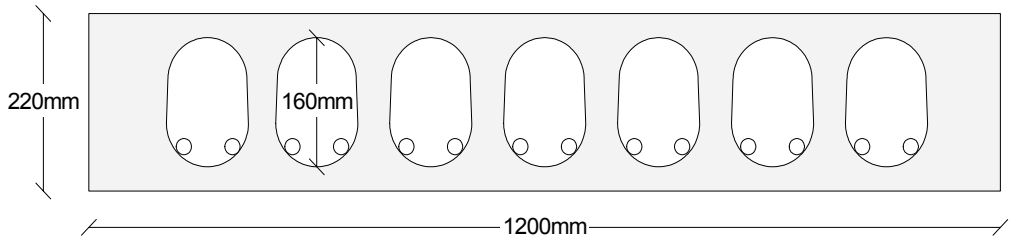

Figure 6.5 Hollow deck with pipe in cavity setup

The placement of the pipe in the floor cavities can be either with one pipe in each cavity or with two pipes placed as a U in each cavity. The U layout means that the pipe needs only to be handled in one end of the deck.

If one pipe is placed in the cavity, it will be placed at the bottom of the cavity, since it should be placed near the ceiling surface, where the largest heat transfer to the room can be achieved. At the same time it is the easiest position, as a position away from the bottom would require some type of suspension system. With two pipes in the cavity, these will be placed in the bottom half of the deck close to each side of the cavity wall. A position at the top and bottom is also possible though again it will require a suspension system.

6.2 Pipe in cavity setup

The pipe in cavity (PIC) setup is a simple way of creating a thermo active component, which has been described in section 6.1.2.

The construction with the pipe placed loosely in the cavities is attractive because it is very simple to implement. However, the thermal properties and cooling capacity are unknown and because of the complex combination of convection and radiation in the heat transfer from the pipe to the concrete deck they cannot satisfactorily be found from simulations, as it will be shown in 6.2.1. Therefore a test setup is needed to find the thermal properties of the PIC deck, which is described in 6.2.2.

In this investigation, a 220mm hollow core concrete deck with seven cavities has been used with the dimensions shown in Figure 6.5.

6.2.1 Simulations

Initially however, it is necessary to assess the accuracy of the modelling using Therm[8]. Therm is a program, which has been developed for calculating the thermal properties of windows. In order to model the combination of radiation and convection in the cavities in both glazing and frame profiles, several different methods have been implemented to account for this heat exchange. The methods have been described in the standards CEN 15099 (ISO, 2001). The methods range from simple models assuming an equivalent heat transfer coefficient in the air cavity to models where radiation and convection are calculated separately as a coupled heat transfer phenomena.

Figure 6.6 shows the temperature distribution in the floor construction with one pipe in the cavity. Further, the cooling capacity in W/m²K of floor surface is shown. The order in which the data are shown is first data for the total cooling capacity, then for the part through the ceiling and finally the part through the floor surface.

The simulation model of the floor is a section of the deck with one half of the pipe. This is due to limitations in Therm, which requires the pipe centerline to be modelled as an external boundary. Therefore the pipe has been implemented as a line with a fixed temperature on the boundary. The pipe is modelled as a material with a very large heat transfer coefficient to ensure that the surface temperature of the pipe is uniform. The assumption that a symmetry axis can be used is correct based on the radiation, but the convection in the cavity can be destroyed by the axis of symmetry since the air will most likely ascend in one half of the cavity and descend in the other half.

[8] See http://windows.lbl.gov/software/therm/therm.html for further information

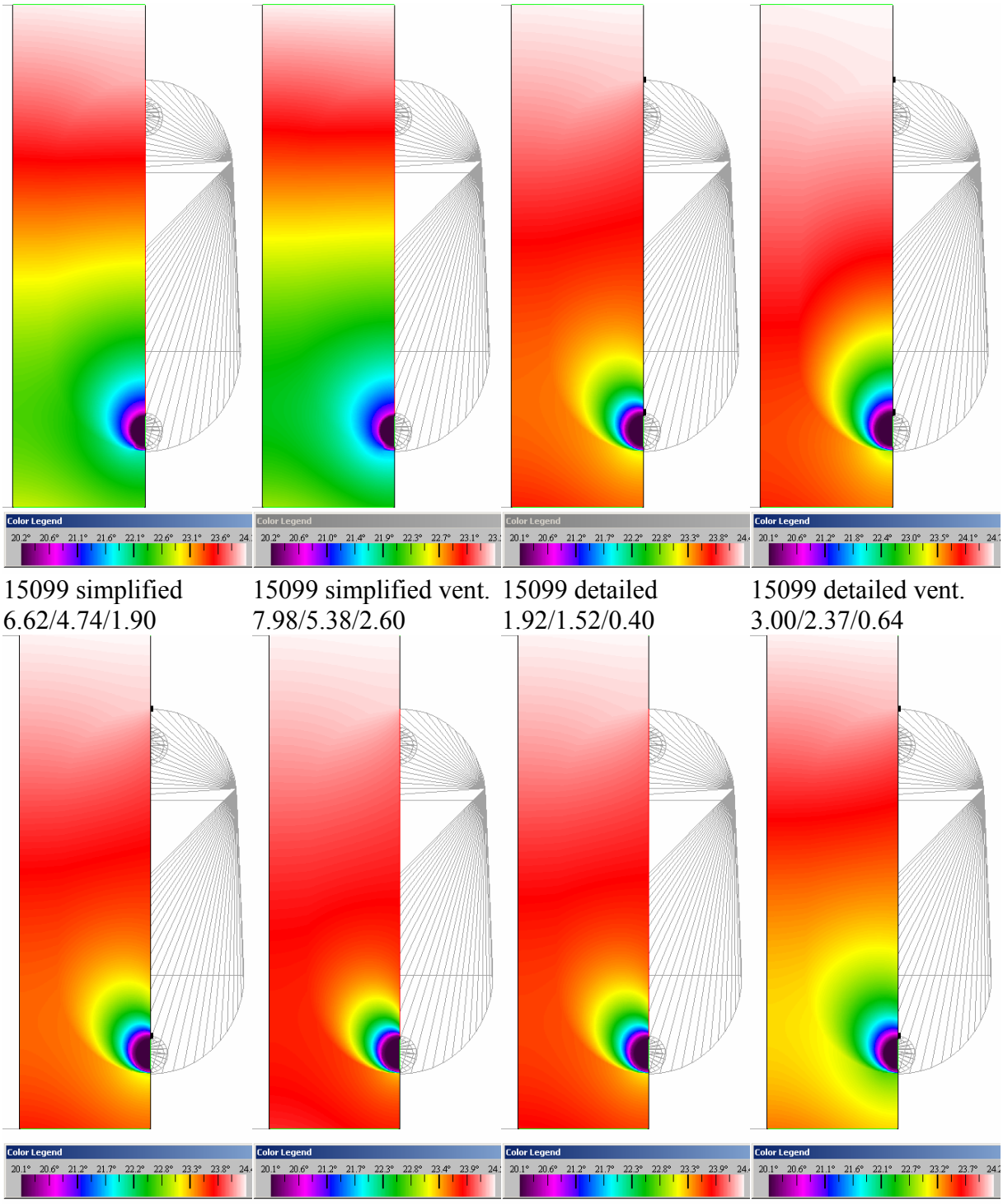

15099 simplified
6.62/4.74/1.90

15099 simplified vent.
7.98/5.38/2.60

15099 detailed
1.92/1.52/0.40

15099 detailed vent.
3.00/2.37/0.64

NFRC detailed left
3.83/2.82/1.31

NFRC detailed down
3.14/2.31/1.08

CEN detailed right
3.51/2.56/1.17

CEN detailed down
4.96/3.60/1.66

Figure 6.6 Temperature profiles and results of the cooling capacity (in W/m²K) for different methods of modelling the cavity. The numbers represent the cooling capacity of the entire deck, ceiling and floor surface respectively. The outline of the cavity can be seen in figure as well, as it is symmetric around the adiabatic line. The wire frame pattern on the right side of the figures shows the cavity of the deck, and is given by the representation in Therm. The method names (15099, NFRC and CEN) refer to the name which each of the methods has been given in Therm.

A few notes should be made to the results from the simulation model:

- There is a large discrepancy in the results, where only the modelling of the cavity is changed. A difference of a factor four is observed between the most optimistic and the most pessimistic, where the simplified models are much more optimistic than the detailed models. Observe also that the simplified models have very different temperature distribution in the section than the detailed models.
- The detailed model is the most correct as the combination of radiation and convection in the cavity is very complex. This is only estimated in the simplified models. In this case, where the heat transfer is both convective and radiative between concrete and pipe surface, the detailed model is most likely superior to the simplified. However, it is uncertain how much the results are influenced by the fact that only half the cavity is modelled, as this most likely prohibits correct determination of both convection and radiation in the cavity.
- There is a smaller (yet noticeable) difference in the results using different methods of modelling for the cavities. These methods are designed for calculations of the thermal transmittance of window frames, and thus not necessarily completely applicable for this investigation.
- If a floor covering (such as a raised floor used for cabling) is used with an assumed heat transfer resistance of 0.3m²K/W, the total cooling capacity coefficient for the calculation using 'ISO15099 detailed' is changed to 1.89/1.64/0.25, compared to 1.92/1.52/0.40 when there is no resistance from floor covering.

The large difference in the absolute values more than indicates that the results should be verified by other means. Therefore, an experimental setup is used to find the properties in the next section.

6.2.2 Test setup

Based on the very inconclusive simulation results, it was decided to make a test setup to find the cooling capacity of the deck. The test setup is placed in the research laboratory on a set of stands thereby raising the deck approximately one meter above the floor. The deck is insulated to the sides to limit the unwanted heat exchange to the surroundings. The supply and return of the pipe is insulated outside the deck. In each end, the cavities have been covered by a plastic sheathing to avoid convection between room air and cavity.

The pipe is placed as a U in each of the seven cavities, such that it only leaves the cavities at one end of the setup. In order to bend the pipe to be narrow enough to fit into the cavity the pipe has been heated before being bent. No special effort was made to ensure the placement of the pipe in the cavities.

Notice, that this setup is different than for the simulation model described above. Firstly, a setup where the pipe is not placed directly in the middle of the cavity cannot be modelled because of the implementation in Therm. Secondly, simulations have shown a large dependence on the position of the pipe in the deck, which in practise is very hard to achieve and thirdly because of the diversity of the results in Figure 6.6 no effort has been made to get a correct implementation.

Figure 6.7 shows pictures of the test setup and details of the position of the pipe in each end of the deck. As it can be seen from the pictures, the pipe position is very difficult to accurately define.

Because of the proximity of the deck to the floor surface, the radiation and convection from the bottom of the deck is not realistic as the floor surface and air under the deck is colder than

in the rest of the room. This means that the test setup will most likely underestimate the cooling capacity of the deck, which means that the measured values will be on the safe side.

Further, it was not possible to control the temperatures of the surrounding air. Therefore, it was difficult to get steady state conditions for the measurements. These factors will be taken into account when analysing the measurements.

Figure 6.7 Pictures of setup. The upper left picture shows the deck during testing. The deck is insulated to the sides and ends. The upper right picture shows the bend of the pipe in the end where it leaves one cavity to enter the next. The lower pictures show two examples of the pipe position at the far end of the deck. The bends are approximately 10 cm from the end of the deck.

The measurement positions in the deck and on the surfaces have been shown in Figure 6.8.

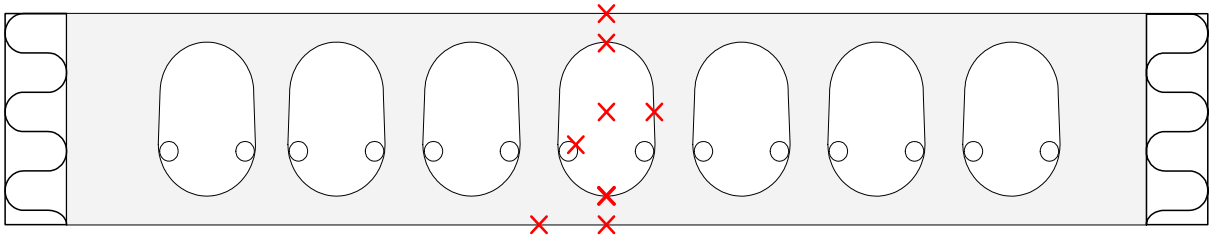

Figure 6.8 Drawing of the PIC-deck showing measurement positions

The measurements have been placed on the upper and lower deck surface and inside the middle cavity.

Besides from the measurements shown in Figure 6.8, additional measurements of the flow and temperature difference between supply and return of the flow in the pipe have been recorded.

The room air temperature has been measured in four different positions in the room away from the deck. All four temperatures have been measured at a height between 0.5m and 1.5m. No temperatures have been recorded below the deck, due to a design flaw in the test setup which also means that the floor surface temperature is not measured. This temperature is expected to be lower than generally in the room, which means that the estimates of the cooling capacity in this investigation will be conservative, since the room air temperature will be overestimated.

The purpose of the measurements is to find the cooling capacity of the deck, the temperatures in the cavities and the temperatures on the floor and ceiling surfaces of the deck.

Notice, that since the test setup has been placed directly in the laboratory, the accuracy of the measurements is not expected to be very good, because there are a large number of factors that cannot be controlled, with the most important being the surrounding temperature. However, the purpose is to find an approximate value of the cooling capacity based on a simple experimental setup, with the purpose of deciding whether or not this concept is interesting enough to continue developing. For the same reason, no effort has been made to find the accuracy of the measurements.

6.2.3 Measurement series

Six measurement series have been carried out, as shown in Table 6.4. Two variations of the setup have been tested. The difference is whether or not the floor surface (the upper surface) of the deck is covered by a layer of insulation. This has been used to model a floor covering with large thermal resistance.

The different measurement series have used different supply temperature to the pipe in the deck to find the variation with temperature.

Table 6.4 Measurement series

Series number	Supply temperature [°C]	Flow [kg/s]	Covering
1	15.9	0.045	None
2	13.0	0.045	None
3	14.6	0.045	None
4	11.6	0.044	None
5	11.7	0.044	50mm insulation
6	15.9	0.045	50mm insulation

In the investigations only steady state conditions have been investigated.

6.2.4 Results

Stability of measurements

An example of the measurement data can be seen in Figure 6.9, from series 2 from Table 6.4. As it can be seen, the conditions are nearly constant for the pipe temperature, while this is not the case for the surrounding air temperature where there are large fluctuations. Two values are shown for the room air temperature; namely the mean room air temperature and the measured minimum value. This will be used to estimate the cooling capacity in the absence of a measurement of the temperature below the deck and on the floor surface.

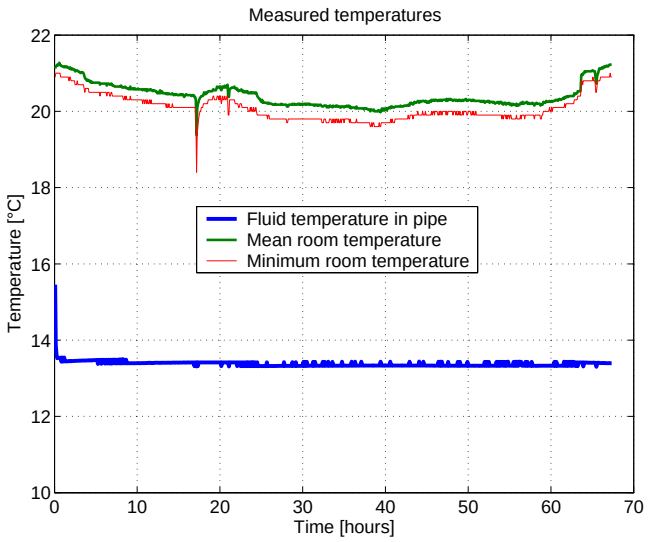

Figure 6.9 Overview of measurement results for pipe temperature and room temperature

The measured heat flow in the pipe is shown in Figure 6.10. Again it can be seen that the value is not constant during the measurement period. However, a fairly long period from around hour 30 to 60 shows nearly constant values. Therefore this period has been used to find the cooling capacity. A similar investigation has been performed for all measurement series.

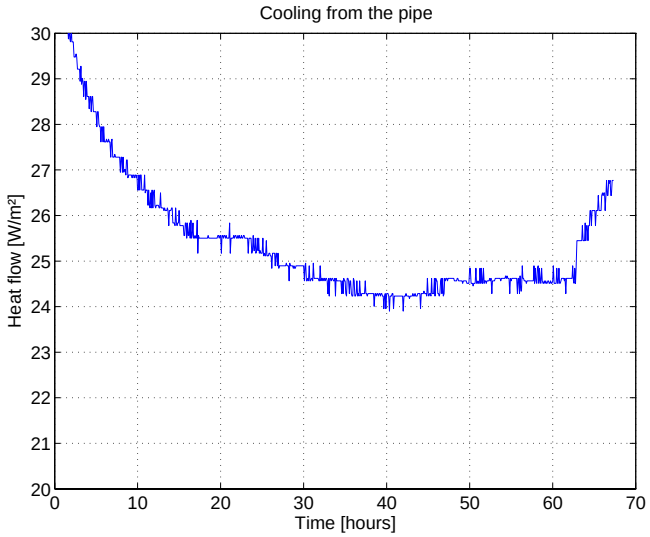

Figure 6.10 Overview of measurement results of heat flow from the deck to the pipe

It is obvious, that stringent requirements for the stability of the measurements cannot be required for the analysis. However, in all of the measurement series, there are periods with fairly stationary conditions. This is considered sufficient for the present analysis.

Temperatures in cavity

The conditions of the temperatures in the cavity are shown in Figure 6.11 for measurement series number 5. The figure shows the pipe temperature, the surface temperature of pipe and concrete in three positions (top, bottom and side) along with the cavity air temperature.

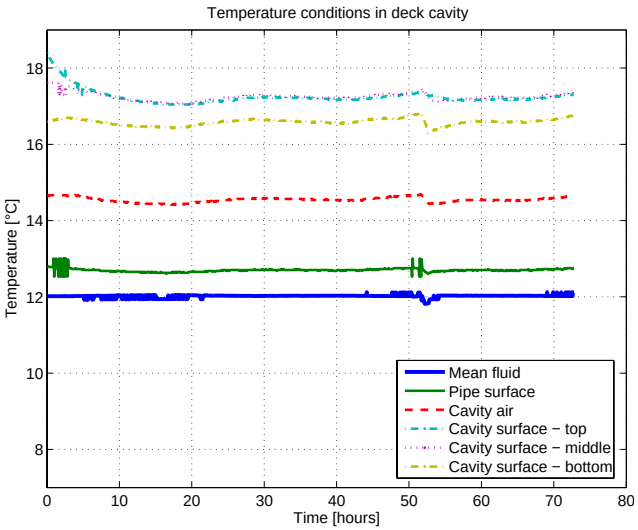

Figure 6.11 Temperature in cavity

As expected, the pipe temperature is the lowest temperature. The surface temperature is around 0.5K higher. The surface temperatures of the concrete deck are the highest temperatures. As expected, the temperature at the bottom of the cavity is lower than for the side and top, which are almost identical. The air temperature in the cavity is placed between the pipe temperature and the surface temperature of the concrete.

The fact that the temperature on the bottom surface of the deck is lower comes from the fact that the pipes are placed at the lower half of the cavity, and that the cold air will drop to the bottom of the cavity. However, more detailed measurements are needed to quantify the distribution of radiation and convection in the cavity.

Surface temperature distribution

The surface temperature of the deck is shown in Figure 6.12 based on measurement series 2, which is one of the series without insulation on the top.

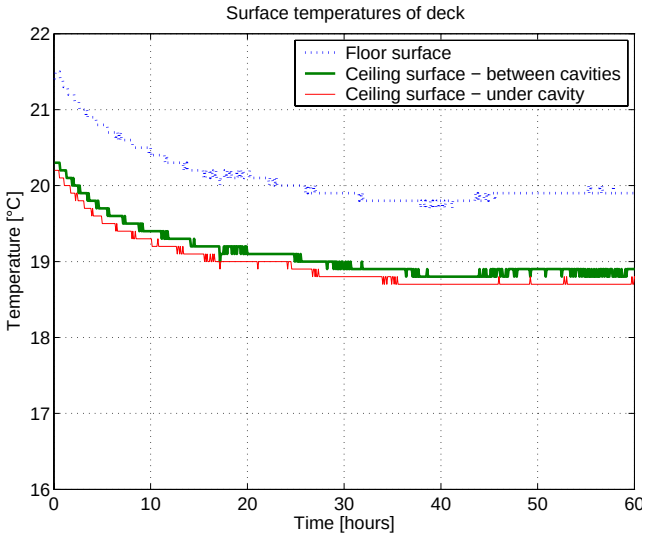

Figure 6.12 Surface temperature of concrete deck above and below the deck in one and two positions respectively

Three surface temperatures are shown; one for the floor surface and two for the ceiling surface. The ceiling surface has been measured in two positions to find the difference of the surface temperature directly under the pipes and between the pipes.

As expected, the surface temperature of the deck is lower for the ceiling surface than for the floor surface, which is a natural consequence of the fact that the temperature in the cavity is lower at the bottom and that the thermal resistance is lower towards downwards than upwards. The temperature distribution on the ceiling surface shows that the temperature is around 0.1K lower directly under the cavity than between two cavities.

Cooling capacity

Two basic equations are used to find the cooling capacity of the deck. The heat flux in the pipe can be found from Eq. (6.1), where the supply and return temperature and the mass flow of the fluid are the variables.

$$q_{fluid} = \dot{m}_{fluid} \cdot c_{p,fluid} \cdot \left(T_{return} - T_{supply}\right) \quad \textbf{(6.1)}$$

The heat flow to the fluid from the deck can be found from Eq. (6.2).

$$q_{deck} = U_{cc} \cdot \left(T_{room} - T_{pipe}\right) \quad \textbf{(6.2)}$$

Here the pipe temperature is defined as the mean value of the supply and return temperature of the fluid to the deck.

$$T_{fluid} \equiv \frac{1}{2} \cdot \left(T_{supply} + T_{return}\right) \quad \textbf{(6.3)}$$

Setting the two heat flows equal to each other, the cooling capacity coefficient, U_{cc}, can be found.

$$U_{cc} = \frac{\dot{m}_{fluid} \cdot c_{p,fluid} \cdot \left(T_{return} - T_{supply}\right)}{A_{deck} \cdot \left(T_{room} - T_{fluid}\right)} \quad \textbf{(6.4)}$$

The room temperature, which is used to calculate the cooling capacity coefficient, is the measured value with the largest degree of uncertainty. This is the case as the temperature in the laboratory is not constant and not the same above and below the deck. The air and surface temperatures below the deck are the most important temperatures for the heat exchange between deck and room. Since this has not been measured, the average room temperature will be used in stead. This temperature will be higher than the temperature below the deck, due to the cooling from the deck. Therefore, using this temperature will result in an underestimation of the cooling capacity coefficient as it can be seen in Eq. (6.4). The implications of this will be analysed below.

The cooling capacity coefficient in the six measurement series is shown in Figure 6.13 grouped by the first four being without floor covering and the last two with floor covering. As it can be seen, the cooling capacity is fairly close to being constant. The cooling capacity for the covered deck is lower than for the uncovered, which is also as expected. The average value for the covered deck is approximately 20% lower than the uncovered deck.

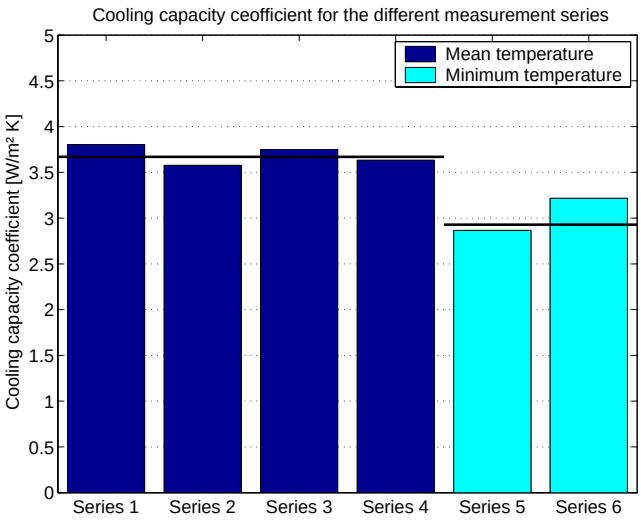

Figure 6.13 Cooling capacity for the six measurement series. Series 1 through 4 are for the uncovered deck, while series 5 through 6 are for the covered deck.

Figure 6.14 shows a plot of the cooling heat flux against the temperature difference between air temperature and fluid temperature. As indicated in Figure 6.13, the cooling capacity is nearly constant. Therefore a linear correlation between heat flux and temperature difference can be observed. In the figure, a linear fit of the measurement data using least squares for U_{cc} in Eq. (6.2) is also shown.

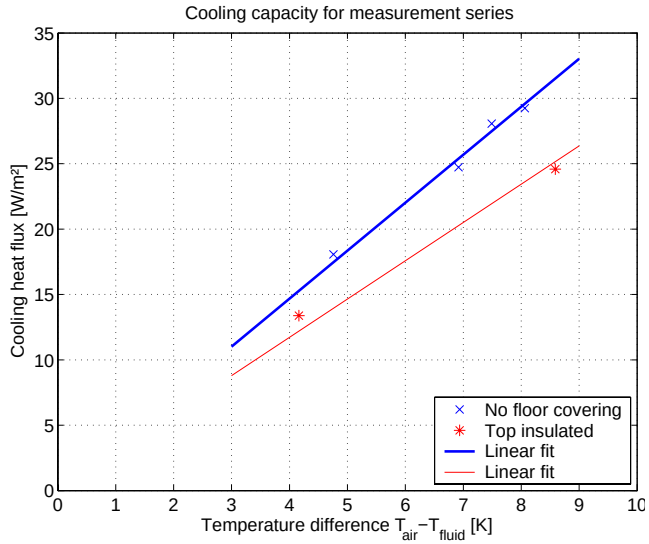

Figure 6.14 Correlation between $\Delta T_{room\text{-}fluid}$ and cooling power

The calculated cooling capacity in Figure 6.13 and Figure 6.14 is based on the average air temperature measured in the surroundings. If instead the lowest temperature is used for the calculation, as the temperature under the deck is lower than around above the deck, the cooling capacity will become larger. This is shown in Table 6.5.

Table 6.5 Cooling capacity based on either mean air temperature or lowest measured air temperature

Cooling capacity	Mean air temperature [W/m² K	Lowest measured air temperature [W/m²K]	Difference [%]
No floor covering	3.7	3.9	6%
Top insulated	2.9	3.1	6%

As it can be seen, using the mean temperature gives a 6% lower estimate of the cooling capacity than using the lowest measured temperature. Since the temperature below the deck is expected to be lower, this will give an even larger cooling capacity. Therefore, using the mean air temperature will give a conservative estimate of the cooling capacity.

6.2.5 Summing up and discussion

The present investigation has aimed at finding the cooling capacity of a concrete deck with a pipe placed directly in the pipe cavities. Initially it has been established, that the conditions of the heat flow in the deck cannot be modelled satisfactorily in a heat transfer simulation program, mainly as a result of the combination of radiation and convection in the cavities. Therefore in order to find the cooling capacity, it is necessary to use test setup.

A simple setup has been used, where the surrounding temperature could not be controlled. Therefore the conditions in the deck could not become steady-state. Still the measurements can be used to find an approximate value for the cooling capacity. Additionally, the deck has been placed close to the laboratory floor, which means that the deck will not have ideal conditions for radiation and convection.

A design flaw in the test setup meant that the temperature below the deck was not measured and instead the temperature in the surrounding laboratory has been used. This has been shown to give a conservative estimate of the cooling capacity.

The investigation has shown that a cooling capacity of around 3W/m²K can be expected when using a pipe in cavity (PIC) setup. The cooling capacity can most likely be optimized by a better placement of the pipe in the cavities and by a larger pipe than the 15mm pipe, which has been used here.

This result means that the PIC setup can cool the room by around 30W/m² assuming an average pipe temperature of 15°C and a room temperature of 25°C. This cooling capacity is the maximum value which can be achieved, and therefore it is probably not sufficient to cool office buildings during periods with large solar income and warm outside temperatures. However, due to the cheap installation cost the system is interesting to investigate further, as it can give a basic cooling of the building which can run both day and night. Therefore, in a consciously designed building, where the energy consumption has been in focus in the design process, it may actually be sufficient to cool the building using this system, so that an air-conditioning system can be avoided altogether.

A question which has not been addressed in this investigation is the dynamical behavior of the PIC-deck. However, it is expected to be equivalent to a system with integrated pipes, as the limiting barrier for the reaction time is in the concrete itself and not in the cavity, which will almost instantly change temperature once the pipe temperature is changed.

A final point is the integration of this deck construction in a simulation model for use in TASim. Based on the current investigation, there are too many unknown factors to satisfactorily model the PIC-deck, as shown by the calculations in Therm. However, it will most likely be possible to create a simple model, i.e. an RC-thermal network model as the one described in Chapter 5. Such a model will neglect the complex heat transfer in the cavity and simplify it to a contact resistance. To create this model, a larger series of measurements is needed. Alternatively, different numerical heat transfer programs can be tested to establish the cooling capacity.

6.2.6 Conclusion

Based on this small investigation, it is recommended that the cooling capacity of the deck with a Pipe In Cavity setup should be examined further, since the results from the measurements indicates that the cooling capacity in the deck is large enough to cool a consciously designed office building. It has been found that the cooling capacity is proportional to the temperature difference between fluid temperature and room temperature. Therefore the cooling capacity coefficient is a constant value.

6.3 Test mock-up

The purpose of the mock-up is to test the thermal and dynamical properties of thermo active components and rooms in buildings with thermo active components based on pre-fabricated hollow core concrete decks.

The main purpose of the test mock-up in this context is to find the maximum cooling capacity of the deck under steady-state conditions and the dynamical behavior for a daily variation of internal heat loads and flow (on/off). In addition to this, the thermal comfort in the room is also measured. The purpose of these measurements of heat flows and temperatures is to validate the program TASim.

The measurements are kept as simple as possible. However, future measurements in the mock-up can include different concepts of suspended ceilings, operable suspended ceilings and different types of ventilation systems and even different types of thermo active components. This has, however, not been possible in the frame of this thesis.

6.3.1 Design

Before describing the design in detail, notice that the mock-up is part of an on-going project sponsored by ELFOR (the Danish union of electricity distributing companies) to investigate the introduction of thermo active components in the Danish building industry. This project is still in an early phase, and therefore the measurements in the mock-up are preliminary in the sense that at the time of the finishing of this thesis, the mock-up has not been completely finished. The influence of this will be described where appropriate. However most importantly, the measurements are well suited for validation of TASim, which is the main interest in this context. The final results from the measurements in the mock-up will be published during 2005.

General description

The main design of the mock-up is a construction consisting of two levels of thermo active components in between which an office room in a building is placed. The room is closed to the four sides by insulating walls. The room is surrounded by a guard box, which separates the room and thermo active component from the rest of the laboratory.

The room has a length of 6.0m and a width of 3.6m, for a total room area of 21.6m², equivalent to a fairly large single person office or a “typical” two-person office. The internal room height is 3.6m. The decks are 6.6m in length, so that they are long enough to be supported by the load bearing construction (described below). The lower deck is raised about 0.5m from the floor in the laboratory. The upper deck is about 4.4m above the laboratory floor.

The total size of the mock-up is 7.6m long, 4.6m wide and 5.4m high.

Two levels of thermo active components have been used to ensure that the room will have a deck with realistic conditions both above and below the room itself. The dimensions of the deck are identical to those in Figure 6.1. That is the deck is 270mm high, 1200mm wide and 6600mm long. The deck has seven cavities with a distance of 150mm. The height is of the cavities is 160mm and the width is 108mm where it is widest. Below each of the cavities a 20mm PEX-pipe is integrated in the concrete. The centerline of the pipe is 50mm above the ceiling surface.

In the test version, individual strings of pipe will be integrated in the deck, which will be connected after creating the deck. A later version will most likely have the pipe placed as a serpentine in the deck.

The ends of the decks have been insulated to minimize unwanted heat losses from the deck to the guard. The temperature in the guard zone will in all cases be controlled to be the same as in the room, to ensure that there will be no heat transfer across the room walls. The air gap in the guard zone will also allow realistic thermal conditions for the deck surfaces facing the guard. However, the radiation is not going to be completely realistic due to small vertical distance between deck surface and guard surface. For the measurements in this work, the thermal guard has not been finished, and therefore the guard temperature has not been controlled. Where this has an influence on the results this will be stressed.

The decks are supported by a load bearing construction placed in the air gap in the guard, designed as four steel columns with beams for supporting the deck-elements. To ensure that the supporting beams will have a minimal influence on the temperature distribution in the deck, a 100mm x 100mm wooden beam is placed on top of the steel beam as a thermal break.

Approximately 50 thermocouples and thermopiles are measuring the temperatures throughout the construction.

The flow in the decks is controlled by two flow units capable of delivering water at a given temperature and flow. The flow units can be turned on or off at a given time schedule to give dynamical conditions for the flow.

Internally in the room, four radiators with a total power output of 1.9kW are installed as heat load. The maximum heat load in the room is therefore 88W/m². The internal heat load is controlled by a power controller which is fed by a continuous 0-10V signal. Therefore for instance, a 5V signal means that the radiators are turned on 50% of the time, resulting in a heat load of 44W/m². The heat load can be controlled, in principle, infinitely variably.

The guard will be controlled by the same type of control, once this has been installed.

In the room, there is no ventilation in the present state of the mock-up. The inner walls and joints between walls and decks have been carefully assembled to avoid leaks.

The measurement and control of the conditions in the mock-up is integrated in a LabVIEW (National Instruments, 2003) application.

Figure 6.15 and Figure 6.16 shows the main dimensions of the mock-up seen from the side and horizontally.

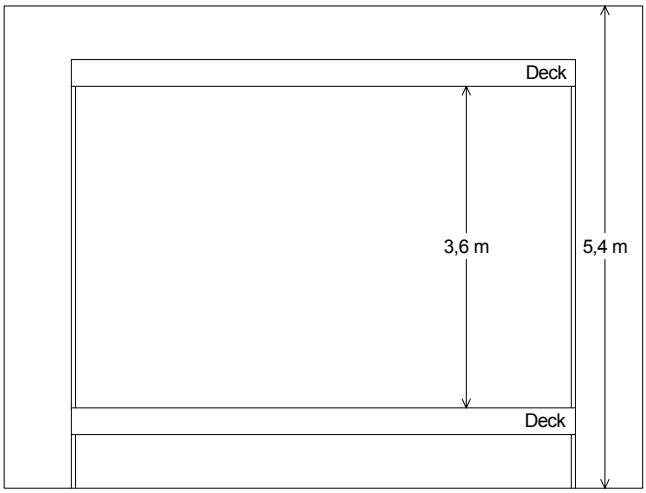

Figure 6.15 Main overview of dimensions in a vertical view of mock-up seen from the side.

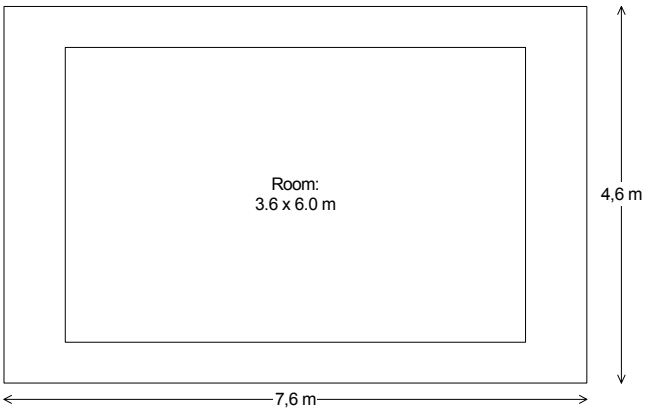

Figure 6.16 Main overview of dimensions in a horizontal view of mock-up seen from above.

Pictures of the construction

To give a better idea about the construction, a few pictures from the construction phase are shown.

Figure 6.17 shows the load bearing construction and the lower deck. Notice the wooden beam placed between the deck and the load bearing steel beam which will break the thermal bridge. Both the lower and upper deck are made from three decks, each with a width of 1.2m for a total of 3.6m.

Figure 6.17 Pictures of the load bearing construction and the lower deck after installation.

Figure 6.18 shows two close-up pictures of the end of the deck. The left picture shows the deck. The pipes are placed directly under each of the cavities and they have not been assembled. This is shown in the right picture where the pipes have been connected as a serpentine layout for each of the three decks which are each fed from a manifold. The picture shows the insulated supply pipe where the supply temperature and warm side of the temperature difference between supply and return are measured, through which the distributing manifold pipe is fed. Further the insulation of the side of the deck can be seen. During the measurements, the box at the end of the deck is insulated.

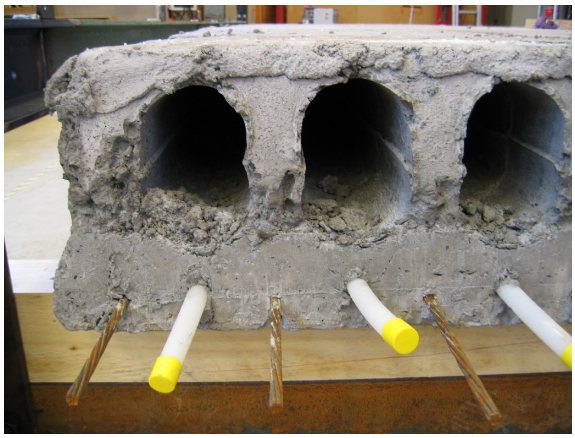

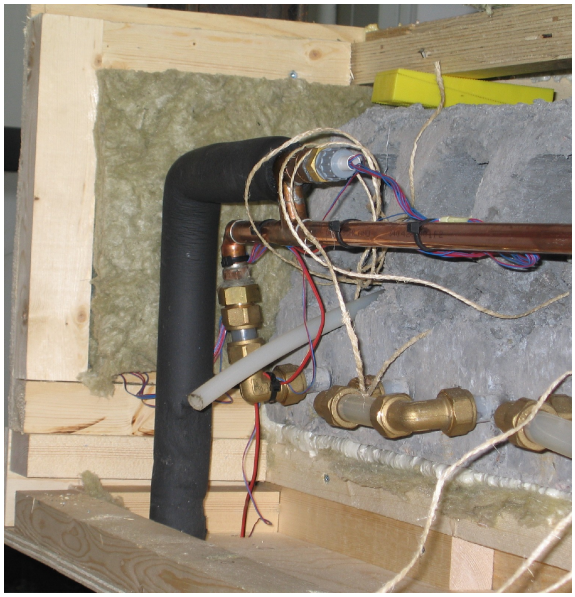

Figure 6.18 Pictures of the end of one of the decks. The left picture shows the deck without the pipe connected, and the right figure shows the deck with manifold.

Figure 6.19 shows the finished insulation box at the end of the deck. The inner wall between room and guard can also be seen.

Figure 6.19 End of upper deck after being finished. The wooden box is filled with insulation thereby minimizing the unwanted heat loss from end of deck and manifold. All four deck ends (upper and lower) have the same insulation box.

Figure 6.20 shows the floor construction in the room. This is constructed as a wooden floor on rafts placed on the concrete deck. In the room, the floor construction is finished by a 6mm parquet floor to make a “nice looking” finish in the room. This has not been installed in the upper deck, as this will not be visible.

Figure 6.20 Floor construction. A wooden floor on rafts is used. A plywood plate of 15mm is used as the floor covering. In the room, a 6mm parquet floor is placed on top of the plywood plate.

Figure 6.21 shows the room after being finished. The pole in the middle of the room is used for air temperatures and the partly hidden pole is used for measurement of operative, radiant and air temperatures as well as air velocity and relative humidity. The picture also shows two of the four radiators with a nominal power output of 500W. These are placed approximately in the middle of each of the walls about 200mm from the floor.

Figure 6.21 Room. Four 500W heating panels (two can be seen here) are installed on each wall. Centrally in the room, measurements of temperatures (air, radiant and operative) are performed as well as air velocity and relative humidity.

Measurement equipment

The temperatures in the mock-up are measured by the use of thermocouples for absolute temperatures and thermopiles for temperature differences. Type TT thermocouples (cupper/constantan) are used. Type TT has an increased accuracy compared to type T. An Agilent 34970A data acquisition/Switch unit equipped with 60 voltage and 6 current measurement slots connected to a PC is used for the measurements.

The temperatures are calculated internally in the instrument by using ITS-90 software compensation.

The accuracy of the temperature measurements can be found from the following relation:

$$Accuracy = \pm(\%\text{ of reading} + \%\text{ of range}) \tag{6.5}$$

This accuracy is very good for the measurement of voltage and conversion of voltage to temperature to temperatures. However, the accuracy of the thermocouple itself is not as good. An accuracy of ±1K is given in the data sheet for the data logger, plus the accuracy from the thermocouples themselves, which are expected to be 0.3% of the reading. This is typical for thermocouple measurements. A very large part of this is due to the fact that a common reference point in the data logger is used. Since the temperature across this data logger board can be up to 1K, this sets the limit to the accuracy.

For the voltage differential measurements (thermopiles), which do not use the reference point in the data logger, the coefficients in Eq. (6.5) for the measurement accuracy are 0.0050+0.0040. Notice that for the thermopiles, three or five elements in the pile are used to increase the measurement signal. This increases the accuracy of these measurements.

The flow is measured using a “Danfoss MASS 1100, DN10” which can measure up to 4.400 kg/h. The output from the unit is a 0-20mA signal, where the maximum rate which will give 20mA can be set on the unit. An accuracy of ±0.5% is given on the output of the signal. The accuracy of the reading in the data logger, the coefficients are 0.050+0.005.

The accuracy of the heat flow in the decks is a combination of the flow measurement and temperature difference measured by the thermopile placed in the supply and return of the decks (see right side of Figure 6.18 for position of the supply side of the thermopile). In a

previous investigation (Weitzmann and Jensen, 2000), the error has been shown to be less than 2% of the actual heat flow.

For the measurement of operative temperature, radiant temperature, air velocity and relative humidity, Brüel and Kjær 1212 and 1213 have been used. For the operative temperature the accuracy is ±0.5K. At the same time, there is an offset error in the device, which has been found by calibrating it using a digital precision thermometer. Here the offset was found to be 0.4K, meaning the device measures too high operative temperature.

Control systems

The control of the radiators in the room is controlled by a Measurement Computing PCI-DAS6014 control and measurement board, which is integrated in the PC. The board sends a 0-10V signal to an electronic analog power controller from IC Electronic. This power controller is using a 'Burst Firing mode', which is in practice a switch which will ensure that the power controller will supply power to the radiators in the part of the time decided by the control signal. Therefore a 5V signal means that the radiators are turned on for 50% of the time.

The temperature in the room is controlled by a PID-control of the heat supply to the radiators in case of steady state measurements and a fixed signal when a fixed heat supply to the radiators is required.

The temperature in the guard is controlled to be identical to the room temperature. This has however not been included in these measurements since the guard walls have not been installed for the measurements.

Measurement positions of temperature

Figure 6.22 shows the temperature positions in the upper deck. Three sections are used, with a different number of measurements in each section. The positions of the sections are shown on the horizontal view. Section 1 is the most detailed, where temperatures are measured in different positions of the deck and on the upper and lower surface of the deck. The temperatures in four internal positions are measured. In all sections, the temperature difference across the floor covering has been measured to find the heat flow. A thermopile with three elements is used in each of three sections. For the lower deck, only one temperature on the lower surface is measured. Otherwise the same positions are installed here.

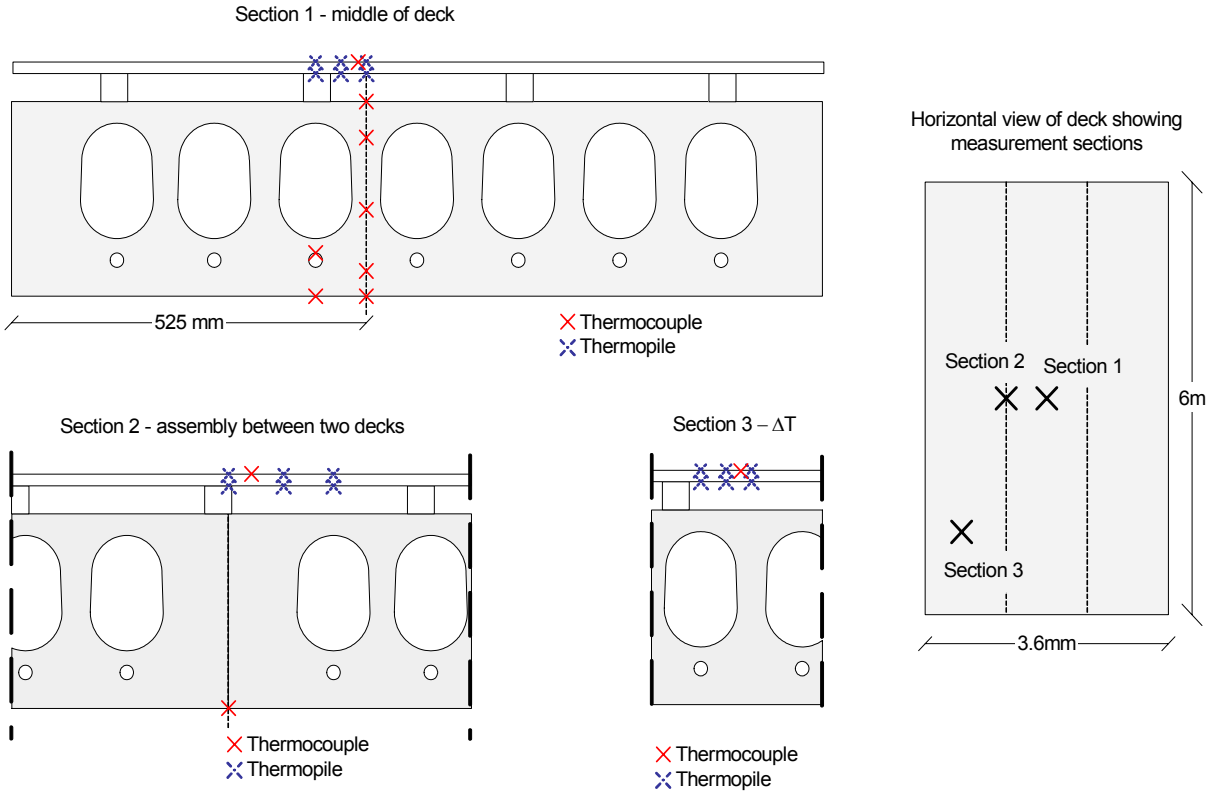

Figure 6.22 Measurement positions in the decks for the three measurement sections. The horizontal view shows the position of the measurement sections, while the vertical views show the actual placement.

Figure 6.23 shows the measurement in the room. The left figure shows the internal surface temperatures. The floor and ceiling surface temperatures are measured in the middle of the surface. On one of the 6m long walls, the surface temperatures are measured at heights of 0.5m, 1.5m, 2.5m and 3.5m. Initially, a test has shown that measuring the temperature in the middle of each of the surfaces gave almost identical surface temperatures, which means that there is no need to measure all four. The right figure shows the air temperature measurements, which are measured at 0.1m, 0.7m, 1.1m, 1.8m and 3.5m (0.1m from the ceiling surface).

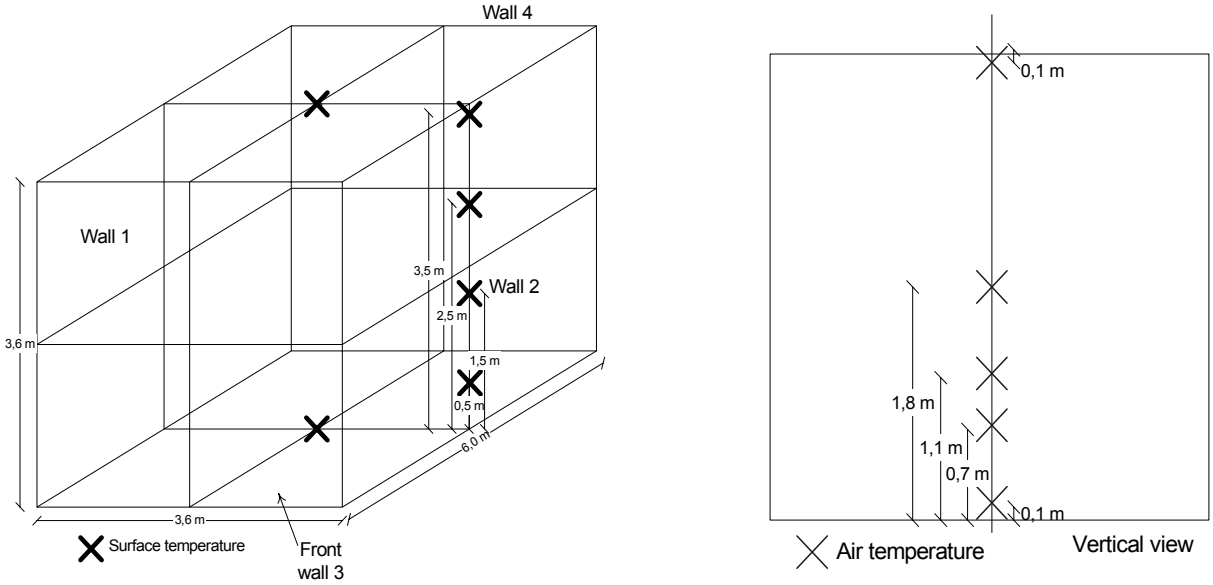

Figure 6.23 Measurement positions in room.

Figure 6.24 shows the control measurements of the temperatures and temperature differences characterising the conditions between room and guard. The measurement positions shown on the left figure are used to find the surface temperature of the end of the deck. The middle figure shows the measurement positions for the temperature difference between the rim of the deck and guard. Finally, the right figure shows the measurement of the temperature difference across the inner walls. One thermopile is installed in each of the four walls.

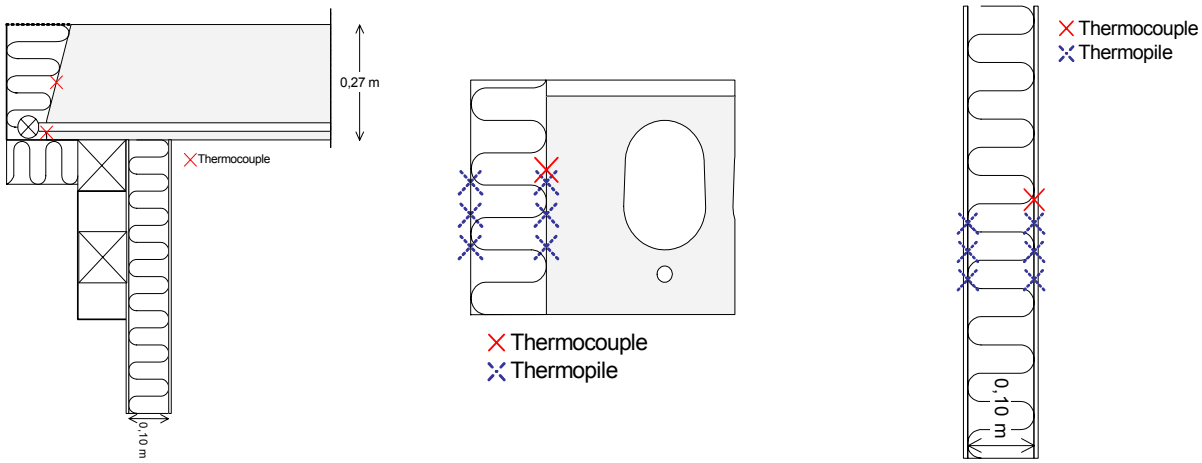

Figure 6.24 Measurement positions between room and guard.

Measurements of flow and temperatures in water loop

Figure 6.25 shows the measurements used for the flow and temperatures in each of to the two decks. The flow is measured in the flow unit while the supply temperature is measured directly at the inlet to the distribution manifold to each of the decks. The temperature difference is measured by a thermopile placed in the inlet and outlet from the manifolds. The same setup is used for both decks.

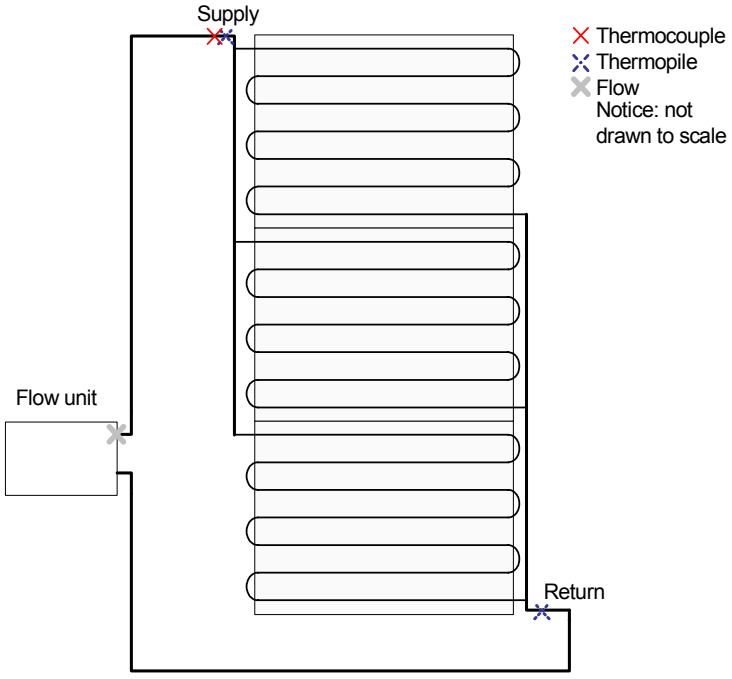

Figure 6.25 Measurement positions used for flow measurement

Heat load in room

The heat load in the room is found from the control signal to the power control units. The following conversion is used, which has been found by measuring the integrated energy consumption for approximately 5-10 minutes for each measurement point while applying the control signal. Based on this, the average heat load during the integration period has been calculated resulting in a linear relation, which is shown in Figure 6.26.

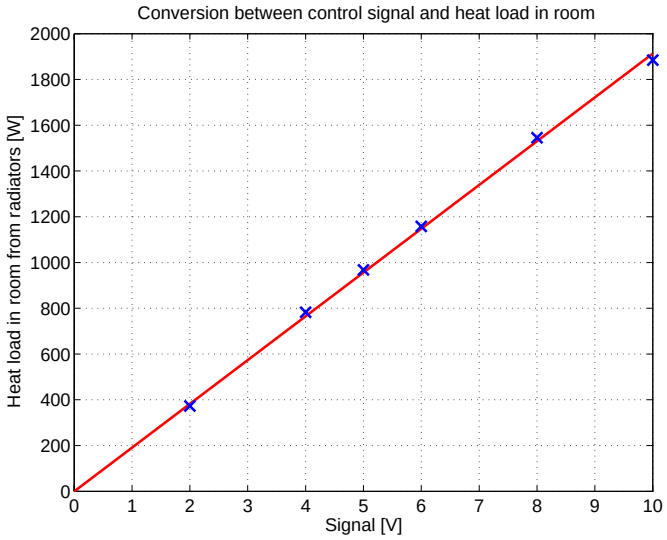

Figure 6.26 Conversion between control signal to power control unit and heat load in room

Using a linear fit, the following correlation between control signal and heat load in the room:

$$q_{room} = 191.3 \cdot V_{signal} \ [\mathrm{W}]$$

or **(6.6)**

$$q_{room} = 8.86 \cdot V_{signal} \ [\mathrm{W/m^2}]$$

This correlation is used for finding the internal heat load in the room. Notice, that when the control signal is 10V, the heat flow rate to the room is only around 1900W instead of 2000W which is the nominal heat load.

A long term comparison spanning two days of measurements between the calculated energy consumption based on the control signal and an integrated measurement shows a deviation of around 2% between measured and calculated heat flow.

6.3.2 Unwanted heat flows in construction

Besides from the accuracy of the measurement equipment, another source limiting the measurement accuracy is the unwanted heat flows in the mock-up.

The following heat flows are considered:

- One-dimensional heat flow through walls between room and guard
- Two-dimensional heat flow through the ends of the decks
- Two-dimensional heat flow through the sides of the decks
- Three-dimensional heat flow through corners
- Infiltration/exfiltration between guard and room

These are treated individually in the following sections. Finally, a section is dedicated to other types of unwanted heat flows in the construction.

The investigation of the unwanted heat flows in this section does not cover the unwanted but required heat flow from the deck surface which is facing the guard. This heat flow is required to give realistic conditions for the temperatures and heat flows in the decks. Therefore the upper deck is not insulated to minimize to unwanted heat loss, since this will cause unrealistic and undesired temperature distribution, especially for the dynamical measurements. At the same time, the heat flow through the floor surface of the upper deck is measured based on measurements of the temperature difference across the floor covering, as shown in Figure 6.22.

One-dimensional heat flow through walls between room and guard

The one-dimensional heat flow through the walls can be estimated by the measured temperature difference across the insulation layer in the wall construction, since the thermal transmittance is well-defined for the wall. The thermal transmittance is 0.38W/m²K or 26W/K, since the area of the inner walls is 69m².

Since the temperature difference between room and guard is typically less than 2K even without the guard installed, since the laboratory temperature during the measurement period is around 23-24°C, a maximum unwanted heat flow of 50W can be expected.

Two-dimensional heat flow through the ends of the decks

The deck end is extended approximately 30cm into the guard zone in each end of the deck. Figure 6.27 shows the end of the deck with the insulation box and manifold. The unwanted heat loss from the deck to the guard is found as the heat flow from the deck to the insulation box and wall below the deck. The two-dimensional section assumes that the temperature at the pipe level is the same in the entire deck, and that there are no air cavities. Different combinations of room/guard and pipe temperature are tested. For all combinations a value of 0.4W/mK is found. The temperature difference refers to the difference between the fluid temperature in the pipe and the guard temperature. For the 7.2m of deck end, a maximum unwanted heat loss of 2.9W/K can be expected.

Since this difference will typically not be larger than 10K, a maximum of approximately 30W for one deck can be expected.

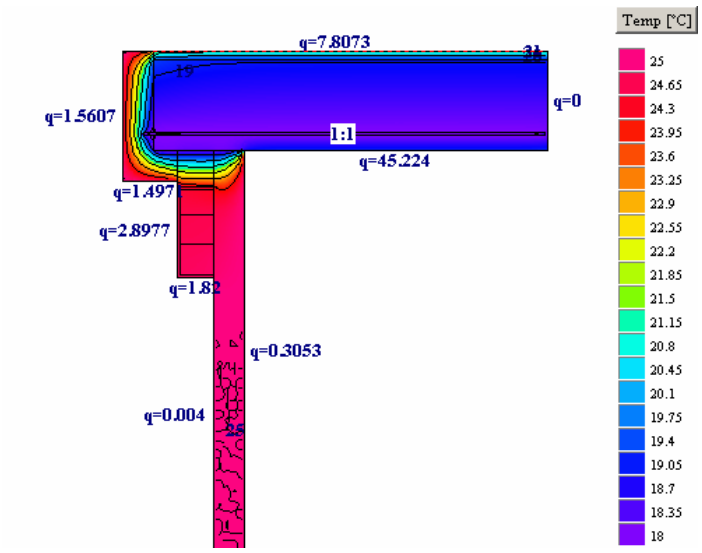

Figure 6.27 Heat2 simulation of temperatures in the end of the deck. Heat flows shown in W/m² surface.

Two-dimensional heat flow through the sides of the decks

The unwanted heat loss along the side of the deck is found in similar way as above. Figure 6.28 shows a calculation using 18°C pipe temperature, 25°C room temperature and 27°C guard temperature. This results in an unwanted heat loss of 0.6W/m of joint, which will result in an unwanted heat loss of 7W for the 12m of thermal bridge. Again different combinations of fluid and room/guard temperature have been tested. In this case the linear thermal transmittance value loss is not the same for all combinations of temperatures. However the value of 0.6W/m was found to be the highest for any of the combinations. A maximum unwanted heat loss of 10W for each of the decks is therefore assumed.

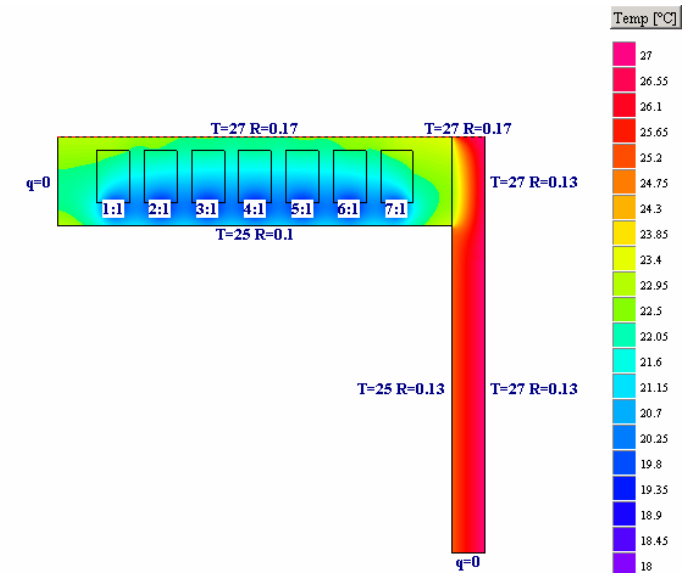

Figure 6.28 Heat2 simulation of temperatures along the rim of the deck. Here shown for the upper deck

Three-dimensional heat flow through corners

The heat flows through the corners also been estimated using a Heat3 simulation. However, in this case it is not possible to use given temperatures as inputs for the pipes. Instead it is necessary to use a heat flow rate, which means that the estimates can not be defined in the same way as when using temperatures as input.

However, a maximum unwanted heat loss of around 1W for each corner is found. For practical purposes, this heat flow can be omitted from the investigations.

Infiltration/exfiltration

The air change rate between room and guard due to infiltration/exfiltration has not been measured. However, even for an air change rate of 5l/s, which is assumed to be very high the unwanted heat loss is 6W/K, or 12W if the temperature difference is 2K between room and guard.

Other sources of unwanted heat flows

A source of unwanted heat loss from the room to the guard is the fact that the radiators are placed on the walls, which means that the walls are heated. The unwanted heat loss from this is not assessed here.

Summing up on unwanted heat flows between deck/room and guard

In this section the unwanted heat losses between deck and guard and room and guard have been investigated. An estimated maximum value of each of the unwanted heat losses has been given based on a worst-case situation.

A combined accuracy of the mock-up has not been found. Firstly, the accuracy in an actual case depends on the relevant heat flows in that case. For instance an energy balance for the upper deck will not be influenced (directly) by the unwanted heat loss through the inner walls. Secondly, since the mock-up has not been finished with the guard wall being installed, the accuracy will depend on the temperature in the laboratory, which is different for all measurement series – and therefore a new estimation of the accuracy is, in principle, needed for each measurement. Considering only the upper deck, it may actually be an advantage that the guard is not finished, since the unwanted heat loss from the floor surface will be smaller since the surrounding temperature in the laboratory is normally lower than in the room.

An assessment of the maximum unwanted heat loss from the deck to the guard has shown that the maximum value is found to be 40W (30W from the ends and 10W from the sides). This is based on a guard temperature which is higher than the room air temperature, which is not the case for the measurements where the guard temperature is typically 1K-2K lower. A correction of 40W is equivalent to 2W/m² floor surface, since the room is 21.6m². As the cooling capacity of the deck in the measurements is between 30W/m² and 60W/m² an error of 3%-7% is the maximum expected value. However as this value is based on maximum expected values, the unwanted heat loss will be lower than given here.

6.3.3 Data analysis

The purpose of the data analysis is to find the main heat flows in the construction and the cooling capacity from the deck to the room. This section sets up equations for calculating the heat flows in the upper deck and the entire room. Further, the measurement data are used to validate TASim.

Energy balance and heat flows in upper deck

The main object for the measurements is to find the heat flows in the upper deck. In this analysis, the deck is considered the object of the measurements while the rest of the mock-up is actually only a means of creating the proper boundary conditions for the deck. The upper deck is used for the investigation. This means that the main heat flow, q_{up}, will consequently be through the ceiling surface of the room.

Figure 6.29 shows the deck with the main heat flows, where q_{pipe} is the heat flow in the pipe, q_{up} is the heat flow through the ceiling surface, q_{down} is the heat flow through the floor surface and q_{guard} is the heat flow between the ends and sides of the deck.

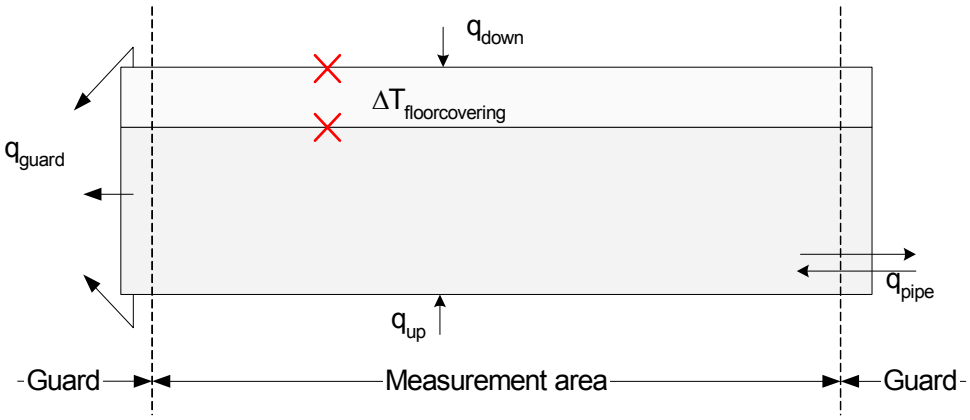

Figure 6.29 Heat flows in upper deck

Eq (6.7) is the main energy balance for the deck assuming steady-state conditions.

$$q_{pipe} = q_{up} + q_{down} + q_{guard} \tag{6.7}$$

The individual heat flows can be found as described below.

The heat flow between pipe and concrete deck, q_{pipe}, is given by the basic relationship between flow and temperature difference between supply and return temperature.

$$q_{pipe} = \dot{m} \cdot c_p \cdot \left(T_{supply} - T_{return}\right) \tag{6.8}$$

The heat flux through the floor surface, q_{down}, is found from:

$$q_{down} = \frac{1}{R_{floorcovering}} \cdot \Delta T_{floorcovering} \tag{6.9}$$

The thermopile is placed directly across the plywood layer in the floor construction. The thermal resistance of the floor covering is therefore the resistance of the plywood plate. The thermal resistance of the plywood plate is well-defined, which means that the measurement of the heat flow based on this thermal resistance will also be well-defined.

The unwanted heat loss from the ends and sides of the deck to the guard, q_{guard}, can be estimated based on simulations using the actual measurement conditions as input. This has been described above in section 6.3.2. In general, the heat loss is a function of geometry and temperatures in room, guard and deck (based on the fluid temperature pipe).

$$q_{guard} = f\left(geometry, T_{room}, T_{guard}, T_{fluid}\right) \tag{6.10}$$

In this investigation, no corrections of the heat flow from the deck to the guard will be made. Notice, that in section 6.3.2, a maximum expected unwanted heat loss of 3%-7% of the total energy balance of the deck is found.

Based on Eq. (6.7) to Eq. (6.10) it is possible to find, q_{up}, which expresses the cooling capacity of the ceiling surface.

This set of equations is equally applicable to both decks, though the upper deck is the most interesting when the decks are used for cooling the room. Notice that the heat flow through

the ceiling surface of the lower deck will not be realistic compared to the upper deck due to the proximity of the floor in the laboratory – especially for radiation.

Heat flows in the room

The heat flows in the room are generally more difficult to measure than in the deck alone. Therefore, the measurement accuracy is expected to be poorer than for the deck alone.

Figure 6.30 shows the heat flows in the room

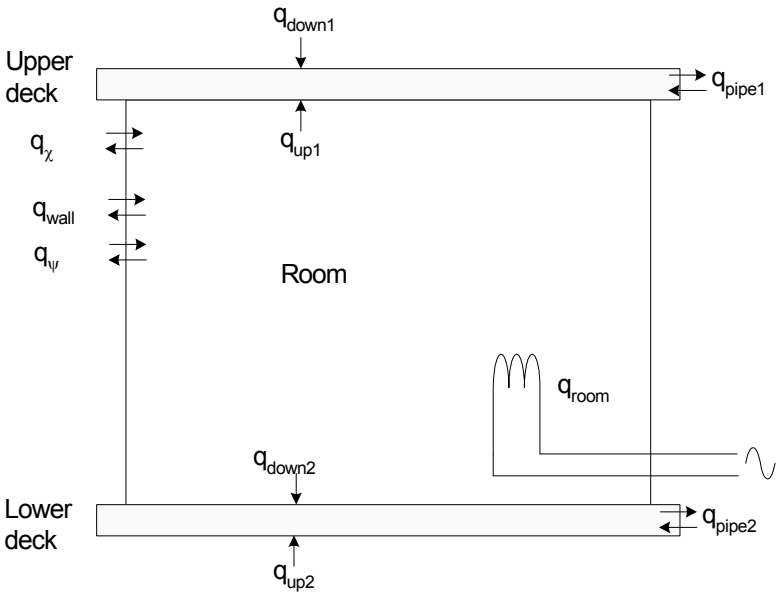

Figure 6.30 Heat flows in room.

Again, an energy balance equation can be set up for the conditions – in this case for the room:

$$q_{room} = q_{up1} + q_{down2} + q_{wall} + q_{\psi} + q_{\chi} \quad \textbf{(6.11)}$$

Where:

q_{room}	Heat load in the room
q_{up1}	Heat flow from room to the upper deck through the ceiling surface
q_{down2}	Heat flow from room to the lower deck through the floor surface
q_{wall}	Unwanted one-dimensional heat flow from room to guard
q_{ψ}	Unwanted two-dimensional heat flow from room to guard
q_{χ}	Unwanted three-dimensional heat flow from room to guard

The heat flows through the wall, q_{wall}, is a function of the temperature in the wall and guard and the thermal transmittance of the wall.

$$q_{wall} = f\left(T_{room}, T_{guard}, U_{wall}\right) \quad \textbf{(6.12)}$$

The heat flows through the assemblies and corners, q_{ψ} and q_{χ}, are as the wall heat transfer a function of the temperature difference between room and guard. The line and point heat transfers can be calculated in for instance Heat2 and/or Heat3, which are used to predict the unwanted heat loss. These two are shown in Eq. (6.13) and (6.14).

$$q_{\psi} = f\left(geometry, T_{room}, T_{guard}, T_{fluid}\right) \quad \textbf{(6.13)}$$

$$q_{\chi} = f\left(geometry, T_{room}, T_{guard}, T_{fluid}\right) \quad \textbf{(6.14)}$$

Notice, that the fluid temperature is also included in the equations, even though it is not directly a part of the heat transfer between room and guard. However, the temperature in the decks will have an influence on the line and point losses from the room to the guard.

The left side of Eq. (6.11) can be found by measuring the heat loads in the room, which comes from the electrical heaters in the room. The relationship between heat loads and control signal has been defined in Figure 6.26 and Eq. (6.6).

$$q_{room} = f\left(heat\,loads\right) \quad \textbf{(6.15)}$$

Cooling capacity

The cooling capacity of the ceiling surface of the upper deck can found based on Eq. (6.7) to Eq. (6.10), using steady-state measurements. In this section the method is applied to the measurement conditions and further, the cooling capacity coefficient is defined.

In brief the method is to find the heat flow through the ceiling surface and divide the heat flow by the temperature difference between the fluid and the room.

The heat flow through the ceiling surface, q_{up}, is found from Eq. (6.16)

$$q_{up} = q_{pipe} - q_{down} - q_{guard} \quad \textbf{(6.16)}$$

That is, the heat flow through the ceiling surface is the heat flow in the pipe minus the unwanted heat flows to the guard through the sides and ends of the deck and to the guard through the floor covering.

The heat flow from the fluid is found from Eq. (6.8) while the heat flow through the floor covering is found from Eq. (6.9).

Therefore, the cooling capacity coefficient, $U_{cc,ceiling}$, can be found from the following relationship:

$$U_{cc,ceiling} = \frac{q_{up}}{A_{deck} \cdot \Delta T} = \frac{q_{up}}{A_{deck} \cdot \left(T_{room} - T_{fluid}\right)} \quad \textbf{(6.17)}$$

Here the fluid temperature, T_{fluid}, is defined as the average value of the supply and return temperature, or:

$$T_{fluid} = \frac{1}{2} \cdot \left(T_{supply} - T_{return}\right) = T_{supply} + \frac{1}{2} \cdot \Delta T_{supply-return} \quad \textbf{(6.18)}$$

The room temperature is more difficult to define, as this depends on both position in the room and the fact that the air and surface temperatures are different. An approach, which is used for guarded hot box measurements for finding the thermal properties of windows using ISO 12567-1 (ISO, 2000), is to calculate the environmental temperature, which is the average of

the air and radiant temperatures weighed by the surface heat transfer coefficients for convection and radiation respectively.

$$T_{room} = \frac{h_{conv} \cdot T_{air} + h_{rad} \cdot T_{rad}}{h_{conv} + h_{rad}} \tag{6.19}$$

The radiant temperature, T_{rad}, is found as the average temperature of measured surface temperatures on the inner walls and floor surface and the air temperature, T_{air}, is found as the average of the measured temperature in 0.7m and 1.1m height. Notice, that the room air temperature is stratified in the room, such that the air temperature is higher in the top of the room than in the bottom.

The radiative heat transfer between two surfaces is given by the following relationship taking the view factors and emissivity of the surfaces into account. (Mills, 1992).

$$q_{12} = \sigma \cdot F_{1,2} \cdot \left(\varepsilon_1 \cdot T_1^4 - \varepsilon_2 \cdot T_2^4\right), \quad 0 \le F \le 1 \tag{6.20}$$

By assuming that all surfaces (except for the ceiling) have the same temperature, and all surfaces have the same emissivity as well as linearizing the temperature difference, Eq. (6.20) can be simplified to:

$$\begin{aligned} q_{12} &= \sigma \cdot \varepsilon \cdot \left(4 \cdot T_m^3\right) \cdot \left(T_{room} - T_{ceiling}\right) \\ &= h_{rad} \cdot \left(T_{room} - T_{ceiling}\right) \end{aligned} \tag{6.21}$$

Here T_m is the average value of all surfaces in the room. In all cases the radiant heat transfer coefficient will be around 5.5m²K/W.

The convective heat transfer coefficient depends greatly on the actual temperature conditions and is difficult to accurately calculate. Therefore, the convective heat transfer coefficient will be based on the actual measurement data, where it is assumed that that the actual measured heat flow between the cooled surface(s) and the room, q_{up}, is equal to the sum of the convective and radiative part of the heat transfer:

$$q_{up} = h_{co} \cdot \left(T_{air} - T_{sur}\right) + h_{rad} \cdot \left(T_{rad} - T_{sur}\right) \tag{6.22}$$

Eq. (6.22) has only one unknown, namely the convective heat transfer coefficient. Using Eq. (6.19) through Eq. (6.22) therefore yields the environmental temperature, T_{room}.

Based on this, the cooling capacity of the ceiling surface of the deck can be calculated.

The influence from the floor surface on the cooling capacity from the lower deck can be included by making a similar calculation to Eq. (6.17) thereby finding the cooling capacity coefficient for the floor, where instead the heat flow through the floor covering, q_{down} is used.

$$U_{cc,floor} = \frac{q_{down}}{A_{deck} \cdot \Delta T} = \frac{q_{down}}{A_{deck} \cdot \left(T_{room} - T_{fluid}\right)} \tag{6.23}$$

Again the same calculations can be used for finding the heat flow and temperature difference.

Therefore a combined cooling capacity coefficient for the ceiling surface of the upper deck and the floor surface of the lower deck can be found by the following relationship, summing the two cooling capacity coefficients to give a combined cooling capacity coefficient of the decks towards the room.

$$U_{cc,room} = U_{cc,floor} + U_{cc,ceiling} \tag{6.24}$$

To check the results from the calculation of the cooling capacity of ceiling and floor surface, an alternative calculation can be made where the room heat load is used in stead of the fluid heat flow in the decks.

$$U_{cc,room} = \frac{q_{internal}}{A_{floor} \cdot \left(T_{room} - T_{fluid}\right)} \tag{6.25}$$

Where,

$$q_{internal} = q_{room} - q_{wall} - q_{inf/exf} \tag{6.26}$$

That is, the cooling capacity of the deck is equal to the heat load in the room minus the unwanted heat losses through wall and from infiltration/exfiltration. Both of these unwanted heat losses are kept small. The same method for finding the room temperature as described in Eq. (6.19) can be used again.

6.3.4 Measurement series

As described previously, the purpose of the measurements in the test mock-up is to find the cooling capacity of the thermo active deck and to validate the simulation model used in TASim. These two purposes are reflected in the design of the measurement series. Both steady-state and dynamic measurement series have been completed.

Table 6.6 shows the steady-state measurement series, where combinations of different supply temperatures and set point temperatures in the room have been tested. In total, six measurement series are undertaken with two different set point temperatures in the room air and two different supply temperatures to the decks. In measurement series 1 and 3, there has only been flow in the upper deck, while in the rest there has been flow in both decks.

Table 6.6 Steady-state measurement series.

Measurement series number	Set point temperature	Supply temperature	Comment
1	25°C	15°C	Upper deck only
2	25°C	15°C	
3	25°C	18°C	Upper deck only
4	25°C	18°C	
5	23°C	18°C	
6	23°C	15°C	

To test the dynamical conditions of the deck, measurement series where two different heat loads can be applied during a 24 hour period where the flow in the deck can be either on or off is used. Therefore, as shown in Table 6.7, the flow is turned on in the evening and left on for 12 hours while the heat load is high during the day time and low during the night time. This is to simulate a situation in an office where there is activity and solar gains during the day but only cooling available during the night time.

Table 6.7 Dynamic measurement series. Notice only flow in upper deck.

Time for flow on/ time for flow off	Supply temperature when on	Time for high heat load/time for low heat load	High heat load/low heat load
21-09 / 09-21	15°C	08-20 / 20-08	48W/m² / 5W/m²

Notice that only the upper deck is used for the measurement series. This is because only one of the flow systems could be turned on and off by the control program.

6.3.5 Assessment of measurements including accuracy and stability

Initially, an assessment of the accuracy of the measurements will be made based on one of the measurement series. For this, the steady-state measurement series 1 will be used. In this series there is only cooling in the upper deck. Before starting the measurement series, the upper deck has been running at the same temperature for several days to ensure stable conditions.

Figure 6.31 shows the heat load in the room, which is calculated based on the control signal as shown in Eq. (6.6). The control is based on a PID-control algorithm, which means that initially it starts by quickly rising to full signal – equivalent to 88W/m² - before dropping down to the desired signal, which in this case is around 58W/m². The control can also be seen in Figure 6.32, where the mean air temperature of the measurement positions 0.7m and 1.1m above the floor level are used to control the room air temperature. In this case it can be seen, that the temperature and heat loads both becomes fairly stable.

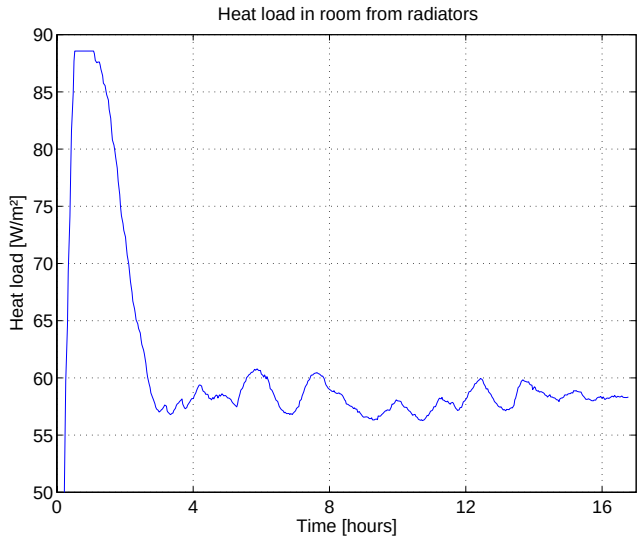

Figure 6.31 Heat load to room during measurement period. Data shown for series 1 in Table 6.6.

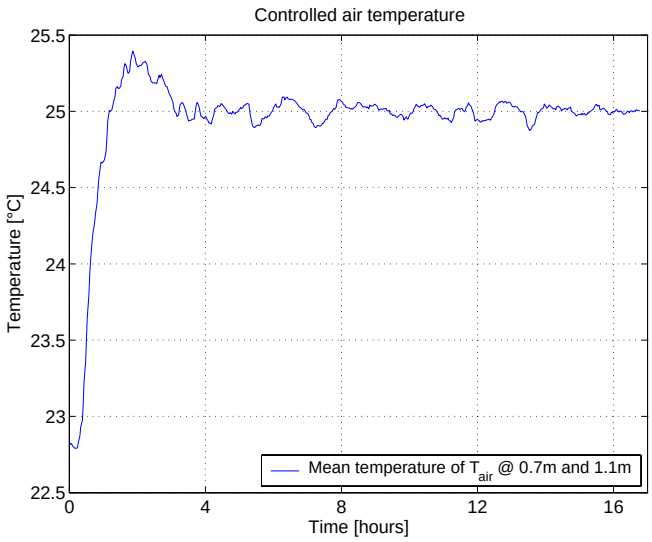

Figure 6.32 Controlled temperature in room found as the mean value of the measured air temperatures at a height of 0.7m and 1.1m. Data shown for series 1 in Table 6.6.

The heat removed through the pipe to the flow unit is shown in Figure 6.33. In this series, the supply temperature is 15°C, the temperature difference from supply to return is approximately 1.7K and the flow is 0.2kg/s.

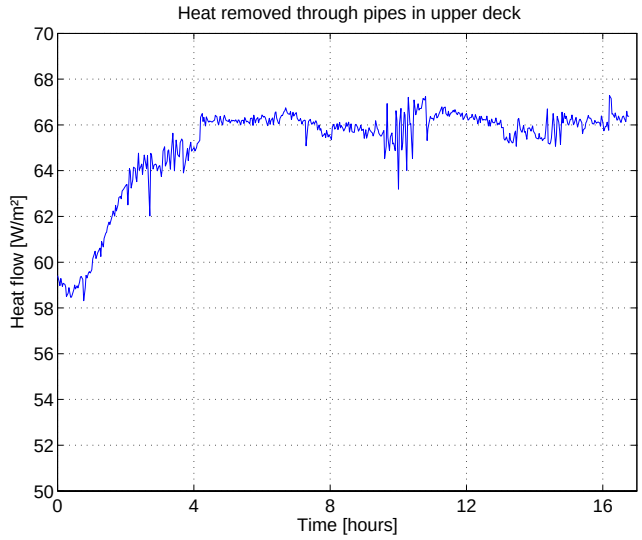

Figure 6.33 Heat removed through the pipe in the upper deck. Data shown for series 1 in Table 6.6.

Since the guard wall has not been installed for these measurements, the temperature in the guard cannot be controlled, and therefore the unwanted heat loss through the inner walls will be larger than when this wall is installed. Figure 6.34 shows the guard temperature in the six measurement positions outside each of the six room surfaces. As it can be seen here, the guard temperature is generally around 1K lower than inside the room, the only exception being the temperature below the deck, where the air is colder than outside the walls and ceiling, where there is a larger air circulation.

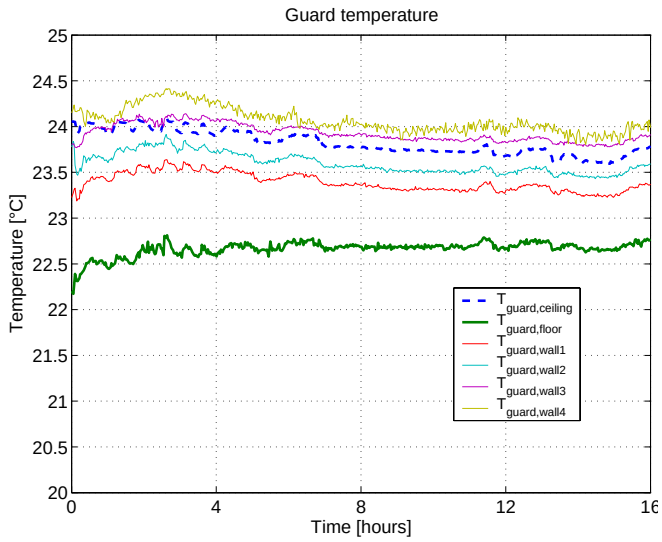

Figure 6.34 Temperatures around the room. The temperature above and below the decks are shown in bold. Data shown for series 1 in Table 6.6.

The temperature difference across the 95mm of insulation in the four walls is shown in Figure 6.35. This difference is between 0.5K and 1K, which also coincides with the fact that the guard (laboratory) temperature is around 1K lower than the room temperature. In this case this corresponds to an unwanted heat loss of around 21W for the 69m² of wall assuming that the average temperature difference in this case is 0.8K. This corresponds to around 1W/m² of heat load in the room.

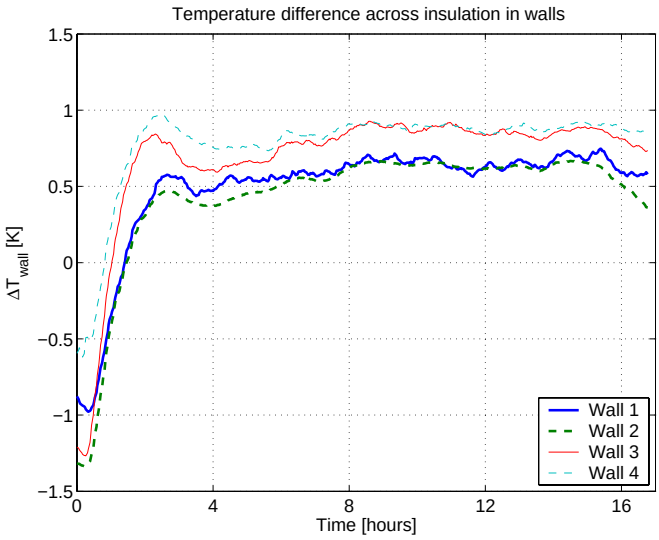

Figure 6.35 Temperature difference across insulation in walls. A 1K difference corresponds to approximately 0.38W/m². Data shown for series 1 in Table 6.6.

The room surface temperature on the walls, floor and ceiling is shown in Figure 6.36 for a situation where the wall temperatures are measured in the middle of the surface. As it can be seen from, the floor and ceiling surface temperatures are very different from the wall surfaces. The wall surface temperatures are, on the other hand very similar, differing by around 0.25K-0.5K.

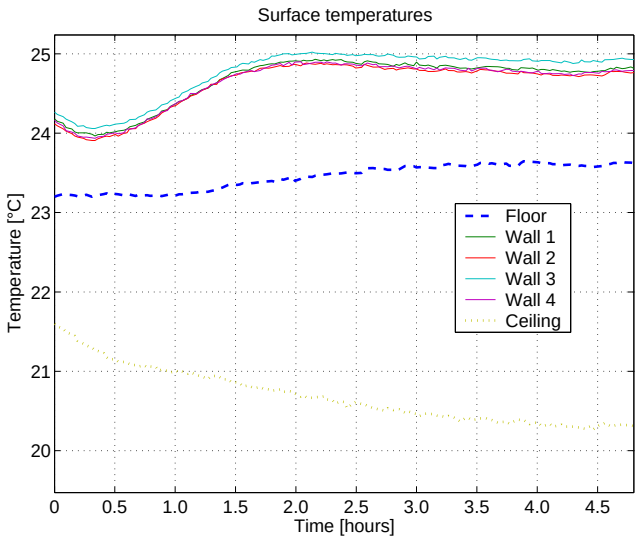

Figure 6.36 Internal surface temperatures in room with one thermocouple placed centrally on each wall. Data shown for series 2 in Table 6.6.

Based on the results for the wall surface temperatures, it was decided to move the measurement position to the same wall surface and place them as shown in Figure 6.23. This is shown in Figure 6.37 for measurement series 5. Again, the temperatures can be seen to be almost identical, differing by around 0.5K. The lowest surface temperature is 0.5K above the wall and the highest is 2.5m above the floor, while the cooling of the wall from the ceiling surface is apparent for the upper part of the wall.

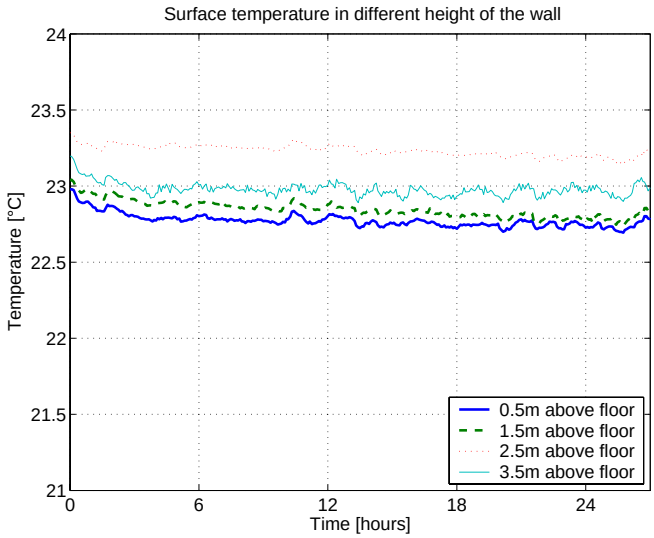

Figure 6.37 Internal surface temperatures placed on the same wall in different height of the wall. Data shown for series 5 in Table 6.6.

The temperature difference between the side of the deck and guard has been measured as shown in the middle drawing in Figure 6.24. This is shown in Figure 6.38. This temperature difference is approximately 4K, with a temperature difference between pipe and guard of approximately 8K. As a comparison to this, the Heat2 calculation shown in Figure 6.28 has a temperature difference across the insulation layer besides the deck is approximately 4.5K in a situation where the temperature difference between pipe and guard is 9K. This seems to confirm the findings in the assessment of the accuracy, which predicted an unwanted heat loss of around 10W for the sides of the deck.

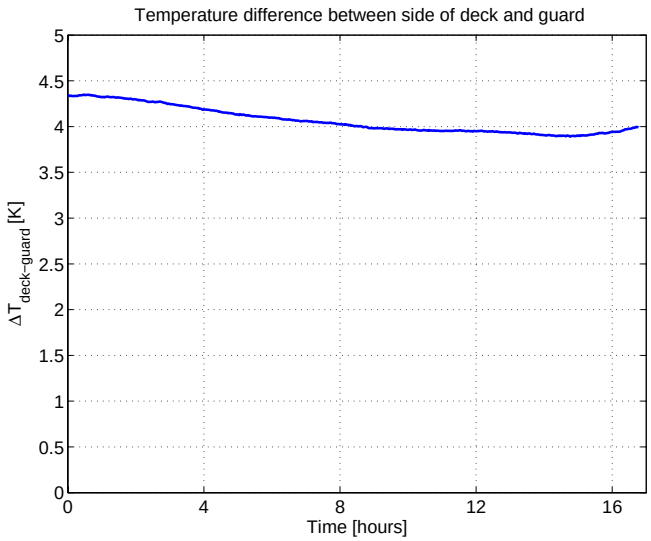

Figure 6.38 Temperature difference between side of deck and guard. Data shown for series 1 in Table 6.6.

Figure 6.39 shows the surface temperature of the deck ends in two positions; in the level of the pipes and in the middle of the deck. Here a direct comparison between the measurements and calculation made in Figure 6.27 is more difficult, since the Heat2 model assumes that the pipe temperature is the same throughout the pipe level. However, the temperatures seem to confirm the simulation results with temperatures that are more influenced by the deck temperature than the guard temperature.

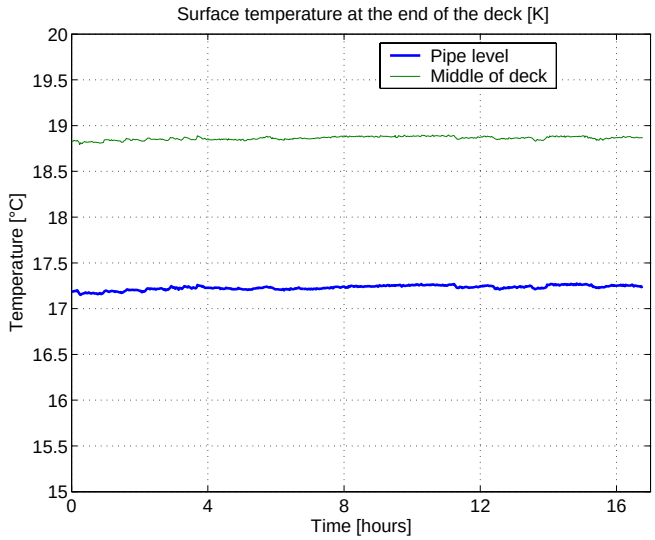

Figure 6.39 Surface temperatures at the end of the deck. Data shown for series 1 in Table 6.6.

Finally the conditions in the two decks are compared. Generally, the flow in the lower deck is only half that of the upper deck, which is due to less pump capacity in the flow unit. This of course influences the conditions. However, conversely to this is the fact that the floor surface in the laboratory building is heavily influenced by the lower “ceiling” surface of the lower deck. This means that less heat is absorbed by the lower deck and therefore a smaller temperature difference than for the upper deck. In most cases, the heat flow from the deck to the fluid in the lower deck is approximately half that for the upper deck.

This is also the case for the temperature difference across the floor covering as shown in Figure 6.40.

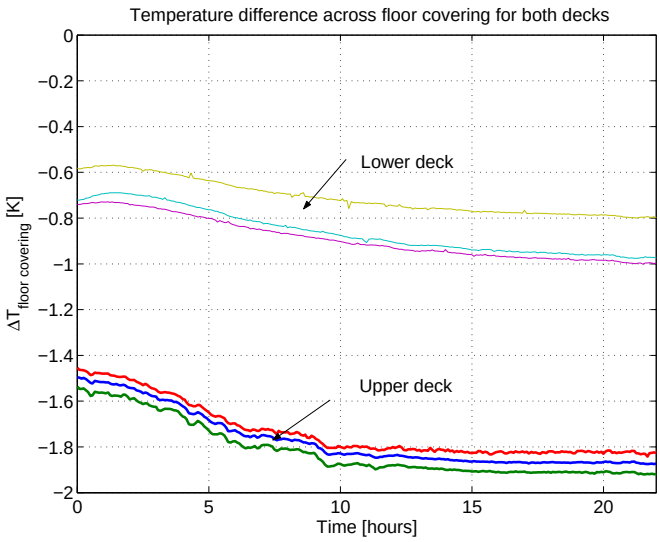

Figure 6.40 Temperature difference across floor covering for the two decks. In both cases, the difference is measured in three positions according to Figure 6.22. Data shown for series 5 in Table 6.6.

This temperature will also lead to different heat flows, which are higher in the lower deck than in the upper. Since the guard wall has not been finished, the upper deck sees a much higher radiant temperature, because the deck is placed directly under the ceiling radiant heating panels in the laboratory which have a surface temperature of approximately 45°C. This is estimated to give a radiant temperature, which is 8K higher than the air temperature above the deck, and therefore an environmental temperature which is around 4K higher than the measured air temperature. Another, but opposing reason is that the lower deck is equipped with a 4mm parquet floor in the room, which of course leads to an extra but small thermal resistance. This problem is expected to be solved once the guard box is finished.

Concluding on the data presented in this section, it has been shown that the test mock-up can be used to measure the thermal conditions and energy flows in the room equipped with thermo active components, and that the measurement conditions have been shown to be satisfactory in spite of the fact that the test mock-up has not been finished at the time of the measurements.

6.3.6 Results from measurements

Steady state

Figure 6.41 shows the ceiling surface temperature of the upper deck, which is measured in three positions. The first two are measured in the central part of the deck respectively directly below and between two pipes, while the third is measured in the assembly between two decks. The difference is around 0.25K in the two central positions, while it is almost 1.5K between the central part of the deck and between two decks. This is as expected.

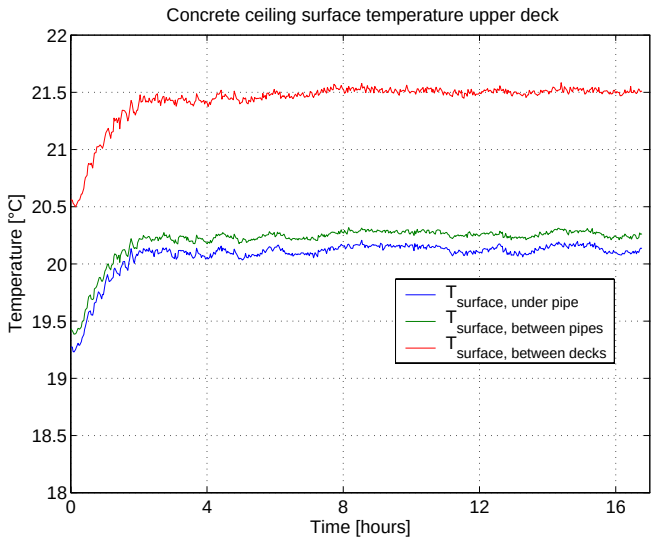

Figure 6.41 Ceiling surface temperature. Data shown for series 1 in Table 6.6. In the figure, the order of the curves from top to bottom is the temperature between two decks, between two pipes and directly below a pipe.

The vertical room air distribution is shown in Figure 6.42 in series 2 from Table 6.6, where both the upper and lower deck are cooled. The lowest temperature is the temperature close to the floor surface and rising with the vertical height in the room. The temperature difference between ankles (0.1m) and head (1.1m) for sedentary persons is found to be around slightly over 1K, which will cause less than 1% dissatisfied due to this temperature difference according to EN ISO 7730 (ISO, 1994). Notice that the air velocity in the room is very small, as there is no air movement from ventilation and at the same time the mainly radiant cooling does not induce convective air movement. The air velocity has also been measured in the middle of the room. It has been found to have an average value of 0.06m/s and a standard deviation of 0.04m/s.

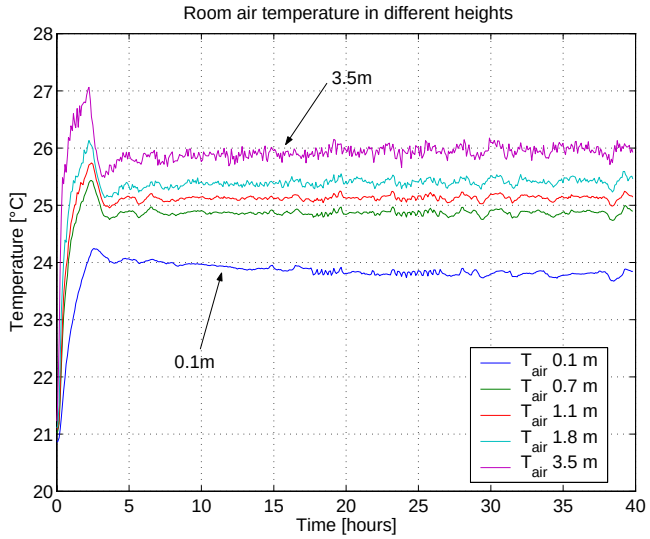

Figure 6.42 Air temperature in room. Data shown for series 2 in Table 6.6.

A simple investigation has shown that as expected the room air rises close to the walls where the heat is supplied by the radiators and drops down in the middle of the room. The temperature distribution has also been assessed in the height between 1.8m and 3.5m, with the result that the air temperature is in fact higher in the upper part of the room, where the

maximum temperature was found between 2.8m and 3.5m. It is therefore expected that the average room temperature will be higher than the temperature measured in the middle of the room.

Figure 6.43 shows the surface temperatures in the room for floor, ceiling and wall temperature in four different heights. In all cases, the wall temperatures are around 24.5°C, all within 0.5K, while the ceiling surface temperature is 20.5°C and the floor surface temperature is around 21.5K. This temperature is in the range which will give less than 10% dissatisfied.

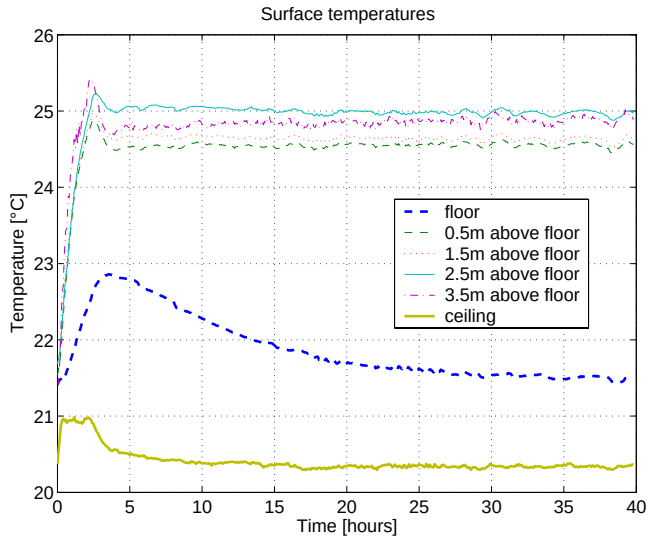

Figure 6.43 Surface temperatures in room. Data shown for series 2 in Table 6.6.

Table 6.8 shows the main parameters from the measurement series. These are the fluid temperature calculated from Eq. (6.18), the heat flow through the ceiling surface from Eq. (6.16), the room temperature (environmental) calculated from Eq. (6.19), the heat flow through the floor covering calculated from (6.9), the heat flow in the pipe based on Eq. (6.8), and the heat load in the room based on Eq. (6.6) minus the heat loss through the walls and from infiltration. In the calculation of the heat flow through the ceiling surface, a heat load of 2W/m² has been subtracted to correct the value for the unwanted heat losses through the sides and ends of the deck corresponding to a total of 40W as it has been found in section 6.3.2. The correction to the heat load in the room is also fairly small, corresponding to approximately 1W/m².

Table 6.8 Main results for temperatures and heat flows for the different measurement series.

Measu-rement series	T_{fluid} (upper/lower deck) [°C]	T_{room} [°C]	q_{up} (upper deck) [W/m²]	q_{down} (upper/lower deck) [W/m²]	q_{pipe} (upper/lower deck) [W/m²]	q_{room} [W/m²]
1	16.1/-	25.0	50	14/-2	66/0	57
2	16.0/15.3	24.7	51	15/10	68/50	62
3	18.7/-	24.9	32	12/-2	46/0	39
4	18.7/18.9	24.8	32	13/8	47/29	42
5	18.5/17.6	23.0	20	16/6	38/27	21
6	15.8/15.0	22.8	35	18/8	55/39	42

In the table, only one room temperature is given, instead of three that differ in the radiant part due to the different surfaces that are included in the calculation. For instance the room temperature seen from the ceiling surface does not include this surface in the calculation, while it is included when the temperature is calculated seen from the floor surface. However,

the difference is fairly small, and therefore only the room temperature seen from the upper deck is included in the table.

The heat flow in the lower deck is approximately 50% lower than for the upper deck, which is due to a smaller cooling from the ceiling surface since this surface is placed 50cm above the laboratory floor, which is cooled by the deck which means that the environmental temperature becomes low for this surface.

Based on the data in Table 6.8, the heat flow through the ceiling surface of the upper deck is plotted in Figure 6.44 as function of the temperature difference between fluid and room.

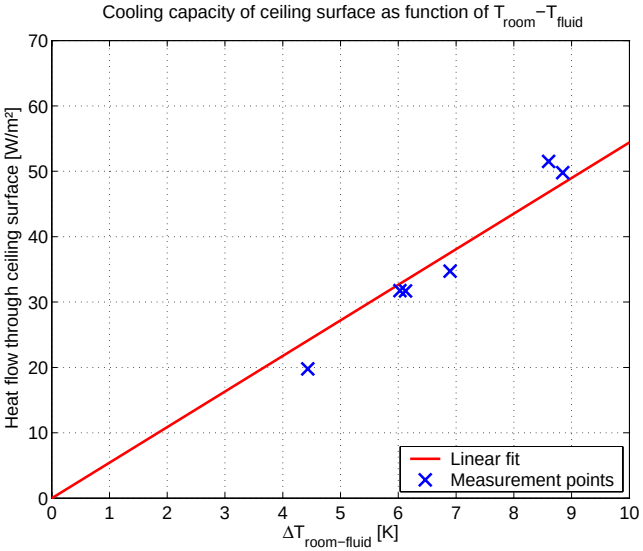

Figure 6.44 Cooling capacity of the ceiling surface of the upper deck as function of the temperature difference between room and fluid.

A linear correlation can be observed, as was the case for the PIC setup (Figure 6.14).This means that the cooling capacity coefficient of the ceiling surface of the thermo active component for the stationary measurements can be expressed as a linear equation where the heat flow in the pipe of the upper deck is equal to the cooling capacity times the temperature difference between room and deck.

The equation for the fitted measurement data is shown in Eq. (6.27) showing the fitted value using a least squares curve fit. Notice, that the equation assumes a proportional correlation without any offset of the cooling capacity.

$$\begin{aligned} q_{up1} &= U_{cc,ceiling} \cdot \left(T_{room} - T_{fluid}\right) \\ &= 5.4 \cdot \left(T_{room} - T_{fluid}\right) \end{aligned} \qquad \textbf{(6.27)}$$

That is, the cooling capacity coefficient of the ceiling surface is 5.4W/m²K.

For the floor surface of the lower deck, the following relation can be observed between the heat flow through the floor surface and the temperature difference between room and fluid temperature in the lower deck. Notice, that only the four measurement series where there is flow in both decks are included.

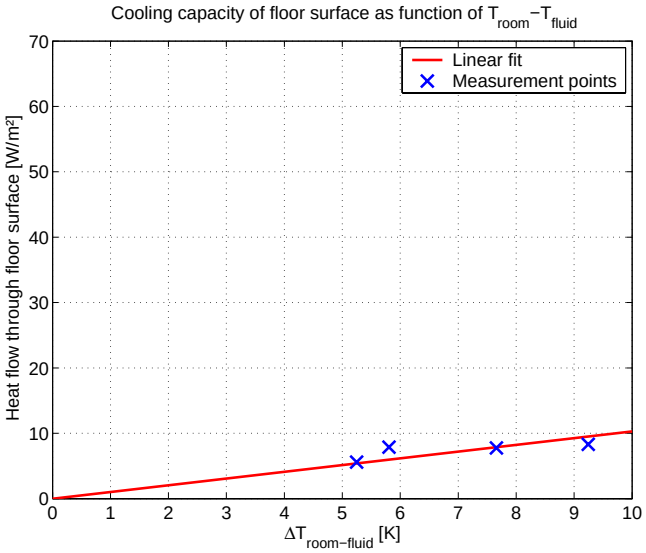

Figure 6.45 Cooling capacity of floor surface as function of the temperature difference between room and fluid.

A linear fit of this gives the following correlation.

$$\begin{aligned} q_{up1} &= U_{cc,floor} \cdot \left(T_{room} - T_{fluid}\right) \\ &= 1.0 \cdot \left(T_{room} - T_{fluid}\right) \end{aligned} \tag{6.28}$$

The cooling capacity coefficients of the ceiling surface of the upper deck and the floor surface of the lower deck using Eq. (6.24), gives the combined cooling capacity coefficients:

$$\begin{aligned} U_{cc,room} &= U_{cc,floor} + U_{cc,ceiling} \\ &= 5.4 + 1.0 = 6.4\,\mathrm{W/m^2K} \end{aligned} \tag{6.29}$$

Finally, based on (6.25), Figure 6.46 shows the room heat load in the room as function of the temperature difference between room temperature and fluid temperature of the upper deck. Again the measurements where there is only flow in the upper deck have been excluded.

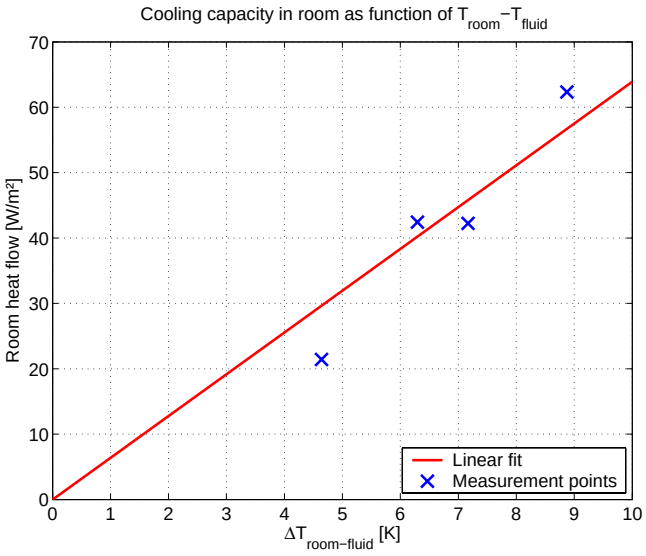

Figure 6.46 Cooling capacity using the room heat load as a function of the temperature difference between room and fluid.

This is fitted to the linear equation in (6.30).

$$\begin{aligned} q_{room} &= U_{cc} \cdot \left(T_{room} - T_{fluid}\right) \\ &= 6.4 \cdot \left(T_{room} - T_{fluid}\right) \end{aligned} \quad \textbf{(6.30)}$$

As it can be seen, cooling capacities found in (6.28) are (6.30) are the same with the shown accuracy, which confirms both results and methods.

Dynamic

The dynamic measurements reveal the temperature response in the room. Only the upper deck is used in these measurements.

Figure 6.47 shows the room air temperature in five different heights. As it can be seen, during periods with low heat supply to the room, the temperature in the room is the same in all heights, while during the period with high heat load the vertical difference becomes the same as for the stationary measurements. This means that during the periods with low heat loads, there is almost no air movement in the room, which shows the mainly radiant heat exchange in the room. Conversely, during periods with high heat loads the air movement creates a temperature stratification of the air in the room, which is growing from 0K when the heat load is set to high to over 2K when the heat load is turned off again. Also notice that immediately after the heat load is turned on, the room air temperature rises quickly for the first short period, after which the increase starts levelling out.

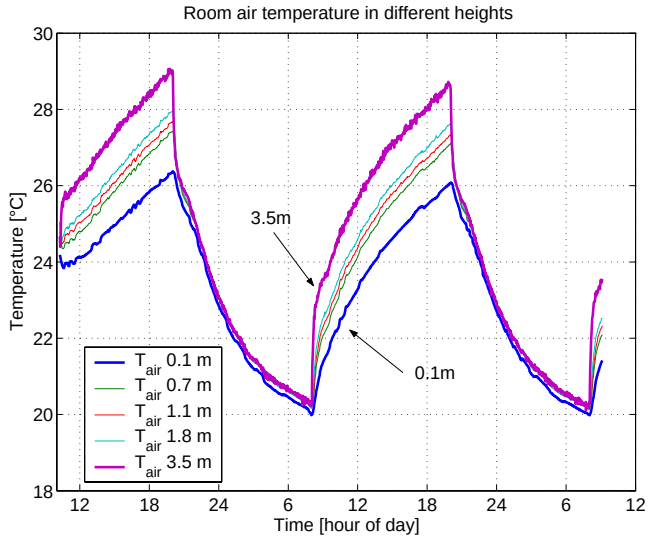

Figure 6.47 Air temperature in room during dynamic measurement series.

Figure 6.48 shows the heat flow in the pipe for two 24 hour periods where the flow is alternating between being on and off for periods each lasting 12 hours. Immediately after turning on the flow, the heat flow in the pipe rises to the peak value of around 140W/m² after which it drops exponentially over the next 12 hours to the minimum value of around 50W/m². This is as could be expected based on theoretical considerations. Notice that the very last part of the period, just before the flow is turned off again, the heat flow starts rising again. This is due to the fact that heat load in the room shifts to high at 8 in the morning, while the flow is not turned off until 9 in the morning, and therefore the heating of the deck will just have time to reach the pipe and increase the heat flow in the pipe slightly.

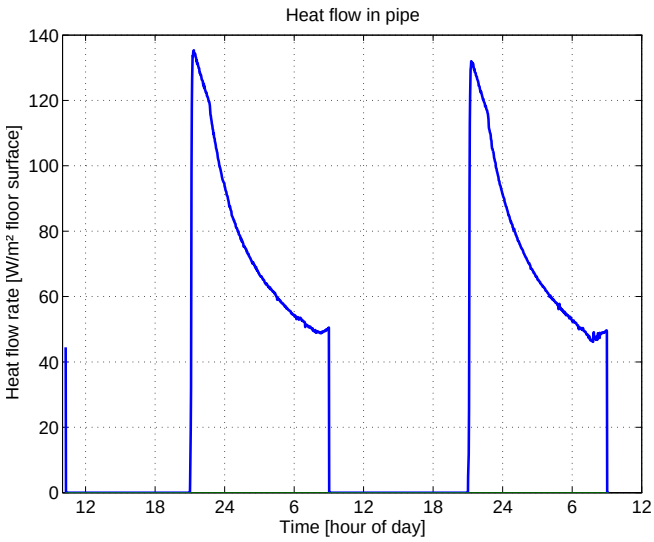

Figure 6.48 Heat flow in pipe during dynamic measurement series.

Figure 6.49 shows the temperatures on the upper and lower surfaces of the deck and the internal temperature close to the pipe. Starting by the lower surface temperature, these are approaching each other when there is no flow in the pipe and approach the stationary results when the flow is on. The upper surface temperature shows a clear shift in the peak values compared to the temperature near the pipe and on the ceiling surface. This is obviously a result of the phase lag caused by the larger thermal mass between the pipe and the upper surface than for the pipe and the lower surface. This shift is around 2.5-3 hours. Finally, the cooling from the pipe is obvious from the internal temperature.

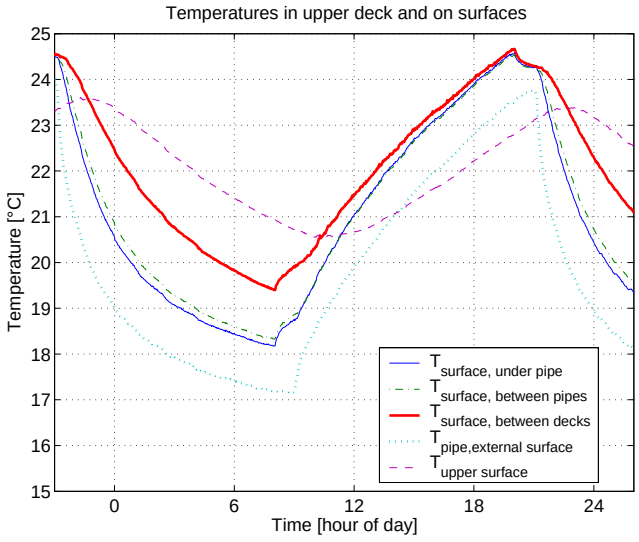

Figure 6.49 Temperatures in upper deck near the pipe and on the upper and lower surfaces.

6.3.7 Measurements vs. modelling (Validation of numerical model)

To compare the measurements to the modelling, a simulation model of the room is developed in TASim based on the dimensions in the mock-up.

As inputs to the simulation model, the supply temperature to the decks, flow rates, average guard temperature and internal heat load are used. The heat load from the radiators is assumed to be 90% convective and 10% radiative, which is distributed evenly on all surfaces.

Generally though, the environmental temperature above the upper deck is increased by 4K compared to the measured air temperature, which is due to the radiant ceiling panels in the laboratory – which has been discussed previously.

Steady-state

Table 6.9 shows a comparison of the main results of measured and simulated heat flows and temperatures for measurement series 2, which is representative for all measurement series with respect to the differences between measured and simulated results, meaning that the same general trend is observed in all measurements. The values are shown for the steady-state part of the measurement period. The data presented for the measured heat flows have not been corrected by the unwanted heat flows, while the measured operative temperature is corrected by the offset of 0.5K, which was found during the calibration – corrected data shown in parenthesis.

Table 6.9 Data for mock-up comparing measured stationary values to simulated values. Data shown for series 2 in Table 6.7.

Parameter	Measured	Simulated	Difference (absolute/relative)
Pipe heat flow upper deck	66.2W/m²	66.5W/m²	-1%
Pipe heat flow lower deck	42.1W/m²	43.3W/m²	-3%
Heat flow through floor covering upper deck	15.4W/m²	13.9W/m²	10%
Heat flow through floor covering lower deck	9.8W/m²	10.1W/m²	-3%
Room air temperature (middle of room)	25.4°C	26.9°C	-1.5K
Ceiling surface temperature (average)	20.3°C	19.3°C	1.0K
Floor surface temperature (average)	21.5°C	22.1°C	-0.6K
Operative temperature	25.9°C (25.5°C)	25.0°C	0.9K (0.4K)

The pipe heat flows are in fairly close agreement between measured and simulated results. For both decks the measured value is 1-2W/m² too high, as it has been found in section 6.3.2.

For the heat flow through the floor surface of the upper deck, the measured value is much higher than the simulated value. This is not the case for the lower deck, where the measured and simulated results are again in fair agreement. The reason for this is as discussed above, that the environmental temperature which can be "seen" from the upper deck is higher than for the room.

The room air temperatures are generally overestimated by TASim. In fact, the temperature is typically close to the air temperature which is measured immediately below the ceiling surface. As described above, the room temperature is generally higher than in the upper part of the room than in the lower, which is as expected. As TASim does not include stratification – as there is only one room air node in the model – the model will find the average room temperature, which is expected to be higher than the temperature measured in the middle of the room, due to the stratification. On the other hand, the ceiling surface temperature is underestimated. This can be explained by the fact that since the air temperature immediately below the deck is higher than in the model, the model will underestimate the convection since the temperature difference between room air and surface is smaller in the model than in the measurements. This also explains that the surface temperature is underestimated by model since the convection is smaller and therefore has less heat flux from convection.

Finally, the operative temperature is underestimated in TASim compared to the measured data, which is described below.

While the results for the heat flows in TASim are close to the measured data, the results for the temperatures are not in as good an agreement, where especially the room temperature is overestimated by the model.

A few probable reasons are listed below:

- Thermocouples are used for the measurements of absolute temperature have an accuracy of ±1K, which brings all but the room air temperature within the accuracy range of the measurement device.
- The air in the room is very still and therefore the temperature will be more stratified than it would otherwise be. This means that the average room air temperature can easily be higher than the temperature in the middle of the room. As it will be shown below in the dynamic case, the simulated temperature is close to the measured when there is low heat load in the room and therefore less stratification of the room air.
- The convective heat transfer coefficients used in the model are perhaps not applicable to this type of measurements and the model underestimates the convection from the ceiling surface. This shows that the convective part is very much depending on the actual air temperature used for the calculation. Therefore a convective heat transfer coefficient needs to refer to the average room air temperature – not the temperature immediately below the deck.
  However, if the combined convective and radiative heat transfer coefficient is calculated for the simulation model, the values are in close agreement to those stated in DS418 (DS, 2002).
- The results from the measured operative temperature using the Brüel and Kjær 1212 measurement device have been found to overestimate the temperature when compared to the temperature in a closed room, which is used for calibration of the device by around 0.4K. This brings the simulated value within the accuracy range of ±0.5K given for the measurement device.

Dynamic

The dynamical conditions are also compared to the measurements.

Figure 6.50 shows the floor surface of the lower deck and the ceiling surface of the upper deck. The measured data are shown as full lines, while the simulated data are shown as dotted lines. For both floor and ceiling, the model is capable of finding the correct dynamical conditions, though with some deviations. Especially the floor surface is not very accurate, as the highest temperature is almost 1K higher for the simulated than for the measured data. However, for the ceiling surface both maximum and minimum values are in close agreement.

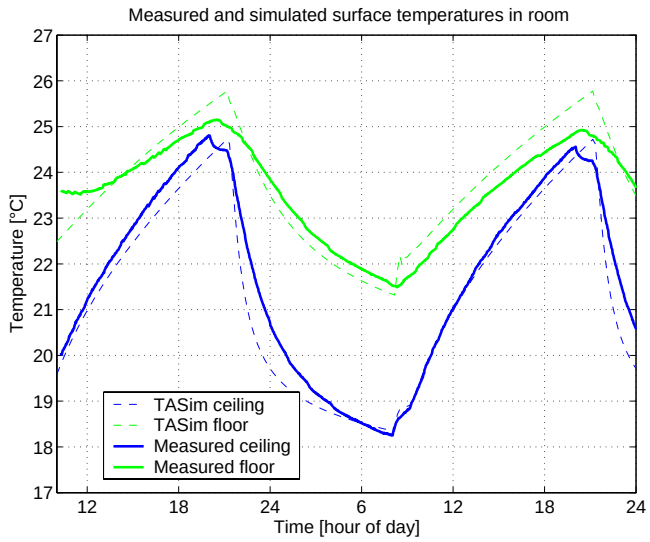

Figure 6.50 Comparison of surface temperatures in the room.

Figure 6.51 shows the pipe temperature during the period from when the flow is turned on and until it is turned off again. Again a close agreement can be observed between measured and simulated.

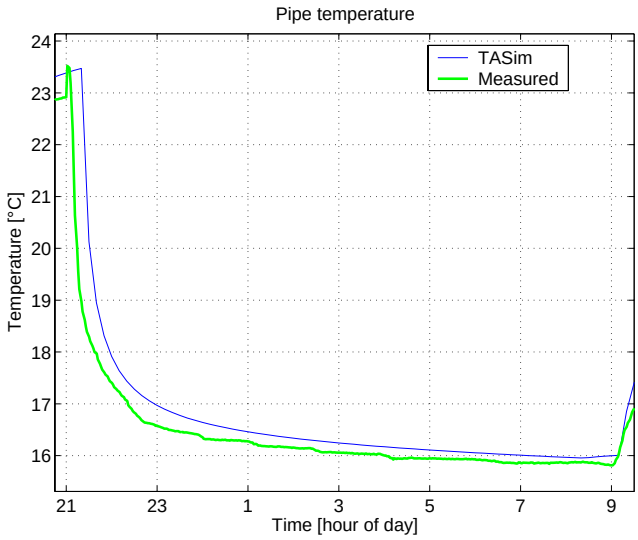

Figure 6.51 Comparison of the measured and calculated pipe temperature, which is only shown for the period when the flow is on – during the period without flow the measured temperature is not measured correctly as it is based on the supply temperature plus half the temperature difference between supply and return.

Figure 6.52 shows the heat flow in the pipe comparing measured and simulated data. A fairly close agreement can be observed both with respect to magnitude and dynamical conditions.

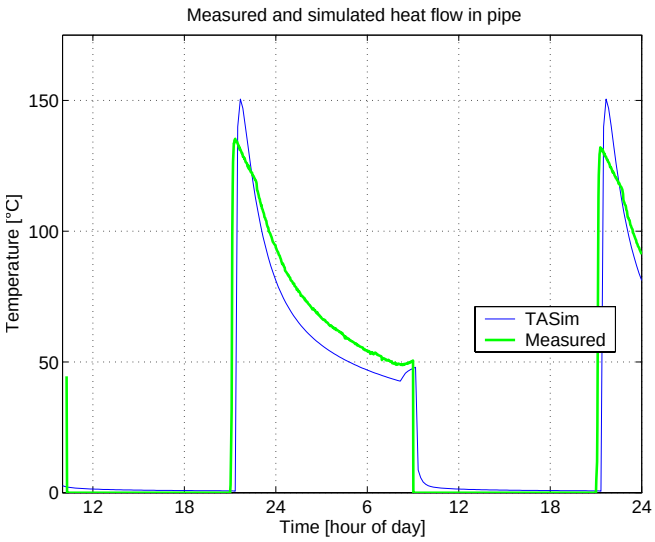

Figure 6.52 Comparison of the measured and calculated heat flow in the pipe.

In total, Figure 6.50 to Figure 6.52 shows that TASim is fully capable of modelling the dynamical conditions in the thermo active deck.

Figure 6.53 shows the measured results for the room air temperature and operative temperature during the measurement period.

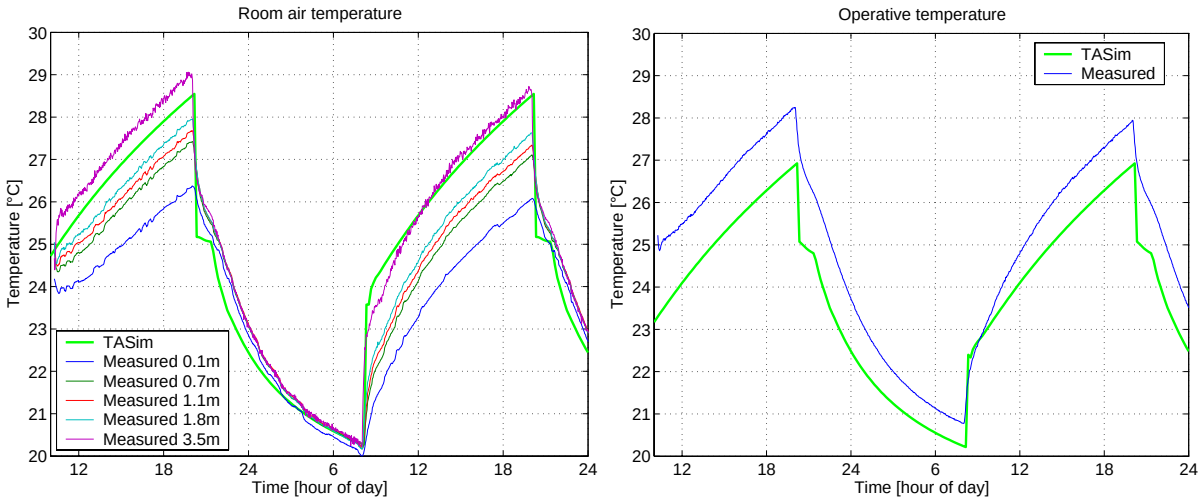

Figure 6.53 Room air temperature and operative temperature compared. The data shown for the operative temperature has been corrected by the offset error on the measurements by -0.4K.

As found above, TASim overestimates the room air temperature while underestimating the operative temperature. As discussed above, the room air temperature is typically close to the highest measured temperature in the room when there is a “high” heat load, while it is in close agreement when there is a “low” heat load, which again indicates that without stratification in the room air (during the cooling periods with low heat load), TASim is fully able to predict the temperature in the room.

6.3.8 Discussion

Initially in this section, the test mock-up has been described with respect to design and measurement positions followed by an analysis of the expected measurement accuracy and unwanted heat losses.

The measurements in the mock-up are as expected and therefore the experimental setup can be used for finding the thermal conditions and energy flows. This is the case in spite of the fact that the test mock-up has not been finished at the time of the measurements, which among others means that the guard box has not been installed. This especially influences the temperature in the guard, which should be identical to the temperature in the room. This gives an unwanted heat flow through the walls. However, it has been shown that this does not have a significant influence since this unwanted heat flux is small because the temperature differences are generally small between room and guard. Unfortunately it has not been possible to achieve the same thermal conditions in both decks due to differences in the flow unit and the fact that the missing guard resulted in different conditions for the floor surfaces where the upper deck was exposed to laboratory conditions and not guard conditions, which gave a much higher radiant temperature, while the lower deck is placed only 0.5m above the laboratory floor resulting in a much lower temperature. This will be improved by the installation of the guard where a fan will ensure air circulation in the guard.

In the stationary measurement series, the cooling capacity has been shown to be proportional to the temperature difference between the fluid temperature and the environmental temperature of the room. This result of a constant cooling capacity coefficient is the same as found for the PIC-setup in section 6.2. This could also be expected since the only causes of non-linearity are the convective and radiative heat transfer coefficients between deck surface and room/guard. While the radiative heat transfer coefficient depends on the temperature difference between the surfaces to the fourth power, it can be linearized in the narrow temperature band in which these measurements take place. Therefore the only “truly” non-linear part is the convective heat transfer coefficient, which again is not non-linear enough to influence the cooling capacity in the temperature band under which the thermo active deck operates.

The use of the environmental temperature, which is the average temperature of the air and surface radiant temperatures weighed by the convective and radiative temperatures respectively, has proven useful for defining the cooling capacity coefficient of the deck. The approach is similar to a method used for characterising windows, where there is often a large difference between air and radiant temperatures, especially between outdoor air and sky temperature during the night. This is – to a lesser degree – also the case for the mainly radiant cooling from the thermo active component. Another advantage is that the method actually does not require the convective heat transfer coefficient to be known, as this parameter has proven difficult to accurately define and measure. This will be discussed further below.

The cooling capacity has been calculated for the floor and ceiling surfaces individually to split the contributions of the actual cooling of the room. This is especially relevant since the measurements should also be applicable to other constructions – for instance other types of floor constructions. In buildings with thermo active components it is expected that the floor construction will have a higher thermal resistance than used in this mock-up, since both cabling and acoustic measures must be handled by the floor surface as the ceiling surface will need to have clear view of the concrete in order to absorb enough heat from the room.

In this investigation the cooling capacity of the ceiling surface has been found to be five times higher than through the floor surface.

The dynamic measurements show that the deck can absorb the heat from the high heat load during the day and remove it through the pipes during the night. This result is as previously shown in the literature based on simulations and field measurements.

The test mock-up has proven a good tool for measuring the thermal conditions of thermo active components and the versatile design means that many different experiments can be investigated. A few can be mentioned:

- Different acoustic measures such as lowered ceilings.
  Installing a lowered ceiling could be used to easily find a "shading" coefficient of the cooling capacity of the deck. This could be used to develop different types of lowered ceilings, perhaps perforated metal sheets that would both act as acoustic measures while also ensuring cooling from the ceiling surface.
  One very interesting type of lowered ceiling, which could unfortunately not be included in this thesis, is an operable lowered ceilings formed as elements of perhaps 40cmx400cm, which can be placed in either horizontal or vertical position. Such a ceiling would have two functions. Firstly, it can be used for acoustic measures both in the horizontal and vertical position. Secondly, the fact that it is operable means that the deck can be cooled more during the night because of the lowered ceiling when placed in the horizontal position will be a thermal resistance for the cooling from the deck to the room. Therefore the room will not be as cool in the morning as it would otherwise be. During the day, when the room starts heating up, the ceiling can be turned and open up for the cool surface of the deck. Further, the operability could be made individually controllable, such that persons with different thermal preferences could themselves control the temperature.
- Heating experiments.
  In this thesis only cooling has been examined. However, the design of the mock-up means that cooling can also be measured, by cooling the air in the guard.
- Ventilation
  Different types of ventilation principles – for instance displacement ventilation – can be tested. One possible investigation would be to use a combination of a lowered ceiling and a ventilation system where the air is pre-cooled by the cool air in the cavity between deck and lowered ceiling and the air is supplied to the room through the perforations in the ceiling surface.
- Alternative deck constructions.
  The mock-up has been designed in such a way that the upper deck can be replaced by an alternative construction with the same dimensions
- External conditions on one of the walls. One side of the walls has been designed in such a way that the guard wall and inner wall can be removed. This means that dynamic conditions can be applied to this surface – for instance solar radiation through a fully glazed façade.
- Pipe in Cavity setup.
  The upper deck has been equipped with a loose pipe in the cavities of the upper deck. The results from these measurements have not been included in this thesis, but the mock-up has been prepared for this. An early assessment in the mock-up seems to find a cooling capacity of around 2W/m²K – or roughly one third of the capacity for the deck with integrated pipes.
- Thermal comfort.
  The mock-up can be used for more detailed measurements of the thermal comfort in the room, for instance through controlled experiments on test persons.
- Convection.
  As found above, the convective part of the heat transfer has been found to be poorly defined especially concerning the validation of TASim. Therefore measurements in the

room can be used to measure the convective heat transfer coefficient and the split between radiant and convective heat transfer from the surface to the room (air and surfaces)

The simulation model has been validated based on the measurements series with the following results:

- For the stationary measurements the simulated heat flows have been found to be in close agreement to the measured data, except for the heat flow through the floor surface of the upper deck which is underestimated by the model. This can however be explained by an unexpectedly high radiant temperature on the surface. While the room air temperature is generally overestimated, the ceiling surface temperature is underestimated. This indicates that the convective heat transfer is not modelled accurately enough as the thermal stratification is not included in TASim. The difference can be explained by the fact that the room air temperature is higher directly under the deck than the modelled value, which causes a higher convection than expected – this also accounts for the underestimated ceiling surface temperature of the upper deck.
- For the dynamic measurements the simulated results of heat flows and temperatures in the thermo active component are shown to be in close agreement with the measurement results. This has shown that the model is fully able to reproduce the thermal conditions in the decks. For the room, the model is fully able to reproduce the dynamic course of the temperature of both air and surface temperatures. However, the absolute value of the room air temperature is overestimated by about 1K when there is a high heat load in the room, where the predictions made by the model agree closely with the highest temperature in the room, namely the temperature immediately below the ceiling surface. On the other hand, during periods with low heat load in the room and therefore less stratification, the temperature predicted by the model is very close to the room air temperature, which is the same in all heights of the room.

In total, the results from the convective part of the room model brings up an interesting discussion on the general use of correlations used in building energy simulation programs where there is only one room air node. A correlation for finding the convective heat transfer refers to an air temperature, but generally it is not well-defined which air temperature this is – in fact what air temperature would be correct to refer it to? Generally in this context it must be concluded that the convective part of the heat transfer is not completely satisfactorily defined. However the problem is most likely of a more fundamental nature towards the definition and use of convective heat transfer coefficients in building energy simulation programs. A natural step is consequently to more accurately define the convective heat transfer. This is also being investigated through detailed analyses using CFD modelling of the air volume in the rooms – but also in building energy simulation programs where the room air can be divided into a few vertical nodes to include the stratification or alternatively through a stratification term on the room air which assumes a linear stratification from bottom to top of the room. In this context, investigations on the convective heat transfer from horizontal surfaces that are heated or cooled in an entire enclosure.

At the same time it is noticed that most of the results from the comparisons shows that the simulated values are within the range of the measurement accuracy.

In total, TASim has proven that it can model the conditions in the test mock-up and reproduce measurement results for heat flows and temperatures.

One final and very important point to mention in this discussion on the validation is that since the room model in TASim has been shown to give credible results for the room model, this is of course also the case for FHSim.

6.3.9 Conclusion on the use of the mock-up

In total, the mock-up has worked according to the design and the versatile design means that it can be used for investigations of the thermal properties of for instance lowered ceilings. At the same time the simulation model in TASim has proven to be able to model the conditions in the mock-up satisfactorily with respect to heat flows and to a somewhat lesser degree with respect to temperatures.

The results from the measurements shows that the thermo active component based on pre-fabricated hollow core concrete decks are able to cool the building and to shift the time when the heat load is high in the room and the time when this surplus heat is removed through the fluid in the pipes in the thermo active component. A linear correlation between the cooling capacity of the deck and the temperature difference between room temperature and fluid temperature has been found. In the measurements, the cooling capacity has been found to be around 5.4W/m²K for the ceiling surface and around 1.0W/m²K for the floor surface.

6.4 Simulation study

A simulation study using the simulation model in TASim has been undertaken in Paper 3, with the title: *Simulation of Temperature in Office with Building Integrated Heating and Cooling System*, which is also a part of this thesis.

In this section a brief description of the paper is made and the main results are extracted. The results are based on a simplified model of the thermo active deck, which is a section around one pipe in the deck. This will give a higher cooling capacity than for the entire deck, as there are no pipes close to the side of the decks.

6.4.1 Simulation model

An office with an area of 25m times 10m is modelled giving a total floor area of 250m². The room height is 3.5m. A south facing façade with 100% glass is used for the simulations. The inner walls are of concrete with a thickness of 100mm. The thermo active component has a height of 320mm, with a pipe spacing of 280mm, and a pipe diameter of 20mm.

A constant air volume system gives 2 air changes pr. hour, with an inlet temperature equal to the outdoor air temperature. An infiltration/exfiltration rate of 0.2 air changes pr. hour is assumed.

Two control strategies are used. One where the water in the pipe is circulated all day, and one where the water is circulated only from 21.00 in the evening until 9.00 in the morning.

For the windows, a low energy window with a U-value of 1.1W/m²K is used. The data for transmission of solar energy, solar light and absorbed solar energy in each of the two glazing layers is shown in Table 6.10.

Table 6.10 Glazing data for windows.

U-value [W/m² K]	g-value [-]	light transmittance [-]	Absorptance [-]
1.1	0.5	0.66	0.28 (0.14 in each layer)

A solar shading with a shading factor of 0.2 is activated when the solar gain through the glazing surpasses 200W/m², and is deactivated when the solar gain is lower than 175W/m².

For the internal heat load the following is assumed: 20 persons with an activity of 100 W, 20 PC's of 150W. For the light 10W/m² in total is assumed. However, it is assumed that only 80% of the heat load from persons, light and equipment is present during the day time. The total heat loads are summed up in Table 6.11.

Table 6.11 Heat loads in office during day time, night time and weekends.

Type	Day time [8-18]	Night time [18-8]	Weekends [all day]
Persons	1600W	0W	0W
Light	2000W	250W	250W
Equipment (PCs)	2400W	300W	300W
Total	6000W	550W	550W

Of the heat loads, half is added convectively to the room air, and half by radiation uniformly distributed to the surfaces based on their area. The heat load directly in the office is therefore 24W/m² during the day time, to which the solar income should be added.

In the model, the fluid temperature is set to a fixed value that does not depend on the actual heat transfer. It is therefore assumed that the actual combination of flow rate and supply temperature will give the required fluid temperature.

The Danish Design Reference Year is used as weather data in the simulations.

6.4.2 Results

The effect of using a thermo active component is shown Figure 6.54 for a summer week.

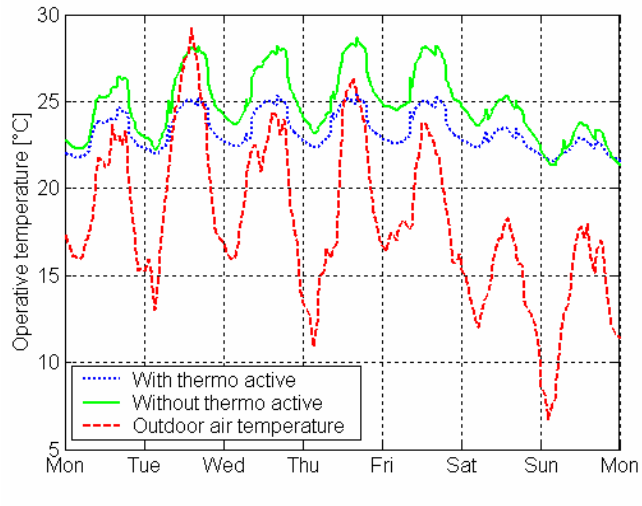

Figure 6.54 Operative temperature in room air with and without cooling from the thermo active component for a summer week (week 27).

The temperature in the office with thermo active cooling is lower than the temperature in the office without cooling. This shows the effect of the thermo active cooling. In this case, a medium temperature of 22°C is used – a lower temperature will give a lower room temperature or enable a higher internal heat load while maintaining the same room temperature.

The temperature profile during the day should be noticed. It can be seen that the air temperature rises from around 21°C in the morning to around 26°C (or more) during the peak temperature of the day. This large temperature difference will normally not be the case in air-conditioned offices, where a more constant temperature can be upheld.

Dynamic properties

The dynamics of the thermo active component is yet another point to comment. In Figure 6.55, a comparison is made between the time the heat is absorbed in the thermo active construction through the surfaces and the time it is removed through the pipes in the construction. A fluid temperature of 16°C is used for the figure.

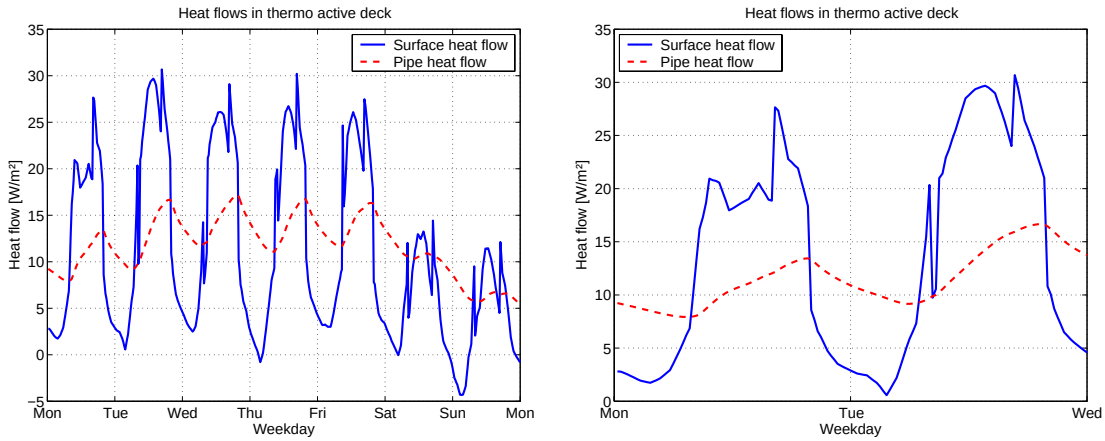

Figure 6.55 Heat fluxes in thermo active component – comparison of heat flux through surface of construction and heat flux through pipe wall. Again, data for week 27 is shown. The right figure shows only the first two days.

As it can be seen, the heat removal from the room and the heat removal from the pipes are very different in time, and also much more evenly distributed during the day than what is the case with the heat load in the room. This means, that a much more efficient cooling system can be designed, where it is not required that all heat is removed during the peak loads as with air condition systems.

Different heat loads and supply temperatures

A series of simulations is performed with different supply temperatures, operation period of the flow in the pipe and heat loads.

Table 6.12 Hours with temperatures above 26 °C and 27 °C. Both data for operative and air temperature is shown. The period of operation is either 24 hours, or from 21 to 9 (night). The heat load is either normal as in Table 6.11 or high, with twice the heat load.

Fluid temperature	Operation	Heat load	Air temperature above		Operative temperature above	
			26 °C	27 °C	26 °C	27 °C
°C	24h/night	high/normal	hours	hours	hours	hours
19	24 h	normal	15	2	0	0
22	24 h	normal	273	109	144	27
19	night	normal	74	17	6	0
22	night	normal	290	118	157	32
19	24h	high	963	655	653	370
22	24h	high	1630	1152	1489	888

Firstly, the difference between the amounts of hours over a given temperature is very different when air and operative temperature is compared. In DS474 the Danish Standard concerning the thermal indoor climate (DS, 1993) a maximum of 100 hours above 26 °C, and 25 hours above 27 °C is recommended.

As it can be seen there are almost no hours with the low supply temperature at 24 h operation, while the high temperature and night time only operation gives many hours with excess temperatures. Also, the high heat load causes problems with overheating. This would also be the case, if no or little solar shading was available.

The difference between air and operative temperature in the zone is also significant, where the air temperature has many more hours with too high temperature. This shows that the cooling is radiant.

6.4.3 Summing up

This section, which is based on Paper 3, has shown the possibilities of using the simulation model in TASim for modelling thermo active components in an office building.

The example illustrates that thermo active components can be used to cool the office and avoid excess temperatures, even using high temperature cooling, represented by fluid temperatures of 19°C or even 22°C.

The functionality of the system is shown by the fact that while the heat transfer through the floor and ceiling surfaces varies with the room temperature, the heat flow to the fluid from the deck is more constant during the day, which shows the levelling of the heat flow.

6.5 Discussion

In this chapter, thermo active components have been investigated. The focus has been placed on the use of pre-fabricated hollow core concrete decks as thermo active components, through testing two different ways of "thermally activating" the deck – one where the pipe is placed in the cavities and one where the pipe is embedded in the concrete layer. To this end, two test setups have been designed at used. In both cases the purpose has been to find the cooling capacity of the decks and to show the possibility of using them as thermo active components in buildings.

For both types, a linear correlation between cooling capacity and temperature difference between room temperature and fluid temperature has been found. This can be explained by the fact that the heat conduction in the concrete deck is linear and the non-linear terms of convection and radiation are not non-linear "enough" in the temperature interval under the measurements conditions, since the maximum temperature difference between pipe and room is not above 10K-15K for typical use of the model. Assuming 10K difference the pipe in cavity setup can cool the room by around 30W/m² and the integrated pipe setup around 65W/m².

The cooling capacity of the deck with pipes in the cavities is most likely not large enough to be used in a typical office building – however in a consciously designed building where emphasis has been made on reducing the heat load, this may actually be enough.

For the deck with embedded pipes, the cooling capacity is large enough to cool a standard office building. However, these maximum values are not a realistic measure for the actual cooling capacity, since it will not be possible to control the temperature in the room using the maximum cooling capacity of the deck – since especially the temperature in the morning will be too cold. This has been shown in the dynamic measurement, where a 50W/m² heat load during the day and 5W/m² resulted in slightly too cool temperatures in the morning and too high in the afternoon.

Based on the measurements, a validation has been carried out for the simulation model used in TASim. This has found that TASim is able to model the conditions in a room with thermo active components. Therefore this model can be used to predict the thermal conditions in a room which is cooled (or heated) by a building integrated system.

Using TASim many different investigations can be made to improve the functionality of buildings equipped with thermo active components. A few are mentioned:

- Predictive control.
  Because of the large thermal mass of the concrete decks and consequent inability to quickly change the temperature, an obvious investigation is to make a predictive control strategy which adapts the temperature of the concrete in the deck to accommodate the

cooling (or heating) which is needed in the next day (or more) in advance. This can also be used to optimize the use of the cooling sources which are available. This can for instance be used to predict if free cooling from the cold air during the night is enough to keep the building cold the next day.

- Heating.
  The model can also be used to find the possibility to heat the rooms during cold periods. This heating capacity is limited by a maximum temperature of the ceiling surface to avoid thermal discomfort
- Building design.
  Is the building even suited for the use of thermo active components?
- Inclusion of a model for the pipe-in-cavity thermo active deck
  Based on the measurements (both existing and new in the large mock-up) as well as numerical analysis (using a program which is more suited for combined radiation and convection), a simple model of the pipe-in-cavity deck, which can be included in TASim.
- Floor heating in multi-storey buildings.
  Floor heating in multi-storey buildings is expected to be introduced in the coming years, and therefore it will be relevant to analyse the thermal behavior especially to avoid unwanted heat flow through the ceiling surface below the deck, which can cause discomfort for occupants.

This investigation has been focused on the design and development of thermo active components based on pre-fabricated hollow core concrete decks, which is often used in the Danish building tradition.

The inclusion of embedded pipes in pre-fabricated decks has many interesting perspectives, as this will push the introduction of this technology in the Danish market. However, the process has proven not to be straight-forward, since the hollow core decks are optimized with respect to both the production process as well as the finished product concerning weight and load bearing capabilities. Further, it will also increase the price of the deck. A change in this process therefore has implications that need to be addressed with respect to the production and price – not to forget the practical problems of avoiding hidden joints in the building construction, where leaks can cause water damage and impede the use of the system.

Therefore, an alternative constructions has been investigated; namely the pipe in the cavities deck. However, the actual cooling capacity is not very large – just as it was expected based on the mode of heat transfer in the cavities. However since the construction is extremely simple and does not require any alterations to the production process of the deck, which means that all the installation work can be made directly on the building site. At the same time, the limited cooling which this system can provide may actually be enough in a consciously designed building where all other measures for limiting the heat loads in the office have already been taken into account. Therefore the system is actually a cheap and simple way to remove any limited surplus heat loads in the rooms, which can be used if it is not possible to avoid cooling in a building.

Another alternative construction type can also be used as thermo active components. Among these is the TT-deck, which has so far mainly been used in warehouse buildings. However, a recent trend is to use these in office buildings as well. This deck will, like the hollow deck with the pipe placed in the cavities, have the advantage that the production will be the same, while the installation of the pipes can be handled on the building site, where the pipe can be embedded in the layer of concrete which in any case is cast on top of the TT-deck once this has been installed. The thermal properties of the TT-deck will be well-defined, since the heat

transfer will exclusively be through conduction. However, on the surfaces the ‘T’ shape of the lower part of the deck will result in different conditions for radiation and convection – especially if the cavity between the T’s is used to install an acoustic ceiling.

Another construction which can be investigated is steel decks, which are used mainly in North America. Here the problem is that they do not have the thermal mass to ensure the ability to store the cooling capacity and shift the load from day to night. In this case thermal mass must be introduced in the deck.

6.6 Conclusion

In this chapter thermo active components based on pre-fabricated hollow core concrete decks have been investigated through measurements in two test setups and through simulations using TASim, which has been validated through the measurements.

Two types of constructions have been tested; a standard pre-fabricated hollow core concrete deck which has been equipped with a pipe placed in the cavity and a pre-fabricated hollow core concrete deck where the pipe has been embedded in the concrete at the time of the production.

The main focus has been on the development and testing of the decks in the test setups with the purpose of finding the cooling capacity coefficient expressed as the cooling per square meter of deck and temperature difference. A cooling capacity coefficient for the first type was found to be 2-3W/m²K and around 6-7W/m²K for the second. For both types of construction a linear correlation between cooling capacity and temperature difference between fluid temperature and room temperature was found. Here the room temperature is defined as the environmental temperature where the convective and radiative temperatures are weighed by their heat transfer coefficients.

The large test setup, which consists of two concrete decks that are floor and ceiling of an office room, has been shown to be a versatile tool towards the design of thermo active components, which can be used for detailed analysis of many different construction types and setups such as lowered ceilings.

7 Thermal energy storage of solar energy in floor construction

This main purpose of the work in this thesis is to model building integrated heating and cooling systems. This has been pursued in Chapter 5 and Chapter 6 for floor heating systems and thermo active components respectively. In both cases the supply of water at the correct temperature is not included in the model, as it is simply assumed that the supply side of the heating/cooling system is capable of delivering the fluid at the predefined temperature.

In this chapter, a slightly different approach is used for the modelling of a house with building integrated heating, as a solar collector is used to supply energy to the lower concrete deck of a floor construction with two decks. The purpose is to investigate the thermal energy storage of the solar energy with the aim of lowering the energy consumption in a house.

The description in this chapter is a very brief introduction to the paper entitled *Numerical Analysis of Heat Storage of Solar Heat in Floor Construction*, which is included as Paper 4 to this thesis. Here only a short description of the system, model and main result from the paper is included.

7.1 System description

The system of heat storage of solar heating consists of solar collector, solar tank and heat storage in the floor. Figure 7.1 shows a sketch of the setup with, the piping between collector, tank and storage. These are only sketched in the sense that different layouts can be imagined; both parallel and serial. The system is a conventional solar heating system with an extra opportunity to use the heat storage to store the solar heat in the floor construction of the house.

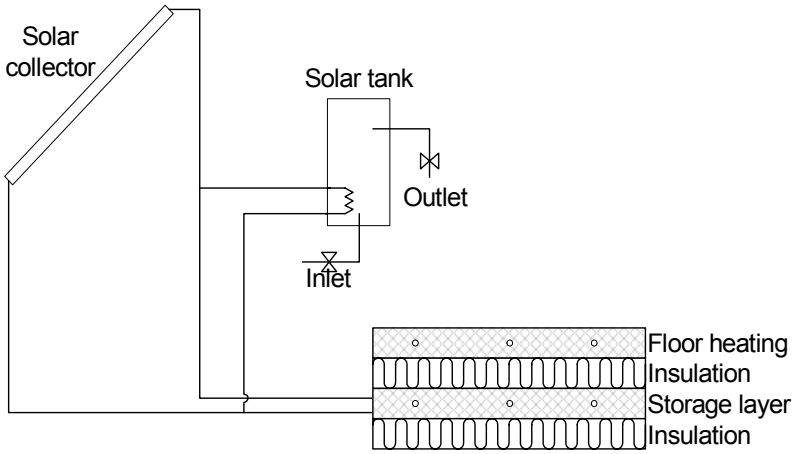

Figure 7.1 Setup used for the analyses of thermal energy storage of solar energy the floor construction of a single family house.

The design of the floor with the heat storage layer is a slab-on-grade sandwich construction with two concrete decks and two layers of insulation, where the lower concrete deck is used as the thermal energy storage and the upper layer is used for the floor heating system in the house. Both floor heating system and energy storage system are made with embedded PEX pipes. This makes the system cheap to install. The solar collector and hot water system are both standard components, which together with the storage system – also constructed by standard components – makes the system cheap to install.

The storage layer is insulated towards both room and ground in order to minimize the heat loss from the heat storage. The downward insulation is obviously installed to prevent heat loss to the ground, while the purpose of the upward insulation is to prevent uncomfortably hot and incontrollable temperatures in the house. It is also important to make sure that the heat storage is well insulated to the sides towards the foundation.

7.2 Simulation model

7.2.1 Numerical model

The construction elements are modelled as simple RC-thermal network models, based on the description in Appendix A. The room model is identical to the model used in FHSim.

The simulation model is implemented in Simulink.

The solar collector is modelled using the flat plate collector efficiency (Duffie and Beckman, 1991).

7.2.2 Building and floor model

The heat storage is installed in a typical Danish single-family house of about 130 m². Two versions of the house are used; with and without heat recovery unit. The energy consumption is approximately 9300kWh (72kWh/m²) with and 5000kWh (38kWh/m²) without heat recovery unit.

The solar heating system is a conventional Danish solar heating system, consisting of a solar collector (and solar tank). The solar collector area is varied between 4m² and 16m².

The floor has 300mm insulation and two concrete decks of each 100mm with a pipe distance of 300mm. The insulation is divided in two parts with 100mm between the decks and 200mm below the lower deck. In the paper, there are six additional floor layouts with different distribution of the insulation thickness and lower deck. The energy consumption in the house is modelled using different size of the solar collector with the Danish Design Reference Year as input.

7.3 Main result from paper

Figure 7.2 shows the energy consumption and reduction in heating demand for increasing solar collector area with and without heat recovery unit installed. For both the model with high and low energy consumption there is a decrease in the heating demand for increasing size of the solar collector, which can be seen from the left figure. The right figure shows the relative reduction of the energy consumption per area of the solar collector. The maximum reduction in the heating demand pr. m² of solar collector is in both cases at 8 m² solar collector area.

Notice, that even for 16m² of solar collector there is still a large reduction of 100kWh/m² solar collector for the house without heat recovery and 70kWh/m² solar collector with heat recovery unit.

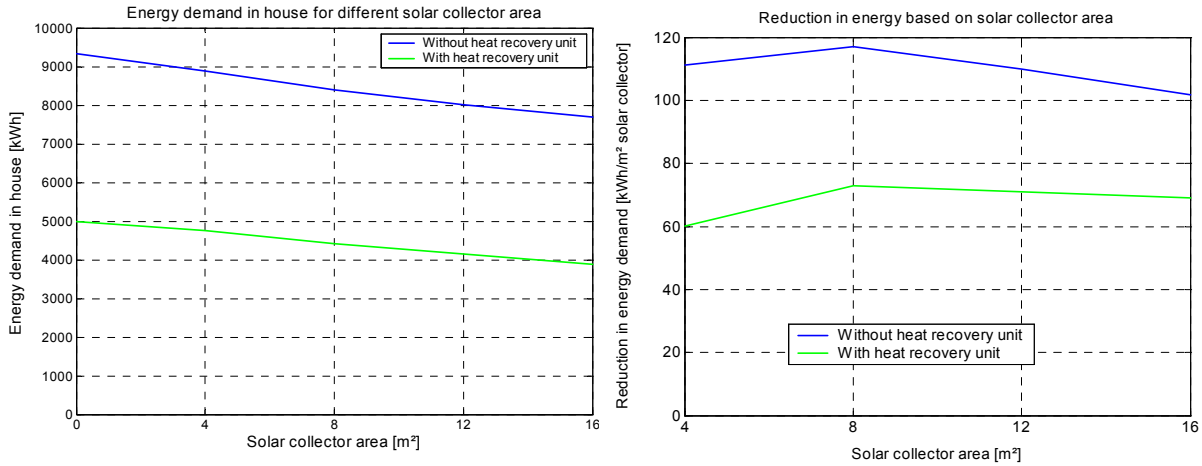

Figure 7.2 Energy consumption as a function of the solar collector area (to the left) and the reduction in energy consumption per square meter of solar collector (to the right)

In the paper, seven different layouts of the floor construction has been modelled. Here it has been found that the size and storage material (concrete or sand) and pipe distance (300mm or 500mm) in the storage had little influence on the savings, while the distribution of the insulation between the layers, solar collector area and heating demand of the house did influence the results.

Concerning the distribution of the insulation thickness, it was found that the smaller the thickness of the upper insulation towards the room, the larger the reduction in the energy consumption. However this meant that the temperature in the summer period in the house became too high, both on the floor surface and in the room. This can however be solved by using a good control strategy

7.4 Summing up

In Paper 4, the energy savings potential from using the lower deck in a floor construction to store solar energy is described.

The results have shown that there is indeed a large potential in the single-family house. For a 16m² solar collector, the reduction in the energy consumption is 17% and 22% with and without heat recovery unit respectively.

This shows that in stead of simply increasing the insulation thickness to lower the energy consumption an equally possible approach is to use solar energy to increase the energy performance of the building, which is the aim of the EU directive (European Parliament, 2003).

8 Conclusion

In this thesis simulation models of building integrated heating and cooling systems have been investigated. Two simulation programs have been developed based on models of building integrated heating and cooling systems coupled to a room model. One called FHSim for modelling floor heating systems, and one called TASim for modelling thermo active components. The models combine detailed modelling of the conditions within the constructions with a room model taking both radiation and convection into account.

It is found that it is possible to model building integrated heating and cooling systems using the models which have been developed as part of this thesis.

The simulation models have been validated against measurements for a slab-on-grade floor with floor heating as well as for a test mock-up for thermo active components. Combining the results from these two investigations, it is found that the simulation models are able to model the conditions in buildings with building integrated heating and cooling systems.

For floor heating it is found that introducing the characteristic dimension – defined as the area divided by half the perimeter – as the width in a two-dimensional slab-on-grade floor model the three-dimensional conditions can be reduced to a two-dimensional problem. This has so far only been shown for models without floor heating. Additionally, it has been shown that in order to correctly model the conditions in the floor construction – as the temperatures in the deck are influenced by the dynamical conditions – it is necessary to model building integrated systems by coupling them to a room model to ensure that the dynamical conditions are included to give correct heat flows

It has been found that both by changing insulation in floor construction and foundation as well as the characteristic dimension, the construction using floor heating is relatively more influenced with respect to heat loss to the ground than a similar construction without floor heating. Therefore there is an extra “penalty” on the heat loss to the ground compared to buildings heated by other means if the slab-on-grade is poorly insulated.

Simulation models with different levels of detail have been compared to find the differences for energy consumption, heat loss to the ground and temperature distribution. The detailed two-dimensional model has been used as reference to the results. Large discrepancies have been found, especially for small insulation thicknesses and compared to the models without foundation included in the models. More specifically it has been found that the best approximation to the detailed model was the simplified thermal network model including the influence of the foundation. Further it has been found that an electrical implementation of the hydronic floor heating system which is modelled here was not adequate.

Thermo active components have been investigated through the use of two test setups, both aiming at characterising the cooling capacity of pre-fabricated hollow core concrete decks. The first is a simple setup designed for testing a deck where the pipe is simply placed directly in the cavities to give a very simple and easy-to-install thermo active component. The second test setup is a made of two decks with pipes embedded in the concrete as ceiling and floor in a room of approximately 20m².

In both setups a linear correlation is found between cooling capacity and temperature difference between room temperature and fluid temperature, where the room temperature is an environmental temperature weighing air and radiant temperatures in the room.

The second test setup has proven to be useful for analysing thermo active components.

Finally thermal energy storage of solar energy in the floor construction of a slab-on-grade floor with two concrete decks has been investigated in a purely numerical analysis. Here it has been found that it is possible to decrease the energy consumption significantly in buildings with an already low energy consumption.

8.1 Recommendations for further work

As described in the conclusion, the simulation models FHSim and TASim have been validated with good results. However, there are still a few issues that could further improve the models. Especially concerning the convective part of the heat transfer in the room the model proved to be not completely able to finding the conditions. Therefore an improvement in the model would be to include a stratification model in the room air, thereby also improving the calculation of the convection between surfaces and room air. The test mock-up would be a good tool for such an analysis.

The investigations on floor heating in this work have been focused on buildings with a minimum energy consumption of around 35kWh/m². An interesting investigation would be to reduce the energy consumption further from this level to a very low value. Especially concerning the control system such an investigation is very relevant, as it is expected that buildings with very low energy consumption will be more or less self controlling with a fluid temperature which is only very few degrees above the room air temperature. This will in practise mean that the control system can be simplified significantly.

FHSim and TASim can be used for a variety of investigations to further advance the knowledge on building integrated heating and cooling systems. A few of these are mentioned below:

- Include supply side of heating/cooling system.
  The present analysis does not include the heating/cooling system in the analyses. However one of the advantages of these low temperature heating and high temperature cooling systems is the versatility in the use of the supply side of the system, where heat pumps, low temperature district heating/district cooling, free cooling using outside night time air and more. Since building integrated heating and cooling systems are so-called low exergy systems the versatility in the supply side is expected to be beneficial towards the energy performance of buildings introduced by the European Parliament. In IEA Annex 37 a large effort is underway to include the supply side – including the results from this effort in FHSim/TASim would further improve the model.
- Further investigations especially on control strategies.
  In this work only a few control strategies have been tested namely fixed and variable supply temperatures for floor heating and intermittent control of the thermo active components using 12 hour cycles. Many alternative control strategies can be tested and also different control algorithms other than simply on/off the flow based on a set point temperature. These investigations can easily be verified by measurements in the test mock-up.
- Method for calculating the linear thermal transmittance in floors with floor heating.
  The results in the work have indicated that the existing methods for calculating the linear thermal transmittance of the foundation are not conservative in their estimates when floor heating is used in the models. Therefore an obvious investigation would be to establish a suggestion for a new method for calculating the linear thermal transmittance of the foundation in floors with floor heating.

- Light floor heating and ground coupling.
  Lightweight floor heating has not been included in this investigation. Based on the thermal properties where more insulation is placed around the floor heating pipe, it can be expected that the penalty on floor heating with respect to higher energy consumption will be smaller than for heavy floor heating.
- Floor heating in multi-storey buildings.
  Are there any problems using floor heating in multi-storey buildings, such as unwanted heat flow through the ceiling surface to the room below the heating system?

A secondary improvement to the simulation model would be to expand the model from being a single zone model, to a multizone model. However, instead of expanding the capabilities of FHSim and TASim it would be more relevant to export the building integrated heating and cooling models to more general building energy simulation programs which are already highly developed multizone models with many other systems of for instance ventilation systems. Therefore, the results from this investigation can be the basis for developing models that can fit into existing programs. Of special relevance to this is the number of inputs required to model hydronic systems, of which a few have been investigated here.

Finally, the mock-up can be used for a number of investigations on further improvements of thermo active components where among others the development of an operable lowered ceiling would be relevant. Such an operable ceiling could be used to impede the cooling in the morning from the ceiling surface and be opened to allow cooling once the temperature in the room starts to rise during the working day. Besides from this the mock-up can be used for testing for instance different ventilation systems, thermal comfort of occupants and other deck constructions. The results from these investigations can subsequently be included in TASim.

9 References

Achermann M and Zweifel G (2003): RADTEST – Radiant Heating and Cooling Test Cases. IEA Task 22, Subtask C, International Energy Agency

Adjali M H, Davies M, Ni Riain C and Littler J G (2000a): In Situ Measurements and Numerical Simulation of Heat Transfer beneath a Heated Ground Floor Slab. In: Energy and Buildings, Vol. 33, pp. 75-83

Adjali M H, Davies M, Rees S W and Littler J (2000b): Temperatures in and under a Slab-on-Ground Floor: Two- and Three-Dimensional Numerical Simulations and Comparison with Experimental Data. In: Building and Environment, Vol. 35, pp. 655-662

Anderson B R (1991): Calculation of the Steady-State Heat Transfer through a Slab-on-Ground Floor. In: Building and Environment, Vol. 26, No. 4, pp. 405-415

Andersson L O and Isfält E (1978): Hus med betongstomme spar 80 procent värme. (In Swedish) In: Byggnadstidningen nr. 18.

Antonopoulos, K. A., Tzivanidis, C. (1997): Numerical Solution of Unsteady Three-Dimensional Heat Transfer during Space Cooling using Ceiling Embedded Piping, In Energy, Vol. 22, No. 1, pp. 59-67

Athienitis A K and Chen Y (2000): The Effect of Solar Radiation on Dynamic Thermal Performance of Floor Heating Systems. In: Solar Energy, Vol. 69, No. 3, pp.229-237

Athienitis A K and Chen Y (1998): A Three-Dimensional Numerical Investigation of the Effect of Cover Materials on Heat Transfer in Floor Heating Systems. In: ASHRAE Transactions 104(2), pp. 1350-1355

Athienitis A K and Chen T Y (1993): Experimental and Theoretical Investigation of Floor Heating with Thermal Storage. In: ASHRAE Transactions, Vol. 99(1), pp. 1049-1057

Awbi H B (1991): Ventilation of Buildings. E & F N Spon.

Bahnfleth W P and Pedersen C O (1990): A Three-Dimensional Numerical Study of Slab-on-Grade Heat Transfer. ASHRAE Transactions 96(2), pp. 61-72

Bansal N K, Shail (1999): Characteristic Paramters of a Hypocaust Construction. In: Building and Environment, No. 34 (1999) pp. 305-318

Barton P, Beggs C B and Sleigh P A (2002): A theoretical study of the thermal performance of the TermoDeck hollow core slab system. In: Applied Thermal Engineering 22, pp. 1485-1499.

Bauer M (1998): Methode zur Berechnung und Bewertung des Energieaufwandes für die Nutzenübergabe bei Warmwasserheizanlagen. Universität Stuttgart, IKE Lehrstuhl für Heiz- und Raumlufttechnik

Beckman, W A (2000): TRNSYS A Transient System Simulation Program, TRNSYS Manual, Version 15, SEL, University of Wisconsin, Madison, WI

Blomberg, T (2001): Heat 3. A PC Program for Heat Transfer in Three Dimensions - Manual with brief Theory and Examples. Lund-Gothenburg Group for Computational Building Physics

Blomberg, T (2000): Heat 2. A PC Program for Heat Transfer in Three Dimensions - Manual with brief Theory and Examples. Lund-Gothenburg Group for Computational Building Physics

Blomberg T (1996): Heat Conduction in Two and Three Dimensions. Computer Modelling of Building Physics Applications. Doctorate Thesis. Lund University, Sweden. ISBN 91-98722-05-8

Boerstra A, Op't Veld P, Eijdems H (2000): The Health, Safety and Comfort Advantages of Low Temperature Heating Systems: A Literature Review. In: Healthy Buildings Conference, 2000

Boligministeriet (1995): Bygningsreglement 1995 (In Danish) (Danish Building Code). Bygge- og Boligstyrelsen, København.

Boligministeriet (1998): Bygningsreglement for småhuse 1998 (In Danish) (Danish Building Code). Bygge- og Boligstyrelsen, København.

Byberg M, Jappe H, Andersen J C, Dagnæs-Hansen M and Bechmann D (1989): Indeklima og energiforbrug – varmeledning i betonelementer (In Danish). Byggeriets Udviklingsråd.

Caluwaerts P, Lebrun J and Marret D (1980): (In German) Wärmeverluste mit unterschiedlichen Heizungssystemen. 2. Internationaler Velta Kongress.

CEN (1994): EN ISO 10211-1: Thermal Bridges in Building Construction – Heat Flows and Surface Temperatures – Part 1: General calculation methods. 1994, CEN

CEN (1995): EN ISO 10211-2: Thermal Bridges in Building Construction – Heat Flows and Surface Temperatures – Part 2: Calculation of linear thermal bridges, 1995, CEN

CEN (1997): EN ISO 1264: Floor Heating – Systems and Components. European Committee for Standardization, CEN

CEN (1998a): CR 1752, Ventilation for Buildings: Design Criteria for the Indoor Environment. Brussels: CEN.

CEN (1998b): EN 832 Thermal Performance of Buildings – Calculation of Energy Use for Heating – Residential Buildings. CEN

CEN (1998c): EN ISO 13370: Thermal Performance of Buildings – Heat Transfer via the Ground – Calculation Methods. CEN.

CEN (2004): EN ISO 13790: Thermal Performance of Buildings – Calculation of Energy Use for Space Heating. CEN.

Chen Y, Athienitis, A K (1998): A Three-Dimensional Numerical Investigation of the Effect of Cover materials on Heat Transfer in Floor Heating Systems, In: ASHRAE Transactions, Vol.104(2), pp. 1350-1355

Claesson J, Hagentoft C-E (1991): Heat Loss to the Ground from a Building – I. General Theory, Building and Environment, Vol. 26, No. 2, pp. 195-208

Comini G and Nonino C (1994): Thermal Analysis of Floor Heating Panels. In Numerical Heat Transfer, Part A, Vol. 26 pp. 537-550

Dascalaki E, Santamouris M, Balaras C A and Asimakopoulos D N (1994): Natural convection heat transfer coefficients from vertical and horizontal surfaces for building applications. In: Energy and Buildings. No. 20 (1994), pp. 243-249.

Davies M, Tindale A and Littler J (1995): Importance of Multi-Dimensional Conductive Heat Flow in and around Buildings. In: Building Serv. Eng. Res. Technol. 16(2), pp. 83-90

Davies M, Zoras S and Adjali M H (2001): Improving the Efficiency of the Numerical Modelling of Built Environment Earth-Contact Heat Transfers. In: Applied Energy, Vol. 68, pp. 31-42

De Boer, R (2003): The Effect of Sub-Floor Heating on House-Dust-Mite Populations on Floors and in Furniture. In: Experimental and Applied Acarology, Vol. 29 Issue 4, p. 315-330.

De Carli M and Olesen B W (2001): Field Measurements of Thermal Comfort Conditions in Buildings with Radiant Surface Cooling Systems. In Proceedings from Clima 2000/Napoli 2001 World Congress

De Carli M and Olesen B W (2002): Field Measurements of Operative Temperatures in Buildings Heated or Cooled by Embedded Water-Based Radiant Systems. In: ASHRAE Transactions. Vol. 108(2), pp. 714-725

Delsante A E (1990): Comparison between Measured and Calculated Heat Losses through a Slab-on-Ground Floor. Building and Environment. 1990, Vol. 25, pp. 25-31

Deru M, Judkoff R, Neymark J (2003): Whole Building Energy Simulation with a Three-Dimensional Ground-Coupled Heat Transfer Model. In: ASHRAE Transactions, Vol. 109(1), pp. 557-565

DS (2002): DS 418. Beregning af bygningers varmetab (In Danish) English title: Calculation of heat loss from buildings. 6th edition

DS (1993): DS 474. Norm for specifikation af termisk indeklima (In Danish). English title: Code for Indoor Thermal Climate. 1st edition.

Duffie J.A. and Beckman W.A. (1991) Solar Engineering of Thermal Processes, 2nd edn. pp. 54-59. Wiley Interscience, New York.

Eijdems H H E W, Boerstra A C, Op ‘t Veld P J M (no year): Low Temperature Heating Systems Impact on IAG, Thermal Comfort and Energy Consumption. Can be found on http://www.vtt.fi/rte/projects/annex37/POVpaper.pdf Part of IEA Annex 37.

European Parliament (2003): Directive 2002/91/EC of the European Parliament and of the Council of the 16 December 2002 on the Energy Performance of Buildings. Official Journal of the European Communities. L 1/65

Fanger P O (1970): Thermal Comfort. Danish Technical Press, Copenhagen. Reprinted in 1972 by McGraw-Hill, New York and in 1982 by Robert E. Krieger, Florida

Farouki, O T (1986): Thermal Properties of Soils, Series on Rock and Soil Mechanics, Vol. 11, Trans Tech Publications, Germany.

Fort K (1989): Dynamisches Verhalten von Fussbondenheizungen. (In German) (English title: Dynamical Behavior of floor heating systems). Juris Druck + Verlag, Zürich.

Fort K (1993): Optimaler Betrieb von Fussbodenheizungen. Forschungsbericht Bundesamt für Energiewirtschaft, Zürich.

Fort K (1999): Type 160: Floor heating and Hypocaust.

Hagentoft C-E (2001): Introduction to Building Physics. Studentlitteratur

Hagentoft C-E and Roots P (2001): How a Building Heating Supply System Affects Energy Demand and Indoor Comfort. In: Buildings VIII

Hagentoft C-E (1988): Heat Loss to the Ground from a Building. PhD thesis, Lund University of Tehcnology.

Hanibuchi H and Hokoi S (1998): Basic Study of Radiative and Convective Heat Exchange in a Room with Floor Heating. In: ASHRAE Transactions. Volume 104(1) part B, pp. 1098-1105

Hansen J O, Jacobsen T and Weitzmann P (2002): Termoaktive konstruktioner. Fase 1 – forprojekt. (In Danish). Energistyrelsen, EFP-2001, j.nr. 1213/01-0020.

Harrysson C (1997): In Swedish: Golvvärme eller radiatorsystem i småhus. (Floor heating or radiators in single-family houses), Falkenberg.

Ho S Y, Hayes R E and Wood R K (1995): Simulation of the Dynamic Behaviour of a Hydronic Floor Heating System. In: Heat Recovery Systems and CHP, Vol. 15, No. 6, pp. 505-519

Hsieh C-S and Hwang C (1989): Model Reduction of Continuous-Time Systems Using a Modified Routh Approximation Method. IEE Proceedings, Vol. 136, Pt. D, No. 4, July

Incropera F P, DeWitt D P (1996): Introduction to Heat Transfer. John Wiley and Sons.

ISO (1994): EN ISO 7730. Moderate Thermal Environments – Determination of the PMV and PPD Indices and Specification of the Conditions for Thermal Comfort. ISO.

ISO (2000): ISO12567-1: Thermal Performance of Windows and Doors – Determination of Thermal Transmittance by Hot Box Method – Part 1: Complete Windows and Doors. ISO.

ISO (2001) ISO/FDIS 15099: Thermal Performance of Windows, Doors and Shading Devices – Detailed Calculations, ISO/FDIS

Janssen H, Carmeliet J and Hens H (2004): The Influence of Soil Moisture Transfer on Building Heat Loss via the Ground. Building and Environment. 2004, Vol. 39, pp. 825-836

Janssen H, Carmeliet J, Hens H (2002a): The Influence of Soil Moisture in the Unsaturated Zone on the Heat Loss from Buildings via the Ground. Journal of Thermal Envelope and Building Science, Vol. 25, No. 4, pp. 275-298.

Janssen, H.; Carmeliet, J.; Hens, H (2002b): The Influence of Soil Moisture in the Unsaturated Zone on the Heat Loss from Buildings via the Ground: a Parametric Study. Proceedings of the 6th Symposium of Building Physics in the Nordic Countries, P. 207-214.

Judkoff R and Neymark J (1995): International Energy Agency Building Energy Simulation Test (BESTEST) and Diagnostic Method. NREL.

Kilkis I B and Coley M (1995): Development of a Complete Design Software for Hydronic Floor Heating of Buildings. In: ASHRAE Transactions. Vol. 101(1), pp. 1201-1213

Kilkis I B and Sapci M (1995): Computer-Aided Design of Radiant Subfloor Heating Systems. In: ASHRAE Transactions. Vol. 101(1), pp. 1214-1220

Kolokotroni M and Aronis A (1999): Cooling-Energy Reduction in Air-Conditioned Offices by Using Night Ventilation. In: Applied Energy. No. 63, pp. 241-253

Koschenz M and Lehmann B (2000): Thermoaktive Bauteilsysteme tabs. (In German) EMPA Energiesysteme/Haustechnik

Lee T., Hawes D. W., Banu D., Feldman D. (2000): Control Aspects of Latent Heat Storage and Recovery in Concrete. Solar Energy Materials & Solar Cells, Vol. 62, pp. 217-237.

Lefebvre G (1997): Modal-Based Simulation of the Thermal Behavior of a Building: the m2m Software. Energy and Buildings, Vol. 25, pp. 19-30.

Mathworks (2002): Using Matlab, Mathworks

Meierhans R A (1993): Slab cooling and Earth Coupling. In ASHRAE Transactions. Vol. 99, pp. 511-518

Meierhans R A (1996): Room Air Conditioning by Means of Overnight Cooling of the Concrete Ceiling. In: ASHRAE Transactions. Vol. 102(1), pp. 693-697

Meierhans R A and Olesen B W (2002): Art Museum in Bregenz – Soft HVAC for a Strong Architecture. In: ASHRAE Transactions. Vol. 108(2), pp. 708-713

Ménézo C, Rox J J and Virgone J (2002): Modelling Heat Transfers in Building by Coupling Reduced-Order Models. Building and Environment, Vol. 37, pp. 133-144

Mills, A F (1992). Heat Transfer. Irwin

Munch-Andersen J., Svendsen S., Tommerup H.M.: Exterior Walls to Meet Future Danish Requirements. In: Detailing design. Towards a Joined-up Industry. Proceedings of the Third international conference on Detail Design in Architecture, September 12 and 13, 2000, University of Brighton, Sussex, UK. Emmitt, S. (Ed.). Leeds. Metropolitan University. Centre for the Built Environment, CeBE. 2001. pp. 95-108.

National Instruments (2003): LabVIEW. Version 7 Express has been used. For further information see http://www.labview.com/

Nelder JA, Mead R (1965): A Simplex Method for Function Minimization, Computer Journal vol. 7 (1965), pp. 308-313.

Nielsen TR, Duer K., Svendsen S. (2001): Energy Performance of Glazings and Windows, Solar Energy, Vol. 69, pp. 137-143.

Nielsen, H., Nielsen, K., Jensen, H. Siggaard (1995): Skruen uden ende – den vestlige teknologis historie (In Danish), Teknisk Forlag

Nordtest (2001): NT VVS127. Floor Heating Systems: Design and Type Testing of Waterborne Heat Systems for Lightweight Structures. Nordtest.

Olesen, B W (1975): Termiske komfortkrav til gulve (In Danish), Ph.d, Laboratoriet for Varme- og Klimateknik,

Olesen B W (1994): Comparative Experimental Study of Performance of Radiant Floor-Heating Systems and a Wall Panel Heating System Under Dynamic Conditions. In: ASHRAE Transactions. Vol. 100(1), pp. 1011-1023

Olesen B W (2000): Cooling and Heating of Buildings by Activating the Thermal Mass with Embedded Hydronic Pipe Systems. In proceedings of ASHRAE/CIBSE conference in Dublin 2000.

Olesen B W (2001): Opvarmning og køling med vandbårne systemer. (In Danish) In Danvak Magasinet 04-2001. pp. 30-33.

Olesen B W (2002): Radiant Floor Heating In Theory and Practice. ASHRAE Journal July 2002 pp. 19-26

Olesen B W, Koschenz M and Johansson C (2003): New European Standard Proposal for Design and Dimensioning of Embedded Radiant Surface Heating and Cooling Systems. In ASHRAE Transactions. Vol.103(1), pp. 565-668

Olsen L and Christiansen C (2004): Byg Boligerne Bedre. Analyse af bygninger med gulvvarme og radiatorer. Teknologisk Institut

Olsen E L and Chen Q (2003): Energy Consumption and Comfort Analysis for Different Low-Energy Cooling Systems in a Mild Climate. In: Energy and Buildings, No. 35, pp. 561-571

Pan S and Pal J (1995): Reduced Order Modelling of Discrete-Time Systems. Applied Mathematical modelling, Vol. 19 March, pp. 133-138

PASSYS (1989): The PASSYS Project Phase 1. Subgroup: Model Validation and Development. Final Report. 1986-1989. Edited by Jensen S Ø. Thermal Insulation Laboratory, Technical University of Denmark for the Commission of the European Communities Directorate – General XII for Science, Research and Development

Peng S and Peterson F (1995): Convection From a Cold Window with Simulated Floor Heating by Means of a Transiently Heated Flat Unit. In: Energy and Buildings, No. 23 (1995), pp. 95-103

Perez R, Ineichen P, Seals R, Michalsky J and Stewart R (1990): Modeling Daylight Availability and Irradiance Components from Direct and Global Irradiance. Solar Energy. Vol 44, No. 5, pp. 271-289

Persson T (2000): In Swedish: Lågtemperaturvärmesystem – En kunskapsöversikt (Low Temperature Heating Systems – A literature Review). SERC, Högskolan i Dalarna.

Radisch N (2001): Vurdering af varmeforbrug i nyere huse med gulvvarme (In Danish). Teknologisk Institut – Energi.

Roots, P (2001): Mätning av fuktförhållande och värmetransport til underliggande mark i en grund som utföres med golvvarme, Working Paper No. 14, University of Gävle, 2001.

Roots P (2002): En litteraturstudie om golvvärme (In Swedish). SP AR 2004:04, Energiteknik, Borås

Roots P, Hagentoft C-E (2002a): Floor Heating – Heating Demand. Proceedings of the 6th Symposium on Building Physics in the Nordic Countries, Trondheim, Norway, pp. 775-782

Roots, P; Hagentoft, C-E (2002b): A Field Study of Heat and Moisture Condition in a Slab on the Ground with Floor Heating – Results. Proceedings of the 6th Symposium of Building Physics in the Nordic Countries, P. 223-230.

Roots, P; Hagentoft, C-E (2002c).: Moisture Conditions in a Slab on the Ground with Floor Heating. Proceedings of the 6th Symposium of Building Physics in the Nordic Countries, P. 215-221.

Roots P and Sandberg P I (2001): Moisture Conditions in a Concrete Slab on Grade with Floor Heating. In: Buildings VIII

Rose J, Svendsen, S, (2002): Single-Family Houses that meet the Future Energy Demand. Proceedings of the 6th Symposium on Building Physics in the Nordic Countries, Trondheim, Norway, pp. 269-276

Rueegg T, Dorer V and Steinemann U (2001): Must Cold Air down Draughts be Compensated when Using Highly Insulation Windows? In: Energy and Buildings 33 (2001), pp. 489-493

Sanchez-Romero M and Alavedra-Ribot P (1996): Experimental Study of the Thermal Behaviour of Radiant Floors. In: Building Research and Information, Vol. 24, No. 6

Schmidt D (2004): Methodology for the Modelling of Thermally Activated Building Components in Low Exergy Design. KTH Civil and Architectural Engineering, Stockholm, Sweden 2004.

Schramek, E. R., Späte, F., Werner, M. (no year): Optimizing Temperature Control in Buildings via Weather Forecasts. Universität Dortmund. Lehrstuhl TGA Technische Gabäudeausrüstung,

Seta T, Gunji T, Maie K and Kondo S (1993): Thermal Properties of Carpets on Floor Heater. Based on paper in Journal of The Textile Machinery Society of Japan, Vol. 46, No. 5, T125-T130

Stetiu C (1998): Radiant Cooling in US Office Buildings: Towards Eliminating the Perception of Climate-Imposed Barriers. Ph.D. Thesis. Energy and Resources Group, Lawrence Berkeley National Laboratory

Strängbetong (1987): Klimatsystem TermoDeck (In Swedish). Brochure

Shukuya M and Hammache A (2002): Introduction to the Concept of Exergy - for a Better Understanding of Low-Temperature-Heating and High-Temperature-Cooling Systems. VTT Resarch notes 2158. Published as part of IEA Annex 37 “Low Exergy Systems for Heating and Cooling of Buildings”

Strand R K and Pedersen C O (2002): "Modeling Radiant Systems in an Integrated Heat Balance Based Energy Simulation Program," ASHRAE Transactions. Vol. 108(2), pp. 979-988.

Thomas H R, Rees S W and Lloyd R M (1996): Measured Heat Losses through a Real Ground Floor Slab. In: Building Research and Information, Vol. 24 (1)

VVS Danvak (1999): In Danish: Gulvvarme giver 40 % merforbrug? (Floor heating leads to 40 % extra energy consumption?). In VVS Danvak, 13, 1999 p. 7. No author name stated

Wallén G (1996): Vetenskapsteori och forskningsmetodik, Studentlitteratur.

Wallentén P (2001): Convective Heat Transfer Coefficients in a Full-Scale Room with and without Furniture. In: Building and Environment. No. 36 (2001), pp. 743-751.

Weber T (2004): Energy Performance of Buildings / Methodologies for Experimental Verification. KTH Civil and Architectural Engineering, Stockholm, Sweden 2004.

Weitzmann P and Jensen C F (2000a): Varmeteknisk analyse af gulvvarmeanlæg (In Danish). English title: Thermal Analysis of Floor Heating Systems. Institut for Bygninger og Energi, Danmarks Tekniske Universitet.

Weitzmann P, Jensen C F and Svendsen S (2000b): Comparison of Calculations of Thermal Transmittance of Windows Using Two- and Three-Dimensional Models. In EuroSun 2000. Paper No. 011.4, p. 84 in Book of Abstracts.

Weitzmann P (2002): Simulation of Temperature in Office with Building Integrated Heating and Cooling. In: Proceedings of the Sixth Symposium on Building Physics in the Nordic Countries, pp. 897-904.

Weitzmann P, Kragh J and Jensen C F (2002): Numerical Investigation of Floor Heating Systems in Low Energy Houses. In: Proceedings of the Sixth Symposium on Building Physics in the Nordic Countries, pp. 905-912.

Weitzmann P, Kalagasidis A S, Nielsen T R, Peuhkuri R and Hagentoft C-E (2003a): Presentation of the International Building Physics Toolbox for Simulink. In: Proceedings of The Eight International IBPSA Conference: Building Simulation 2003, pp. 1369-1376

Weitzmann P, Holck O and Svendsen S (2003b): Numerical Analysis of Heat Storage of Solar Heat in Floor Construction. In: Proceedings of ISES Solar World Congress 2003. Paper number 02 15.

Weitzmann P, Kragh J, Roots P, Svendsen S (not yet published): Modelling Floor Heating Systems Using a Validated Two-Dimensional Ground Coupled Numerical Model. Accepted for publication in Buildings and Environment.

Weitzmann P, Svendsen S (submitted): Method for Calculating Thermal Properties of Lightweight Floor Heating Panels Based on an Experimental Setup. Submitted to the International Journal of Low Energy and Sustainable Buildings

Youcef L (1991): Two-Dimensional Model of Direct Solar Slab-on-Grade Heating Floor. In: Solar Energy, Vol. 46, No. 3, pp. 183-189

10 Nomenclature

Variable	Description	Unit
ε	Emissivity	-
ψ	Linear thermal transmittance	W/mK
τ	Time constant	s
χ	Point heat loss	W/K
σ	Stefan-Boltzmann's constant	W/m^2K^4
λ	Heat transfer coefficient/thermal conductivity	W/mK
θ	Temperature	
q	Heat flow	W (or W/m^2)
a	Power product factors	-
A	Area	m^2
B	System dependent coefficient	-
B'	Characteristic dimension	m
Bi	Biot number	-
c_p	Heat capacity	kJ/kgK
d	Distance/length	m
F	View factors	-
h	Heat transfer coefficient	W/m^2K
L_c	Characteristic length	m
M	Month of year	month
m	Power factor	-
$\dot{m}$	Flow	kg/s
P	Perimeter	m
R	Thermal resistance	m^2K/W
t	time	s
T	Temperature	˚C
U	Thermal transmittance	W/m^2K
U_{cc}	Cooling capacity coefficient	W/m^2K
V	Volume	m^3
V_{signal}	Voltage signal	V
w	Distance/length	m
x	Distance/length	m

Generally used indices

Index	Description
ψ	Linear
χ	Point
1D	One-dimensional
air	Air
cc	Cooling capacity
ceiling	Ceiling
conc	Concrete
conv	Convective
deck	(Thermo active) deck
down	Downwards
ext	External

floor	Floor
floorcovering	Floor covering
fluid	fluid in pipe
foundation	Foundation
ground	Towards the ground
guard	Guard
H	Hydronic
i	Counter
inf	Infiltration
l	Length
m	Average
material	Material
out	Outside conditions
pipe	Pipe
rad	Long wave thermal radiation
ref	Reference point
return	Return from pipe
room	Room
si	Surfaces (inside and outside)
supply	Supply to pipe
sur, surface	Surface
tot	Total
up	Upwards
wall	Wall

Appendix A Modelling procedures

In this appendix the simulation models used in FHSim and TASim is presented. Emphasis will be placed on the implementation of the different types of models for floor constructions and thermo active components with different implementation of the pipes. A certain overlap with the description found in the main chapters of the thesis cannot be avoided, as this description aims at including all parts of the modelling process which are needed to understand the simulation programs. A few overlaps between the description in the different implementations cannot be avoided either. Where possible references to similar sections will be made in stead of making almost identical descriptions of the implementations to avoid overlaps.

The methodology in this appendix is written mainly based on the floor heating model presented in Chapter 5, while the thermo active components are only briefly mentioned. However, the same simulation models are used in both cases, and since the floor heating model is slightly more advanced especially concerning the boundary conditions, the floor heating is used for the description. Therefore, thermo active components are essentially a simplification of the floor heating model.

Notice, that the symbols are not explained in the text. This has been supplied in a nomenclature at the end of the appendix.

A.1 Finite Control Volume

The finite control volume method is the main carrying element of the simulation models used in this thesis, based on different level of detail in the implementations ranging from simple one-dimensional models to detailed two-dimensional models. Emphasis is placed on the two-dimensional simulation model of the ground coupled floor heating model, which is the most detailed of the models used in this thesis.

In general a Finite Control Volume (FCV) method is a way to discretize a differential equation so that an otherwise unsolvable problem can be solved for a given domain by applying a set of boundary conditions.

In this documentation, a brief overview of the FCV method is given. A more thorough description can be found in many textbooks in the field of numerical modeling.

A.1.1 Description of simulation models

A number of different FCV models are developed as part of this work, each with different levels of detail in the modelling and features. These are:

- Detailed two-dimensional model with floor construction, foundation and ground volume.
- Two-dimensional model around one pipe in the construction. This model is called a 1.5D model in this thesis.
- One-dimensional model with a hydronic implementation of the pipe
- One-dimensional model with an electrical implementation of the pipe

The reason for developing these very different models is to be able to compare models with very different levels of detail and – more importantly – different time requirements in the simulations. Therefore, if a simple model with low simulation time gives the same results as a more detailed model, there is no need to use the detailed model, assuming that the same inputs can be included in the model.

Two-dimensional FHSim floor model

Figure A.1 shows the floor model, which is based on the description in EN ISO 10211-1 (CEN, 1994) and EN ISO 10211-2 (CEN, 1995). It consists of the floor construction, the foundation, and a 20 m by 20 m ground volume to ensure undisturbed boundary conditions at the vertical and horizontal cut-off planes. The floor width is variable to accommodate for different building geometries. As discussed in Chapter 3, the three-dimensional conditions can be simplified to two-dimensional conditions by introducing the characteristic dimension as the width of the floor construction. Therfore it is also assumed that there is no cooling along the length of the pipe. It is also assumed that the temperature is the same in the pipe from inside the foundation to the central part of the floor.

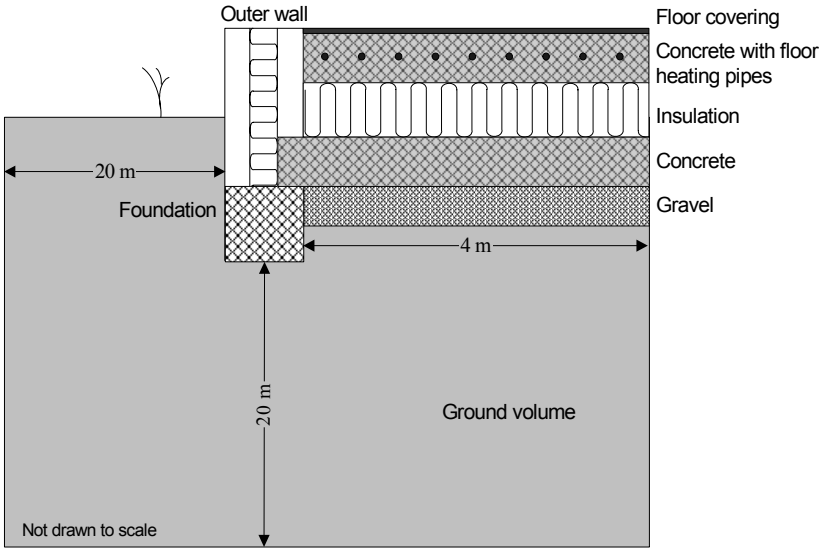

Figure A.1 Two-dimensional section of floor model used in FHSim with floor heating. Here the model is shown with a width of the floor construction of four meters.

The boundary conditions used in the model are shown in Figure A.2. They are:

- Adiabatic on the sides and bottom of the ground volume
- Adiabatic on top of the outer wall and at the far side of the floor construction
- On the floor surface interior climate is used
- On the ground surface and on the side of the outer wall exterior climate is used
- The pipes are included as a fluid with a given temperature

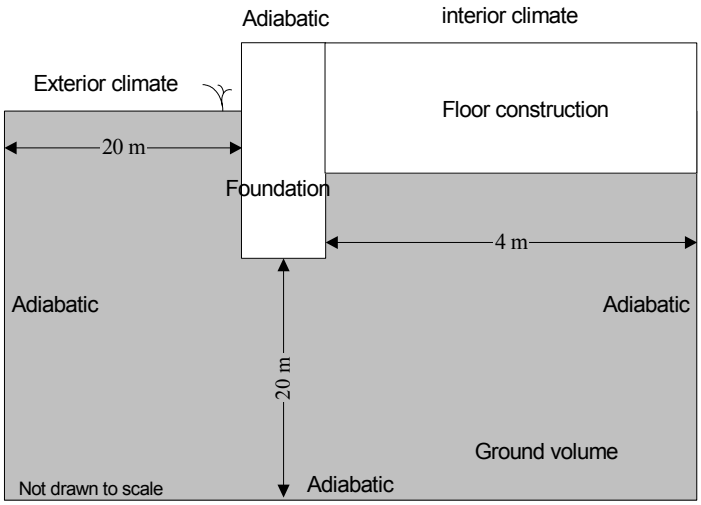

Figure A.2 Boundary conditions in model

Two-dimensional section model in FHSim (1.5D)

A simpler two-dimensional model – which is called a 1.5D model since though it is two-dimensional it has few details compared to the slab-on-grade floor – has also been implemented in FHSim. This model is shown in Figure 5.25 and Figure 5.26. Figure 5.25 shows the floor construction and the lines of symmetry in the floor construction. These lines will be adiabatic, thereby assuming that there is the same pipe temperature in all the adjacent pipes in the floor.

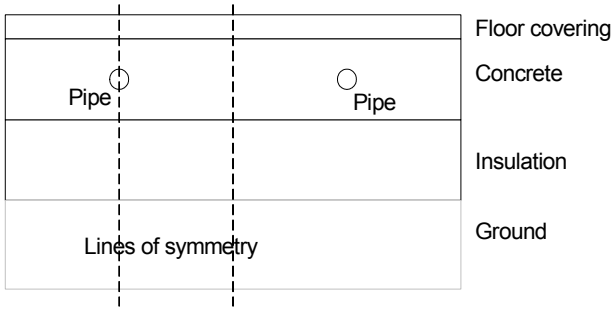

Figure A.3 1.5D section showing the lines of symmetry

Consequently, the model presented in Figure 5.26 is the model, which is used by the simulation model.

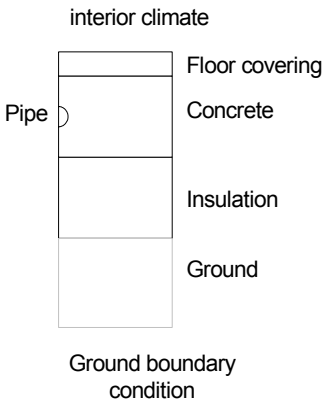

Figure A.4 1.5D floor heating model with pipe included

One-dimensional FHSim model with hydronic pipe

Figure 5.24 shows the 1D model with the floor heating pipe is again using a normal 1D mesh definition with the standard implementation of the FCV model. The pipe has been included as an extra nodal point, which can interact with one of the nodal points in the normal 1D mesh. A thermal resistance is included between the pipe and the concrete. The value of this resistance is difficult to accurately define and will be subject to an investigation later in the chapter.

The conditions in the model are considered to be the average values for the entire floor construction. Therefore, the temperature of the fluid in the pipe is calculated as the mean temperature of supply and return, which is calculated, based the flow rate and the temperature in the concrete next to the pipe, through a thermal resistance between fluid and concrete deck, which takes the convective resistance of the fluid, the pipe resistance and geometric resistance into account.

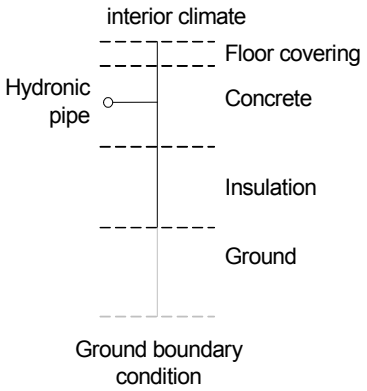

Figure A.5 1D floor heating model with pipe included

One-dimensional FHSim model with electrical pipe

The electrical floor heating model shown in Figure 5.23 has a 1D mesh definition. Floor heating is included as a supply of an energy flux directly in one of the nodal points in the concrete layer of the model. This approach is similar to that used in typical building energy simulation programs if such a model exists.

The figure shows the different elements of the model with floor covering, concrete layer, insulation and optional ground volume.

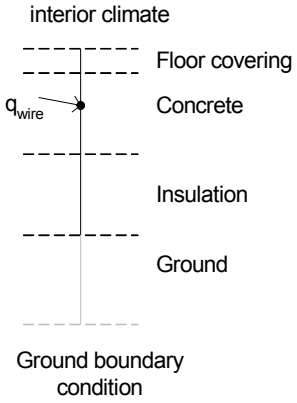

Figure A.6 1D floor heating model with electrical implementation of the pipe

Two-dimensional TASim model

The two-dimensional model of a thermo active deck which is used in TASim is shown in Figure A.7. The deck is made of concrete with a floor covering. The cavities of the hollow deck are modelled as air with an equivalent thermal resistance given based on tabulated values in the literature. The sides of the deck are adiabatic as it is assumed that each deck is place next to another deck.

The pipes are included as hydronic pipes.

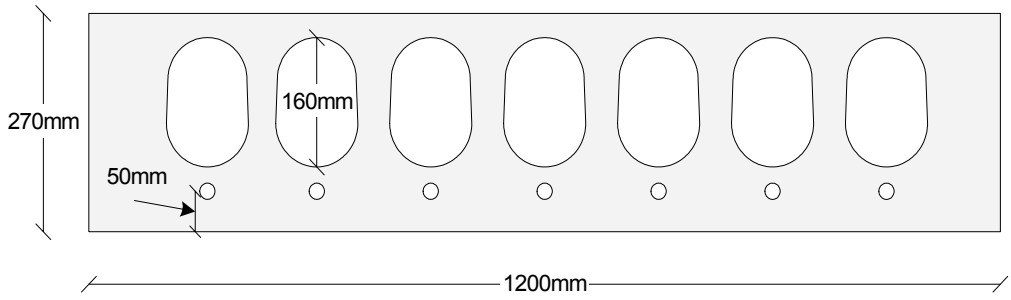

Figure A.7 Two-dimensional model of thermo active component

Two-dimensional section model in TASim

The two-dimensional section model of a thermo active component is shown in Figure A.8 and is a simplified version of the model shown in Figure A.7, as it is only the section around half a pipe which is included in the model. This simplification means that the surface temperature will be more influenced by the pipes than the "full" model where the sides are not as influenced.

The pipe is included as a hydronic pipe.

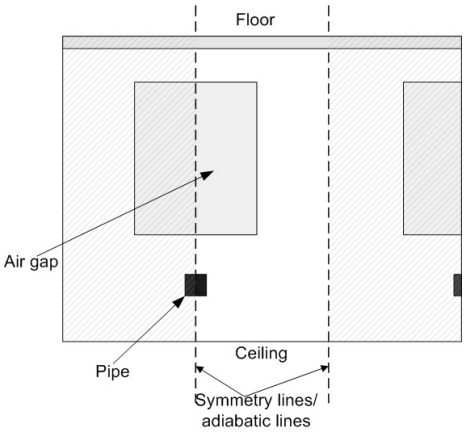

Figure A.8 Two-dimensional model of section of thermo active component

A.2 General heat transfer equation

The general formulation of the heat transfer equation is a three-dimensional partial differential equation. This is shown in Eq. (A.1).

$$\frac{\partial}{\partial x}\left(\lambda_x \cdot \frac{\partial T}{\partial x}\right)+\frac{\partial}{\partial y}\left(\lambda_y \cdot \frac{\partial T}{\partial y}\right)+\frac{\partial}{\partial z}\left(\lambda_z \cdot \frac{\partial T}{\partial z}\right)+\dot{q}=\rho c_p \frac{\partial T}{\partial t} \qquad \textbf{(A.1)}$$

The heat transfer equation is a differential diffusion equation, with three spatial terms, a heat flux term and a time dependent term. A thorough description of the equation and its implications can be found in the literature (Milss, 1992; Incropera and DeWitt, 1996).

A typical simplification, which is often used in building physics applications, is to assume that the thermal conductivity is constant, rather than temperature dependent. This is a good approximation for most building materials in the fairly narrow temperature interval in which buildings typically operate. Further, it is also assumed that the thermal conductivity is constant in all three spatial directions, which is also a good approximation for typical building materials, with wood as one exception.

This leads to the simpler equation shown in (A.2)

$$\lambda\left(\frac{\partial^2 T}{\partial x^2}+\lambda\frac{\partial^2 T}{\partial y^2}+\lambda\frac{\partial^2 T}{\partial z^2}\right)+\dot{q}=\rho c_p\frac{\partial T}{\partial t} \quad \textbf{(A.2)}$$

This form of the equation is used in the work presented here.

Different types of boundary conditions can be applied to the equations. As an example a combined convective and radiative boundary condition is shown in Eq. (A.3).

$$-\lambda\left.\frac{\partial T}{\partial x}\right|_{x=L}=\alpha_{conv}\cdot\left(T\big|_{x=L}-T_{air}\right)+\sigma F\left(T\big|_{x=L}^4-T_e^4\right)^4 \quad \textbf{(A.3)}$$

Finally, some type of initial condition must also be applied to be able to solve the heat transfer equation. Typically an isothermal starting condition is used, unless more detailed knowledge exist.

The heat transfer equation can be solved in simple cases with only on material and two boundary conditions. However, the equation very quickly becomes impossible to solve through analytical solutions. Therefore, in order to solve the heat transfer equation, some sort of numerical solution technique must be used.

A.3 Two-dimensional model

In order to model the floor, a discretization of the general equation for heat transfer must be created in order to accommodate for implementation of numerical solution techniques.

A.3.1 Discretization of heat transfer equation

By discretizing the equation a number of control volumes are created. The numbering of these are shown in the figure below around a central control volume called (*i,j*):

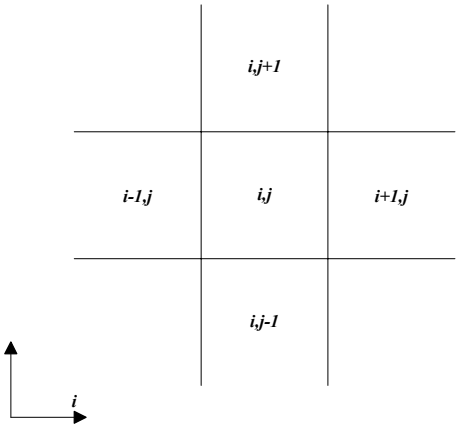

Figure A.9 Numbering of numerical mesh as seen from central nodal point (*i, j*)

The terms ‘nodal point’ refer to the point in the numerical mesh for which the temperature is calculated. The term ‘control volume’ refer to the area surrounding the nodal point – or rather the area in which the same conditions as in the nodal point is assumed. Notice, that in this context some nodal points will not have a control volume as they are only defined on a surface without a physical spatial definition.

In order to discretize the heat transfer equation, resistances (spatial and contact) and dimensions must be defined. This is shown in the figure below:

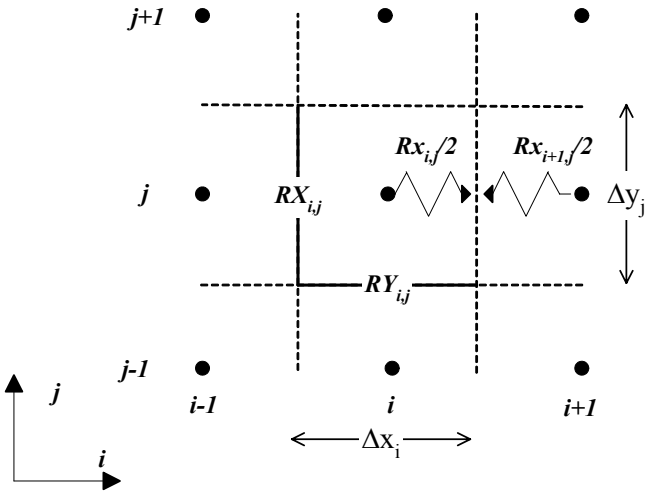

Figure A.10 Discretization of numerical mesh and inclusion of line resistances. Notice the distinction between Rx, which is the resistance between two nodal points and RX which is a contact resistance, which is typically placed between two layers.

This equation is the discretized for the x and y coordinates. One equation of this type must be created for each of the n times m control volumes in the floor model.

$$\frac{\left(\rho c_p\right)_{i,j}\Delta x_i \Delta y_j}{\Delta t}\left(T_{i,j}^{new}-T_{i,j}^{old}\right)= \frac{\left(T_{i-1,j}^{new}-T_{i,j}^{new}\right)\cdot\Delta y_j}{\frac{\Delta x_{i-1}}{2\lambda_{i-1,j}}+RX_{i,j}+\frac{\Delta x_i}{2\lambda_{i,j}}}+\frac{\left(T_{i+1,j}^{new}-T_{i,j}^{new}\right)\cdot\Delta y_j}{\frac{\Delta x_i}{2\lambda_{i,j}}+RX_{i+1,j}+\frac{\Delta x_{i+1}}{2\lambda_{i+1,j}}} + \frac{\left(T_{i,j-1}^{new}-T_{i,j}^{new}\right)\cdot\Delta x_i}{\frac{\Delta y_{j-1}}{2\lambda_{i,j-1}}+RY_{i,j}+\frac{\Delta y_j}{2\lambda_{i,j}}}+\frac{\left(T_{i,j+1}^{new}-T_{i,j}^{new}\right)\cdot\Delta x_i}{\frac{\Delta y_j}{2\lambda_{i,j}}+RY_{i,j+1}+\frac{\Delta y_{j+1}}{2\lambda_{i,j+1}}} \quad \textbf{(A.4)}$$

An interpretation of the equation is that the left side of the equation represents the heat storage and temperature change over time in the central nodal point, while the four parts on the right side represent the heat transfer between the central point and each of the four nodal points around the central point. At the same time, the equation is set up to be implicit, which means, that the temperature in one point cannot be solved without solving the equation for all other nodal points at the same time.

Five variables $Rx_{i,j}$, $Ry_{i,j}$ og $Hx_{i,j}$, $Hy_{i,j}$ og $H0_{i,j}$, are defined to rewrite the equation

$$Rx_{i,j}=\frac{\Delta x_i}{2\cdot\lambda_{i,j}} \qquad Ry_{i,j}=\frac{\Delta y_j}{2\cdot\lambda_{i,j}} \quad \textbf{(A.5)}$$

And

$$Hx_{i,j} = \frac{\Delta y_j}{Rx_{i-1,j} + RX_{i,j} + Rx_{i,j}}$$

$$Hy_{i,j} = \frac{\Delta x_i}{Ry_{i,j-1} + RX_{i,j} + Rx_{i,j}} \qquad \textbf{(A.6)}$$

$$H0_{i,j} = \frac{\left(\rho c_p\right)_{i,j} \cdot \Delta x_i \cdot \Delta y_j}{\Delta t}$$

By introducing the heat transfer functions, *H*, a simpler appearance of Equation (A.4) can be presented:

$$\begin{aligned} &H0_{i,j}\left(T_{i,j}^{new} - T_{i,j}^{old}\right) = \\ &Hx_{i,j}\left(T_{i-1,j}^{new} - T_{i,j}^{new}\right) + Hx_{i+1,j}\left(T_{i+1,j}^{new} - T_{i,j}^{new}\right) \\ &+ Hy_{i,j}\left(T_{i,j-1}^{new} - T_{i,j}^{new}\right) + Hy_{i,j+1}\left(T_{i,j+1}^{new} - T_{i,j}^{new}\right) \end{aligned} \qquad \textbf{(A.7)}$$

And by introducing another six variables or coefficients it is again rewritten to be solved for the new temperatures.

$$-A_{i,j} \cdot T_{i-1,j}^{new} - C_{i,j} \cdot T_{i+1,j}^{new} - D_{i,j} \cdot T_{i,j-1}^{new} - E_{i,j} \cdot T_{i,j+1}^{new} + B_{i,j} \cdot T_{i,j}^{new} = F_{i,j} \cdot T_{i,j}^{old} \qquad \textbf{(A.8)}$$

These six coefficients are therefore defined as:

$$\begin{aligned} A_{i,j} &= -Hx_{i,j} \\ B_{i,j} &= H0_{i,j} + Hx_{i,j} + Hx_{i+1,j} + Hy_{i,j} + Hy_{i,j+1} \\ C_{i,j} &= -Hx_{i+1,j} \\ D_{i,j} &= -Hy_{i,j} \\ E_{i,j} &= -Hy_{i,j+1} \\ F_{i,j} &= H0_{i,j} \cdot T_{i,j}^{old} \end{aligned} \qquad \textbf{(A.9)}$$

By assembling the n times m equations the following coefficient matrix shown in Eq. (A.10) can be created. Notice, that there is a shift in the indices for the matrices *A* through *F*, which are transformed to vectors, where the first element of the second row in the matrix is placed after the last element of the first row.

$$\begin{bmatrix} B_1 & C_1 & & & E_1 & & & & & & \\ A_2 & B_2 & C_2 & & & E_2 & & & & & \\ & \cdot & \cdot & \cdot & & & \cdot & & & & \\ \cdot & & \cdot & \cdot & \cdot & & & \cdot & & & \\ & D_l & & A_l & B_l & C_l & & & E_l & & \\ & & \cdot & & \cdot & \cdot & \cdot & & & \cdot & \\ & & & & \cdot & & \cdot & \cdot & \cdot & & \\ & & & & & D_{nm-1} & & A_{nm-1} & B_{nm-1} & C_{nm-1} & \\ & & & & & & D_{nm} & & A_{nm} & B_{nm} & \end{bmatrix} \begin{bmatrix} T_{1,1}^{new} \\ T_{2,1}^{new} \\ \cdot \\ \cdot \\ T_{i,j}^{new} \\ \cdot \\ \cdot \\ T_{n-1,m}^{new} \\ T_{n,m}^{new} \end{bmatrix} = \begin{bmatrix} F_1 \\ F_2 \\ \cdot \\ \cdot \\ F_l \\ \\ \\ F_{nm-1} \\ F_{nm} \end{bmatrix} \quad \textbf{(A.10)}$$

By solving the matrix system, the temperature distribution in the floor construction can be found. But before being able to solve the system, it is necessary to define boundary conditions. Also, the coefficient matrix is sparse with an almost tridiagonal structure, as it consists of five bands containing data with nonzero values. The reason for this structure where all non-zero elements are placed in diagonals is due to the fact that the nodal points can interacts with only four other nodal points, which by the nature of the equations, will be placed in a diagonal structure.

If the coefficients in the matrix system above are compared to the way the nodal points interact, the scheme shown in Figure A.11 can be set up. The way the scheme should be read is by looking at the central nodal point (*i,j*) to see through which equations the other nodal points are attached to the central point. The central nodal point (denoted by $B_{i,j}$) can only "see" the nodal points adjacent to the central point. For instance, the heat transfer to the nodal point placed "above" the central point (denoted *i,j*+1) will de defined through the $E_{i,j}$ coefficient. This can also be seen in Equation (A.8) and (A.9). Also, it should be noted that the coefficient $F_{i,j}$ contains information on the temperature in the previous time step and together with $B_{i,j}$ contains data for the heat storage in the control volume and therefore the rate at which the temperature is changing within the material.

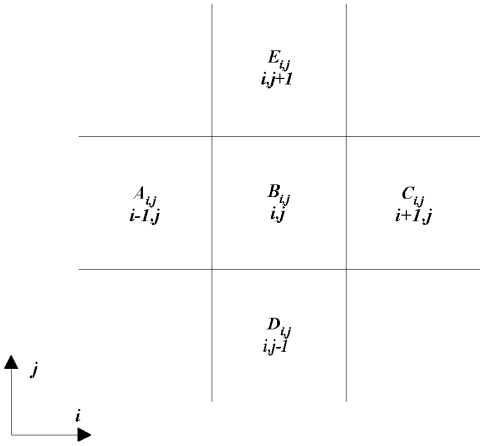

Figure A.11 Interaction scheme for a nodal point

An understanding of this interaction is important in setting up the coefficients for the nodal points placed on the boundaries of the construction.

A.3.2 Boundary conditions

For each of the types of boundary conditions used in the model, a drawing representing the numerical mesh at the surface and the equations used to include the boundary into the numerical model, by creating coefficients for equation (A.10).

For the floor surface

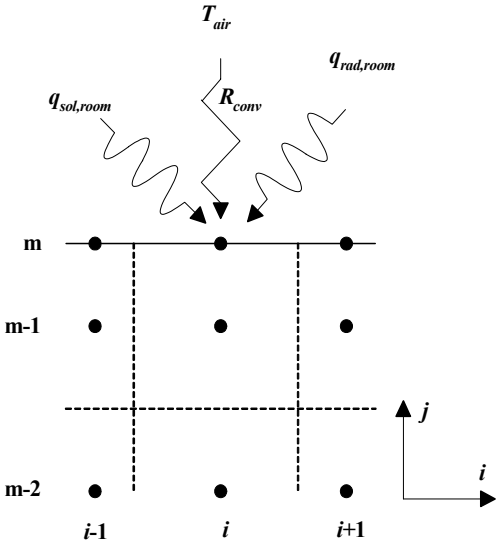

Figure A.12 Floor surface

For a node point (i,m) on the surface the following equations apply:

$$\frac{\left(T_{room} - T_{i,m}\right)\cdot \Delta x_i}{R_{conv}} + \left(q_{sol,room} + q_{rad,room}\right)\cdot \Delta x_i = \frac{\left(T_{i,m} - T_{i,m-1}\right)\cdot \Delta x_i}{\frac{\Delta y_{m-1}}{2\lambda_{i,m-1}}} \qquad \textbf{(A.11)}$$

$$\Delta y_m = 0$$

This can be translated into the following coefficients, which are applied to the matrix system in equation (A.10).

Notice, that while the short wave solar gain on the surface is independent of temperature, this is not the case for the long wave internal thermal radiation. This is however calculated in a separate model based on the actual floor surface temperatures and therefore the internal radiation is treated as an input which is independent of temperature.

$$A_{i,m} = C_{i,m} = E_{i,m} = 0$$
$$B_{i,m} = 1$$
$$D_{i,m} = -\frac{\frac{2\lambda_{i,m-1}}{\Delta y_{m-1}}}{\frac{1}{R_{conv}} + \frac{2\lambda_{i,m-1}}{\Delta y_{m-1}}} \qquad \textbf{(A.12)}$$
$$F_{i,1} = \frac{\frac{T_{air}}{R_{conv}} + q_{sol,room} + q_{rad,room}}{\frac{1}{R_{conv}} + \frac{2\lambda_{i,m-1}}{\Delta y_{m-1}}}$$

For the side of the outer wall

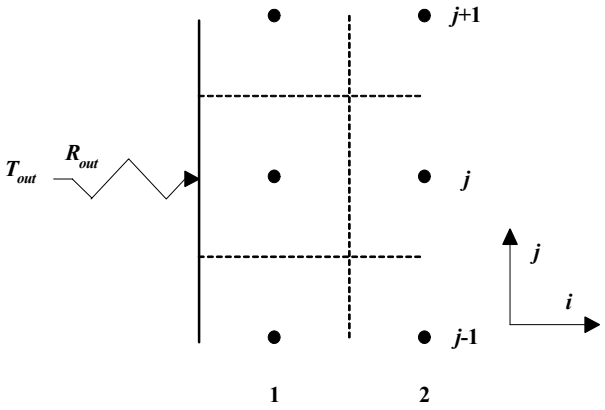

Figure A.13 Side of outer wall

The boundary conditions towards the outside conditions are different from the other boundary conditions used here (except for the adiabatic ones) in that the surface temperature is not calculated. This is due to the way the numerical mesh is created. In stead, an approach is used to setting up an equation for the nodal point within the construction.

Keeping Figure A.11 in mind, it can be seen, that the only two coefficients in the matrix system needs to be changed; namely the A and B coefficient. And also the F coefficient must be changed.

$$A_{1,j} = 0$$
$$B_{1,j} = H0_{1,j} + Hx_{2,j} + Hy_{2,j} + Hy_{2,j+1} + \frac{\Delta y_j}{R_{out} + \frac{\Delta x_1}{2\lambda_{1,j}}} \qquad \textbf{(A.13)}$$
$$F_{1,j} = H0_{1,j} \cdot T_{1,j}^{old} + \frac{\Delta y_j}{R_{out} + \frac{\Delta x_1}{2\lambda_{1,j}}} \cdot T_{out}$$

For the ground surface

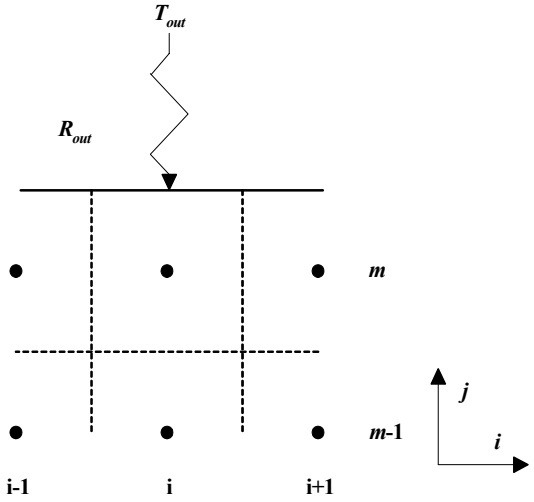

Figure A.14 Ground surface boundary condition

The same type of equations as for the ground side of the outer wall can be used for the ground surface.

$$B_{i,m} = H0_{i,m} + Hx_{i,m} + Hx_{i+1,m} + Hy_{i,m} + \frac{\Delta x_i}{R_{out} + \frac{\Delta y_m}{2\lambda_{i,m}}}$$

$$E_{i,m} = 0 \qquad \textbf{(A.14)}$$

$$F_{i,m} = H0_{i,m} \cdot T_{i,m}^{old} + \frac{\Delta x_i}{R_{out} + \frac{\Delta y_m}{2\lambda_{i,m}}} \cdot T_{out}$$

For the sides and bottom

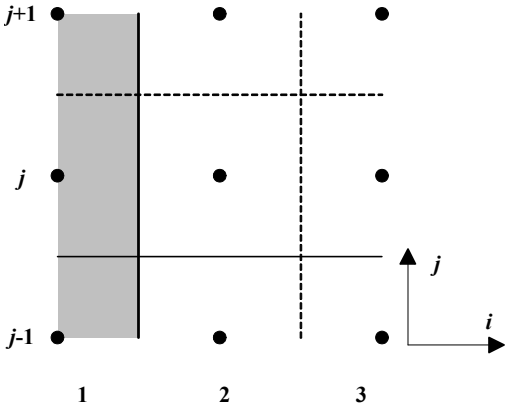

Figure A.15 Adiabatic boundary condition

The following equation can be stated for the adiabatic node point (1,*j*)

$$T_{1,j} = T_{2,j}$$
$$\Delta x_1 = \Delta x_2 \qquad \textbf{(A.15)}$$

This is again translated into a set of coefficients.

$$\begin{aligned} A_{1,j} &= D_{1,j} = E_{1,j} = F_{1,j} = 0 \\ B_{1,j} &= 1 \\ C_{1,j} &= -1 \end{aligned} \qquad \textbf{(A.16)}$$

The same approach can be used for the right side and bottom adiabatic. Only here it is the coefficient called $A_{n,j}$ and $E_{i,1}$ which should be assigned the value –1 in stead of $C_{1,j}$

Corners

There is no need to pay attention to the corners in the model, as they will be included in the other boundary conditions. However, the position of the nodal points in the corners is shown in Figure A.16, to give an idea about this particular detail of the model.

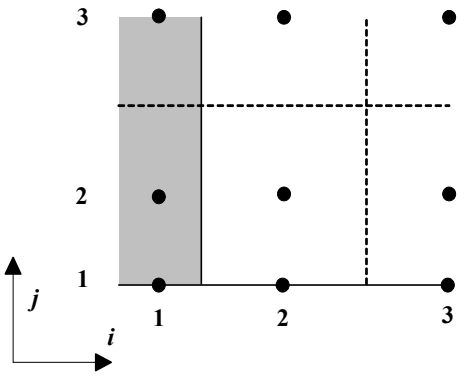

Figure A.16 Corner in two-dimensional model

A.3.3 Pipe implementation

For the pipe, the following figure applies for the equations shown for the pipe and around the pipe.

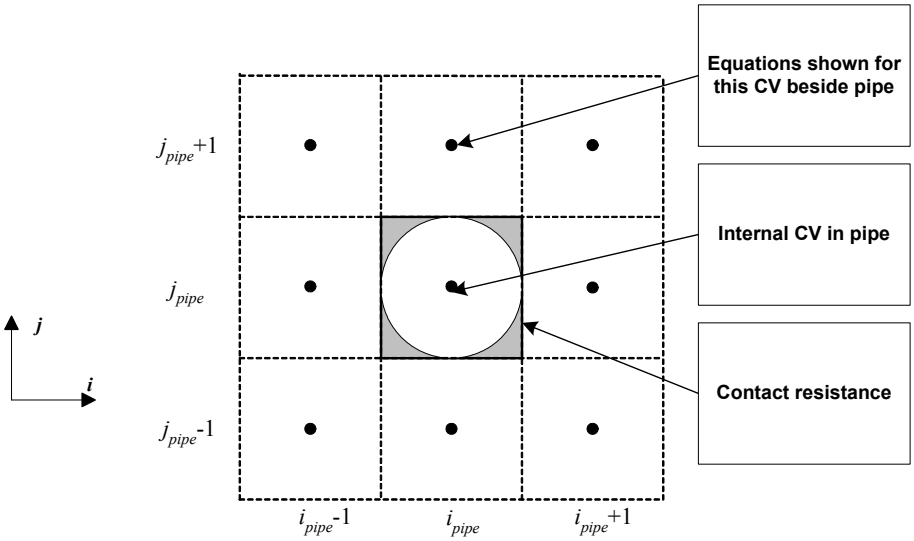

Figure A.17 Control volume in and around pipe

In the pipe, the following equation is applicable when the flow is turned on in the floor heating system.

$$T_{i,j} = T_{fluid} \tag{A.17}$$

Resulting in the following coefficients for the pipe

$$\begin{aligned} A_{i,j} &= C_{i,j} = D_{i,j} = E_{i,j} = 0 \\ B_{i,j} &= 1 \\ F_{i,j} &= T_{fluid} \end{aligned} \tag{A.18}$$

These coefficients are valid when the floor heating system is turned on. When this is not the case, the coefficients are calculated as described in section A.3.1.

Around the pipe the following equation is valid, for a node point placed immediately above the pipe:

$$\begin{aligned} &\frac{\left(\rho c_p\right)_{i,j}\Delta x_i \Delta y_j}{\Delta t}\left(T_{i,j}^{new} - T_{i,j}^{old}\right) = \\ &\frac{\left(T_{i-1,j}^{new} - T_{i,j}^{new}\right)\cdot \Delta y_j}{\frac{\Delta x_{i-1}}{2\lambda_{i-1,j}} + RX_{i,j} + \frac{\Delta x_i}{2\lambda_{i,j}}} + \frac{\left(T_{i+1,j}^{new} - T_{i,j}^{new}\right)\cdot \Delta y_j}{\frac{\Delta x_i}{2\lambda_{i,j}} + RX_{i+1,j} + \frac{\Delta x_{i+1}}{2\lambda_{i+1,j}}} \\ &+ \frac{\left(T_{i,j-1}^{new} - T_{i,j}^{new}\right)\cdot \Delta x_i}{RY_{i,j} + \frac{\Delta y_j}{2\lambda_{i,j}}} + \frac{\left(T_{i,j+1}^{new} - T_{i,j}^{new}\right)\cdot \Delta x_i}{\frac{\Delta y_j}{2\lambda_{i,j}} + RY_{i,j+1} + \frac{\Delta y_{j+1}}{2\lambda_{i,j+1}}} \end{aligned} \tag{A.19}$$

By comparison to Equation (A.4), it can be seen that the only difference is in the third part on the right side of the equation that is influenced by the pipe. That is, the heat transfer functions $Hx_{i,j}$, $Hx_{i+1,j}$ $Hy_{i,j+1}$ and $HO_{i,j}$ are as found above. Therefore the coefficients $A_{i,j}$, $C_{i,j}$, $E_{i,j}$ and $F_{i,j}$ are the same while $B_{i,j}$ and $D_{i,j}$ must be altered to:

$$\begin{aligned} D_{i,j} &= -\frac{\Delta x_i}{RY_{i,j} + \frac{\Delta y_j}{2\lambda_{i,j}}} \\ B_{i,j} &= H0_{i,j} + \frac{\Delta y_j}{RY_{i,j} + \frac{\Delta x_i}{2\lambda_{i,j}}} + Hx_{i,j} + Hx_{i+1,j} + Hy_{i,j+1} \end{aligned} \tag{A.20}$$

A.3.4 Pipe implementation

The pipe temperature is calculated from the assumption that the heat flow from the pipe to the surroundings is equal to the heat added to the pipe by the flow. That is the following two equations must be equal to each other

$$q = \dot{m} \cdot c_p \cdot \Delta T = \dot{m} \cdot c_p \cdot \left(T_{supply} - T_{return}\right) \tag{A.21}$$

$$q = \frac{T_{fluid} - T_{bp}}{R_{bp}}$$

In the first of the equations, the return temperature is not known. This value is not required by the program, therefore it is eliminated since $\Delta T = T_{supply} - T_{return}$. The fluid temperature is defined as the average fluid temperature, T_{fluid}:

$$T_{fluid} \equiv T_{supply} - \frac{\Delta T}{2} \quad \textbf{(A.22)}$$

Therefore:

$$q = \dot{m} \cdot c_p \cdot \Delta T = \dot{m} \cdot c_p \cdot 2 \cdot \left(T_{supply} - T_{return}\right) \quad \textbf{(A.23)}$$

In the second of the equations in Eq. (A.21), a correction must be made to get the heat flow in W, where it in the equation is given in W/m² pipe surface. The correction is performed by multiplying by the pipe length pr. area and pipe perimeter.

$$q = \frac{T_{fluid} - T_{bp}}{R_{bp}} \cdot \frac{A_{floor}}{w_{center}} \cdot P_{pipe} \quad \textbf{(A.24)}$$

Setting the two expressions equal, the following expression is found for the pipe temperature:

$$T_{fluid} = \frac{\dot{m} \cdot c_p \cdot T_{supply} + 2 \cdot d_{eq} \dfrac{A_{floor}}{w_{center}} \cdot \dfrac{1}{R_{bp}} \cdot T_{bp}}{\dot{m} \cdot c_p + 2 \cdot d_{eq} \dfrac{A_{floor}}{w_{center}} \cdot \dfrac{1}{R_{bp}}} \quad \textbf{(A.25)}$$

Here it is also assumed that:

$$P_{pipe} = 4 \cdot d_{eq} \quad \textbf{(A.26)}$$

Finally, notice that the same fluid temperature in the pipe is assumed in all the pipes in the section. An alternative approach would be to have a cooling from one pipe to the next. This approach would however require far more details on the layout of the pipe and the flow direction, which in any case is most likely unknown until the detailed planning of the building. Consequently, the same pipe temperature is used in all pipes in the model.

The heat flow from the pipe to the concrete is found from the following equation:

$$Q_{pipe,up} = \sum_{pipesurface} \frac{1}{R_{pipe-concrete}} \cdot \Delta l_{pipe} \left(T_{fluid} - T_{concrete}\right) \quad \textbf{(A.27)}$$

That is the sum of the flow through the four pipe surfaces in the quadratic mesh definition, found by the reciprocal value of the resistance in each of the four directions between the pipe nodal point and the corresponding concrete nodal point, multiplied by the side length of the nodal point and multiplied by the temperature difference between the pipe nodal point and the concrete.

A.4 Two-dimensional section models

The two-dimensional section models are shown in Figure 5.26.

A.4.1 Discretization

The same type of discretization as above has been used, as the model is also two-dimensional.

A.4.2 Boundary conditions

The same type of boundary conditions can be used for the tow-dimensional section models for the floor surface and sides, as these are adiabatic. Only the lower surface towards the ground needs to be described

Lower surface towards ground

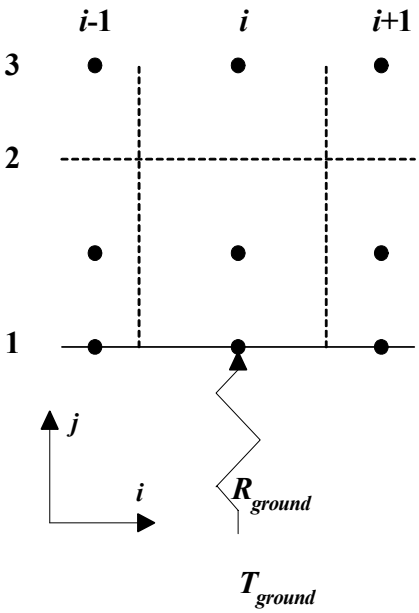

Figure A.18 Bottom of model towards ground in two-dimensional section model

The following equation can be stated for a node point (i,1).

$$\frac{\left(T_g - T_{i,1}\right)\cdot \Delta x_i}{R_g} = \frac{\left(T_{i,1} - T_{i,2}\right)\cdot \Delta x_i}{\frac{\Delta y_2}{2\lambda_{i,2}}} \qquad \textbf{(A.28)}$$

$$\Delta y_1 = 0$$

This translates into the following coefficients

$$A_{i,1} = C_{i,1} = D_{i,1} = 0$$
$$B_{i,1} = 1$$
$$E_{i,1} = -\frac{\frac{2\lambda_{i,2}}{\Delta y_2}}{\frac{1}{R_g} + \frac{2\lambda_{i,2}}{\Delta y_2}} \quad \textbf{(A.29)}$$
$$F_{i,1} = \frac{\frac{T_g}{R_g}}{\frac{1}{R_g} + \frac{2\lambda_{i,2}}{\Delta y_2}}$$

A.4.3 Pipe implementation

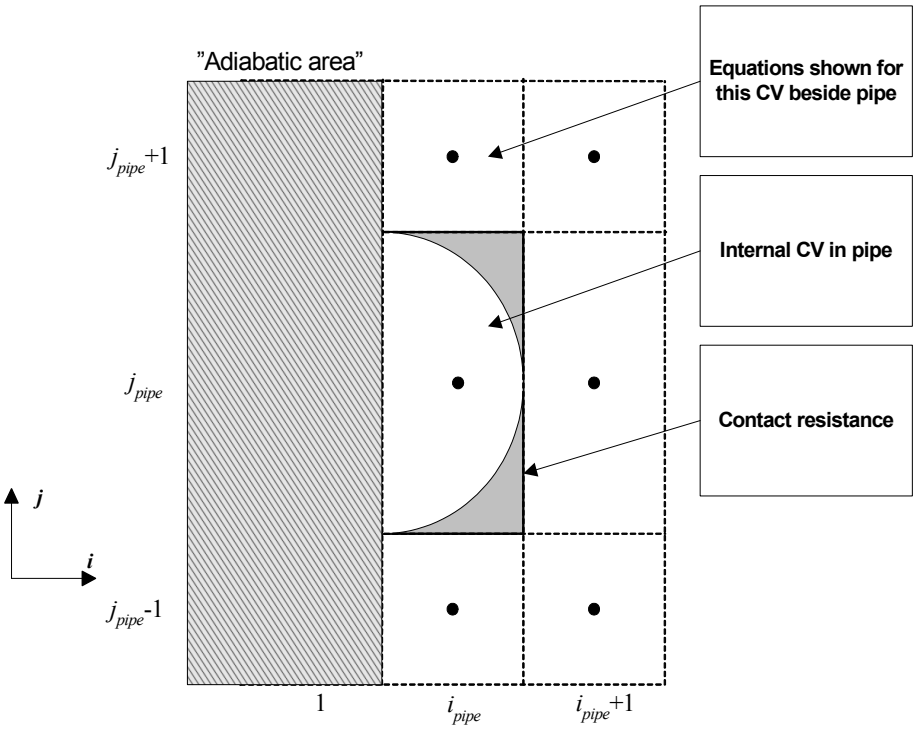

Figure A.19 Control volumes in and around pipe in two-dimensional section model

In the pipe, the following equation is applicable when the flow is turned on in the floor heating system.

$$T_{i,j} = T_{fluid} \quad \textbf{(A.30)}$$

Resulting in the following coefficients for the pipe

$$\begin{aligned} A_{i,j} &= C_{i,j} = D_{i,j} = E_{i,j} = 0 \\ B_{i,j} &= 1 \\ F_{i,j} &= T_{fluid} \end{aligned} \tag{A.31}$$

These coefficients are valid when the floor heating system is turned on. When this is not the case, the coefficients are calculated as described in section A.4.1.

Around the pipe the following equation is valid, for a node point placed immediately above the pipe:

$$\begin{aligned} &\frac{\left(\rho c_p\right)_{i,j}\Delta x_i \Delta y_j}{\Delta t}\left(T_{i,j}^{new} - T_{i,j}^{old}\right) = \\ &\frac{\left(T_{i-1,j}^{new} - T_{i,j}^{new}\right)\cdot \Delta y_j}{\frac{\Delta x_{i-1}}{2\lambda_{i-1,j}} + RX_{i,j} + \frac{\Delta x_i}{2\lambda_{i,j}}} + \frac{\left(T_{i+1,j}^{new} - T_{i,j}^{new}\right)\cdot \Delta y_j}{\frac{\Delta x_i}{2\lambda_{i,j}} + RX_{i+1,j} + \frac{\Delta x_{i+1}}{2\lambda_{i+1,j}}} \\ &+ \frac{\left(T_{i,j-1}^{new} - T_{i,j}^{new}\right)\cdot \Delta x_i}{RY_{i,j} + \frac{\Delta y_j}{2\lambda_{i,j}}} + \frac{\left(T_{i,j+1}^{new} - T_{i,j}^{new}\right)\cdot \Delta x_i}{\frac{\Delta y_j}{2\lambda_{i,j}} + RY_{i,j+1} + \frac{\Delta y_{j+1}}{2\lambda_{i,j+1}}} \end{aligned} \tag{A.32}$$

By comparison to Equation (A.4), it can be seen that the only difference is in the third part on the right side of the equation that is influenced by the pipe. That is, the heat transfer functions $Hx_{i,j}$, $Hx_{i+1,j}$ $Hy_{i,j+1}$ and $HO_{i,j}$ are as found above. Therefore the coefficients $A_{i,j}$, $C_{i,j}$, $E_{i,j}$ and $F_{i,j}$ are the same while $B_{i,j}$ and $D_{i,j}$ must be altered to:

$$\begin{aligned} D_{i,j} &= -\frac{\Delta x_i}{RY_{i,j} + \frac{\Delta y_j}{2\lambda_{i,j}}} \\ B_{i,j} &= H0_{i,j} + \frac{\Delta y_j}{RY_{i,j} + \frac{\Delta x_i}{2\lambda_{i,j}}} + Hx_{i,j} + Hx_{i+1,j} + Hy_{i,j+1} \end{aligned} \tag{A.33}$$

Fluid temperature in pipe

The same procedure as in section A.3.4 is used.

A.5 One-dimensional models

The one-dimensional discretization is essentially a simplification of the two-dimensional case. However, there are a few exceptions to this. Therefore the discretization and pipe implementation are described in this section, while the boundary conditions are skipped, however, with very few comments for the discretization.

A.5.1 Discretization

The discretization of the heat transfer equation is shown in Eq. (A.34).

$$\frac{(\rho c_p)_i \Delta x_i}{\Delta t}\left(T_i^{new} - T_i^{old}\right) = \frac{T_{i-1}^{new} - T_i^{new}}{\frac{\Delta x_{i-1}}{2\lambda_{i-1}} + RX_i + \frac{\Delta x_i}{2\lambda_i}} + \frac{T_{i+1}^{new} - T_i^{new}}{\frac{\Delta x_i}{2\lambda_i} + RX_{i+1} + \frac{\Delta x_{i+1}}{2\lambda_{i+1}}} \quad \textbf{(A.34)}$$

In case there are only two adjacent nodal points, which means that a discretization only has to include three nodal points in the equation system; namely the central nodal point and the two points to each side.

Again the resistance can be defined as

$$R_i = \frac{\Delta x_i}{2\lambda_i} \quad \textbf{(A.35)}$$

and the heat admission term:

$$H_i = \frac{1}{R_{i-1} + RX_i + R_i} \quad \textbf{(A.36)}$$

Here RX_i is the linear thermal resistance between the i'th-1 and the i'th element.

$$H0_i = \frac{(\rho c_p)_i \Delta x_i}{\Delta t} \quad \textbf{(A.37)}$$

Rearranging the discretization equation, the following equation for the i'th nodal point is found

$$A_i \cdot T_{i-1}^{new} + B_i \cdot T_i^{new} + C_i \cdot T_{i+1}^{new} = D_i \quad \textbf{(A.38)}$$

This means, that A_i, B_i, C_i and D_i are defined by:

$$\begin{aligned} A_i &= -H_i \\ B_i &= H0_i + H_i + H_{i+1} \\ C_i &= -H_{i+1} \\ D_i &= H0_i \cdot T_i^{old} \end{aligned} \quad \textbf{(A.39)}$$

Or for all nodal points, this can be written in the following coupled system of equations.

$$\begin{bmatrix} B_1 & C_1 & & & & \\ \cdot & \cdot & \cdot & & & \\ & A_i & B_i & C_i & & \\ & & \cdot & \cdot & \cdot & \\ & & & A_n & B_n \end{bmatrix} \begin{bmatrix} T_1^{new} \\ \cdot \\ T_i^{new} \\ \cdot \\ T_n^{new} \end{bmatrix} = \begin{bmatrix} D_1 \\ \cdot \\ D_i \\ \cdot \\ D_n \end{bmatrix} \quad \textbf{(A.40)}$$

Notice, that this equation system has the same structure as in the two-dimensional situation with bands of non-zero elements from upper left corner to lower right corner. In this case the structure is tri-diagonal and therefore simpler to solve than the two-dimensional case.

A.5.2 Boundary conditions

The boundary conditions are not described in the one-dimensional case, as these are only simplifications of the two-dimensional case. This is not described further here.

A.5.3 Pipe implementation

The pipe implementation is different for the one-dimensional than the two-dimensional case. Where the resistance from the pipe to the concrete in the two-dimensional model has been built into the construction through the geometry, the one-dimensional model must rely on a thermal resistance between the pipe and the concrete.

Electrical

The electrical inclusion of the floor heating pipe is shown in Figure A.20.

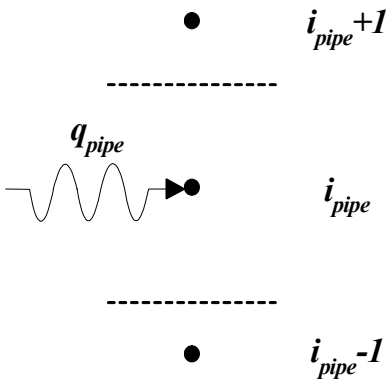

Figure A.20 Control volumes used for implementation of pipe in one-dimensional model using electrical inclusion of pipe

The only difference in the model including floor heating and the standard one-dimensional discretization is the extra term for the supplied heat flux to the nodal point in which the floor heating is applied. This means than only the *D* coefficient needs to be changed in order to include floor heating, which is shown in Eq. (A.41)

$$D_i = H0_i \cdot T_i^{old} + q_{pipe} \quad \textbf{(A.41)}$$

As it can be seen, this type of inclusion does not need (and cannot calculate) the pipe temperature.

Pipe

The pipe inclusion in the one-dimensional simulation model requires an extra nodal point to be inserted into the equation system in Eq. (A.40) to include the effect of the pipe. Figure A.21 shows the extra nodal point, which is introduced in the simulation model. The pipe is included in such a way that it only sees one nodal point in the one-dimensional model. Therefore, the extra nodal point requires that the equation system be expanded by an extra set of equations.

The pipe resistance can be found by different means, typically by an optimization if more detailed data exist, which can be used to calibrate the model. In this work a "realistic" value has been used, which gives essentially the same heat flow from the pipe to the room as the one-dimensional section model (1.5D model).

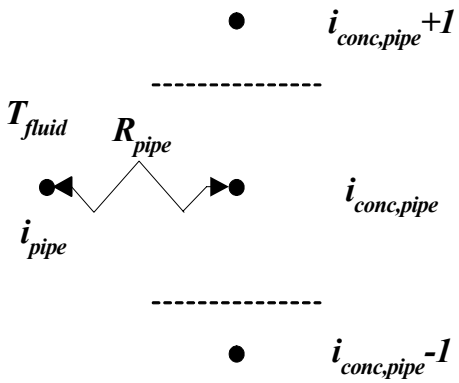

Figure A.21 Control volumes used for implementation of pipe in one-dimensional model using pipe inclusion of the pipe

For the node in the concrete next to the pipe, the following equation has been used for the *B* coefficient – the others remain unchanged compared to Eq. (A.39):

$$B_{conc,pipe} = H0_{conc,pipe} + H_{conc,pipe} + H_{conc,pipe+1} + \frac{1}{R_{pipe}} \tag{A.42}$$

For the pipe node, the following equations have been used when the flow is turned on

$$\begin{aligned} A_{pipe} &= 0 \\ B_{pipe} &= 1 \\ C_{pipe} &= 0 \\ D_{pipe} &= T_{fluid} \end{aligned} \tag{A.43}$$

When it is turned off, the following equations are used

$$\begin{aligned} A_{pipe} &= 0 \\ B_{pipe} &= \frac{(\rho \cdot c_p)_{water}}{dt} A_{pipe} + \frac{1}{R_{pipe}} \\ C_{pipe} &= 0 \\ D_{pipe} &= \frac{(\rho \cdot c_p)_{water}}{dt} A_{pipe} \cdot T_{pipe} \end{aligned} \tag{A.44}$$

Eq. (A.45) shows the equation system when the pipe has been included as an extra equation at the bottom of the system.

$$\begin{bmatrix} B_1 & C_1 & & & & \\ . & . & . & & & \\ & A_i & B_i & C_i & & \\ & & . & . & . & \\ & & & A_n & B_n & \\ & & & & & B_{pipe} \end{bmatrix} \begin{bmatrix} T_1^{new} \\ . \\ T_i^{new} \\ . \\ T_n^{new} \\ T_{pipe}^{new} \end{bmatrix} = \begin{bmatrix} D_1 \\ . \\ D_i \\ . \\ D_n \\ D_{pipe} \end{bmatrix} \quad \textbf{(A.45)}$$

Notice that the heat flow between the pipe and the concrete nodal points are not included by terms in the equation systems away from the tri-diagonal structure, as is the case for the two-dimensional implementation, as is the case in the two-dimensional implementation. In stead, this information is included in the B-coefficients for B_{pipe} and $B_{conc,pipe}$.

A.6 RC thermal network model

The thermal network model is a very simplified model compared to the finite control volume models above. The main difference is that the thermal resistances and capacities are lumped in just a few nodal points. This is of course to save simulation time.

The method is widely used in a number of simulation commercial simulation programs as for instance ESP-r and EnergyPlus.

In this context, the main differences between the RC thermal network and the one-dimensional inclusion of the pipe are;

- Fewer nodal points in the RC-model, where the heat capacities and resistances have been lumped in a few central nodal points.
- Where the one-dimensional model assumes identical conditions over the entire surface which is modelled, the RC-model can through the definition of the thermal capacities include a section of the floor, which will therefore – in a sense – become multidimensional.

A.6.1 General thermal network model

The thermal network model used in this work is shown in Figure A.22. Three nodal points are used for the internal conditions in the floor construction and two for the upper and lower surfaces. The internal nodal points have a thermal capacity while it is set to zero for the surface nodal points. This means that effectively there are only three nodal points, as the surface points are effectively just heat balances, which can be calculated by the actual surrounding temperatures.

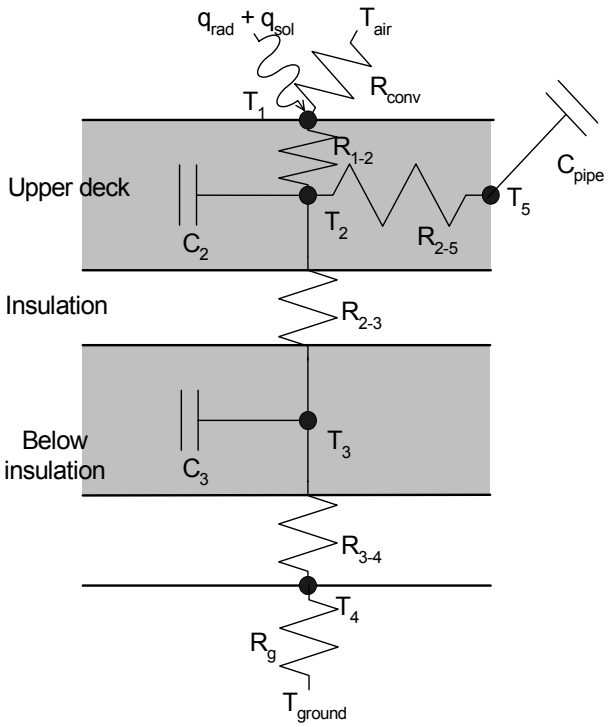

Figure A.22 RC-Thermal network model

Governing equations for each of the five nodes

$$1:\ 0 = \frac{1}{R_{conv}} \cdot \left(T_{air} - T_1\right) + \frac{1}{R_{1-2}} \cdot \left(T_2 - T_1\right) + q_s + q_r \qquad \textbf{(A.46)}$$

$$2:\ C_2 \frac{dT_2}{dt} = \frac{1}{R_{1-2}} \cdot \left(T_1 - T_2\right) + \frac{1}{R_{2-3}} \cdot \left(T_3 - T_2\right) + \frac{1}{R_{2-5}} \cdot \left(T_5 - T_2\right) \qquad \textbf{(A.47)}$$

$$3:\ C_3 \frac{dT_3}{dt} = \frac{1}{R_{2-3}} \cdot \left(T_2 - T_3\right) + \frac{1}{R_{3-4}} \cdot \left(T_4 - T_3\right) \qquad \textbf{(A.48)}$$

$$4:\ 0 = \frac{1}{R_{3-4}} \cdot \left(T_3 - T_4\right) + \frac{1}{R_g} \cdot \left(T_g - T_4\right) \qquad \textbf{(A.49)}$$

$$5:\ C_{pipe} \frac{dT_5}{dt} = \left(1 - \alpha\right) \cdot \left(\frac{1}{R_{2-5}} \cdot \left(T_2 - T_5\right) \right) \qquad \textbf{(A.50)}$$

For nodal point 5, the factor α is introduced to accommodate for the flow being on or off. In case the flow is on (α=1), the right hand side of the equation is equal to 0, which results in an infinite amount of solutions to the equation. However, the desired temperature is passed to the previous solution. The results will therefore not change.

Replacing $\frac{dT}{dt}$ with $\frac{\Delta T}{\Delta t} = \frac{\left(T^{new} - T^{old}\right)}{\Delta t}$ and solving the resulting system of equations gives the following matrix equation:

$$K \cdot T = F \tag{A.51}$$

Where,

$$K = \begin{bmatrix} \frac{1}{R_c}+\frac{1}{R_{1-2}} & -\frac{\frac{1}{R_{1-2}}}{\frac{1}{R_c}+\frac{1}{R_{1-2}}} & 0 & 0 & 0 \\ -\frac{1}{R_{1-2}} & \frac{C_2}{\Delta t}+\frac{1}{R_{1-2}}+\frac{1}{R_{2-3}}+\frac{1}{R_{2-5}} & -\frac{1}{R_{2-3}} & 0 & -\frac{1}{R_{2-5}} \\ 0 & -\frac{1}{R_{2-3}} & \frac{C_3}{\Delta t}+\frac{1}{R_{2-3}}+\frac{1}{R_{3-4}} & -\frac{1}{R_{3-4}} & 0 \\ 0 & 0 & -\frac{1}{R_{3-4}} & \frac{1}{R_g}+\frac{1}{R_{3-4}} & 0 \\ 0 & (1-\alpha)\cdot\left(-\frac{1}{R_{2-5}}\right) & 0 & 0 & (1-\alpha)\cdot\left(\frac{C_{pipe}}{\Delta t}+\frac{1}{R_{2-5}}\right)+\alpha \end{bmatrix} \tag{A.52}$$

$$T = \begin{bmatrix} T_1 \\ T_2 \\ T_3 \\ T_4 \\ T_5 \end{bmatrix} \tag{A.53}$$

and

$$F = \begin{bmatrix} \frac{1}{R_c}\cdot T_{air} + q_s + q_r \\ \frac{C_2}{\Delta t}\cdot T_2^{old} \\ \frac{C_3}{\Delta t}\cdot T_3^{old} \\ \frac{1}{R_g}\cdot T_g \\ (1-\alpha)\cdot\left(\frac{C_{pipe}}{\Delta t}\cdot T_5^{old}\right)+\alpha\cdot T_{pipe} \end{bmatrix} \tag{A.54}$$

If a linear thermal transmittance is included (by the term $P \cdot \psi$ in the equation 2 above), the coefficient matrix will now become:

$$K = \begin{bmatrix} \frac{1}{R_c}+\frac{1}{R_{1-2}} & -\frac{\frac{1}{R_{1-2}}}{\frac{1}{R_c}+\frac{1}{R_{1-2}}} & 0 & 0 & 0 \\ -\frac{1}{R_{1-2}} & \left(\frac{C_2}{\Delta t}+\frac{1}{R_{1-2}}+\frac{1}{R_{2-3}}+\frac{1}{R_{2-5}}+P\cdot\psi\right) & -\frac{1}{R_{2-3}} & 0 & -\frac{1}{R_{2-5}} \\ 0 & -\frac{1}{R_{2-3}} & \frac{C_3}{\Delta t}+\frac{1}{R_{2-3}}+\frac{1}{R_{3-4}} & -\frac{1}{R_{3-4}} & 0 \\ 0 & 0 & -\frac{1}{R_{3-4}} & \frac{1}{R_g}+\frac{1}{R_{3-4}} & 0 \\ 0 & (1-\alpha)\left(-\frac{1}{R_{2-5}}\right) & 0 & 0 & \left((1-\alpha)\left(\frac{C_{pipe}}{\Delta t}+\frac{1}{R_{2-5}}\right)+\alpha\right) \end{bmatrix} \quad \textbf{(A.55)}$$

and the F-vector (the Temperature vector is identical to Eq. (A.53))

$$F = \begin{bmatrix} \frac{1}{R_c}\cdot T_{air}+q_s+q_r \\ \frac{C_2}{\Delta t}\cdot T_2^{old}+P\cdot\psi\cdot T_{air} \\ \frac{C_3}{\Delta t}\cdot T_3^{old} \\ \frac{1}{R_g}\cdot T_g \\ (1-\alpha)\cdot\left(\frac{C_{pipe}}{\Delta t}\cdot T_5^{old}\right)+\alpha\cdot T_{pipe} \end{bmatrix} \quad \textbf{(A.56)}$$

The resistances $R_{1\text{-}2}$, $R_{2\text{-}3}$, $R_{3\text{-}4}$ and $R_{2\text{-}5}$ are found according to:

$R_{1\text{-}2}$, $R_{2\text{-}3}$, $R_{3\text{-}4}$ are taken as the 1D resistance between the layers. The value of $R_{2\text{-}5}$ is fitted to give the correct heat supply to the room at a given supply temperature.

The pipe temperature is found from the cooling in the pipe in the previous time step. This is valid when the flow is turned on in the floor heating system.

$$q_1 = \dot{m}c_p\Delta T = \dot{m}c_p\left(T_{supply}-T_{return}\right) \quad \textbf{(A.57)}$$

$$q_2 = \frac{1}{R_{2-5}}\cdot\left(T_5-T_2\right) \quad \textbf{(A.58)}$$

Also, the average pipe temperature is (assuming a linear temperature drop in the pipe)

$$T_{pipe} \equiv \frac{T_{supply}+T_{return}}{2} \quad \textbf{(A.59)}$$

Setting these equal and substituting for the return temperature yields:

$$T_{pipe} = T_{supply} - \frac{1}{2}\left(\frac{\frac{1}{R_{2-5}} \cdot \left(T_{pipe}^{old} - T_2 \right)}{\dot{m} c_p} \right) \quad \textbf{(A.60)}$$

Here T_2 is the temperature of the concrete deck. The term T_{pipe} is identical to T_5.

When the floor heating system is turned off, the following relation holds:

$$C_{pipe} \frac{T_{pipe} - T_{pipe}^{old}}{\Delta t} = \frac{1}{R_{2-5}} \left(T_2 - T_{pipe/5} \right) \quad \textbf{(A.61)}$$

Solving for T_p gives:

$$T_{pipe} = \frac{\frac{C_{pipe}}{\Delta t} T_{pipe}^{old} + \frac{1}{R_{2-5}} T_2}{\frac{C_{pipe}}{\Delta t} + \frac{1}{R_{2-5}}} \quad \textbf{(A.62)}$$

A.6.2 Parameter estimation

A problem concerning very simplified models such as a thermal network model is to estimate the parameters in the model compared to finite control volume models, which (generally) do not require parameter estimation.

Different simplified models and methods for parameter estimation have been presented in the literature. This has been discussed in Chapter 3. For the thermal network models, typical methods involve comparison to finite element methods and/or measurements using time domain or frequency domain analysis.

In this work two methods are used for the parameter estimation. The first is simply a geometrical estimation in which the physical dimensions form the parameters. In the second the estimation has been defined as an optimization problem. Both methods are described below.

Figure 5.52 shows the thermal network model with the parameters included.

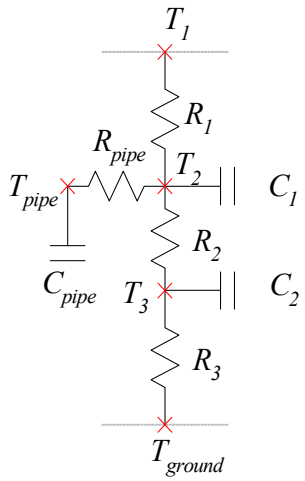

Figure A.23 RC thermal network showing thermal resistances, heat capacities and temperature nodes

Geometrical parameter estimation

The geometrical parameter estimation is based on physical dimensions of the model. The resistances are found by the simple one-dimensional sum of the thermal resistance of each material layer.

$$R = \sum_{mat} \frac{x_{mat}}{\lambda_{mat}} \tag{A.63}$$

The thermal capacities are found by the sum of the heat capacities of the materials which the lumped capacity covers.

$$C = \sum_{mat} \left(\rho \cdot c_p\right)_{mat} \cdot A_{mat} \tag{A.64}$$

In the estimation of the thermal capacities, the smallest possible section is used for the capacities. That is, the same as the two-dimensional section model, as it is shown in Figure 5.26.

Optimized parameter estimation

The data fitting problem is defined in this section.[9] The data fitting problem described here is an overestimated system of non-linear equations defined by a residual vector between a data set and a mathematical model intended for representing the data. The data set is calculated by applying a transient temperature profile in the floor heating pipe. A sinusoidal temperature profile with m time steps has been applied.

The purpose of the data fitting is to estimate the “central” parameters for the heat flow from the pipe to the room in a transient calculation compared to the 1.5D model, which in this case is considered to be the correct solution. Therefore, the data set which the measurements are compared to is given as:

[9] The optimization procedure used in this section has been developed in cooperation with Frank Pedersen, a fellow PhD student at BYG·DTU who specialises in optimization procedures applied to building energy problems. The results from this limited paramter estimation study will be used as basis for further work on parameter estimation.

$$q_{1.5D}, \in \Re^m \tag{A.65}$$

The model shown in Figure 5.52 is the RC thermal network which is intended to represent the data set given by Eq. (A.65).

The following model parameters, x, are fitted:

$$x = \left[R_{pipe}, R_1, C_1\right]^T \in \Re^n \tag{A.66}$$

Consequently the model for q_{RC} is:

$$q_{RC} : \Re^n \rightarrow \Re^m \tag{A.67}$$

Notice, that since $m>n$, the system is over determined.

The difference between the model and the data set can be defined by the residual vector, $r(x)$.

$$r(x) = q_{RC} - q_{1.5D} = \begin{bmatrix} q_{RC,1} - q_{1.5D,1} \\ q_{RC,2} - q_{1.5D,2} \\ . \\ . \\ . \\ q_{RC,m} - q_{1.5D,m} \end{bmatrix}, r : \Re^n \rightarrow R^m \tag{A.68}$$

The purpose is therefore to find a solution, x^*, such that

$$q_{RC,i}(x^*) \approx q_{1.5D,i}, i = 1,...,m \tag{A.69}$$

As a measure of the size of the residuals in Eq. (A.68), the l_2 vector norm is used, which is given by:

$$R(x) = \|r(x)\|_2 = \sqrt{\sum_{i=1}^{m} r_i(x)^2} \tag{A.70}$$

Other norms can also be used, i.e. the one-norm.

The data fitting problem can finally be defined as the following optimisation problem:

$$x^* = \arg\left\{\min_x R(x)\right\} \tag{A.71}$$

Eq. (A.71) can be solved by various numerical methods, whose description is beyond the scope of this thesis. Here the "Nelder and Mead's simplex method" (Nelder and Mead, 1965) has been used. This has been implemented in the optimization toolbox in Matlab as the 'fminsearch' method. The advantage of this method is that it is very robust and does not require the gradients to be known, which proved necessary in this case. The reason is most likely that the gradients of the model are very small.

A.7 Additional modelling elements

In this section the additional modelling elements used in FHSim and TASim are described.

A.7.1 Weather data

The Danish weather data year DRY (Design Reference Year) is used as input in all the simulations in this thesis. The average temperature during the year is 7.8 °C. All data are given as hourly values. Figure A.24 shows the monthly average outside temperature.

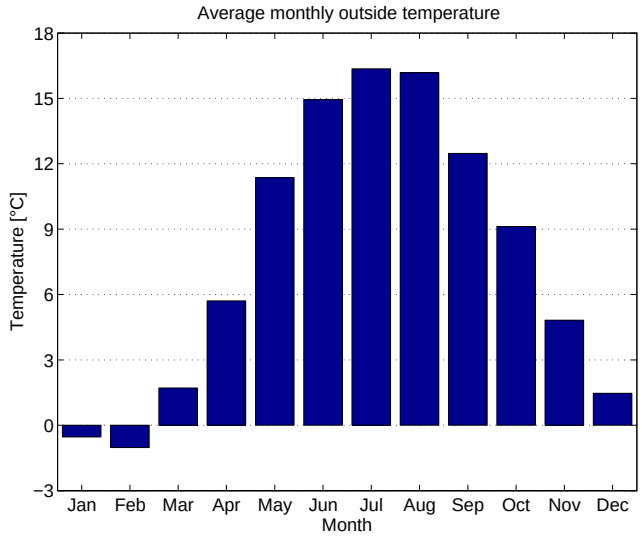

Figure A.24 Monthly average outside temperature in Danish Design Reference Year

The solar algorithm used is the Perez solar algorithm (Perez et al, 1990). In this algorithm the global, direct and diffuse radiation on tilted surfaces at any given direction can be calculated based on the data for global and diffuse radiation from measured data or weather data. Both parameters are available in the Danish Design Reference Year.

A.7.2 Windows

Two main parts are used in the window model: heat transfer between room and outside and solar transmission through the glazing.

The window model requires input of the U-value and area of frame and glazing, the linear thermal transmittance and length of the assembly, as well as data for the transmission and absorption coefficient for the incoming short wave solar radiation preferably, but not necessarily, depending on the angle of the incoming solar radiation. These data can be found in many specialised programs for almost any configuration of glazing unit and frame profile. In this work, data from WIS (http://windat.ucd.ie/wis/html/index.html) are used as input to the model.

U-value

The U-value of the window is given by Eq. (A.72). The equation takes the U-value of the glazing (center value) and frame weighed by their respective areas along with the influence from the linear thermal transmittance, ψ, of the assembly between frame and glazing.

$$U_{window} = \frac{A_{glazing} \cdot U_{glazing} + A_{frame} \cdot U_{frame} + l_{\psi} \cdot \psi}{A} \quad \textbf{(A.72)}$$

Notice, that the effect of corners is excluded from this equation. This is for two reasons: firstly the value is negative and generally small (Weitzmann et al, 2000b) and secondly because these data are fairly difficult to arrive at.

Figure A.25 shows the model of the glazing unit. A double-glazed unit is used. Four nodal points are used for the model, one centrally in each glass layer and one on each of the outer surfaces. A finite control volume is used for the modelling of the heat load.

On the surface nodes long wave radiation and convection make up the boundary conditions, while heat can be absorbed in each of the glass layers.

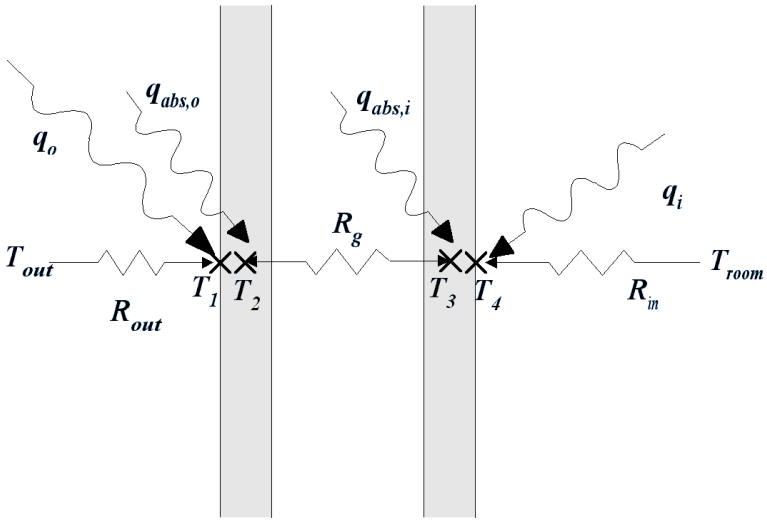

Figure A.25 Model of glazing unit in window model

The actual values of long wave radiation and convective thermal resistance are found based on the description given in sections below.

The thermal resistance between the two central nodal points are given in (A.73)

$$R_g = \frac{1}{U_{glazing}} - \left(R_i + R_o + \frac{1}{2} R_{pane1} + \frac{1}{2} R_{pane2} \right) \quad \textbf{(A.73)}$$

The frame model is not shown here. However, do notice that the part of the heat transfer from the linear thermal transmittance is included in the model of the frame as shown in (A.74) as an extra heat transfer term.

$$R_f = \frac{1}{U_{frame} + \frac{\psi \cdot l_\psi}{A_{frame}}} - \left(R_i + R_o \right) \quad \textbf{(A.74)}$$

Solar transmission

As written above in A.7.1, the solar radiation on the outside surfaces is modelled using the Perez solar algorithm. Figure A.26 shows a somewhat simplified presentation of the conditions of the solar radiation through the glazing unit.

For the calculation of the solar radiation, the simulation model needs data for the absorptance in each of the glass layers and the total transmittance.

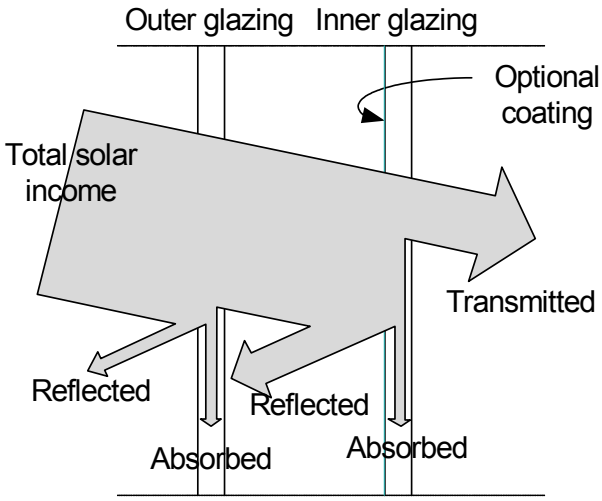

Figure A.26 Principal design of solar income to room

The solar transmission through the window is calculated from the solar radiation on the outside surface split into direct and diffuse radiation and the angle of the direct solar radiation. Eq. (A.75) shows the transmitted solar radiation from the surface to the room, split into direct, diffuse and reflected radiation. The transmittance depends on the angle of the incoming solar radiation. This is calculated by the solar algorithm, which of course also means that the data for the transmittance, *g*, must depend on the angle of the position of the sun.

$$q_{sol,trans} = g_{\beta} \cdot I_{direct} + g_{60} \cdot \left(I_{diffuse} + I_{reflected}\right) \quad \textbf{(A.75)}$$

Equivalent to the transmission, the absorption in each of the layers can be calculated in (A.76).

$$q_{sol,abs} = \alpha_{\beta} \cdot I_{direct} + \alpha_{60} \cdot \left(I_{diffuse} + I_{reflected}\right) \quad \textbf{(A.76)}$$

External radiation from surface to surroundings

Especially during clear nights, the sky temperature can drop considerably below the outside temperature. This will give a large heat loss from radiation from the external surfaces to the surroundings. This heat loss will be especially important for windows, where the small thermal mass means the glazing will cool down considerably, thereby giving a large heat loss from the room.

The radiation exchange between external surfaces and the surroundings is given by the relation shown in (A.77). Here the heat loss is split into two components; radiation to the ground and to the sky. By default the view factors are set to 0.5 for both ground and sky.

$$q_{rad,o} = \sigma\left(\varepsilon \cdot F_{sur,ground} \cdot \left(T_{sur}^4 - T_{ground}^4\right) + \varepsilon \cdot F_{sur,sky} \cdot \left(T_{sur}^4 - T_{sky}^4\right)\right) \quad \textbf{(A.77)}$$

The ground temperature is assumed to be equal to the air temperature, which is not correct. However, no data exist for the ground temperature, which is depending on such factors as the type of ground surface (soil, tiles, grass) and if it is covered by snow.

The surface emissivity for building materials is assumed to be equal to the absorptivity, as these are normally grey surfaces, which means that they will ensure a diffuse emission of radiation from the surface.

$$\alpha = \varepsilon \tag{A.78}$$

This assumption is generally used in the program.

A.7.3 Walls and ceiling

The walls and ceiling are modelled by finite control volume models, which have already been introduced above for the floor heating models. The models used here are one-dimensional.

A.7.4 Room model

The central part of the building simulation model used in both FHSim and TASim is the room model. A single node is used for the room air temperature, while radiation exchange is calculated for all surfaces. For a room with a heated floor, and probably also for a cooled ceiling, the temperature distribution is very uniform in the vertical direction. Therefore the simplification introduced by using a single air node model is acceptable.

The following "systems" are considered part of the room model:

- Ventilation
- Infiltration
- Venting

In addition to the systems, a few auxiliary components are used in the calculation procedure:

- Distribution of solar radiation
- Radiation between surfaces
- Convection from surfaces to room air
- Internal heat load
- Thermal comfort

Notice, that the radiation exchange between the surfaces is considered a part of the room model, which is strictly speaking not true, as the surfaces are not part of the room.

A general remark is made to the models of the models using an air change rate; namely the mechanical ventilation, infiltration and venting. The model uses constant values of the first two and for venting the required venting rate is calculated based on the thermal conditions. Far more advanced models exist for this – models that can fairly easily be implemented in this model in stead of the existing procedure. However, these models often require more information on the building geometry, air tightness and more factors and system layout. These data are not defined in the program and would complicate the process of data input beyond what is otherwise needed by the simulation model. These procedures have therefore been omitted in the model.

Mechanical ventilation

A simple balanced mechanical ventilation system is used, shown in Eq. (A.79)

$$q_{vent} = \left(\rho c_p\right)_{air} \cdot V_{room} \cdot n_{vent} \cdot \left(T_{inlet} - T_{room}\right) \tag{A.79}$$

The inlet temperature can be either the outdoor air temperature or it can be sent through a heat recovery unit. The heat recovery is based on the temperature efficiency, as shown in Eq. (A.80)

$$\eta = \frac{T_{inlet} - T_{out}}{T_{room} - T_{out}} \tag{A.80}$$

Typical values of the temperature efficiency are between 0.7 and 0.9 for modern heat recovery units. The inlet temperature can therefore be found from

$$T_{inlet} = T_{out} + \eta \cdot \left(T_{room} - T_{out}\right) \tag{A.81}$$

Notice, that if the efficiency is set to zero, the inlet temperature will be equal to the outside temperature.

Infiltration

Equivalently to the ventilation system, infiltration is included in Eq. (A.82). Again a simplified model is used, where a constant air change rate is used as input. However, it is well known that the rate depends on other factors – mainly wind pressure. This has not been included in the model, since this dependency in any case is unknown, as it depends on the air tightness of the building.

$$q_{inf} = \left(\rho c_p\right)_{air} \cdot V_{room} \cdot n_{vent} \cdot \left(T_{out} - T_{room}\right) \tag{A.82}$$

Notice the similarity between Eq. (A.79) and Eq. (A.82)

Venting

Venting is the opening of windows to cool the room air. Again a similar equation to the ventilation case can be used to quantify the heat exchange to the surroundings by venting.

$$q_{venting} = \left(\rho c_p\right)_{air} \cdot V_{room} \cdot n_{venting} \cdot \left(T_{out} - T_{room}\right) \tag{A.83}$$

Venting is assumed activated once the room air temperature rises above a given set point temperature – typically 25 °C or 26 °C. In this model, the venting air flow rate is changed to ensure that the room air temperature will end up at the set point temperature, where Eq. (A.84) contains a calculation of the needed air change rate to decrease the temperature in the room to the venting set point temperature, $T_{venting}$. At the same time a maximum air flow rate is used to ensure that this value cannot become unrealistically high.

$$n_{venting} = \min\left(\frac{q_{conv} + q_{\mathrm{int},conv} + q_{sun,conv}}{\left(\rho c_p\right)_{air} \cdot V_{room} \cdot \left(T_{out} - T_{venting}\right)}, n_{venting,\max} \right) \tag{A.84}$$

The use of venting requires that the outside air temperature is lower than the indoor temperature, to be able to cool the room. Therefore the room air temperature can rise above the temperature where the windows are opened. This is also the case, if the air change rate required to cool down the room air to the maximum allowed temperature is larger than the maximum value of the air change by venting.

Radiation

The internal radiation exchange between surfaces in the room is determined by the surface temperatures of the individual surfaces and the view factor between the surfaces. The description in this section is based on descriptions in Mills' book on heat transfer (Mills, 1992). The description requires a room with perpendicular surfaces in an enclosure where all surfaces can see each other.

The heat exchange is found by:

$$Q_{12} = \sigma F_{1,2}\left(\varepsilon_1 T_1^4 - \varepsilon_2 T_2^4\right), \quad 0 \le F \le 1 \tag{A.85}$$

Here, Q_{12} is the radiation exchange from surface 1 to 2, while $F_{1,2}$ is the view factore between the two surfaces. The view factor is determined by purely geometrical considerations, and expresses how much of the horizon of a given surface another surface occupies. If another surface is completely surrounding another surface the view factor from this surface to the surrounding surface is unity, while it is zero if they cannot see each other.

The view factor can be mathematically determined by the surface integral presented in (A.86), where the view factor is found by a semi sphere placed on the surface element, which will therefore include the entire horizon seen from the surface.

$$F_{1,2} = \frac{1}{A_1}\int_{A_1}\int_{A_2}\frac{\cos\theta_1 \cos\theta_2}{\pi r^2} dA_1 dA_2 \tag{A.86}$$

Here θ is the angle between zenith and directional angle from the surface towards to second surface.

For any surface, the sum of all view factors must equal 1, as shown below.

$$\sum_j F_{1,j} = 1 \tag{A.87}$$

The heat balance by radiation from surface number i in the room can be found from Eq. (A.88).

$$Q_i = A_i \cdot \left(G_i - J_i\right) \tag{A.88}$$

The heat transfer, Q_i, is the net radiation on the surface, as an imbalance simply means that energy can be exchanged with the material "behind" the surface. G_i is the incident radiation and J_i radiation to the surface.

The radiosity of the surface for an opaque surface is given by:

$$J_i = \sigma \varepsilon_i T_i^4 + \left(1 - \varepsilon_i\right) G_i \tag{A.89}$$

The total radiation to the surface, G_i, is given by.

$$A_i G_i = \sum_{j=1}^{N} A_j F_{j,i} J_j \tag{A.90}$$

Or since $F_{i,j} \cdot A_i = F_{j,i} \cdot A_j$

$$A_i G_i = A_i \sum_{j=1}^{N} F_{i,j} J_j \quad \textbf{(A.91)}$$

Subsitituting Eq. (A.91) in (A.89)

$$J_i = \sigma \varepsilon_i T_i^4 + (1-\varepsilon_i) \sum_{j=1}^{N} F_{i,j} J_j \quad \textbf{(A.92)}$$

And by rearranging to equation

$$\sigma \varepsilon_i T_i^4 = \sum_{j=1}^{N} \{\delta_{i,j} - (1-\varepsilon_i) F_{i,j}\} J_j \quad \textbf{(A.93)}$$

Here $\delta_{i,j} = 1$ for $i = j$ and $\delta_{i,j} = 0$ for $i \neq j$. Assuming that $F_{ii} = 0$, which means that a surface is not allowed to see itself, the follwowing is found from the surfaces in the enclosure.

$$\mathbf{T}_i = \sigma \varepsilon_i T_i^4, \quad \mathbf{F}_{i,j} = \delta_{i,j} - (1-\varepsilon_i) F_{i,j} \text{ og } \mathbf{J}_i = J_i \quad \textbf{(A.94)}$$

Or,

$$\mathbf{T} = \mathbf{FJ} \Rightarrow \mathbf{J} = \mathbf{F}^{-1}\mathbf{T} \quad \textbf{(A.95)}$$

Inserting the solution from J_i into Eq. (A.88) and (A.89) the net radiation to a surface can be found by:

$$Q_i = A_i \frac{\varepsilon_i}{1-\varepsilon_i} \left(J_i - \sigma T_i^4\right) \quad \textbf{(A.96)}$$

The practical calculation of view factors is not described here. However, this can be found in the literature.

Distribution of solar radiation

The distribution of solar radiation on the internal surfaces to the room is a fairly complex calculation, requiring the angle of the sun, geometry and position of the window – for each of the windows. Since each wall, floor and ceiling is modelled as one surface with the same conditions, an advanced model for the distribution on the individual surface will be too detailed. Therefore the model simply uses a uniform distribution of the total solar radiation which is transmitted through any of the windows. The total solar gains through the windows are summed as shown in Eq.(A.97).

$$q_{sol,room} = \sum_{windows} q_{sol,trans} \quad \textbf{(A.97)}$$

The total solar heat gain is split into two components by introducing a factor, ξ, to account for the fact that parts of the solar radiation will be emitted almost directly to the room as a convective contribution to the heat balance, when the radiation hits for instance furniture in the room. The convective part is shown in (A.98) and the radiative part in (A.99)

$$q_{sol,conv} = \xi \cdot q_{sol,room}, \quad 0 \le \xi \le 1 \tag{A.98}$$

$$q_{sol,radiation,sur,i} = (1-\xi) \cdot q_{sol,trans} \cdot \frac{A_i}{A_{tot} - A_{ceiling}}$$
$$q_{sol,radiation,ceiling} = 0 \tag{A.99}$$

It is assumed that the solar radiation is evenly distributed on all surfaces except for the ceiling surface, which will almost never be struck by direct solar radiation, which is consequently set to zero.

Convection

Numerous correlations for the heat transfer coefficient between surfaces and room air can be found in the literature, (Mills, 1992; Awbi, 1991 and more). This has been discussed in Chapter 3. In this section, only the actual correlations used are shown. All correlations in this thesis are based on (Schramek et al, no year). The reason for using these correlations is that they have different values for the horizontal heat transfer coefficients depending on the direction of the heat flow. Such direction dependent correlations are being implemented in for instance the proposal for the upcoming CEN standard for building integrated heating and cooling (Olesen et al, 2003) and the newest revision of the Danish standard for calculating the heat loss from buildings DS418 (DS, 2002).

Between (vertical) walls and room air, the following expression is used.

$$\alpha_{conv,wall} = 1{,}45 \cdot \left| T_{wall} - T_{room} \right|^{(0{,}32+0{,}14 \cdot h)} \tag{A.100}$$

Here, h, is the height of the wall in meters.

Between ceiling and room the following correlation is used:

$$\alpha_{conv,ceiling} = 0{,}5 \cdot \left| \Delta T \right|^{0{,}31} \text{ for } \Delta T \ge 0$$
$$\alpha_{conv,ceiling} = 2{,}0 \cdot \left| \Delta T \right|^{0{,}31} \text{ for } \Delta T < 0 \tag{A.101}$$
$$\text{hvor } \Delta T = T_{ceiling} - T_{room}$$

And for the floor surface:

$$\alpha_{conv} = 2{,}0 \cdot \left| \Delta T \right|^{0{,}31} \text{ for } \Delta T \ge 0$$
$$\alpha_{conv} = 0{,}5 \cdot \left| \Delta T \right|^{0{,}31} \text{ for } \Delta T < 0 \tag{A.102}$$
$$\text{hvor } \Delta T = T_{floor} - T_{room}$$

Internal heat load

An internal heat load, q_{int}, can be supplied to the room. Again a factor can be used to split the heat load in a convective and a radiative part

$$q_{int,conv} = \xi \cdot q_{int} \tag{A.103}$$

$$q_{int,rad} = (1-\xi)\cdot q_{int} \quad \textbf{(A.104)}$$

The distribution of the radiative part of the internal surfaces is evenly distributed on all internal surfaces.

Heat balance in room

The heat balance in the room is generally given by Eq. (A.105), with contributions from convection, ventilation, infiltration, venting, internal heat loads and convective solar contributions.

$$(\rho c_p)_{air}\frac{dT}{dt} = q_{conv} + q_{vent} + q_{inf} + q_{venting} + q_{int,conv} + q_{sol,conv} \quad \textbf{(A.105)}$$

Here, the convective contribution is given by:

$$q_{conv} = \sum_i \frac{1}{R_{si}}\cdot A_i \cdot (T_{sur} - T_{room}) \quad \textbf{(A.106)}$$

For simplicity, the storage capacity of the room air node is omitted. This is because the thermal mass of the air corresponds to only a few millimetres of the thickness of the walls, which means that the influence from this heat storage can be neglected in the models. Therefore steady-state conditions are assumed for the room air on the left side of Eq. (A.105)

$$q_{conv} + q_{int} + q_{vent} + q_{venting} + q_{inf,conv} + q_{sol,\mathrm{cov}} = 0 \quad \textbf{(A.107)}$$

Temperature in room

Three temperatures to classify the room are included in the model:

- Room air temperature
- Mean radiant temperature
- Operative temperature

Room air temperature

The room air temperature is calculated by inserting Eq. (A.106) into Eq. (A.107) and solving for T_{room}, shown in Eq. (A.108)

$$T_{room} = \frac{\sum_i \frac{A_{si}}{R_{si}}\cdot T_{sur,i} + (\rho c_p)_{air}\cdot V_{room}\cdot (n_{vent}\cdot T_{inlet} + n_{inf}\cdot T_{out}) + q_{sol} + q_{int}}{\sum_i \frac{A_{si}}{R_{si}} + (\rho c_p)_{air}\cdot V_{room}\cdot (n_{vent} + n_{inf})} \quad \textbf{(A.108)}$$

Along with the mean radiant temperature in the room, the room air temperature is used for the assessment of thermal comfort and for the controlling parameter for the floor heating system.

Mean radiant temperature

The mean radiant temperature is defined as the average radiant temperature which will give the same heat exchange by radiation to the surrounding surfaces in the room as the actual conditions give.

The mean radiant temperature for a person is based on the view factors from each of a persons five surfaces to each of the surrounding surfaces. The five surfaces are the four "sides" (front, back and sides) and top of head. The sixth surface (the feet) is omitted as they typically touch the ground surface and therefore must be treated as a local discomfort. The view factors are calculated based on the same procedure as for the view factors between the walls in the room. For each of the person's five surfaces the view factor to each of the surfaces are given as a vector in F_{person,sur_i}

The radiant temperature of surface *j* of a person is given by:

$$T_{rad,j}^4 = \sum_i \left(\left(T_{sur,i} + 273{,}15 \right)^4 \cdot F_{person,sur\_i} \right) \quad \textbf{(A.109)}$$

The mean radiant temperature for each of the five surfaces is the sum of the temperature of a given surface times the view factor to that surface.

The total mean radiant temperature can be calculating by weighing the radiant temperatures for each of the persons surfaces by the area of that surface.

$$T_{mr} = \left(\frac{T_{rad,1}^4 \cdot A_1 + T_{rad,2}^4 \cdot A_2 + \ldots + T_{rad,5}^4 \cdot A_5}{A_1 + \ldots + A_5} \right)^{\frac{1}{4}} - 273{,}15 \quad \textbf{(A.110)}$$

Operative temperature

The operative temperature is defined as the uniform temperature which will give the same heat transfer from a person to the surroundings as the actual climate does.

The operative temperature can finally be calculated as:

$$T_o = \xi \cdot T_{air} + (1 - \xi) \cdot T_{mr}, \quad 0 \le \xi \le 1 \quad \textbf{(A.111)}$$

The weighing factor depends on the relative air velocity to the person in the room for whom the operative temperature is calculated. In typical buildings, the factor is equal to 0.5, which means that the air and radiant temperature are equally important for the thermal sensation for a person.

A.7.5 Thermal comfort

Two types of thermal comfort are considered; general and local (dis)comfort. The general thermal comfort is based on Fanger's PMV index (Fanger, 1970). The local discomfort focuses mainly on temperature asymmetry between the surfaces.

General thermal comfort

The Predicted Mean Vote (PMV) and Predicted Percentage of Dissatisfied (PPD) indices are the main parameters for characterising the level of thermal comfort for a person in a room.

The PMV index is based on a seven point scale, with the following values.

+3 hot
+2 warm
+1 slightly warm
0 neutral
-1 slightly cool
-2 cool
-3 cold

The PMV-value can be found from the following equation:

$$\begin{aligned} PMV = {} & \left(0{,}303 \cdot e^{-0{,}036 \cdot M} + 0{,}028\right) \cdot \\ & \left\{(M - W) - 3{,}05 \cdot 10^{-3} \cdot \left[5733 - 6{,}99 \cdot (M - W) - p_{da}\right]\right. \\ & - 0{,}42 \cdot \left[(M - W) - 58{,}15\right] - 17 \cdot 10^{-6} \cdot M \cdot \left(5867 - p_{da}\right) \\ & - 1{,}4 \cdot 10^{-3} \cdot M \cdot \left(34 - T_{cl}\right) \\ & \left. - 39{,}6 \cdot 10^{-9} \cdot f_{cl} \cdot \left[(T_{cl} + 273)^4 - (T_{rad} + 273)^4\right] - f_{cl} \cdot \alpha_{conv} \cdot \left(T_{cl} - T_{air}\right)\right\} \end{aligned} \quad \textbf{(A.112)}$$

Notice that a lot of details have been left out in the calculation of the PMV-index. These are plentifully described (Fanger, 1970).

And the PPD index is based on the PMV index, which is given by:

$$PPD = 100 - 95 \cdot e^{-\left(0{,}03353 \cdot PMV^4 + 0{,}2179 \cdot PMV^2\right)}, \quad 5 \le PPD \le 100 \quad \textbf{(A.113)}$$

Local thermal discomfort

The local thermal discomfort includes an assessment of the percentage of dissatisfied (PD) due to the floor surface temperature and the PD due to temperature asymmetry of the surfaces in the room.

A.7.6 Control systems

Different control algorithms are used in the simulation programs. These are described in the relevant sections.

However, the basic control system is described in this section. This is a simple on/off algorithm with a dead band, whose states are shown in Table A.1.

Table A.1 Control system table for on/off flow configuration (DB = dead band)

Control state	Flow
$T_{room} < T_{set} - DB$	On
$T_{set} - DB < T_{room} < T_{set} + DB$	If the flow is on it will remain on If the flow is off it will remain off
$T_{room} > T_{set} + DB$	Off

A.8 Calculation procedure in simulation models

In this appendix, the simulation model used in the two programs FHSim and TASim have been documented with respect to the equations used. In this section the calculation procedure is explained. The description is very general in the description of the use, as this is very different in the two programs and the interfaces that it uses.

Initially, it is important to stress the difference between 'the simulation model', which has been described in the preceeding sections and implemented in FHSim/TASim, and 'the input model', which is the actual input parameters of building geometry, material properties and heating/cooling system properties.. In this section, no specific details are given to the input of data to the simulation model. Chapter 4 has a brief description of a graphical user interface, which can be used for inputting data to the simulation model. Further, no specific details are given on the actual implementation of the programs, as this is not considered relevant for the understanding of the work in this thesis.

The calculation procedure used in the simulation model is given in the following table:

Table A.2 Calculation procedure used in FHSim/TASim

Step	In this step	Comments
Initialisation	Input parameters	Definition of the input model of geometry, material properties of walls/ceiling/floor, glazing units, control parameters, floor heating/thermo active component, and so on. View factors are calculated based on geometry.
	Temperature fields in walls, ceiling and floor construction	Based on assumed data – or if this exist temperature fields from previous simulations on the same model. This is especially used for the large ground volume model, where several years of simulations are needed for periodic stationary conditions
	Weather data	Required data are extracted from the Design Reference Year. Both temperatures and solar data
Dynamic simulation	Weather data	Data for actual time step
	Radiation	Distribution of solar radiation and heat exchange between surfaces
	Room temperature	Room air temperature calculated based on weather data
	Control	On/off of flow in system
	Constructions	The temperature distribution and heat flows in the constructions are calculated for walls, ceiling and floor construction
	Room temperature	Recalculation of room air temperature

Step	In this step	Comments
	Control	Recalculation of control parameters for next time step
	Saving variables	Transfers data from the current time step to the results arrays
	Advancing time step	
Post processing	Saving results	Predefined data are saved and key data are calculated (i.e. sums of heat flows in model)
	Data analysis	I.e. plotting of data

A.9 Nomenclature used in appendix A

Variable	Description	Unit
α	Convective heat transfer coefficient	W/m²K
α	Absorption coefficient of solar radiation in glazing	-
ε	Emissivity	-
η	Efficiency factor	-
ξ	Factor	-
π	Pi	-
ψ	Linear thermal transmittance	W/mK
ρ	Density	kg/m³
σ	Stefan-Boltzmann's constant	W/m²K⁴
λ	Heat transfer coefficient/thermal conductivity	W/mK
Δx, Δy	Distances	m
$\dot{q}$, q	Heat flow	W (or W/m²)
A	Area	m²
A, B, C, D, E, F	Coefficients used by numerical method	W/mK
C	Heat capacity (used in thermal network model)	W/mK
c_p	Heat capacity	kJ/kgK
DB	Dead band	K
d_{eq}	Equivalent diameter of pipe	m
F	View factors	-
g	Transmission coefficient of solar radiation (for windows)	
G	Radiation	W/m²
h	Heat transfer coefficient	W/m²K
$Hx, Hy, H0$	Heat transfer functions	W/mK
I	Incident radiation	W/m²
J	Radiosity	W/m²
L, l	Length	m
$\dot{m}$	Flow	kg/s
M	Activity	Met

n	Air change rate	1/hour
n, m	Number of nodal points in the x and y direction respectively	-
p	Pressure	Pa
P	Perimeter	m
PMV	Predicted Mean Vote	
PPD	Predicted Percentage of Dissatisfied	%
r	Residual vector	-
R	Thermal resistance	m²K/W
Rx, Ry	Spatial resistances in model	m²K/W
RX, RY	Contact resistances	m²K/W
t	time	s
T	Temperature	˚C
U	Thermal transmittance	W/m²K
V	Volume	m³
W	External work	
w_{center}	Pipe spacing	m
x, y	Distances	m

Generally used indices

Index	**Description**
ε	Emissivity
β	Incident angle
ψ	Linear thermal transmittance
abs	Absorbed part
air	Air
bp	Nodal point next to pipe
ceiling	Ceiling
cl	Clothing
conv	Convective
diffuse	Diffuse part of radiation
direct	Direct part of radiation
down	Downwards
e	Exterior
eq	Equivalent diameter of pipe
floor	Floor
fluid	fluid in pipe
frame	Opaque part of window
g, glazing	Transparent part of window
ground	Towards the ground
i	Counter or inside
in	Internal
inf	Infiltration
inlet	Air to room from ventilation/infiltration
int	Internal
j	Counter
L, l	Length
m	Nodal points in y-direction
mat	Material

mr	Mean radiant
n	Nodal points in x-direction
out	Return from floor heating pipe or outside conditions
pane	Glazed part of window
person	Person
pipe	Pipe
rad	Long wave thermal radiation
room	Room
set	Set point
sol	Short wave solar radiation
supply	Supply to floor heating pipe
sur	Surface
tot	Total
trans	Transmitted part of radiation
vent	Ventilation
venting	Air change due to venting
wall	Wall
x	x-direction
y	y-direction

Paper 1

Presentation of the International Building Physics Toolbox for Simulink

Peter Weitzmann, Angela Sasic Kalagasidis, Toke Rammer Nielsen Ruut Peuhkuri and Carl-Eric Hagentoft

In: Proceedings of the Eighth International IBPSA Conference Building Simulation 2003

PRESENTATION OF THE INTERNATIONAL BUILDING PHYSICS TOOLBOX FOR SIMULINK

Peter Weitzmann[1], Angela Sasic Kalagasidis[2], Toke Rammer Nielsen[1], Ruut Peuhkuri[1] and Carl-Eric Hagentoft[2]

[1] Department of Civil Engineering, Techical University of Denmark, DK-2800 Lyngby, Denmark

[2] Chalmers University of Technology, Department of Building Physics, SE-412 96 Göteborg, Sweden

ABSTRACT

The international building physics toolbox (IBPT) is a software library specially constructed for HAM system analysis in building physics. The toolbox is constructed as a modular structure of the standard building elements using the graphical programming language Simulink. Two research groups have participated in this project. In order to enable the development of the toolbox, a common modelling platform was defined: a set of unique communication signals, material database and documentation protocol. The IBPT is open source and publicly available on the Internet. Any researcher and student can use, expand, and develop the contents of the toolbox. This paper presents the structure and the backbone of the library. Three examples are given to visualize the possibilities of the toolbox.

INTRODUCTION

The numerical modelling of heat, air and moisture (HAM) flows in buildings is an essential part of studying these phenomena – it might be as a part of research work, building design or for educational purposes. Examples of HAM models can be found in Hens (1996), Wit (2000) and Hagentoft (2002a).

A host of commercially available computer tools models already exist for modelling single components or whole buildings. For modelling whole buildings, there are models for the hourly energy balance programs (in some cases also including moisture) Bsim[1], ESP-r[2], EnergyPlus[3], and more. While these tools are fully appropriate for designing standard buildings, they are not suitable for modelling innovative building elements such as building integrated heating and cooling systems, ventilated glass facades and solar walls, as these have not been defined in the program. A different approach is the use of modular simulation tools, represented i.e. by TRNSYS[4] and SPARK[5]. In Strand et al. (2002), the differences in the two types of tools are discussed. Here it was found that the major shortcomings of building energy simulation programs have so far been the inability to accurately model HVAC systems that are not "standard". This argumentation can easily be expanded to include advanced building elements. The modular models, on the other hand, have the advantage that components and systems can be modelled as the need appears.

Should a detailed and transparent tool be usable by a large number of people working individually to develop models, it must be modular. In addition, transparency of the existing components is essential, if the user/developer wishes to implement any modifications. A transparent, modular and open source system for modelling heat and moisture flows in buildings should therefore be a user-friendly tool that can be expanded as needed in the future.

The above-mentioned concerns have given rise to a need to develop an open and freely available building physics toolbox among the Authors. The start of the International Building Physics Toobox (IBPT) was laid by two groups of researchers working independently of each other with developing building physics models in Simulink. For both groups, the reason for starting to use Simulink as the development environment was a need to being able to model, in great detail, the processes of heat, air and moisture transfer. In both groups the reason for choosing Simulink, which is part of the Matlab package[6], was a large degree of flexibility, modular structure, transparency of the models and ease of use in the modelling process.

Simulink has already previously been used by other research communities (SIMBAD[7] and CARNOT[8]), but the models have either not been open source, free of cost or have not been directly applicable to building physics modelling.

[1] www.bsim.dk
[2] www.esru.strath.ac.uk/programs/ESP-r.htm
[3] www.eren.doe.gov/buildings/energy_tools/energyplus
[4] sel.me.wisc.edu/trnsys
[5] simulationresearch.lbl.gov
[6] www.mathworks.com
[7] evl.cstb.fr
[8] www.sij.fh-aachen.de/projekt_energiesysteme/carnot_1.shtml

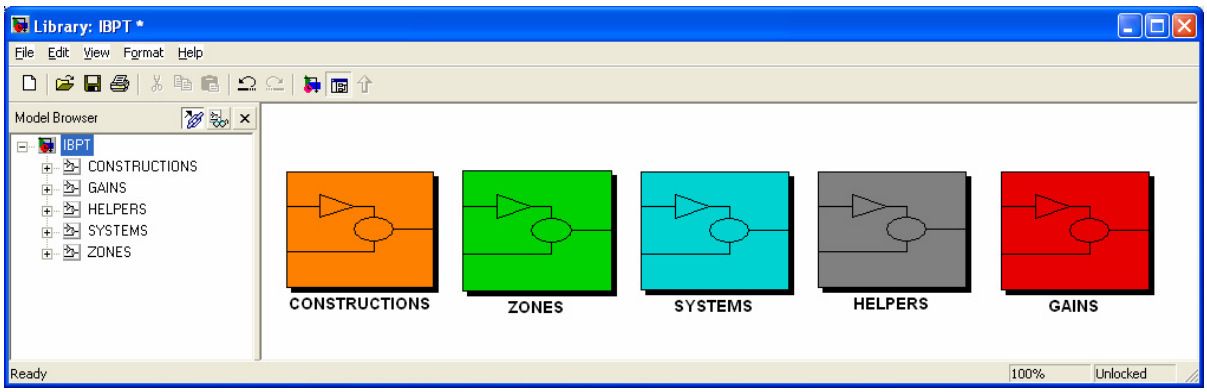

Figure 1 Main window of the International Building Physics Toolbox

The modular structure in Simulink - using systems and subsystems - makes it easier to maintain an overview of the models, and new models can just as easily be added to the pool of existing models. Another advantage of using Simulink is the graphical programming language based on blocks with different properties such as arithmetic functions, input/output, data handling, transfer functions, state space models and more. Furthermore, Simulink has built-in state of the art ordinary differential equation (ODE) solvers, which are automatically configured at run-time of the model. Therefore, only the physical model needs to be implemented, and not the solver. Further, models can be created using a number of different approaches. These include assembling models directly in Simulink using the standard blocks, Matlab m-files, S-functions, and Femlab[9] models using one-, two-, or three-dimensional finite element calculations. This wide variety of modelling techniques with different advantages and disadvantages means, that the optimal choice can always be made with respect to the task.

The graphical approach also makes it easy to show the very complex interaction between the different parts of the model. In addition, people who are not used to programming can easily get started building their own models or altering existing ones. Therefore, the toolbox also represents a good way to teach building physics.

Comparing IBPT to other modular building energy simulation programs (i.e. TRNSYS, SPARK and EnergyPlus), a few notes can be made. (1) IBPT does not require the same level of detailed programming knowledge (but advanced programming is possible), (2) it can use Simulink's built in solvers (but new solvers can be added by the user), (3) a large degree of integration using the Matlab package can be achieved and as described below (4) all programming code is freely available from the website.

The vision behind the development of the IBPT is to create a website (http://www.ibpt.org) with a set of block models for modelling building physics. On the website, the blocks are freely available for download.

A 'block' is a common term for the basic elements used during the modelling process. Five categories of blocks have been defined. They are:

- constructions (e.g. walls and windows)
- zones (e.g. room models)
- systems (e.g. HVAC systems)
- helpers (e.g. handling of weather data)
- gains (e.g. internal heat gains).

These five categories are organized in a Simulink block library as shown in Figure 1.

New blocks can be added by the users, thereby ensuring the development of the contents of the toolbox.

The cornerstone of the IBPT is made up of the definition of a set of data arrays for exchange of data between blocks. A total of seven different arrays have been defined. The use of these data arrays ensures that the blocks can communicate with each other – even if different people have developed the blocks independently of each other!

Besides the data arrays, two more key elements exist. They are: a key for the documentation of the blocks and a database of material properties. This can be found in Sasic (2002) and Nielsen et al. (2002). On the website, a description of the functionality of each of the blocks is available. Also, a detailed description (Rode et al., 2002) of the interface between the blocks can be downloaded, so new blocks can be created and be in compliance with the existing blocks from the toolbox.

Different blocks can have different levels of details and processes. Some construction blocks may model only heat transfer while others may have both heat, air and moisture transfer. Also, the blocks can use different modelling techniques and have different accuracy in the modelling.

In this paper, the International Building Physics Toolbox (IBPT) for Simulink is presented. The paper describes the work that has led to the present state of

[9] www.comsol.com

the toolbox and the background for the choices that have been made.

TOOLBOX

As described above, the IBPT consists of three cornerstones, which are: (1) the set of seven data arrays, (2) a material database and (3) the requirements for describing and documenting the blocks.

Initially however, the blocks presently existing in the toolbox are briefly presented

BLOCKS IN THE TOOLBOX

In the first version of the IBPT, which is presently available for download, a limited number of blocks are available. These include a zone model, input of weather data, ventilation and inner walls, outer walls and windows. These blocks can be used to perform simple energy balance calculations on simple rooms. Below in the examples, the development of two new blocks is described.

An example of a block is shown in Figure 2. The block accepts three input arrays and returns one output array. All data exchange between blocks is in the form of arrays, which contains a predefined set of data.

DATA ARRAYS

Seven data arrays have been defined for the data exchange between the blocks in the models. The arrays have been given the following names:

- Surface weather data array
- Construction array
- System array
- Geometry array
- Zone array
- Radiation array
- Gain array

Each of the arrays includes the necessary physical states and properties at the interfaces of the boundaries between the blocks. This way the data exchange between the blocks can always be handled using the pre-defined arrays, regardless of the level

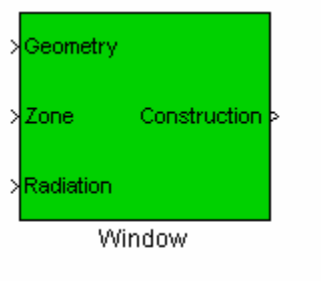

Figure 2 Example of block used in toolbox. In this case a window.

Table 1 Construction array

Symbol	Description	Unit
R_c	Convective thermal surface resistance	m² K/W
T_s	Surface temperature	°C
R_p	Moisture surface resistance	Pa s m²/kg
p_s	Surface vapour pressure	Pa
R_a	Air flow resistance	$m^3/(s\ Pa)$
P_a	Air pressure	Pa
Q_{sun}	Transmitted solar energy	W/m²
ε	Surface emissivity	-
T_{air}	Inlet temperature of air flow	°C
φ_{air}	Relative humidity of air flow	-
Snr	Surface number	-

of detail used in the models. An example of the data the arrays is the construction array shown in Table 1. The construction array is the output from a construction element (wall, window), and it includes the conditions at the surface along with data for transmitted solar energy and air flow through the construction. This array covers both opaque, translucent and transparent constructions, and constructions with air gaps or openings

The reason for using the predefined arrays is that the output from any type of component is known, concerning type and order of data in the array. Therefore, when creating new models, the type of input and output from other blocks is already known. The blocks just need to be connected, and they will be able to communicate with each other. This approach will inevitably give arrays where one or more of the data positions in the array are not activated. However, at the same time the same array can be used from all components of the actual type regardless of the model.

From Table 1, it can be seen that some choices have been made with respect to which data should be exchanged. As an example, the convective thermal surface resistance has been defined to be an output from the construction – and not an input from the zone array. Therefore, the calculation of the convective thermal surface resistance must be performed in the construction block. Of course, this could also have been done in the zone model. This example illustrates the type of choices and considerations involved in the design process of the communication arrays.

In case it should be necessary to include further data in the exchange between blocks (i.e. if a control system variable depends on a given parameter which is not included in the pre-defined arrays), this can be done by using a user-defined array.

MATERIAL DATABASE

The material parameters are arranged in a material library created in the form of **structures**. Structures are multidimensional Matlab arrays with "data containers" called fields. Each field has certain name and can contain any kind of data: text, scalar or array/matrix. Here is an example:

```
data(1).name='insulation'
data(1).dry_density=100
data(1).lambda_dry=0.04
data(1).absorption_RH=
       [0.05 0.015 0.025 ...]
data(1).absorption_U=
       [0.001 0.002 0.008 ...]
```

Each material from the library is described by the same set of data, but with the different index, e.g. (data(2)). These structures called "data()" are saved to a Matlab file, e.g. *DATABASE.mat*. In order to access this structure from Simulink, the file must be loaded either in the Matlab Workspace or by the block mask initialisation to the local Workspace. Now there is an access to the structure, which can be used in the model as any other variable. The different materials can be given an index in the block mask by using a pop-up menu and after choosing the material; all the material parameters in this block are valid only for the material chosen.

Keeping the same structure, and especially field names, any user can create his/her own material library. It should be stressed, anyway, that a range of field names are already definite for particular uses. Any other material property can be added, just with another describing name. This allows users and developers to use their preferable material parameter presentations matching their models.

DOCUMENTATION

Each block in the toolbox is documented according to the following paradigm:

- Description – a short description of the use of the block
- Block diagram – the "front page" of the block as it appears in the toolbox
- Input to the block – which arrays does it require as inputs?
- Output from the block – which arrays does it output?
- Block mask – here different properties for the block can be set. E.g. the insulation thickness in a wall
- Variables – variables used in the mathematical model
- Mathematical model – a documentation of the mathematical model used
- Simulink model – the implemented model
- Miscellaneous – connection to the neighbouring blocks, logging of results, etc
- Validation – if a block has been validated, this must be included. The validation can be a comparison to hand calculations and/or measurements

This documentation is important in the use of the IBPT, as it is here the model is described with respect to the level of detail (what is included and what has been left out). The documentation is also a help file for the user in case of difficulties in using the block.

EXAMPLES

Three examples are given on the use and flexibility of the IBPT. Example 1 shows the implementation of an outer wall with heat, air and moisture transport, which is directly modelled using Simulink blocks. In Example 2, a floor heating system is modelled. This is done using an S-function. Finally, in Example 3, a room model including the blocks from the two first examples is created. It should be noticed, that the blocks in the two examples have been created by different research groups. They have been built in accordance with the requirements of the IBPT, and are thereby able to work together in the room model.

Notice that where the numerical model in Example 1 has been validated, this is not the case for the models presented in Example 2 and 3. Work is in progress to validate the models used here.

EXAMPLE 1: WALL

The wall is treated as a multi-layered structure of different materials in direct contact or connected through a ventilated or non-ventilated air gap. 1D heat, air and moisture (HAM) transfer through the wall is solved numerically using the control volume method.

An example of a numerical procedure and Simulink model for a simple, one material external wall is given in Figure 3. The block icon named as "External wall" corresponds to the numerical scheme given on the right, where the space discretization is obtained by dividing the total wall thickness into five control volumes. Each volume is presented by separate Simulink blocks that are connected following the numerical scheme. The complete Simulink model of the considered wall is shown in Figure 3: one External surface node, three One nodes (used internally in the material) and one Internal surface node.

The layer of the considered material is modelled as a porous structure, consisting of the skeleton of the main (dry) material and pores filled with moisture and air. The output of the system gives temperature, water vapour partial pressure and moisture content of the volume – it's hygrothermal state. Material and geometrical data of the volume are placed either in the model or in a material data file, from which they are called during simulation.

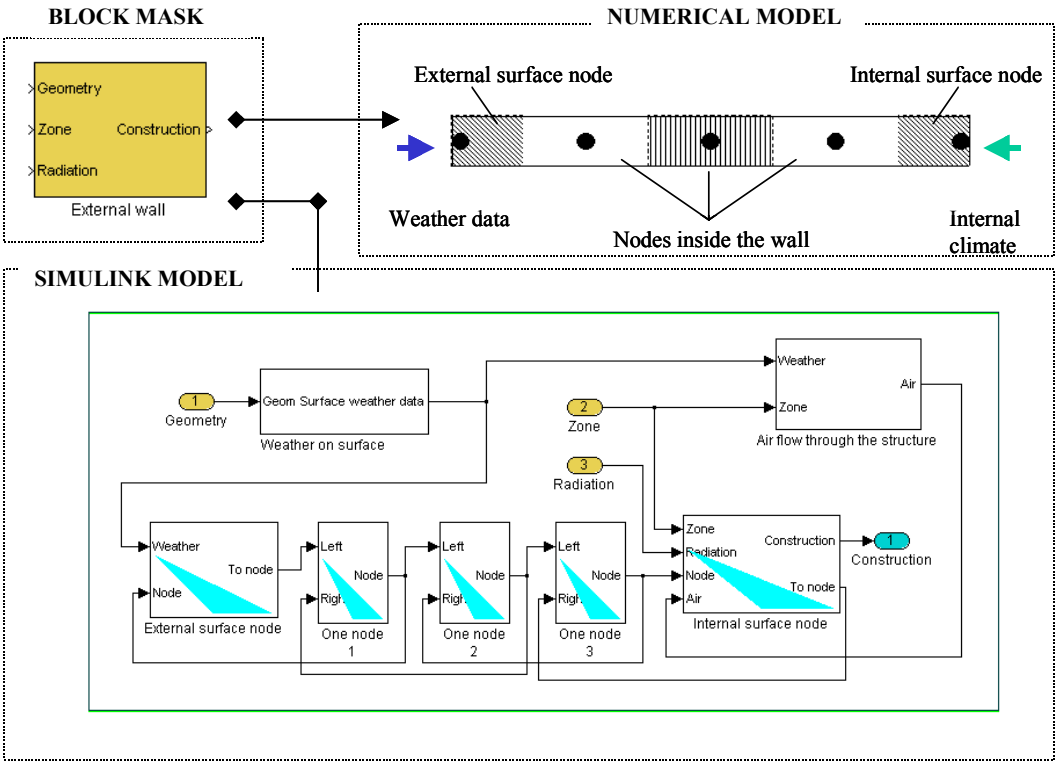

Figure 3 Model of wall with heat, air and moisture transport

External and internal surface nodes describe the surface transfer coefficient between the wall and surrounding air. The model assumes that the external wall surface is exposed to convective heat and moisture exchange with outdoors air, incident solar radiation, long wave radiation, transfer of latent heat, air and rain. Internal wall surface is exposed to convective heat and moisture exchange and transfer of latent heat with inner air, and long wave radiation exchange with other surfaces.

VALIDATION OF THE WALL MODEL

The HAM wall block is validated through the inter-model comparison performed within the HAMSTAD project, which was initiated in order to develop a platform for assessment of computational modelling of HAM transport mechanism in building physics. In this project, five benchmark tests were defined. Details are provided in the project report (Hagentoft, 2002b).

Some results for one of the benchmarks, which covers heat, air and moisture transfer, are given in Figure 4. The benchmark deals with an air transfer through a single material layer. Moisture transfer is caused mainly by the airflow through the layer, and by the moisture and temperature gradients across the layer. The left hand side of the layer is vapour tight, but air-open.

Validation of the HAM room model (like the one in Figure 6) with the measurements taken on the real object is the work in process.

EXAMPLE 2: FLOOR HEATING MODULE

Another approach to creating models in Simulink is to use so-called S-functions. An S-function is "a computer language description of a Simulink Block" (MathWorks, 2002). The S-function can be written in C, C++, Fortran, Matlab or Ada. The advantage of using an S-function is the fast execution, which due to the special syntax can communicate directly with Simulink's equations solvers, much in the same way

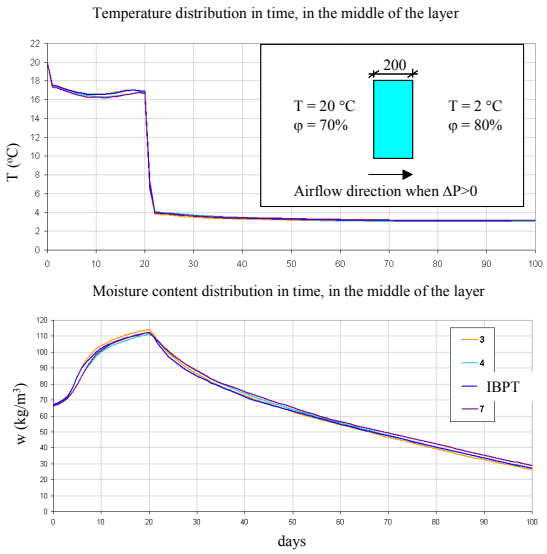

Figure 4 Validation results for the IBPT HAM wall block. Comparison with different solutions

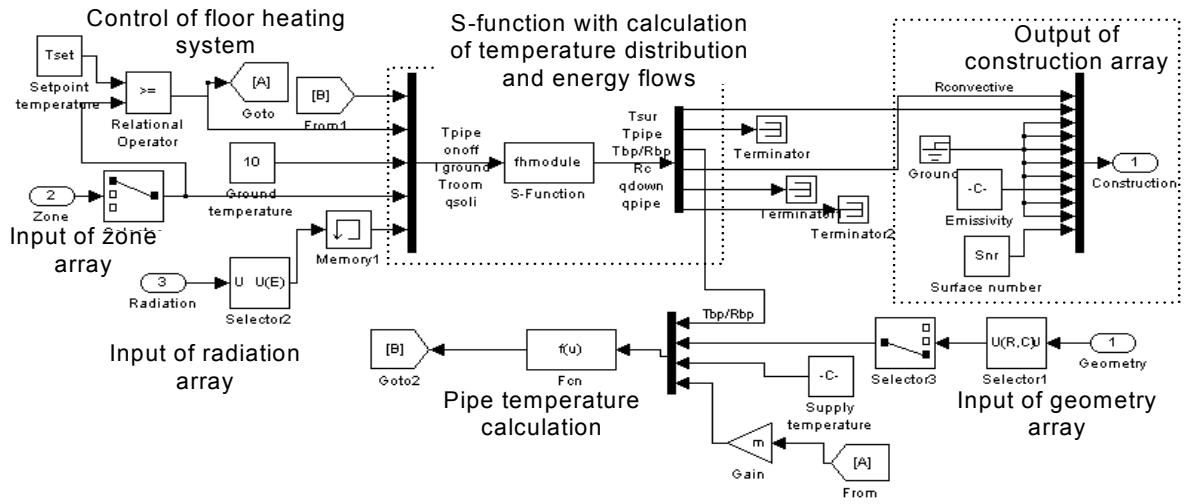

Figure 5 Floor heating block. The numerical model of the floor heating system is placed in the S-function called 'fhmodule', placed in the middle of the block.

as the built-in Simulink blocks do.

A section of the floor around a floor heating pipe has been modelled and implemented into an S-function. The model is described in detail in Weitzmann (2002), and in Weitzmann et al (2002), where the same model was used in the form of a Matlab m-function.

The implementation of the floor heating module includes a two-dimensional finite control volume calculation of the temperature distribution and energy flows in the floor. Notice that in the floor model, the temperature and energy flows are calculated within the model and not by the built-in Simulink solver. However, this is not a problem for Simulink as it only passes the parameters to and from the S-function and therefore does not have problems accepting the calculated values from the S-function

The model, includes both radiation and convection exchange with the room. The pipe temperature is calculated based on the heat flow through the floor heating pipe boundary. The control system is a simple on-off type based on the room air temperature.

The model of the floor heating block can be seen in Figure 5. The temperature distribution and energy flows are calculated in the block called 'fhmodule', which is the S-function. The block is set to have a discrete sampling time, where, the output from the block is assumed constant between the samples. This approach has been used because a finite control

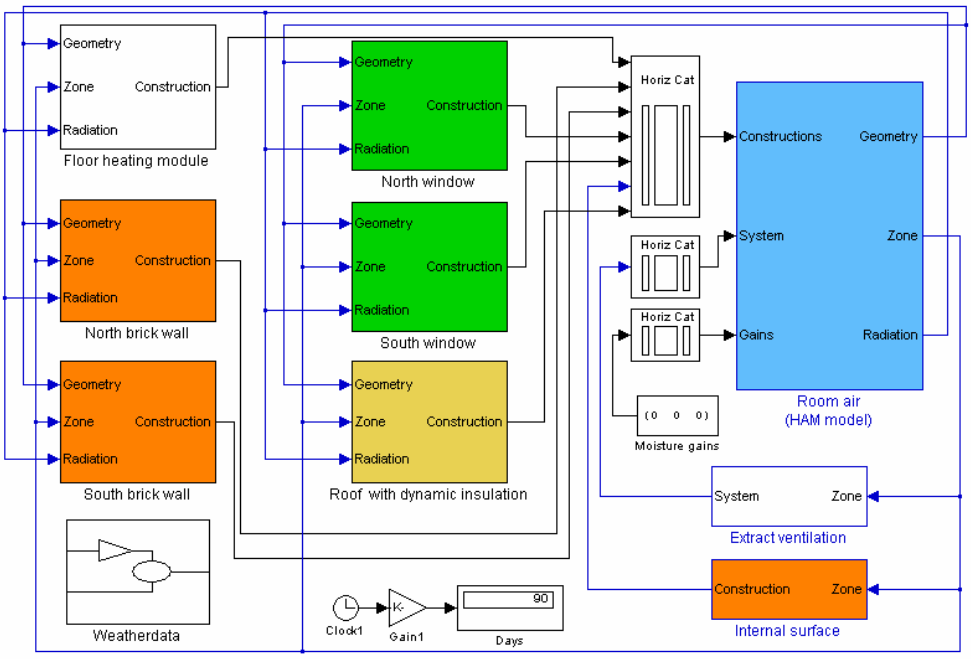

Figure 6 Room model with HAM walls and floor with floor heating. The other blocks have been taken directly from the toolbox

volume method requires a fixed discrete timestep. Notice also, how the construction output array is assembled in the upper right of the figure. Here most of the values have been grounded (signal equal to zero). The fact that they have been included is that the other blocks expect a construction array with 11 values.

EXAMPLE 3: ENTIRE ROOM MODEL

The two blocks shown so far are used in a complete room model where the remaining blocks have been taken from the toolbox.

The temperature, relative humidity and air pressure of the ventilated space is calculated accounting for the heat and moisture gains through the building envelope, internal sources and HVAC equipment placed in the space. All geometrical data like areas, orientations and tilts of the attached construction elements are given as input to the room air block.

The room model assumes well mixed air (one air node), and calculates long wave radiation between the internal surfaces.

The room air model, the constructions and HVAC equipment are represented by different Simulink block models, shown in Figure 6. The number of attached elements is not limited, as well as the number of additional zones. Structural details, materials, meteorological data and applied equipment are designed in such details to represent the reality in a credible way.

Some of the results from this simulation are presented in Figure 7. They illustrate the sensitivity of the model regarding the surrounding and working conditions.

CONCLUSION

In this paper, the International Building Physics Toolbox is presented and a few examples of the usability are shown.

The modular approach together with the definition of the communication arrays gives a versatile and easy-to-use environment for creating building physics models. The toolbox is open source and the blocks that make up the modelling elements are freely available from the website www.ibpt.org. Therefore, there is no need to start over when creating models. Also, anyone is free to contribute their models, as long as they are in compliance with the requirements concerning data exchange and documentation.

So far, the IBPT only contains fairly simple models containing only heat transfer. But as shown in the paper, more advanced models including air and moisture and building integrated heating systems can also be included. Furthermore, there are many different ways of modelling the blocks in the toolbox. In the paper, two were shown: One using only the graphical environment of Simulink and the other using S-functions. Other possibilities of modelling can be found in Femlab and the other toolboxes available in Matlab. In addition, there is no need to worry about the solver, as Matlab has an extensive list of state-of-the-art ODE-solvers available.

Simulink and Matlab also have many advanced features for post processing of the results from the simulation, as it can be seen from the figures in the text above.

The graphical programming environment is useful for teaching building physics as the interaction between different parts of the model can easily be visualized.

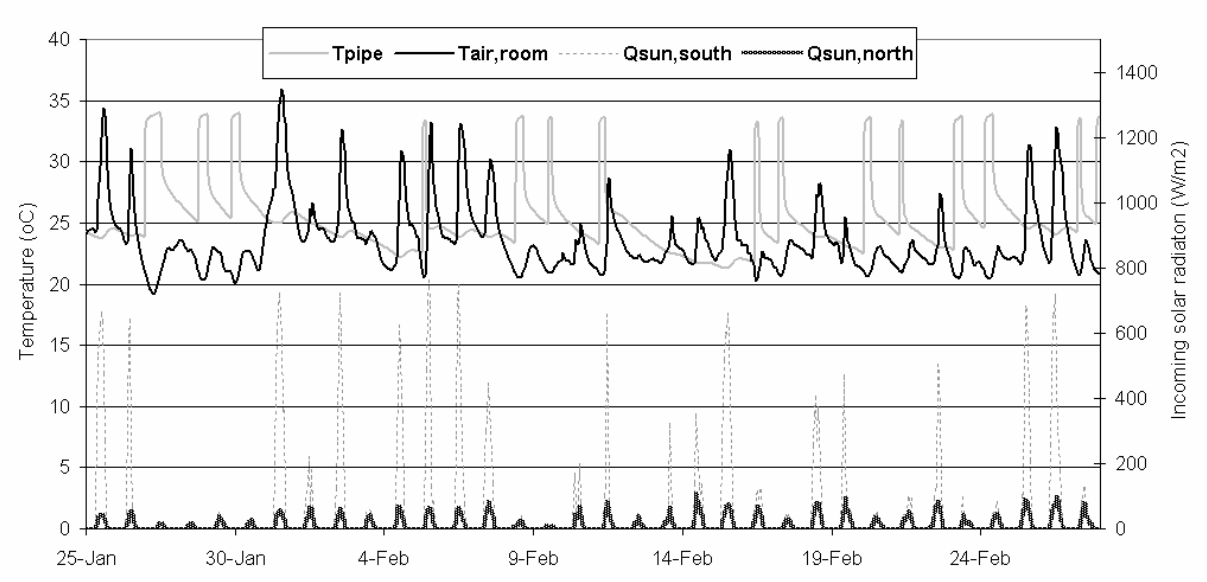

Figure 7 Results from simulation of the example model

One initial concern about the development of the toolbox where different people develop models independently of each other was that it would not work, and that Simulink would refuse to do simulations. This has been proven wrong, because of the strict definition of the communication arrays.

A few drawbacks should also be mentioned. The calculation time is not impressive and cannot compete with native code in other programming languages such as Fortran, C or C++. However, the implementation time is much quicker. Finally, the availability of Matlab should also be mentioned as a problem, as the program is very expensive.

To sum up, the IBPT represents an open and user friendly way of modelling building physics processes. If a researcher (or student) wishes to investigate a certain part of a building and see how it interacts with the entire building – for instance a solar wall, she does not need to create the entire model of the building from scratch. She can focus on the modelling of the solar wall and get the rest from the existing blocks in the IBPT. She can then choose a set of blocks with the level of detail in modelling that she is interested in including into the investigation. When the development and investigation of the solar wall has been completed and documented according to the requirements, she is welcome to upload the block to the website where it will become part of the toolbox and thereby freely available by other researchers and students! In this way, it is hoped that the toolbox over time, will develop into a full modelling tool with open source and fully documented code for the modelling of building physics processes.

Finally, the authors of this paper therefore invite anyone who is interested to participate in the further development of the IBPT. All information on the use of the toolbox and further development of the blocks can be found on the website.

REFERENCES

Hagentoft, C.-E. (2002a): *HAMSTAD – WP2 Modeling, Version 4, Report* R-02:9. Gothenburg, Department of Building Physics, Chalmers University of Technology. Available on www.buildphys.chalmers.se

Hagentoft, C.-E. (2002b): *HAMSTAD – Final report: Methodology of HAM-modeling*, Report R-02:8. Gothenburg, Department of Building Physics, Chalmers University of Technology. Available on www.buildphys.chalmers.se

Hens, H. (1996): *IAE Annex 24, Final report, Volume 1, Modelling*. K.U. Leuven, Belgium: Laboratorium Bouwfysica, Departement Burgerlijke Bouwkunde.

MathWorks (2002): *Writing S-functions*. Available from www.mathworks.com

Nielsen, T.R., Peuhkuri, R., Weitzman, P. and Gudum C. (2002): *Modelling Building Physics in Simulink, Working draft*, Report SR-02-03, BYG DTU. Available on www.ibpt.org

Rode, C., Gudum, C, Weitzmann P, Peuhkuri R. H., Nielsen, T. R., Kalagasidis, A. S., Hagentoft, C-E. (2002): *International Building Physics Toolbox, General report*, R-02:4. Gothenburg: Chalmers University of Technology, Department of Building Physics. Available on www.ibpt.org

Sasic Kalagasidis A. (2002): HAM-Tools, *International Building Physics Toolbox, Block documentation, R-02:6.* Gothenburg: Chalmers University of Technology, Department of Building Physics. To be published. Available on www.ibpt.org

Strand, R.K., Liesen, R.J., Fisher, D. E., Pedersen, C.O. (2002): *Modular HVAC Simulation and the Future Integration on Alternative Cooling Systems in a New Building Energy Simulation Program*, ASHRAE Transactions Vol. 108 Issue 2, Page No. 1107-1117.

Weitzmann, P. (2002): *A floor heating module using an S-function approach for the International Building Physics Toolbox*. Lyngby: Technical University of Denmark, Department of Building Physics. To be published. Available on www.ibpt.org

Weitzmann, P., Kragh, J, Jensen, C.F. (2002): N*umerical Investigation of Floor Heating Systems in Low Energy Houses*. Proceedings of the 6th Symposium on Building Physics in the Nordic Countries.

Wit, M.: *WAVO. A simulation model for the thermal and hygric performance of a building*. Faculteit bouwkunde, Technische Universiteit Eindhoven. 2000

Paper 2

Modelling floor heating systems using a validated two-dimensional ground coupled numerical model.

Peter Weitzmann, Jesper Kragh, Peter Roots and Svend Svendsen

Accepted for publication in Buildings and Environment.

Modelling floor heating systems using a validated two-dimensional ground coupled numerical model

Peter Weitzmann[*] [1], Jesper Kragh [1], Peter Roots [2] and Svend Svendsen [1]

[1] Department of Civil Engineering, Technical University of Denmark. Address: Department of Civil Engineering, Technical University of Denmark, Building 118, DK-2800 Kgs. Lyngby, Denmark.

[2] Swedish Energy Agency. P.O Box 310, SE-631 04 Eskilstuna, Sweden

Abstract

This paper presents a two-dimensional simulation model of the heat losses and temperatures in a slab on grade floor with floor heating which is able to dynamically model the floor heating system. The aim of this work is to be able to model, in detail, the influence from the floor construction and foundation on the performance of the floor heating system. The ground coupled floor heating model is validated against measurements from a single-family house. The simulation model is coupled to a whole-building energy simulation model with inclusion of heat losses and heat supply to the room above the floor. This model can be used to design energy efficient houses with floor heating focusing on the heat loss through the floor construction and foundation. It is found that it is important to model the dynamics of the floor heating system to find the correct heat loss to the ground, and further, that the foundation has a large impact on the energy consumption of buildings heated by floor heating. Consequently, this detail should be in focus when designing houses with floor heating.

Keywords

Floor heating, numerical modelling, ground coupling, energy consumption, model validation.

Introduction

The dynamical behaviour of the ground heat loss is not very well known for single-family houses with floor heating. Especially the influence of the foundation must be better investigated. This is of interest since the heat loss to the ground is larger when floor heating is used and since the ground heat loss is becoming increasingly more important, as the parts of the building above ground are getting still better insulated [1].

Hydronic floor heating

Simulation models of floor heating focusing mainly on the heat transfer from pipe to room can be found in the literature as basis for characterisation and dimensioning. Different types of floor heating systems have been investigated using finite element models with respect to thermal properties [2], and dynamical behaviour [3]. A classification of the thermal output to the room for floor heating systems has been established with the purpose of being able to design and dimension such systems in EN1264 [4]. Different control strategies are investigated in [5], concluding that they have a large impact on the energy consumption. Different floor covering materials have been found to impact temperatures, reaction time and energy consumption [6]. Dynamical models of hydronic floor heating combined with a room model in building energy simulation have been elaborated [7, 8, 9]. These models have the advan-

[*] corresponding author: email: pw@byg.dtu.dk, fax: +45 4588 3282

tage of realistic dynamic properties of hydronic floor heating. However the simple ground geometry omits the influence from foundation and ground volume.

Heat loss from floors without floor heating

Another field of interest for this work is the so-called ground coupling between floor and ground volume. Analyses have been carried out to account for the floor construction and foundation, focusing on especially boundary conditions, multidimensional analysis and level of detail including material properties for the ground volume conditions [10, 11, 12, 13, 14].

The outside boundary condition between air and ground surface depends, among others, on the incident radiation, snow, wind and rain. In the simulations different boundary conditions can be applied ranging from simple convective conditions to more detailed ones including short and long wave radiation, evaporation and rain. In a theoretical investigation on a basement structure [14], a comparison of different level of detail in the boundary condition shows that while a simple convective heat transfer gives the same average temperature at the ground surface as a formulation including radiation, evaporation and rain, the temperature amplitude on the ground surface is much smaller, which means that the heat loss during the winter period will be underestimated. In this case the simplification leads to about 10 % lower predicted heat loss.

In Janssen et al. [15], moisture conditions have been included in a fully coupled model of heat and moisture transport. Here it is found that material properties depend on a long list of factors, which cannot be taken into account when constant values are applied; i.e. the heat transfer coefficient of soil varies by a factor 10 depending on moisture levels and composition of the soil material. It is concluded that for a poorly insulated basement, a model without coupling with simple convective boundary conditions underestimates the heat loss of 10-15% compared to the detailed coupled model. However, this underestimation becomes smaller with better insulation level and when floor slabs are considered in stead of basements. In total these simplifications leads to an underestimation of the heat loss, which cannot however be predicted based on the literature available.

In addition, it is acknowledged that considering the uncertainties in especially ground volume material properties, the use of coupled heat and moisture modelling cannot be defended because of the relatively small difference in the results [14, 15]. This is also the case for simplified boundary conditions compared to more detailed ones.

The importance of using multidimensional ground coupling for poorly insulated constructions is well illustrated in [11]. Here analyses are carried out on the consequences of using one-dimensional rather than two- or three-dimensional modelling of temperature and heat flow, reporting discrepancies of up to 22 % between two- and three-dimensional simulations and up to 41 % between one- and three-dimensional simulations. In other studies the difference between one-, two-, and three-dimensional analysis [10, 12, 13] generally finds through both measurements and theoretical considerations that ground heat loss is a three-dimensional process. Anderson [12] introduces a characteristic dimension of the floor defined as the floor area divided by half the exposed perimeter. If this dimension is used in the two-dimensional simulation model in stead of half the width of the building, the three-dimensional problem can be simplified to a two-dimensional one. This is shown in Eq. (1).

$$B' = \frac{A}{½ \cdot P} \qquad \textbf{(1)}$$

Here B' is the characteristic dimension, while A is the area and P is the perimeter.

Another investigation [10] has found that large floors can be considered two-dimensional. However, a three-dimensional calculation is needed to accurately account for the heat flows in the corner regions and for assessing risk of condensation due to the lower temperatures in the corners.

A standard for calculating heat loss to the ground has been established in EN ISO13370 [16], where the width of the floor construction is required to be at least as large as the characteristic dimension defined in [12]. The basis for calculating heat losses through building components has been described in EN ISO10211.1 [17] and EN ISO10211.2 [18]. Here the total heat loss can be summed from one-, two- and three-dimensional contributions. For a floor construction this corresponds to the slab, the foundation and the corners of the building. In [19] and [13] it is found that the heat loss through the slab and foundation must be found by transient analysis while the heat loss through the corners can be found from steady state analysis.

Modelling ground coupling

Different approaches can be used to model the heat flow from buildings. The most detailed (and time consuming) are achieved by numerical models based on finite element, finite difference or finite control volume methods. Once the method is implemented, it is straight-forward to create accurate geometrical models with detailed boundary conditions. Other methods uses are (semi)-analytical models [20, 21, 22, 23, 24] to reduce the simulation time considerably compared to numerical implementations. The reduction in simulation time is achieved through simplifications by finding eigenvalues or response factors, typically using numerical pre-processing. This approach requires simplifications of the geometry, but once they have been established, fast and numerous analyses can be carried out.

Therefore the difference between numerical and analytical methods is a trade-off between simulation time and ability to model details in the construction. In this case geometrical details are analysed, which makes a numerical model the most appropriate.

Heat loss from floors with floor heating

None of the investigations on ground coupling described above consider floor heating. Heated ground floor slabs combined with ground coupling have been examined in a large office building [25], comparing measurements and three-dimensional numerical modelling. While giving good results, the fact that a large office building is investigated means that the results of temperature distribution are not applicable to single-family houses. A two-dimensional numerical model of a slab on grade floor with solar heated floor has been examined and compared to measurements [26]. Good agreement is reported between measured and simulated values, though for a relatively short measurement period. Further, the investigated slab was only insulated at the perimeter of the building, which is not the case in modern well-insulated buildings. Foundation heat loss in heated slab on grade floors has been examined using a semi-analytical model [27] of heat loss to the ground and temperature distribution in the ground with steady-state and steady-periodic (monthly) variations for different configurations of insulation, while assuming constant heating demand in the house. Here it is found that it is important to correctly model the temperature in the floor heating system because this heavily influences the heat loss to the ground.

Ground coupled floor heating

To summarise the introduction, investigations on floor heating have focused mainly on the interaction between heating system and room, while not considering the heat loss to the ground. Conversely, ground coupling has been investigated to find the heat loss to the ground, while not including the house. The combination of heat loss to the ground and interaction with the room has only been very scarcely investigated. Such a model can be used for calculating

energy consumption and thermal conditions in houses with floor heating, thereby helping to increase the energy efficiency, whose importance is reflected in the new EU-directive on the energy performance of buildings [28].

Therefore, a two-dimensional finite control volume model of a slab on grade floor with floor heating including foundation and ground volume has been created for modelling well-insulated houses with floor heating including the coupling to the ground volume, or more specifically the effect of edge and ground insulation. The effect of building corners has been included by using the characteristic dimension [10] to represent the actual house shape. This approach has not been tested for a heated floor and therefore it is relevant to check if this simplification also holds in this case.

The model of the floor is validated against measurements performed in a house in Bromölla, Sweden, which due to a width of only five meters is heavily influenced by three-dimensional conditions. Therefore, if the two-dimensional model can satisfactorily model these conditions, wider buildings can also be modelled correctly. At the same time it can be shown if the use of the characteristic dimension is also valid for a heated floor.

The validated floor model is used together with a simulation model of a house, where the advantages of using dynamic modelling of floor heating systems coupled to a ground coupled floor model will be shown. Different parameters are investigated with the purpose of being able to design low energy houses based on predictions made by the model. Finally, conclusions will be drawn towards the design of energy efficient floor heating systems.

Model of floor construction

The general design of the two-dimensional model of the slab on grade floor can be seen in Figure 1. The model has correct geometrical inclusion of the floor construction with floor heating pipes and foundation. It is possible to change constructions, material properties and dimensions according to the actual floor construction. In addition to the floor construction, the surrounding ground volume has been included to be able to find the heat loss from the floor construction to the ground through the entire slab and through the foundation.

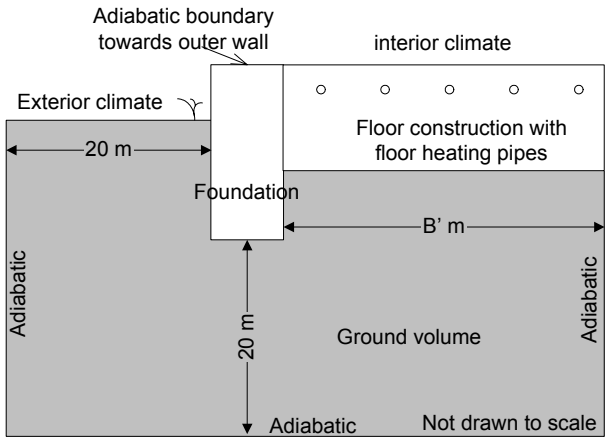

Figure 1 Two-dimensional model of slab on grade floor construction used in FHSim. The width of the floor construction is equal to the characteristic dimension of the building. The actual design of floor construction and foundation is freely created.

The characteristic dimension is used as the width of the floor construction to include three-dimensional effects of the actual building. This approach has been shown to give good agreement between two- and three-dimensional calculations for models without floor heating.

Floor heating is integrated in the form of a hydronic floor heating system. The pipes are included as physical areas, where the temperature in the pipe is based on the flow, supply temperature and cooling from the fluid to the surrounding concrete. The round geometry of the pipe is approximated by introducing a thermal resistance between the four sides of the pipe and the surrounding concrete. Therefore the importance of such factors as pipe distance and placement in the construction can be accurately investigated. Consequently, the model can be used to model arbitrary floor heating systems and constructions in combination, to investigate the implications on temperatures and energy consumption when using floor heating.

The model is implemented using a finite control volume approach [29] where only heat transfer is considered. The model uses constant values for material properties. As described in the introduction the use of constant material properties will cause the predicted heat loss to the ground to be underestimated compared to a model where heat and moisture has been coupled.

Like for the material properties, simple boundary conditions are applied. Towards the ground surface a convective heat transfer with constant surface resistance has been applied. As described in the introduction, this simplification is expected to influence the results for the amplitude of the temperature in the ground volume close to the ground surface, while the average temperature during the year is not expected to be influenced [14, 15]. This will cause a small underestimation of the heat loss.

To ensure undisturbed boundary conditions from the far field, the ground volume is extended 20 m downward and outward from the floor construction, where adiabatic boundaries are applied. This approach has been chosen based on descriptions in EN ISO10211 [17, 18].

The internal boundary condition from floor surface to the room is a combination of convection with room air and radiation exchange with internal surfaces, which will be described further below.

Building energy simulation model

The model of the floor construction can be used in a modular simulation model of the thermal conditions in a room with floor heating under dynamic influence from measured weather data. The model considers heat transfer with constant material properties. The single zone room model includes detailed calculation of radiation exchange between internal surfaces based on view factors, which is important when modelling floor heating, as the room is heated mainly by radiation. Walls, ceiling, floor and windows are modelled using a finite control volume method with an implicit solution scheme. Except for the two-dimensional floor construction, the models are one-dimensional. The ventilation system is a simple balanced system optionally with heat recovery. Hourly weather data (measured or from a design reference year) can be used as input. The model is implemented in a simulation program with models for walls (including internal distribution of solar radiation), ceiling, floor, ventilation, room, and weather data called FHSim for Floor Heating Simulation.[1] Using this program, floor heating can be modelled in detail to find the energy consumption and heat loss to the ground while at the same time being able to include the dynamic coupling to the room model.

[1] FHSim is a program for modelling the energy flows and temperatures in rooms equipped with floor heating systems. The program has been developed at the Department of Civil Engineering at the Technical University of Denmark

Validation of ground coupled floor heating model

The validation of the ground coupled floor heating model will be presented in this section. Initially a description of the house and the measurements will be made before the procedure is described and results shown.

Description of house and measurements

The validation of the numerical model of the floor construction has been performed for a well insulated wooden frame single-family house in Bromölla, Sweden. The house is L-shaped with a size of 137m².

A partial floor plan of the house is shown in Figure 2 indicating measurement positions. Figure 3 shows the foundation and floor construction as well as measurement points. The measurements are performed in the living room, which is appended as an L-shape to the house. The reason for using the living room was, among others, that no installations would disturb the measurements. Two main measurement positions were used – one under the central part of the floor and one under the outer wall/foundation.

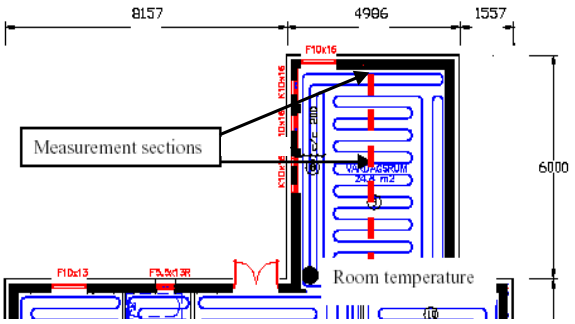

Figure 2 Partial floor plan of the house in Bromölla, Sweden, showing the vertical position of the measurements

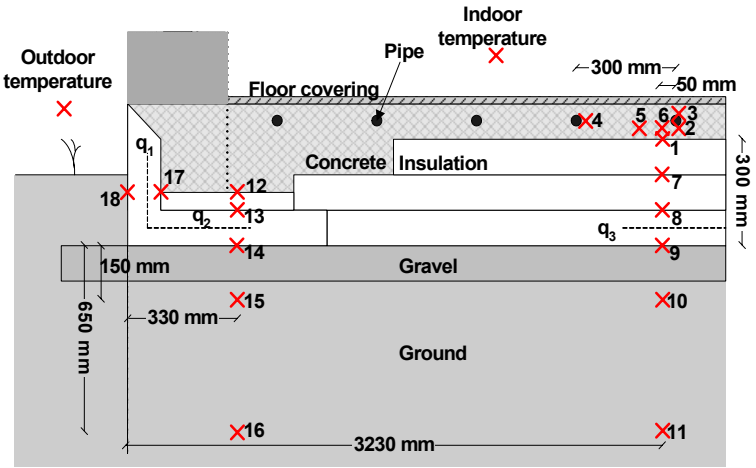

Figure 3 Vertical view of foundation and floor construction of house in Bromölla, Sweden. Measurement of temperatures is marked with x'es, while the heat flow meters are indicated by dotted lines. Notice the figure is not drawn to scale

18 temperatures in the floor and ground below have been recorded, along with indoor and outdoor temperatures. The heat flux to the ground has been measured in three positions using heat flow meters. In addition, measurements were recorded for flow, supply, and return temperature in the floor heating system. In total, hourly data of a little more than three years exist from August 20-1999 until September 30-2002. Figure 4 shows measured outdoor, room air

and mean pipe temperature. The measurement accuracy is ±0.3K for temperature and ±5% for the heat flow meters.

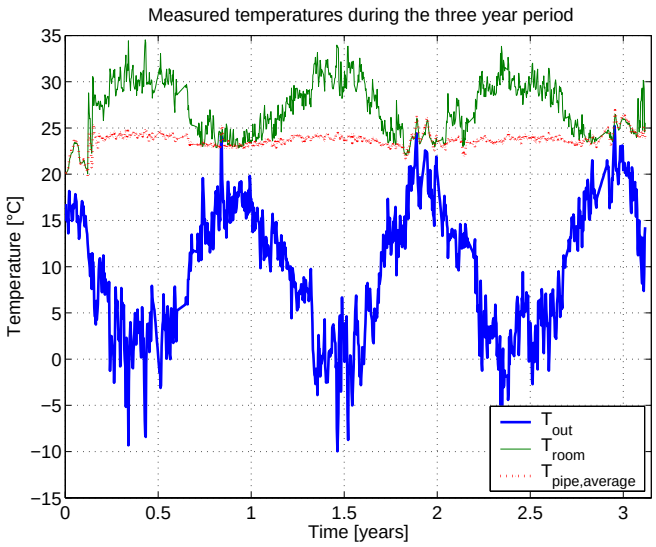

Figure 4 Outdoor temperature. The time zero corresponds to August 20, 1999. Data are shown as daily average values.

One very important aspect of the measurements must be emphasized; the measurement sections are placed under the living room, which is only 5.0m wide. This means that the conditions are very much under the influence of three-dimensional conditions, which consequently cannot be neglected. This will influence temperatures, heat flows and time delay for the outdoor climate to impact the measurement positions in the ground volume.

Validation procedure for the floor model

A validation procedure based on the comparison of measured and simulated heat flows in the floor construction is used along with a comparison of temperatures in the ground volume. As described in the introduction, large differences can be expected between two- and three-dimensional conditions. The heat flows are compared by using a two-dimensional model using the characteristic dimension of the building, defined in Eq. (1), as the width of the model. With an area of the L-shaped living room of 24.8m² and a perimeter of 22m, the characteristic dimension is therefore 2.25m. The measured hourly values of outdoor, indoor and mean pipe temperature have been used as input.

Table 1 Material data used in simulation model of floor construction and ground volume

Material	Thermal conductivity [WmK]	Heat capacity [kJ/m³K]
Ground	1.5	2000
Gravel	0.7	2000
Insulation (foundation)	0.033	42
Insulation	0.043	42
Insulation (between concrete and foundation)	0.039	42
Concrete	1.7	1620

The material properties used for the modelling of the floor model are shown in Table 1. The values for all insulation materials, density, specific heat capacity and heat transfer coefficient are based on data supplied by the manufacturer. Material data for the ground soil have been estimated according to literature [14, 30], with respect to temperature, amount of rain, moisture content and composition and type of soil for Bromölla, Sweden.

For the validation of the floor model, the internal boundary condition between floor surface and room is applied with a fixed combined convective and radiative thermal resistance coefficient with a value of 0.1m² K/W, since only the room air temperature is known, which means that radiation cannot be taken into account. The external boundary condition between ground surface and outside conditions uses a fixed thermal resistance coefficient of 0.04m² K/W, again because of the measurement data.

The initial condition of the temperature distribution in the ground volume is unknown prior to the beginning of the measurement period. The initial temperature distribution is therefore found by applying the average indoor and outdoor temperatures during the measurement period to find a steady state solution. While this is not correct, because the building had only just been erected prior to the start of the measurement period, the temperature under the floor construction will quickly become influenced by the heating from the house. Therefore the calculated steady-state temperature distribution will be a better initial condition than one based on the average outdoor temperature without the house for the ground volume.

Comparison of heat flows

Figure 5 and Figure 6 shows the heat loss to the ground through the central part of the floor construction and the entire slab on grade floor for the measurement period. The central part of the floor is defined as the last 0.5m of the floor. As it can be seen, there is a very good agreement between measured and simulated values for both absolute values and dynamic behavior. The simulated heat loss under the central part of the floor is 5% lower than the measured, while the difference is only 2% for the total heat loss.

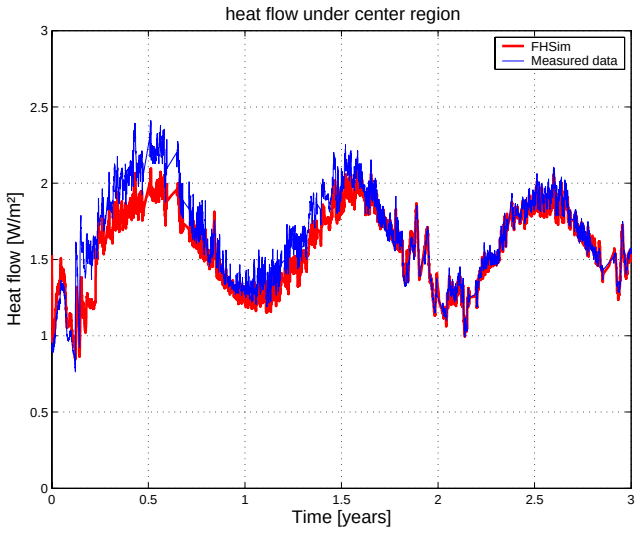

Figure 5 Heat flow from under the central part of the floor construction to the ground

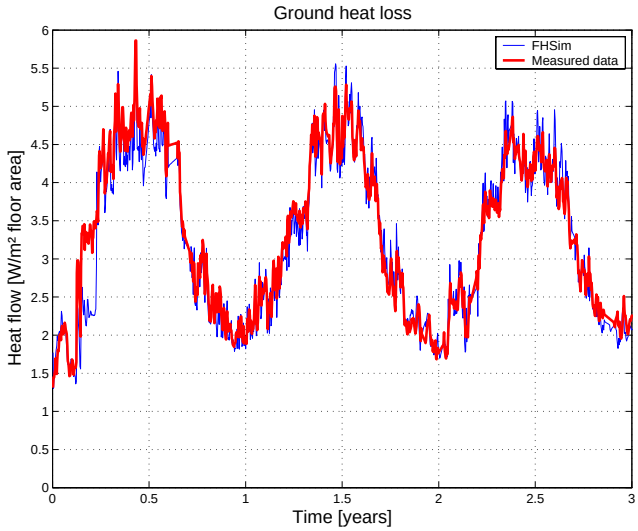

Figure 6 Total heat loss through the entire slab to the ground

Figure 7 shows the heat flow from the floor heating pipe for two periods. Here it can be seen that the model tends to overestimate the heat flow in one of the periods, while it is close to the measured in the other period. In total the simulated heat flow is around 14% larger than the measured. The fairly large discrepancy is due to the simple boundary condition which is needed since only the room temperature is measured. The heat flow to the room is not determined as accurately as it would be if both radiation and convection were included in the measurements. Therefore small changes in the conditions in the room will have large influence on the heat flow to the room and consequently also from the pipe. However, the dynamic behavior is good while the absolute value is also close to the measured.

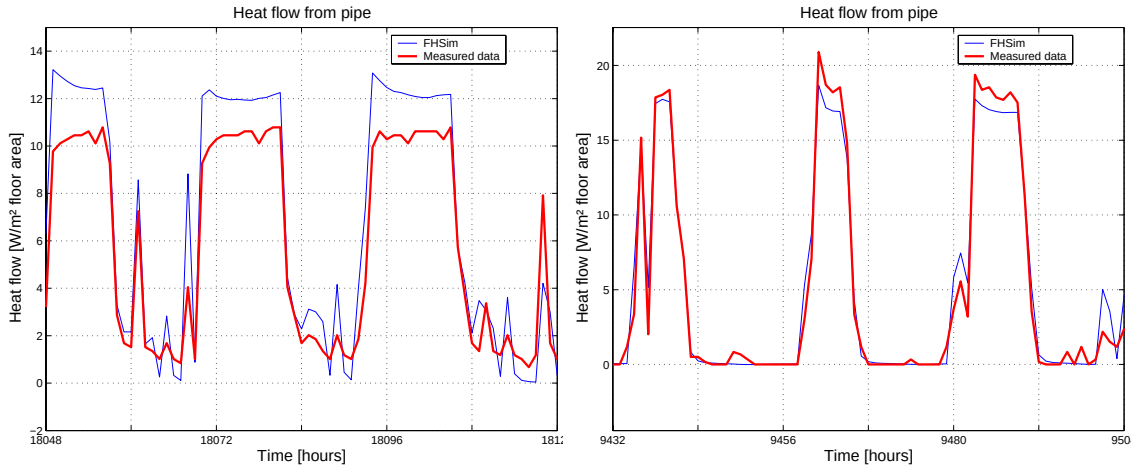

Figure 7 Calculated and simulated heat flow from pipe shown for two periods of three days

Comparison of temperatures

Figure 8 shows the temperature distribution in the floor construction and ground volume immediately below. Only around 0.5 meter of ground is shown away from the foundation in the horizontal direction while 4 meters is shown in the vertical direction of the total 20 meters in each direction. The figure shows the floor construction with a width of 4.5 meters from the foundation including the measurement points 9 and 11, as shown on Figure 3. This model has only been used to compare the temperatures, not for the simulation of the heat flows where the characteristic dimension was used. As it can be seen, the isotherms are fairly one-

dimensional from the position of the characteristic dimension and further into the construction in the floor construction itself and the uppermost part of the ground volume.

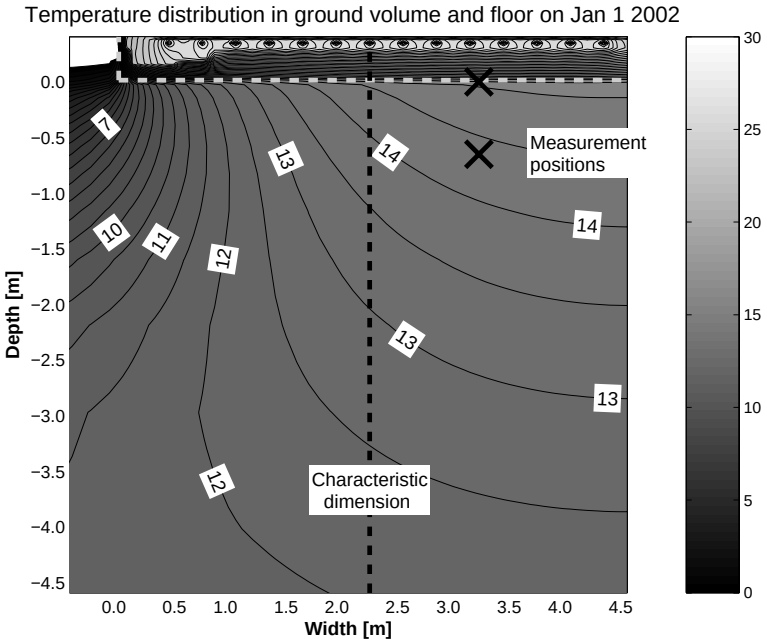

Figure 8 Simulated temperature distribution in ground volume shown for Jan 1, 2002, for a model which is wider than the characteristic dimension to be able to show the measurement positions of point 9 to 11. The outline of the floor construction is shown with the dotted grey line. The figure therefore also shows the characteristic dimension, which is used for the calculation of the heat loss to the ground. The isotherms are shown for each 0.5K.

Figure 9 shows a comparison of the measured temperature in point 9 and 11 and the simulated temperatures in the position of the characteristic dimension, using the model which is only as wide as the characteristic dimension. This comparison is possible because the isotherms are nearly one-dimensional from the point of the characteristic dimension as Figure 8 shows. Again a close agreement between the measured and simulated temperatures can be observed in both of the measurement points, especially considering the measurement accuracy of ±0.3K

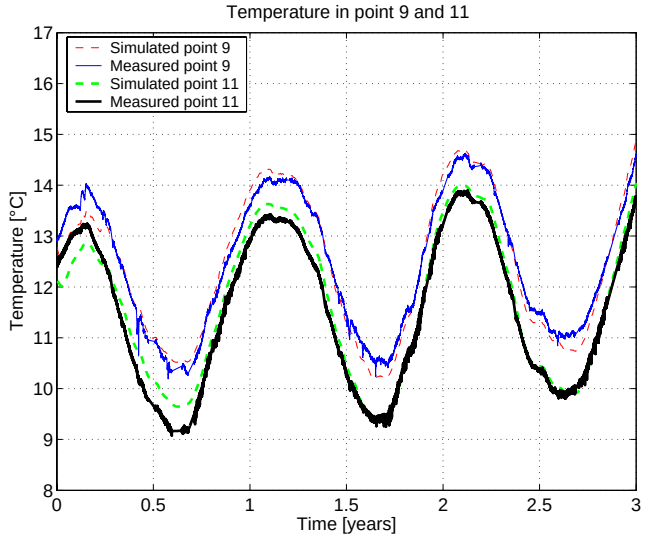

Figure 9 Comparison of temperature in the ground volume under the central part of the floor construction in measurement point 9 to 11

Returning to Figure 8, an illustration of the importance of correct geometrical implementing the floor heating pipes can be seen. Firstly the temperature in the concrete slab is not uniform, especially close to the outer wall because of the different conditions in the central part of the floor and near the outer walls. Secondly the temperature below the floor is not uniform and therefore a one-dimensional model will have difficulties modelling this.

The importance of correct dynamical implementation has been investigated by using a constant temperature in the floor heating pipe as opposed to a dynamical one. EN IOS 13370 prescribes the use of a constant pipe temperature for calculating the heat loss to the ground when the floor is heated. This constant temperature must be found based on the expected required heat supply to the room. However, this value is difficult to estimate. Therefore two simulations using constant temperatures have been tested: One using the measured average pipe temperature of 24.8°C and one using 30°C. The latter is to model a situation where the average temperature in the slab is guessed. Figure 10 shows the calculated ground heat loss for two simulations compared to the measurement data. As it can be seen, both models overestimate the heat loss during the summer periods (with low heat loss) while especially the model using the average pipe temperature of 24.8°C underestimates the heat loss during the winter periods (with high heat loss). In total the simulation with average pipe temperature predicts a 2% lower heat loss to the ground and the model with 30°C finds a 23% higher heat loss. The last one shows the need for an accurate estimate of the average pipe temperature. For the model using the average pipe temperature, it is obvious that even though the model finds an average heat loss that is very close to the measured value, the heat loss is underestimated during the winter period, where it is most important to find accurate values for the heat loss. The fact that the dynamical implementation of the floor heating pipe both finds the most accurate value and does not need to use an estimate of the average temperature clearly illustrates the advantage of using a dynamical model.

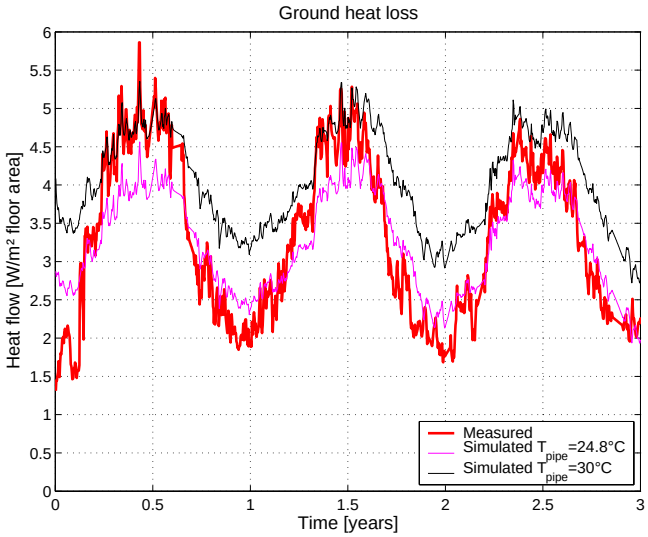

Figure 10 Ground heat loss using a constant pipe temperature as input in the simulation model, using the average temperature during the measurement period and 30°C shown together with the measured heat loss

Based on the comparison of the measured and simulated heat flows and temperatures, it can be seen that the simulation model used here is able to fully predict the conditions for both heat flows and temperatures.

Parametric analysis

The validated floor model is used together with the building model in FHSim to simulate the interaction between the floor heating system and the house to find the thermal indoor climate and energy consumption as well as the heat loss to the ground. The purpose of the investigation is to find the influence of the linear thermal transmittance of the foundation and the thermal transmittance of the floor construction in a dynamical simulation using the Danish Design Reference Year as input.

A somewhat different model of foundation and floor construction than above has been used. However, as it is based on the same numerical scheme, the validation is assumed general. In the investigation six different insulation thicknesses in the floor construction and three different levels of insulation in the foundation has been used for the parametric analysis. The insulation of the foundation has been altered by changing the thermal conductivity of the insulation material in the foundation, thereby maintaining the geometry of the foundation.

Room model

A simple reference room for the parametrical analysis has been created. The well insulated square room of 36m² has two outer walls each with a 4m² window. The ventilation system is a simple balanced system with an airchange rate of 0.5 times an hour and an infiltration rate of 0.1 times an hour. It was chosen not to include a heat recovery unit on the ventilation system. This is a de-facto requirement for energy efficient houses, but here it was omitted to see the effects of changing the parameters more clearly. A supply temperature of 40°C to the floor heating system has been used and a set point temperature of 21°C controlled by an on/off type control. The remaining inputs to the model are shown in Table 2. In the simulations a fixed value of the characteristic dimension of 4.6 meters has been used. This does not correspond to a building with the dimensions given here, but to a larger one. However the results are valid for a room of this size placed in a building with a characteristic dimension of 4.6 meters.

Table 2 Simulation input for reference room model used in the parametric analysis

Parameter	Area [m²]	U-value [W/m²K]
Outer walls	22	0,18
Window	8	1,50
Inner walls	32	-
Roof	36	0,12
Floor	36	0,12
Ventilation & Infiltration		$0{,}5\ h^{-1} + 0{,}1h^{-1}$
Internal heat load		5W/m²
Control strategy of heating supply		On/Off
Supply temperature		40ºC
Set point temperature		21ºC
Weather data (Danish reference year)		DRY

Because of the influence of the orientation of the room, two simulations are carried out with a south/west and a north/east orientation of the outer walls. An average of the energy consumption for the two orientations is used for the comparison of the results. The difference in the energy consumption is typically 20%.

Figure 11 shows the slab on grade floor, which is a sandwich construction with two concrete decks around the insulation layer. The floor heating system is placed in the upper concrete deck, with a pipe distance of 300mm. The floor covering is a 20mm wooden floor. The simulations have been allowed to run for several years to ensure periodic stationary results before the final results have been extracted from the simulations.

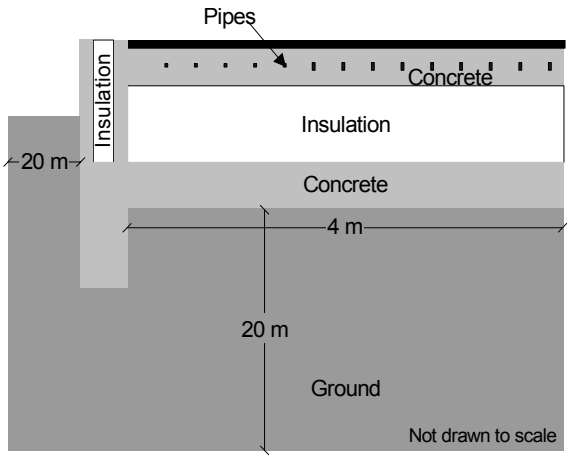

Figure 11 The simulation model of foundation and floor construction. Pipe distance 300 mm. Not drawn to scale.

Calculation of linear thermal transmittance and thermal transmittance

The linear thermal transmittance of the foundation, $\psi_{foundation}$, has been found using a dynamical simulation with a seasonal variation of the outdoor temperature and a fixed indoor temperature. The heat loss is split into two components: the heat loss under the central part of the floor and the heat loss through the entire floor and foundation. The two components are compared and the heat loss, which cannot be attributed to the heat loss through the central part of the floor, is considered to be through the foundation and is consequently the linear thermal transmittance. Floor heating is omitted in the calculation of the size of the linear thermal transmittance. This value is only used to characterise the floor construction and has not been included in the simulations as an input since the foundation already included in the geometric definition of the floor model.

The thermal transmittance of the floor construction, U, has been found as the sum of the one-dimensional resistances from the floor surface to the bottom of the floor construction. The inside and ground surface resistances have also been included.

Results

Linear thermal transmittance and U-value

The higher floor temperature compared to other heating systems increases the heat loss through the foundation. Figure 12 shows the yearly energy consumption as a function of the thermal transmittance, U, for three different values of the linear thermal transmittance, $\psi_{foundation}$. A linear correlation between energy consumption and U-value can be observed in all three cases with a significant influence on the energy consumption. It can be seen that regardless of the U-value savings in the energy consumption can be expected when improving the foundation. In this example, the energy consumption is the same for a $\psi_{foundation}$-value of 0.41W/mK and a U-value of 0.08W/m²K as with a $\psi_{foundation}$-value of 0.25W/mK and a U-value of 0.19W/m² K. Therefore, these results show the foundation should be carefully designed in new houses with floor heating regardless of the insulation thickness in the floor.

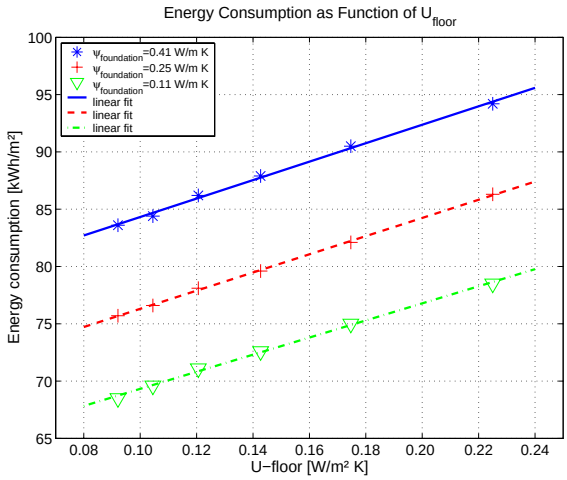

Figure 12 Annual energy consumption as function of U-value of the floor construction

Heat loss to the ground

The heat loss to the ground through the slab on grade floor is larger for houses with floor heating than for houses with other heating sources. Figure 13 shows the heat loss to the ground with and without floor heating for different U-values for the entire year and for the heating season only (September to May). In order to compensate for the larger heat loss caused by the floor heating, extra insulation can be used. If a U-value of 0.2W/m² K of the floor construction in houses without floor heating is considered, this can be seen to result in a heat loss to the ground of around 11kWh/m² during the heating season. In order to get the same heat loss in a house with floor heating, the U-value of the floor constructions must be reduced to around 0.11W/m² K. This is equal to an extra insulation thickness of app. 150mm. If the heat loss for the entire year is used, the U-value should only be lowered to 0.14W/m²K, corresponding to 75mm.

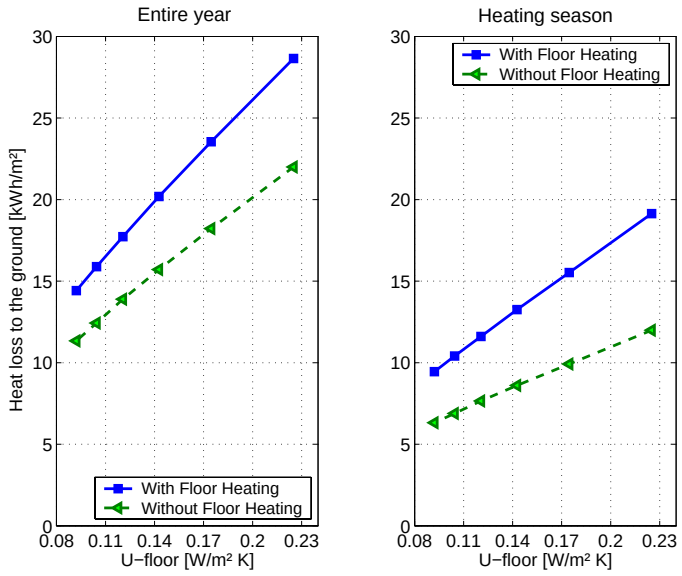

Figure 13 Heat loss to the ground for the entire year (left) and for the heating season (right) as a function of the U-value of the floor construction using models with and without floor heating. A $\psi_{foundation}$ of 0.11W/mK has been used for the simulations

Discussion

In this paper, a two-dimensional model of a house with floor heating has been implemented in order to find the thermal behaviour of the floor with floor heating in contact with both ground volume and house. The scope of this is to create a simulation model of a floor construction with floor heating as part of a building energy simulation program. Normally the coupling to the ground is not included, which means that the influence of the foundation cannot be found. This latter part is shown in this paper to have a large impact on the energy demand for heating, which is influenced by the floor heating system.

The two-dimensional model has been validated against measurements from a building in Bromölla, Sweden, with good results, in spite of a number of limitations with respect to the level of details, such as constant thermal properties and simplified boundary conditions for the ground surface. By introducing the characteristic dimension of the floor, which is defined as the floor area divided by half the perimeter of the building, the comparison of measured and simulated heat flows and temperatures shows that the model is fully able to predict the heat flows. In particular the characteristic dimension has been found to be useful, also for heated floors. This has not previously been shown.

One very interesting aspect of the measurements is that they have been made for a very small and narrow building, which is very much under the influence of three-dimensional conditions. Consequently, the accurate prediction of heat flows and temperatures suggests that larger buildings can also be modelled accurately based on this model and using the characteristic dimension.

At the same time such a dynamic model can be directly used in a building energy simulation program, where the strengths of the accurate implementation of the geometry can be used to find the effect of changing different parameters in the floor construction.

In addition, it has also been shown to be important to use a dynamical simulation of the temperature in the floor heating pipe to accurately find the heat loss to the ground if both accurate average and maximum heat flows are needed. Normally an average value of the temperature of the heated floor is used. However this value is difficult to estimate, as this value depends on a long list of factors, including the energy consumption of the house and the thermal resistance between the floor heating system and room and small errors in this estimate leads to large differences in the predicted heat loss to the ground.

The model, which has been implemented in this paper, can be used to model the influence from foundation and floor construction on the energy consumption and heat loss to the ground by coupling the floor model to a room model. Using this integrated model, dynamical simulations of room and floor heating system can be performed. Here the influence of the insulation in the floor construction and foundation has been shown to be important for the energy consumption for the house.

The drawback of the model is that it is slow and requires a large number of inputs. The model can therefore be seen as a step towards implementing detailed hydronic floor heating systems in energy simulation programs. An investigation is underway to test different approaches for simplifying the models while maintaining the dynamic properties and ground coupling, or alternatively to quantify the error introduced by using simpler models.

Conclusion

In this paper a two-dimensional ground coupled floor heating model has been validated against measurements that are heavily under three-dimensional influence as a very narrow building has been used. By introducing the characteristic dimension (the area divided by half

the perimeter) of the floor construction in the model, it has been shown to give accurate predictions of the heat loss to the ground. The characteristic dimension has not been tested on heated floors, but here it is shown that it is also valid for these.

It has also been shown that an accurate dynamic implementation of the floor heating pipe is required to accurately find heat loss to the ground, while using the average concrete temperature cannot fully account for dynamical and absolute values of the heat loss. At the same time, the model of the floor construction can be used together with a room model to find the energy consumption from a house with floor heating. In this paper the influence on the design of the floor construction has been found. Especially the foundation has been found to have a large influence on the energy consumption and heat loss to the ground.

Acknowledgement

The work presented here has been supported by a grant for the measurements on the house in Bromölla, Sweden, by the knowledge foundation and a part of the producer of thermal insulation (polystyrene) and a grant from Danish Energy Agency for the calculations of energy efficient floor heating. Also, thanks to Professor Johan Claesson from Chalmers Technical University for helping to develop the method of comparing two- and three-dimensional heat flows by creating a difference function.

References

[1] Claesson J, Hagentoft C-E: Heat loss to the ground from a building – I. General Theory, *Building and Environment*, 1991, Vol. 26, No. 2, pp. 195-208

[2] Comini G, Nonino, C: Thermal Analysis of Floor Heating Panels, *Numerical Heat transfer*, Part A, 1994:26:537-550.

[3] Ho SY, Hayes RE, Wood RK: Simulation of the Dynamic Behaviour of a Hydronic Floor heating System, *Heat Recovery Systems & CHP*, 1995, Vol 15., No. 6, pp. 505-519

[4] CEN: EN ISO 1264: Floor Heating – Systems and components. European Committee for Standardization, 1997, CEN

[5] Cho, S-H, Zaheer-uddin M: Predictive Control of Intermittently Operated Radiant Floor Heating Systems, *Energy Conversion and Management*, 2003, Vol. 44, pp. 1333-1342

[6] Chen Y, Athienitis, A K: A Three-Dimensional Numerical Investigation of the Effect of Cover materials on Heat Tranfser in Floor Heating Systems, *ASHRAE Transactions. Proceedings of the 1998 ASHRAE Annual Meeting*, 1998, Vol.104 Issue.2, pp. 1350-1355

[7] Fort, K: Dynamisches Verhalten Von Fussbodenheizungen. 1989, ETH Zürich. Juris Druck + Verlag Zürich

[8] Fort, K: The dynamic behaviour of floor heating systems, *Fuel and Energy Abstracts*, 1996, Volume 37 Issue 5, p. 377

[9] Weitzmann P, Kragh J, Jensen C F: Numerical Investigation of Floor Heating Systems in Low Energy Houses. *Proceedings of the 6th Symposium on Building Physics in the Nordic Countries*, 2002 Trondheim, Norway, pp. 905-912

[10] Adjali MH, Davies M, Rees WS, Littler J: Temperatures in and under a slab-on-ground floor: two- and three-dimensional numerical simulations and comparison with experimental data. *Building and Environment*, 2000, Vol. 35, pp. 655-662.

[11] Davies M, Tindale A, Littler J: Importance of multi-dimensional conductive heat flows in and around buildings. *Building Serv eng Res Technol* 1995. Vol. 16, pp. 83-90

[12] Anderson BR: Calculation of the Steady-State Heat Transfer through a Slab-on-Ground Floor. *Building and Environment*, 1991, Vol. 24, No. 4, pp. 405-415

[13] Hagentoft, C-E: Heat Loss to the Ground from a Building. PhD thesis, 1988, Lund University of Tehcnology.

[14] Janssen H, Carmeliet J, Hens H: The Influence of Soil Moisture in the Unsaturated Zone on the Heat Loss from Buildings via the Ground. *Journal of Thermal Envelope and Building Science*, 2002, Vol. 25, No. 4, pp. 275-298.

[15] Janssen H, Carmeliet J and Hens H: The influence of soil moisture transfer on building heat loss via the ground. *Building and Environment*. 2004, Vol. 39, pp. 825-836

[16] ISO/CEN: EN ISO13370 – Thermal performance of buildings – Heat transfer via the ground – calculation method. 2000, CEN

[17] CEN: EN ISO 10211-1: Thermal bridges in building construction – Heat flows and surface temperatures – Part 1: General calculation methods. 1994, CEN

[18] CEN: EN ISO 10211-2: Thermal bridges in building construction – Heat flows and surface temperatures – Part 2: Calculation of linear thermal bridges, 1995, CEN

[19] Delsante A E: Comparison between measured and calculated heat losses through a slab-on-ground floor. *Building and Environment.* 1990, Vol. 25, pp. 25-31

[20] Lefebvre G: Modal-based simulation of the thermal behavior of a building: the $m2^m$ software. *Energy and Buildings*, 1997, Vol. 25, pp. 19-30.

[21] Davies M, Zoras X and Adjali M H: Improving the efficiency of the numerical modelling of built environment earth-contact heat transfers. *Applied Energy*, 2001, Vol. 68, pp. 31-42.

[22] Pan S and Pal J: Reduced order modelling of discrete-time systems. *Applied Mathematical modelling*, 1995 Vol. 19 March, pp. 133-138

[23] Hsieh C-S and Hwang C: Model reduction of continuous-time systems using a modified Routh approximation method. *IEE Proceedings*, 1989, Vol. 136, Pt. D, No. 4, July

[24] Ménézo C, Rox J J and Virgone J: Modelling heat transfers in building by coupling reduced-order models. *Building and Environment*, 2002, Vol. 37, pp. 133-144

[25] Adjali MH, Davies M, Ni Riain C, Littler JG: In situ measurements and numerical simulation of heat transfer beneath a heated ground floor slab. *Energy and Buildings* 2000:22:75-83.

[26] Youcef L: Two-Dimensional Model of Direct Solar Slab-on-Grade heating Floor, *Solar Energy*, 1991, Vol. 46, No. 3, pp. 183-189

[27] Chuangchid P and Krarti M: Foundation heat loss from heated concrete slab-on-grade floors. *Building and Environment*, 2001 Vol. 36, pp. 637-655

[28] European Parliament: Directive 2002/91/EC of the European Parliament and of the Council of the 16 December 2002 on the Energy Performance of Buildings. 2003, Official Journal of the European Communities. L 1/65.

[29] Patankar S V: Numerical heat transfer and fluid flow. 1980, New York: Hemisphere

[30] Farouki, O T: Thermal Properties of Soils, *Series on Rock and Soil Mechanics*, 1986, Vol. 11, Trans Tech Publications, Germany.

Paper 3

Simulation of temperature in office with building integrated heating and cooling

Peter Weitzmann

In: Proceedings of the Sixth Symposium on Building Physics in the Nordic Countries, pp. 897-904. 2002

Simulation of Temperature in Office with Building Integrated Heating and Cooling System

Peter Weitzmann, Ph.D.-student, Msc(Eng)*

1. INTRODUCTION

Present day (2002) office buildings are designed in such a way, and have such high internal heat loads and solar gains, that some kind of cooling is normally necessary for most of the year. Even in as cool climates as the Nordic countries. The way the cooling is often achieved is through air cooling, which has a high energy consumption when used for cooling.

Another cooling method is to use building integrated cooling in the concrete slabs in the floors between storeys in the building. This technique utilizes the thermal mass of the concrete to absorb heat from the room. The heat is removed from the slabs by integrated PEX pipes with cool water. By thereby maintaining the temperature of the concrete to a level slightly below the desired room temperature, the concrete will work as an absorber for the excess heat in the office. This can significantly reduce the need for air cooling, which will give both improved indoor climate and lower energy costs in the building. At the same time, the building integrated system can also heat the office during cold periods. Using the concrete slab for cooling and heating the rooms in the building can also be called "activating the building core", or that the floor is "thermo active". The latter term will be used as well as "building integrated heating and cooling system" in this paper.

The ventilation system can then be designed only to supply enough air to the room to meet the requirements for acceptability of the air quality.

Building integrated heating and cooling is used mainly in office buildings in Germany and Switzerland (Meierhans), (Olesen, 2000). In (Olesen, 2000) a number of different buildings are presented, among these are an art museum and an office building with an almost 100 % glass façade. This indicates the span of different building types the building integrated heating and cooling system can be employed in.

In this paper, the principle of thermo active heating and cooling is presented. Furthermore, the temperature in an office is examined for various window glazings, heat loads, different control strategies and supply temperatures for the cooling water. In addition, the dynamics of the thermo active component is shown. The analyses are performed by a numerical investigation of the thermal indoor environment in an office with building integrated hydronic heating and cooling system.

2. GENERAL DESCRIPTION OF THERMO ACTIVE COMPONENTS

A thermo active component, or a building component with integrated heating and cooling system, can be seen in the figure below. This model is based on a hollow block floor, which is typically used in Danish office buildings. The hollow block floor, with and without integrated heating and cooling is shown in Figure 1

* Technical University of Denmark, Department of Civil Engineering, Brovej, Building 118, DK-2800 Lyngby, Denmark, pw@byg.dtu.dk

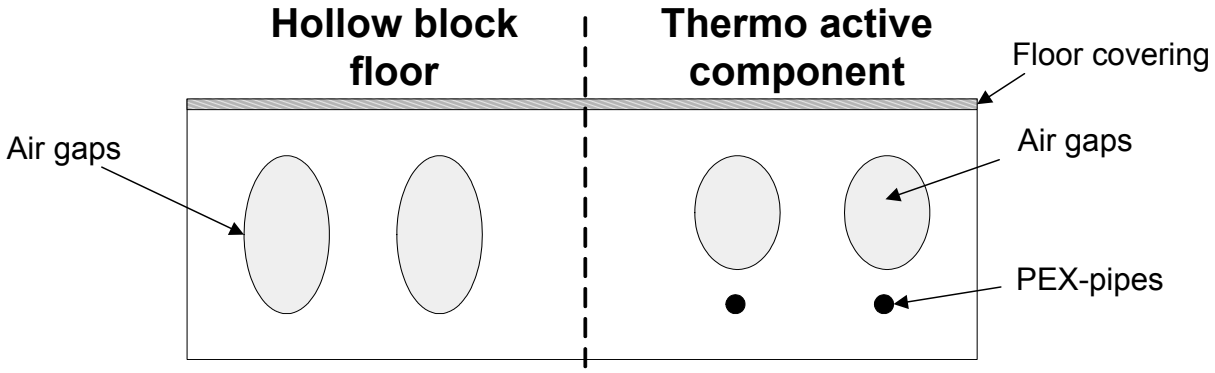

Figure 1 Section of hollow block floor. On the right side, as it is normally built, and to the left as a thermo active component. Not drawn to scale

As it can be seen, the pipes are in the bottom half of the construction, which means, that the primary exchange of energy with the surrounding rooms will be through the ceiling. This is also the best way to remove energy from the room, since the convective heat transfer coefficient is higher for cooling through the ceiling than through the floor (Olesen, 2000).

The principle of the thermo active component is then, that water at close to the desired room temperature is circulated in the PEX-pipes to keep the temperature of the concrete lower than the room temperature in case of cooling, or higher than the room air temperature in case of heating.

In addition, the system works by shifting the time when heat is absorbed from the room, to the time heat is removed from the construction through the pipes from the daytime to the night time. This fact makes the thermo active component attractive in terms of free cooling, where the cool night time air is used for cooling the water in the pipes. This is however not discussed further here.

Further, the thermo active component has the advantages, that the installations are hidden so no radiators can be seen, and the ventilation system does not have to be dimensioned to be able to cool the air – or rather, an air cooling system can be avoided.

The disadvantages are, that the construction makes it impossible to use suspended ceilings for acoustics and lighting, and that the maximum heat that can be removed from the room is not as large as in an air conditioned office.

3. SIMULATION MODEL

To examine building integrated heating and cooling systems, a simulation model has been created and implemented in Matlab. The model is able to calculate heating and cooling demand, temperatures and thermal comfort parameters.

The simulation model can be used for calculating situations with both cooling and heating demands. Using the model, it is therefore possible to assess the thermal environment, and furthermore to calculate the energy consumption required for both heating and cooling. In 3.2, the model is presented. The program is called TASim for **T**hermo **A**ctive **Sim**ulation.

3.1 Existing simulation tools

Starting out, it was attempted to find a program that could perform simulations of thermo active components, and their influence on the thermal indoor climate. While it was no problem to find programs that could do either the detailed calculations of the thermo active components, or programs that could do calculations of the thermal indoor climate and heating/cooling demand for buildings, a program that could couple both parts did not exist.

An example of the former is Heat2 (Blomberg, 2000), and for the latter BSIM2000 (Wittchen et al., 2000).

An obvious choice would be to use TRNSYS (Klein, 1996) for the development of the simulation model, but because it is difficult to use for inexperienced programmers, in case of developing new functionality, it was chosen not to use TRNSYS. Therefore, it was necessary to develop a model of the building with the thermo active component, and implement it into some kind of simulation program. It was decided to use Matlab (Mathworks, 2001) as the programming language, since it is easy to use, even for inexperienced programmers.

3.2 TASim – Thermo Active Simulation

The functionality of the program TASim is shown in Figure 2.

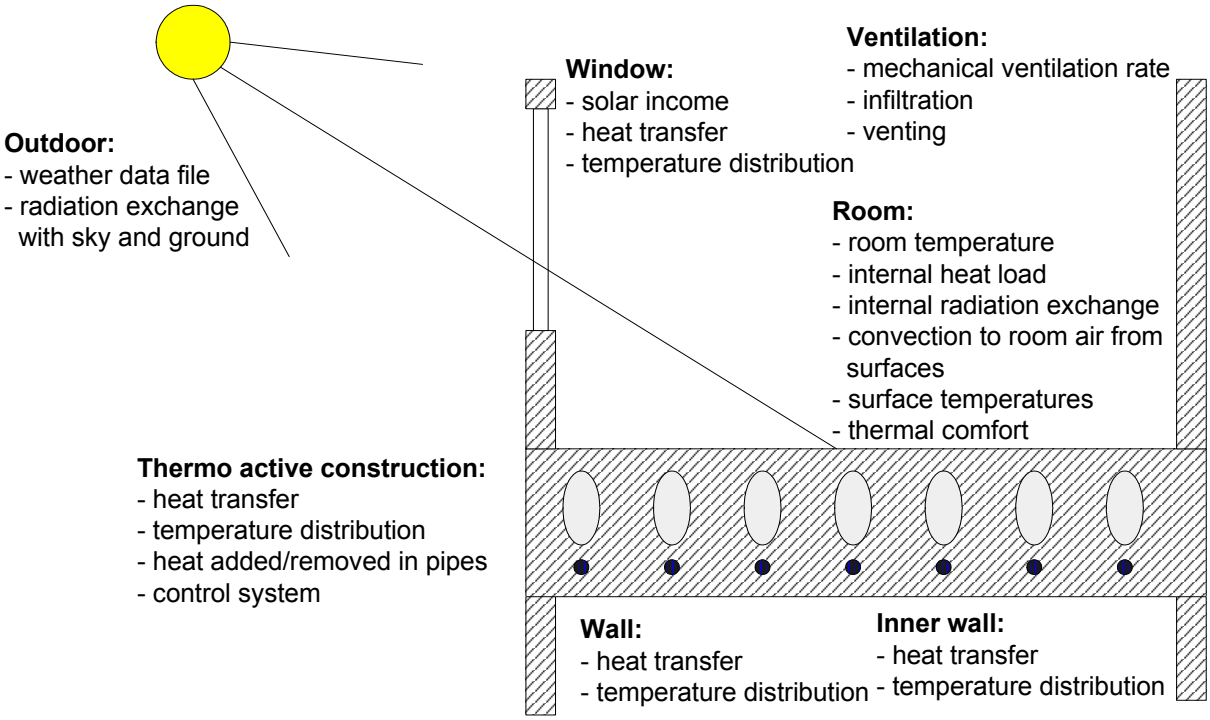

Figure 2 Functionality of TASim based on the different parts of the program

As it can be seen from Figure 2, it is a rather complex model that is used. The calculations use dynamic conditions based on a weather data file for the outdoor temperature, solar radiation and sky temperature. In the walls, inner walls and windows calculations of the heat transfer and temperature distribution are performed using a Finite Control Volume model. For the windows, the transmitted and absorbed solar radiation is also found based on the solar radiation from the weather data file. The ventilation system is a simple balanced mechanical system with a fixed ventilation rate. In addition, infiltration and venting is included in the model.

The room air temperature is calculated using an energy balance for the heat fluxes to the room, the solar gains (of which 30 % is given as a convective term to the room air), the internal heat load and the ventilation system.

The thermo active component is modelled based on a 2D section of the construction. The section shown in Figure 3, takes advantage of all possible lines of symmetry. That is, adiabatic lines are used to make as small a modelling section as possible.

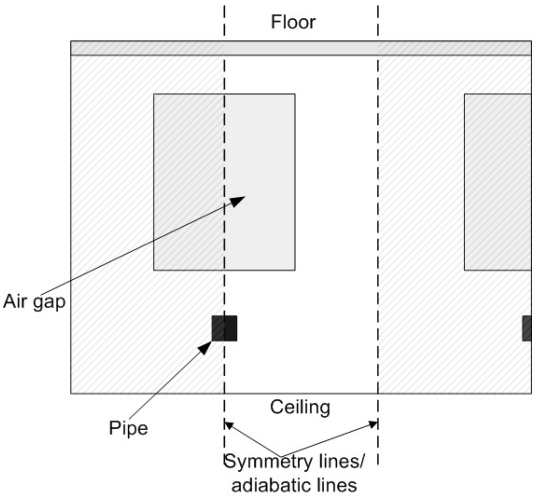

Figure 3 Section of thermo active construction used for simulation in TASim. Indicated by the lines of symmetry

Notice, that the model uses a square approximation to the real geometry. In the approximation, the cross sectional area of the air gap and pipe is the same as in the real geometry.

The model used in TASim is a single zone model for the room. This means, that only one thermo active construction is used for the modelling, and faces both ceiling and floor of the room. This approach is possible as long as it is assumed that there is an office of the same type above (or below) the offices, which is modelled.

4. SIMULATION

A simulation model of an office is created in the simulation program.

4.1 Model of office

An office with an area of 25 m times 10 m is modelled giving a total floor area of 250 m². The room height is 3.5 m. One wall of 25 m times 3.5 m is the façade, while the three other walls are inner walls, assumed to face rooms of the same type as the simulated office. A façade with 100 % glass was used for the simulations. The façade is facing south. The inner walls are of concrete with a thickness of 10 cm. The thermo active component of 320 mm in height is used, and with a pipe spacing of 280 mm, and a pipe diameter of 20 mm.

The ventilation consists of a constant air volume system that gives 2 air changes pr. hour, with a inlet temperature equal to the outdoor air temperature. Further, an infiltration rate of 0.2 air changes pr. hour is assumed.

Two control strategies are used. One where the water in the pipe is circulated all day, and one where the water is circulated only from 21.00 in the evening until 9.00 in the morning. This is to simulate the use of "free" cooling from either cool nighttime air, or radiation exchange with the night sky. Such a system design has been discussed in (Meierhans, 1996)

For the windows, a low energy window is used. It has a U-value of 1.1 W/m² K. The data for transmission of solar energy, solar light and absorbed solar energy in each of the two glazing layers is shown in Table 1. For the calculation, Glas98 was used (Pilkington, 98).

Table 1 Glazing data for windows

Type	U-value [W/m² K]	g-value [-]	light transmittance [-]	Absorptance [-]
1	1,1	0,5	0,66	0,28 (0,14 in each layer)

A solar shading of 0.2, corresponding to an outside solar shading is activated when the solar gain through the glazing surpasses 200 W/m², and is deactivated when the solar gain is lower than 175 W/m².

4.2 Heat loads

For the internal heat load the following is assumed: There can be 20 persons of 100 W (approximately 1 person pr. 12 m²) in the room, who each have one PC of 150 W. For the light 10 W/m² in total is assumed. The total heat loads are summed up in Table 2.

Table 2 Heat loads in office during daytime, nighttime, weekends. The assumed usage is shown in parenthesis.

Type	Daytime [8-18]	Nighttime [18-8]	Weekends [saturday/sunday]
Persons	1600 W (80 %)	0 W (0 %)	0 W (0 %)
Light	2000 W (80 %)	250 W (10 %)	250 W (10 %)
Equipment (PCs)	2400 W (80 %)	300 W (10 %)	300 W (10 %)
Total	6000 W	550 W	550 W

Of the heat loads, 50 % is added convectively to the room air, and 50 % by radiation uniformly distributed to the surfaces based on their area. Only 80% of the maximum heat load is assumed during the daytime, since not all persons can be expected to be present at all times.

In the model, the pipe temperature is set to a fixed temperature that does not depend on the actual heat transfer, which is done to simplify the calculations, because the system is dimensioned to have a difference between supply and return temperature of no more than 2K. The mean temperature of the fluid can be calculated by the flow and supply temperature. It is here assumed that a combination of flow and supply temperature that gives the required temperature is used.

5. RESULTS

5.1 Temperature profiles

First, the effect of using a thermo active component is shown, as it can be seen in Figure 4.

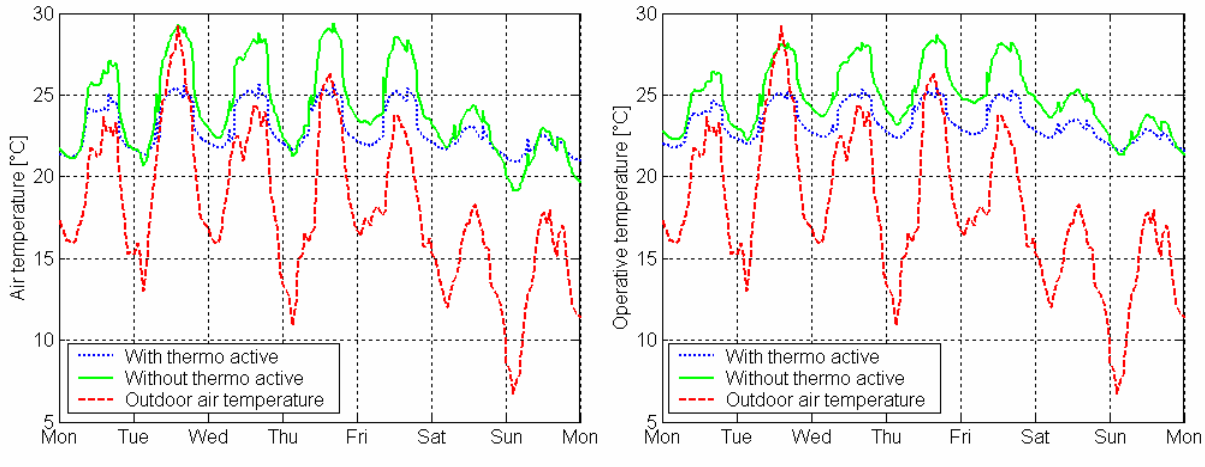

Figure 4 Temperature in room air with and without cooling on a summer week (week 27). To the left the air temperature is shown, and to the right the operative temperature. The operative temperature is determined in the middle of the room.

Two things should be noted from these figures. Firstly, the temperature in the office with thermo active cooling is lower than the temperature in the office without any cooling. This shows the effect of the thermo active cooling. In this case, a medium temperature of 22 °C is used – a lower temperature will give a lower room temperature.

Secondly, comparing air and operative temperature it can be seen that while they are nearly identical in the office without cooling – the operative temperature is lower than the air temperature for the thermo actively cooled office. This shows an important feature of thermo active cooling, namely that the operative temperature is lowered at the same room air temperature. This because building integrated systems are mainly radiant in removing/adding heat to the room.

Also, the temperature profile during the day should be noticed. It can be seen that the air temperature rises from around 20 °C in the morning to around 26 °C (or more) during the peak temperature of the day. This large temperature difference will normally not be the case in air-conditioned offices, where a more constant temperature can be upheld.

5.2 Dynamic properties

The dynamics of the thermo active construction is yet another point to comment. In Figure 5, a comparison is made between the time the heat is absorbed in the thermo active construction and the time it is removed through the pipes in the construction.

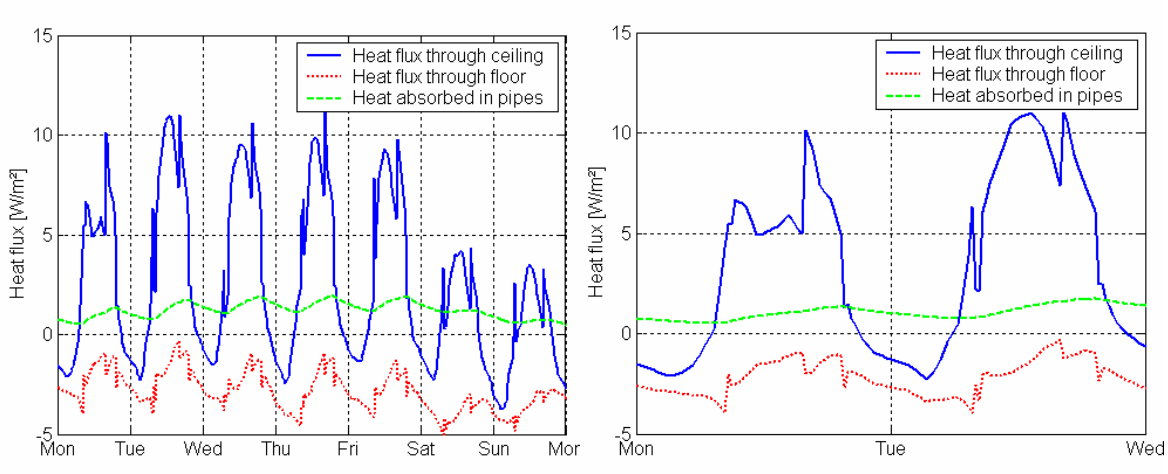

Figure 5 Heat fluxes in thermo active construction – comparison of heat flux through surface of construction and heat flux through pipe wall. Again, data for week 27 is shown. To the right, only the first two days of week 27

As it can be seen, the heat removal from the room and the heat removal from the pipes are very different in time, and also much more evenly distributed during the day than what is the case with the heat load in the room. This means, that a much more efficient cooling system can be designed, where it is not required that all heat is removed during the peak loads as with air condition systems. This point is central for the use of thermo active components.

5.3 Control strategies

Two control strategies are examined in this paper, one where the system is circulating water in the pipes at all times and one where the system is running only during the night.

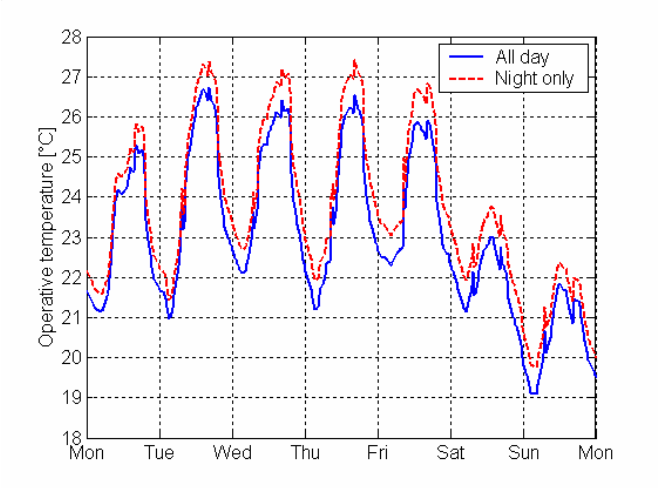

Figure 6 Operative temperature in room with different control strategies

As it can be seen, there is a lower temperature when the system is running all day compared to only during the night time. However, the difference is small, indicating, that if the supply temperature can be low enough, it will be sufficient to use only the night time for operation. This will enable the use of free cooling, where the source in normally only available during the night.

5.4 Different heat loads and supply temperatures

A series of simulations is performed with different supply temperatures, operation period and heat loads. The supply temperature was set to 19 °C and 22 °C, using the two different control strategies. Two different values for internal heat loads were used; the one shown in Table 2, and one where the heat load is twice as high. In the table below, the amount of hours with temperatures above 26 °C and 27 °C are shown. In (Dansk Standard, 1993) a maximum of 100 hours above 26 °C, and 25 hours above 27 °C is recommended.

Table 3 Hours with temperatures above 26 °C and 27 °C. Both data for operative and air temperature is shown. The period of operation is either 24 hours, or from 21 to 9 (night). The heat load is either normal as in Table 2 or high, with twice the heat load.

Supply temperature °C	Operation 24h/night	Heat load high/normal	Air temperature above 26 °C hours	27 °C hours	Operative temperature above 26 °C hours	27 °C hours
19	24 h	normal	15 h	2	0	0
22	24 h	normal	273	109	144	27
19	night	normal	74	17	6	0
22	night	normal	290	118	157	32
19	24h	high	963	655	653	370
22	24h	high	1630	1152	1489	888

Firstly, the difference between the amounts of hours over a given temperature is very different when air and operative temperature is compared.

As it can be seen there are almost no hours with the low supply temperature at 24 h operation, while the high temperature and night time only operation gives many hours with excess temperatures. Also, the high heat load gives problems. This would also be the case, if no or little solar shading were available.

It should be noted that the amount of hours with a too low temperature is not included in this comparison, which is due to the fact, that a control strategy that covers the entire year has not yet been implemented in the model.

6. DISCUSSION

In this paper, the functionality of thermo active components (or building integrated heating and cooling systems) has been examined. Initially the principle of using building integrated heating and cooling system is introduced, and the advantages and disadvantages of the system are explained. The thermo active component cools the room mainly through radiation, which means that the operative temperature in the room is lower, compared to a room with no cooling or with air condition at the same room air temperature. A simulation model is created and implemented in the simulation program TASim (for **T**hermo **A**ctive **Sim**ulation).

Using this model, it has been shown that the temperature can be held below 26 °C with the use of thermo active cooling for a large period of the time. This means that the system is able to cool the office space by means of a hydronic system, rather than using air cooling; and that both heating and cooling at supply temperatures close to room temperature is sufficient. For high heat loads, however, an air condition system is still required. This implies that the use of thermo active components in office buildings should be considered when a new building is being designed. This is especially the case, since the use of thermo active components most likely will result in a cheap building, during both construction and operation – a fact that needs to be examined further.

Presently only the cooling part of the system has been examined, which is due to the fact, that no control strategy has been employed in the simulation model, in which the entire year is covered with respect to heat loss/gains, outdoor temperature and solar income. This is an aim for further work. Also, a more direct comparison to air conditioned offices will be made. Finally, the use of free cooling to cool the circulating water or simply circulating cool air in the air gaps of hollow block floors will be examined. This work will be possible by the simulation model, which has been presented here.

7. REFERENCES

Blomberg, Thomas: Heat2. A PC program for heat transfer in two dimensions. Lund-Gothenborg Group for Computational Building Physics, Lund University, 2000

Dansk Standard. 1993. Specification of thermal indoor environment (in Danish: Norm for specifikation af termisk indeklima). DS 474. Copenhagen, Denmark. (in Danish).

Klein, S. A.: TRNSYS, Solar Energy Laboratory, University of Wisconsin – Madison, USA, 1996.

Mathworks: Matlab, 2001. For further information see: www.mathworks.com

Meierhans, Robert A.: Room Air Conditioning by Means of Overnight Cooling of the Concrete Ceiling, Ashrae, AT-96-8-2, 1996.

Olesen, Bjarne W.: Cooling and Heating of Buildings by Activating the Thermal Mass with Embedded Hydronic Pipe Systems, ASHRAE-CIBSE, Dublin 2000, 2000.

Pilkington: Glas98, 2001

Wittchen, K. B., Johnsen, K., and Grau, K.: BSim2000 User's Guide. Danish Building and Urban Research, Hoersholm, Denmark, 2000

Paper 4

Numerical analysis of heat storage of solar heat in floor construction

Peter Weitzmann, Ole Holck and Svend Svendsen

In: ISES Solar World Congress 2003 Solar Energy for a Sustainable Future.

NUMERICAL ANALYSIS OF HEAT STORAGE OF SOLAR HEAT IN FLOOR CONSTRUCTION

Peter Weitzmann, Ole Holck and Svend Svendsen
Department of Civil Engineering, Technical University of Denmark, Building 118, Brovej, 2800 Kgs. Lyngby, Denmark, Phone: +45 45 25 18 58, Fax: +45 45 88 32 82, pw@byg.dtu.dk

Abstract – In this paper, heat storage of solar heating in the floor construction of single-family houses is examined. A floor construction with two concrete decks is investigated. The lower is used as heat storage while the upper deck has a floor heating system. The potential for a reduction of the energy consumption for heating, by using heat storage in the floor construction is calculated using a dynamic simulation model of solar collector, solar tank and heat storage coupled to a building model, using the Danish Design Reference Year as input. The model calculates the performance of the solar heating system room temperature and energy consumption. A single-family house with and without heat recovery unit on the ventilation system of 130 m² with heating demand of approximately 70 kWh/m² and 40 kWh/m² is investigated. A parametrical analysis was performed for the solar collector area, and floor layouts including pipe spacing, storage materials, and distribution of insulation around the thermal storage layer. The energy consumption, reduction due to the heat storage and total performance of the solar heating system was calculated. The largest reduction of 100 kWh/m² solar collector occurred in the house with the highest energy consumption. The reduction depends on the solar collector area, distribution of the insulation thickness, heating demand and control strategy, but not on pipe spacing and layer thickness and material. Finally, it is shown that the system can also be used for comfort heating of tiled floors during the summer period.

1. INTRODUCTION

In a new EU directive on the energy performance of buildings (European Parliament, 2003), it is stated that the energy consumption in the residential and tertiary sector (i.e. public and private offices), in which the building mass has a large part, is consuming as much as 40% of the total energy consumption in the EU. Therefore, increased energy efficiency in buildings is important to be able to comply with the Kyoto Protocol. This increased energy efficiency will be implemented through the definition of the so-called energy performance of buildings. In the directive, the energy performance includes heating, hot water, cooling, lighting and ventilation and must include the thermal characteristics of the building. In the directive, the use of active solar energy will give a positive influence on the energy performance. This means, that energy from active solar energy sources can be used to improve the energy performance of buildings.

Typically decreasing the energy consumption is obtained by increased insulation thickness, low energy windows and heat recovery units in the ventilation system. However, the practise of using more insulation to reduce the heating demand is becoming increasingly difficult and expensive, since especially the outer walls are becoming thick. This gives architectonic and economic problems; architectonic because of the appearance of the thick walls and economic because the increased wall thickness requires a new and more expensive type of foundation. Therefore just adding extra insulation to the building envelope may not be the cheapest way to reduce the heating demand. (Munch-Andersen et al., 2000).

To lower the energy consumption for heating in buildings by other means than just increased insulation thickness, different types of passive and active solar heating can be used. In passive applications, the choice of glazing and windows can have a large impact on the energy performance of buildings (Nielsen et al, 2001). In Athienitis (1997), a theoretical study of passive solar utilization for a house with radiant floor heating was undertaken. Different control strategies of the floor heating system and different thermal mass were investigated. Active systems can be used to lower the energy consumption for heating by using heat directly from the solar collector. This can be with or without the use of phase change materials, as reported in Lee et al. (2000). Solar heating can also be used as part of a district heating system using seasonal storage of solar heating. (Heller, 2000; Lund and Ostman, 1985)

In this work, lower energy consumption is investigated using building integrated heat storage of solar heating.

The basic idea is to use the heated water from the solar collector to heat the building envelope, making it serve as a layer for heat storage. Here the floor construction was used as heat storage. The storage is made of concrete or sand – both are cheap and have high thermal mass. The heat storage is embedded in a sandwich construction in a slab on ground floor, which from the bottom and up is made of a layer of insulation, the heat storage layer, another layer of insulation and finally a concrete layer with floor heating.

In this paper, a method for utilizing building integrated heat storage of solar heating in typical Danish single-family houses is introduced. Based on simulations performed for different types of layout of the heat storage and floor construction, recommendations are made with respect to the performance of using heat storage of solar heat in the floor construction.

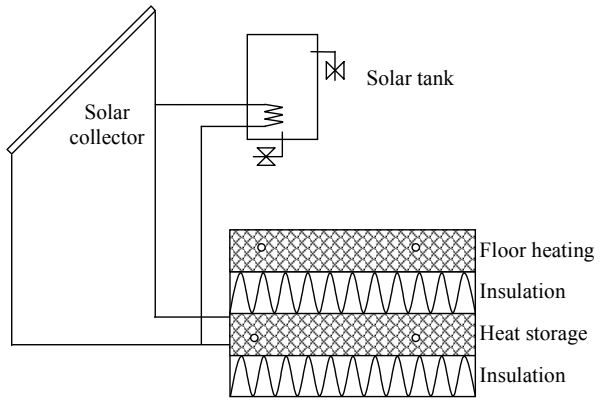

Figure 1 System for heat storage of solar heating

2. SYSTEM DESCRIPTION

The system of heat storage of solar heating consists of solar collector, solar tank and heat storage in the floor of the house. This is shown in Figure 1.

The heat storage analysed in this project is placed in a single-family house of 130 m². The house is built in accordance with the present Danish Building Code (Boligministeriet, 1995), and will, by adding a heat recovery unit on the ventilation system be in accordance with the coming Danish Building Code scheduled for 2005. The house has 190 mm insulation in the walls, 250 mm in the ceiling and 300 mm in the ground, divided into two layers of variable thickness distributed around the heat storage layer. The windows are low energy windows with a total U-value of 1.44 W/m² K.

The solar heating system is a conventional Danish solar heating system. The system consists of solar collector and solar tank. The area of the solar collector is in the analysis varied between 4 m² and 16 m². The solar tank has a volume of 250 L with a spiral heat exchanger.

In Figure 1, the piping between collector, tank and storage is only sketched in the sense that different layouts can be imagined; both parallel and serial. The system is a conventional solar heating system with an extra opportunity to use the heat storage to store the solar heat in the floor construction of the house.

The design of the floor with the heat storage layer is a somewhat unconventional slab on the ground sandwich construction with two concrete decks and two layers of insulation. From the bottom and up the construction consists of Expanded Polystyrene (EPS) insulation, lower concrete deck used for heat storage, another insulation layer and finally upper concrete layer equipped with a floor heating system, which is the primary heating system of the house. The entire house is assumed to have floor tiles as cover material.

This type of floor construction with two concrete decks is used by a Danish producer of single-family houses. This means that cheap installation of the heat storage can be expected.

The heat storage layer is made up of the concrete floor with embedded PEX pipes, placed in the middle of the concrete layer. These pipes are also used for the floor heating system.

The storage layer is insulated towards both room and ground in order to minimize the heat loss from the heat storage. The downward insulation is obviously installed to prevent heat loss to the ground, while the purpose of the upward insulation is to prevent uncomfortably hot and incontrollable temperatures in the house. It is also important to make sure that the heat storage is well insulated to the sides towards the foundation.

The system is cheap to install, as it only requires the installation of PEX-pipes in the lower concrete layer and a simple distribution system between solar collector and heat storage.

3. SIMULATION MODEL

A model of the house is created using Matlab and Simulink (Mathworks, 2002). Furthermore, the finite element program Femlab (Comsol, 2002) has been used.

In short, the simulation model consists of the house including the heat storage, a solar tank and a solar collector, all coupled in a building energy simulation model of the house.

3.1 Solar collector

The production from the solar collector can be found from equation (1), which is a simple representation of a solar collector, based on the efficiency of the collector.

$$C \cdot A \frac{dT}{dt} = A \cdot G \cdot \eta + \dot{m} \cdot c_p \cdot (T_{in} - T_{out}) \qquad \textbf{(1)}$$

In the equation, the temperature on the left side is equal to the outlet temperature of the solar collector when there is flow in the collector. When there is no flow in the collector the temperature is considered the average temperature of the solar collector.

The solar collector efficiency is the flat plate collector efficiency as defined in Duffie and Beckman (1991).

3.2 Solar tank

The solar tank is built using the principles from the methodology used in the EMGP3 program, put forth in Dutré (1991). A model with three internal nodes has been modelled. This means that the model includes stratification of the temperature in the tank, and therefore a more realistic heat exchange is found. The model is not explained further, as it is not included in the further analyses in this paper.

3.3 Building envelope and room model

The building envelope is modeled used in this analysis is based on a simple RC-model for the thermal network including a dynamic response to the heat loads in the building. Here R means thermal resistance and C heat capacity.

The RC-model is a simple approach in which only a few nodal points are used to create the thermal network used to model a building element like a wall or a window.

The model of the house (room) is created by linking the RC-models of walls, windows including solar radiation to the internal surfaces, ceiling and floor together around the air node of the model. In the air node the different heat loads on the room is found. This includes convective heat transfer from room surfaces, internal heat load, and heat loss by ventilation and infiltration. A detailed calculation of the heat exchange by radiation between surfaces is also included in the model. The calculation takes into account the view factors between surfaces. It is necessary to have a detailed model of the radiation exchange since as much as 80 % of the heat emitted from the heated floor is by radiation.

3.4 Floor with storage

The floor with the heat storage has, in order to simplify the calculation as much as possible, been modeled to include as many adiabatic lines of symmetry as possible. The symmetry lines are placed in such a way, that it is only necessary to include half the distance between two pipes. This is shown in Figure 2. The upper part shows the floor – the dashed lines show the symmetry lines. The lower part shows the model that is used in the simulations.

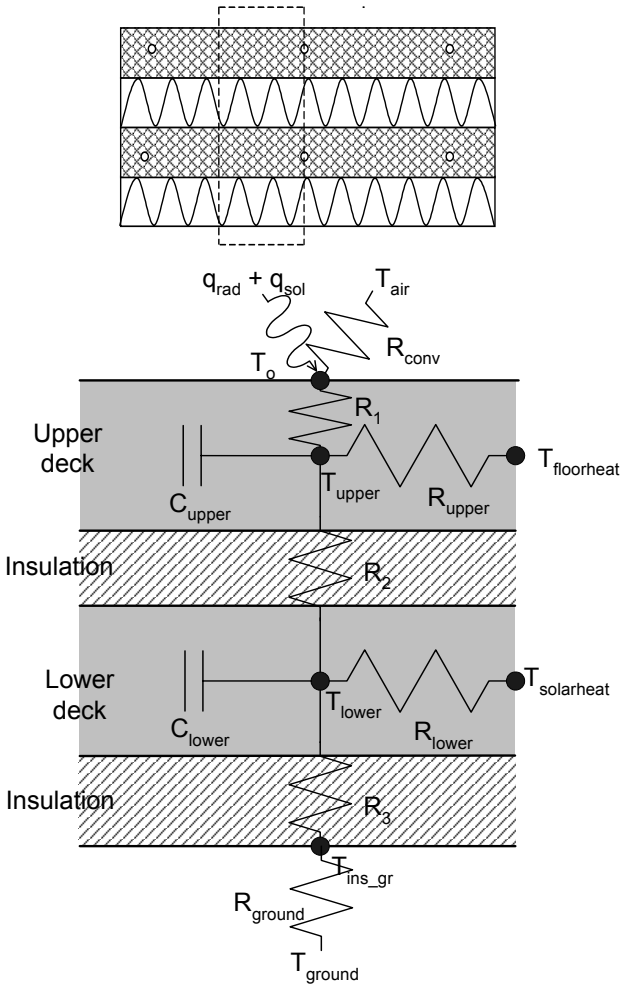

Figure 2 Floor construction and RC-model of floor used for the simulations

Furthermore, inputs and outputs of the model are shown. These include temperature and heat fluxes. The procedure of using adiabatic symmetry lines means, that the model will become an average for the entire floor. The extra heat loss from foundation is taken into account by an average heat loss coefficient found using the description in CEN (2000), using a two-dimensional heat transfer calculation.

Using the thermal network defined in Figure 2, the governing equations stated in equation (2) to (5) can be formulated for four of the six nodal points. The nodal points are placed in the upper and lower concrete deck, at the floor surface and immediately below the lower insulation layer. The two surface nodal points are just energy balances, while the nodal points in the concrete decks also include the thermal capacity. The influence of the foundation is included in equation (3) and (4), by including the linear thermal transmittance of the foundation as an extra term. The extra term is not shown in Figure 2. The last two nodal points, the pipes in each of the concrete decks, are treated below.

$$0 = \frac{1}{R_{conv}} \cdot \left(T_{air} - T_o\right) + \frac{1}{R_1} \cdot \left(T_{upper} - T_o\right) + q_{rad} + q_{sol} \tag{2}$$

$$C_{upper} \frac{dT_{upper}}{dt} = \frac{1}{R_1} \cdot \left(T_o - T_{upper}\right) + \frac{1}{R_2} \cdot \left(T_{lower} - T_{upper}\right) + \frac{1}{R_{upper}} \cdot \left(T_{floorheat} - T_{upper}\right) + P_{house} \cdot \psi_{upper} \cdot \left(T_{upper} - T_{out}\right) \tag{3}$$

$$C_{lower} \frac{dT_{lower}}{dt} = \frac{1}{R_3} \cdot \left(T_{ins\_gr} - T_{lower}\right) + \frac{1}{R_2} \cdot \left(T_{upper} - T_{lower}\right) + \frac{1}{R_{lower}} \cdot \left(T_{solarheat} - T_{lower}\right) + P_{house} \cdot \psi_{lower} \cdot \left(T_{lower} - T_{out}\right) \tag{4}$$

$$0 = \frac{1}{R_{ground}} \cdot \left(T_{ground} - T_{ins\_gr}\right) + \frac{1}{R_3} \cdot \left(T_{lower} - T_{ground}\right) \tag{5}$$

It was initially decided to use a finite element calculation of the temperature distribution in the floor. For this end, a model of the floor was created in Femlab. Though more accurate, this approach unfortunately proved to be extremely time consuming for actual simulations. In

stead, the RC-model of the floor was developed and the parameters for thermal resistances and heat capacities were based on calculations in Femlab. The parameters were found by applying sinusoidal boundary conditions to the finite element model and record the thermal response. The fitted parameters were used in the RC model and compared to the detailed finite element model with good results.

The last two nodal points, the pipes, have been included as the mean temperature of the fluid in each of the pipes, which was found from the supply temperature and volume flow. A heat balance is set up in equation (6), here shown for the upper deck. An equivalent equation was made for the lower deck.

$$\left(\rho c_p\right)\cdot V\cdot\frac{dT_{floorheat}}{dt}=\dot{m}c_p\cdot\left(T_{supply}-T_{return}\right)-\frac{1}{R_{upper}}\cdot\left(T_{floorheat}-T_{upper}\right) \quad (6)$$

When the flow in the pipe is turned on, the temperature of the fluid, calculated in equation (6) is the outlet temperature of the fluid in the deck. When the flow is turned off, it is considered the mean temperature of the deck. This approach is the same as described for the fluid in the solar collector.

Further, the return temperature from the concrete deck is used as the supply temperature to the solar collector.

3.5 Control

An on/off control type is used. This means, that if the solar collector is able to produce enough heat to increase the temperature more than 6 K and the temperature at the outlet is higher than in the floor, the system is turned on. When the increase in temperature is less than 1 K or the outlet temperature is lower than the temperature in the floor, the system is turned off. A minimum incident solar radiation of 50 W/m² on the solar collector is required.

In this investigation, heat is only sent to the heat storage and not the solar tank. In practical use however, the system's control strategy will be much more advanced, and would in addition include the possibility to send heat to the solar tank. This is also indicated in Figure 1.

The upper deck is controlled as a standard floor heating system whose purpose is to ensure that the room temperature is always kept above the set point temperature of 20°C. A supply temperature to the floor heating pipe of 35 °C was used.

Table 1 Layout of the seven types of floor tested

	Insulation thickness (upper/lower)	Storage type	Storage thickness	Pipe distance
a	100 mm/200 mm	concrete	100 mm	300 mm
b	100 mm/200 mm	concrete	100 mm	500 mm
c	50 mm/250 mm	concrete	100 mm	300 mm
d	250 mm/50 mm	concrete	100 mm	300 mm
e	250 mm/ 50 mm	sand	300 mm	300 mm
f	250 mm/ 50 mm	concrete	300 mm	300 mm
g	100 mm/200 mm	concrete	300 mm	300 mm

3.6 Parametrical analysis

The primary investigation in this work is to test seven different layouts of the floor construction with the heat storage layer included. These are named 'a' through 'g'. The different layouts are shown in Table 1.

In all cases, the total insulation thickness and upper concrete deck is the same: 300 mm and 100 mm respectively. The type called 'a' is considered the reference case. In this type, the insulation thickness in the upper insulation layer is 100 mm, the storage is 100 mm, the lower insulation thickness is 200 mm and the pipe spacing is 300 mm. The storage (the lower deck) is in this case concrete.

The distribution of the insulation thickness has been chosen to be able to see the difference in the results if the storage is mainly insulated towards the room or the ground. Three different ways of distributing the insulation thickness is used in the simulations.

Two different thicknesses of the heat storage are used. Further, sand is tested as an alternative to concrete in one simulation.

In one simulation, the pipe distance is changed from 300 mm to 500 mm.

In all, three different distributions of the insulation, two different thicknesses of the lower deck, two different types, and two different pipe distances are tested.

The analyses performed here has also been used to model different types of control systems between the solar collector and the distribution between solar tank and the heat storage. Different layouts have been tested. However, the results have been inconclusive so the results will only be briefly mentioned.

4. RESULTS

The model described above has been used to perform simulations on the system. The simulations are based on the Danish Design Reference Year (DRY).

A few notes to the simulations should be pointed out initially.

- The maximum room temperature is set to 26 °C. Should the temperature rise above this level, it is assumed, that the air is cooled enough to lower the temperature to 26 °C, i.e. through opening of windows.
- The same type of solar tank and solar collector is used throughout the simulations. Only the solar collector area is changed
- All heat from the solar collector is sent to the heat storage in the floor, except for an example of different use of the system.
- The same pipe distance is used in both the floor heating system, and in the heat storage. This is not

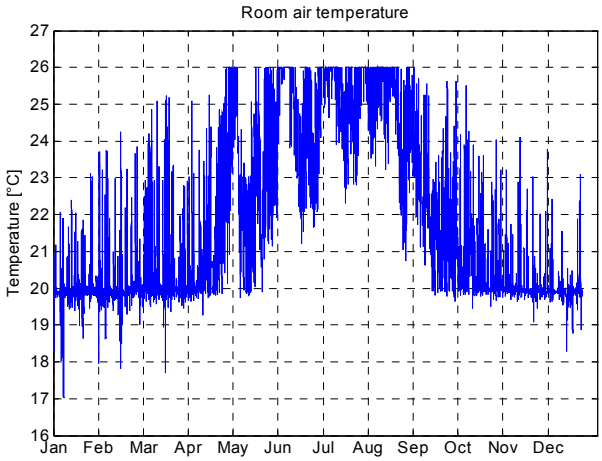

Figure 3 Air temperature in house for a yearly simulation

realistic as the pipe distance in the layer would probably be larger than in the floor heating layer.

4.1 Assessment

Initially an assessment of the results is made. In Figure 3 the results for the indoor temperature is shown.

As it can be seen the temperature is around 20 °C or above for most of the year, except for a few periods where the temperature falls below 19 °C, which is due to very cold outdoors temperatures.

The production of the solar collector and total heating demand of the house is as could be expected. For the house without heat recovery unit and use of the heat storage layer, an energy consumption of around 9300 kWh (or 72 kWh/m²) was found. For the house with a heat recovery unit, a value of 5000 kWh (or 38 kWh/m²) was found. If a 4 m² solar collector was used in the simulation and all heat was sent to the solar tank, the solar collector yielded around 1300 kWh. These data was as expected. In total the model behaves, as it should. A more thorough validation, however, is not described here.

However, a comment must be made to the simulation results shown below. In some cases, Simulink was unable to finish the simulations due to a periodic numerical instability. This is also the reason for the very simple control system used in the investigation. It is, however, not an indication of problems with the reliability of the results for the simulations that did finish.

4.2 Simulation results

In Figure 4, the energy consumption and the reduction of the energy consumption is shown for the floor of type 'a' for the calculations with and without heat recovery unit installed. All heat from the solar collector is sent to the heat storage layer.

As it can be seen in the left graph, the energy consumption is much lower for the house with heat recovery unit. It can also be seen, that the reduction increases with larger area of the solar collector. There is a steady decrease in the energy consumption using larger solar collectors.

On the right side of the figure, the loss pr. m² solar collector is shown. Even if a 16 m² solar collector is used, there is still a reduction of over 100 kWh/m² for the house without heat recovery unit, and around 70 kWh/m² with the heat recovery unit.

The maximum reduction pr. m² solar collector is in both cases at 8 m² solar collector area. In addition, the curve is very flat which means, that there is a potential for lowering the heating demand even for a large solar collector area. The same general trend can be observed for all seven different floor layouts. However, the data should not be extrapolated for even larger solar collectors, as this has not been tested here. Therefore, the largest possible saving is not found here, as the might drop off sharp if the solar collector area is increased further.

If the reduction in energy consumption were calculated in terms of the floor area in the house, the energy con-

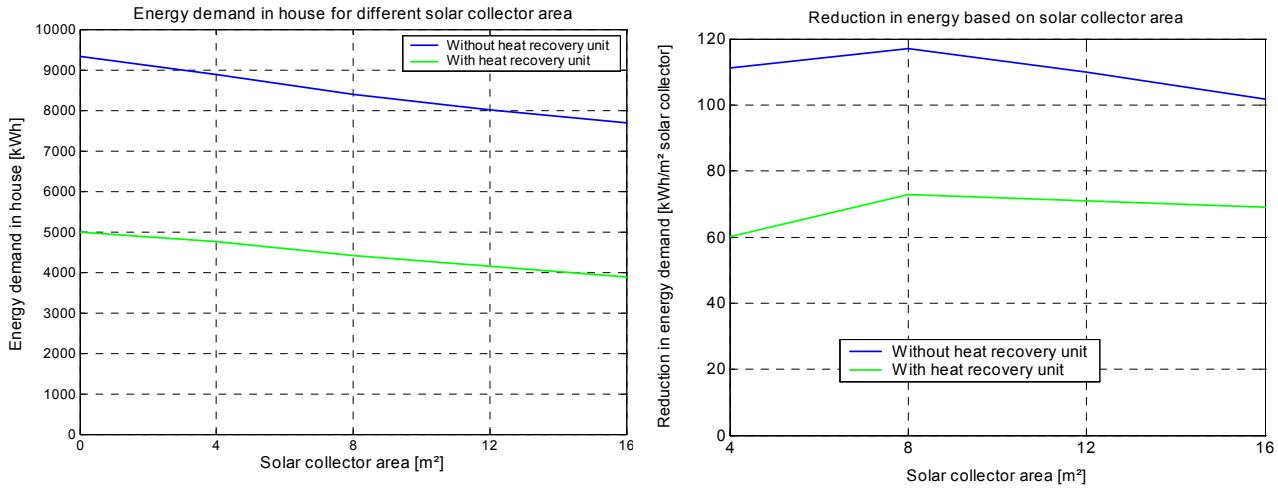

Figure 4 Heating demand for type 'a' as a function of the solar collector area (to the left) and the reduction in heating demand pr. m² solar collector area (to the right)

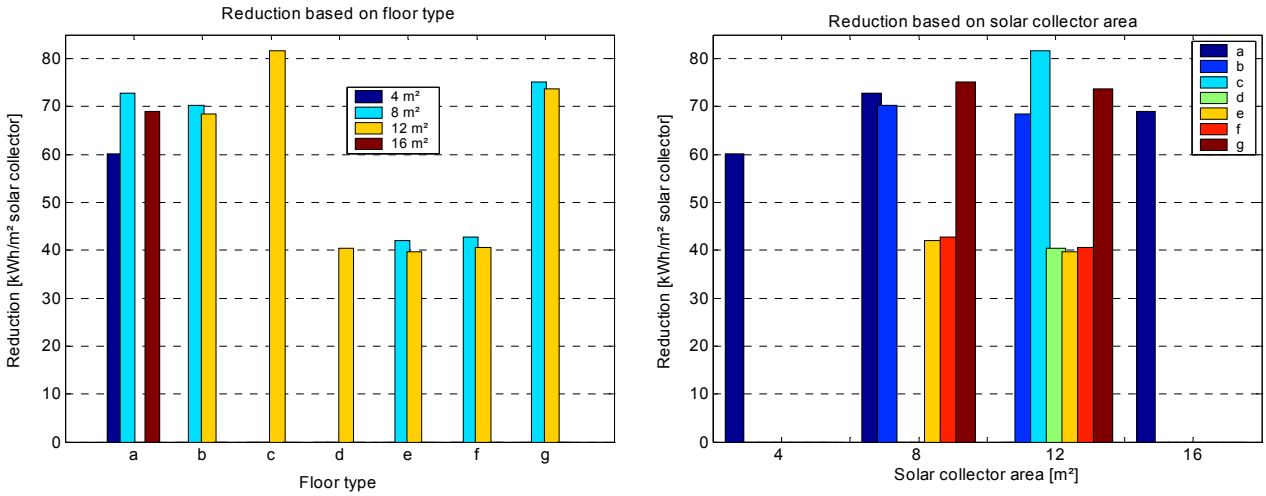

Figure 5 Reduction in heating demand pr. m² solar collector area for different floor types and different solar collector areas – for house with heat recovery unit on the ventilation system

sumption would fall from 72 kWh/m² to 68 kWh/m² and 59 kWh/m² for 4 m² and 16 m² solar collector respectively, in the house without heat recovery unit. In the house with heat recovery unit, the figures would be 38 kWh/m², 37 kWh/m² and 30 kWh/m². In percent, the reductions without heat recovery unit are 5% and 17% for 4 m² and 16 m², while they are 5% and 22% for the house with heat recovery unit. Therefore, the system has relatively better performance for the house with the lowest heating demand.

In Figure 5 and Figure 6, the reductions are shown for the different floor layouts. In the figures, the same data are shown using different x-axes. In the left figure, the data are shown for the different floor types, so that the development can be found when different solar collector area is used. In the right figure, the different floor types can be compared as a function of the solar collector area.

In Figure 5 and Figure 6, the different floor types are compared. In both figures, it can be seen that type 'a', 'c' and 'g' give the largest reduction in the heating demand. Therefore, the smaller the insulation thickness between the two decks, the bigger the reduction of the heating demand. The drawback to the lower heating demand is discussed below.

If comparing type 'a' and 'g', where the only difference is the thickness of the heat storage 10 cm vs. 30 cm, there is no or only little difference between the results. This shows that a storage layer of 10 cm is sufficient. Actually an even smaller storage thickness will be sufficient, but this would require either a thinner deck, or to layout the pipes differently in the floor. This is not examined here. It is noted, that this conclusion is in agreement with the findings in Athienitis (1997) where a small concrete layer was found to perform as well as a larger layer.

The heat storage medium is compared in type 'e' and 'f', where two identical layouts are tested. The only difference is that 'e' is with sand and 'f' with concrete. As it can be seen, there is very little difference between the two. If type 'd' is included in the comparison, where 'd' has 10 cm layer instead of the 30 cm used in 'e' and

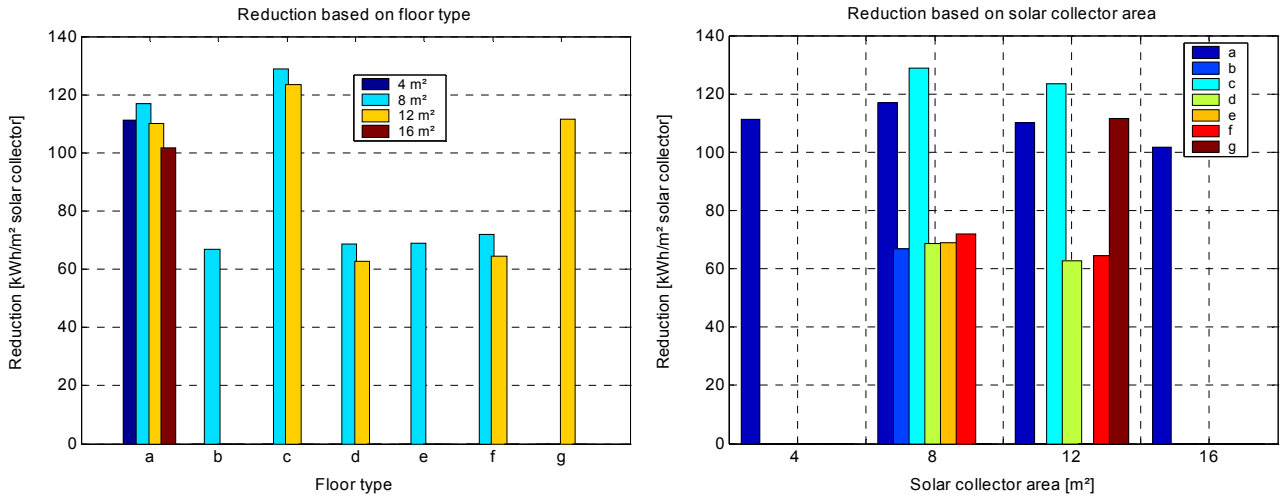

Figure 6 Reduction in heating demand pr. m² solar collector area for different floor types and different solar collector areas – for house without heat recovery unit on the ventilation system

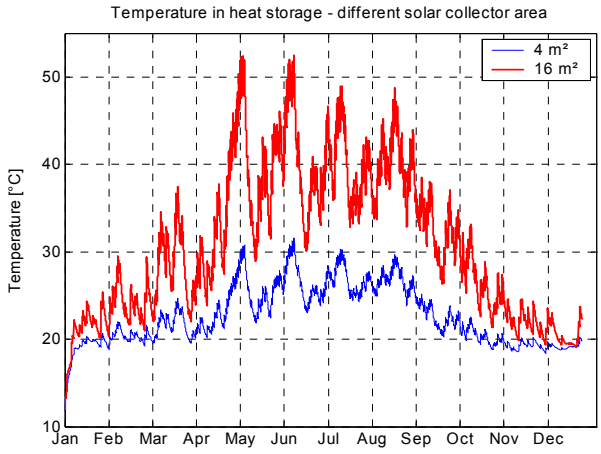

Figure 7 Temperature of heat storage for floor layout type 'a'

'f', the same conclusion as above can be drawn regarding the size of the layer.

The effect of using a larger pipe spacing, thereby reducing the cost of the layer, can be found by comparing type 'a' and 'b'. Here the results are a little more diffuse. In Figure 5, without heat recovery, type "b" has a much lower reduction, while the two are almost identical in Figure 6 with heat recovery unit. In the first case however, the system was not able to heat the room sufficiently because of the large pipe distance, so this result is not usable. Therefore, the two types are likely to have the same potential for heat storage in the house with low energy demand.

4.3 Temperatures of deck and surface

In Figure 7, the temperature in the deck is shown for type 'a' with different solar collector area. As it can be seen, the temperature in the storage reaches over 50 °C during the summer period when the solar collector has an area of 16 m² and just over 30 °C with 4 m² solar collector.

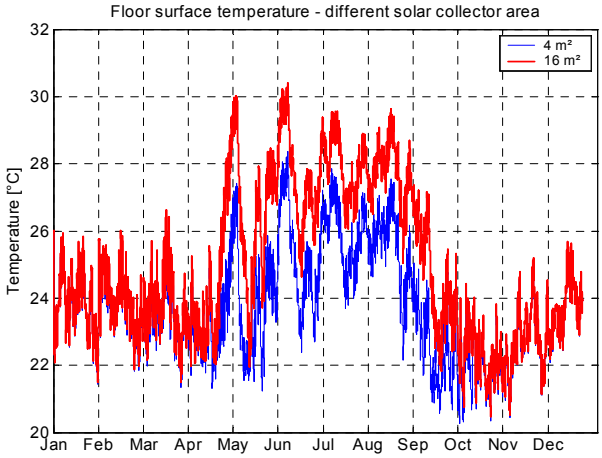

Figure 8 Floor surface temperature for floor layout type 'a'

In the previous section it was found, that the system that gave the best performance was the one with the smallest insulation thickness between the two decks. There is however one thing to be aware of when assessing the heat storage. This is the temperature of the deck, and consequently floor surface temperature. The temperature is highest during the summer. The surface temperature is over 30 °C in the summer, using large solar collector, as it can be seen on Figure 8. This is too warm for comfort, and it will also heat the room to a very high temperature. In Olesen (1977), it was found that the upper limit for comfort for bare feet are 29 °C, but cooler temperatures can also be accepted Normally a temperature of 24 °C is sufficient for comfort for people with indoor shoes.

This means, that using heat storage of solar heating, which is not well insulated, from the room, will result in too high floor temperatures, and consequently too high room temperatures. This problem can most likely be removed by setting a maximum allowed temperature of the heat storage layer, also without decreasing the performance of the system.

However, it also means that the system can be used for comfort heating of tiled floors during the summer period. That is, the system can by adding heat to the heat storage be used to maintain a comfortable temperature in for instance bathrooms and kitchens.

4.4 Control strategies

Two different types of control strategy were tested based on different pipe configurations; with the pipes serial and parallel. The parallel configuration, where the outlet temperature from the solar collector controlled if the flow should be sent to solar tank or heat storage proved to be either a domestic hot water system or a heat storage system. The serial configuration first sent the water to the solar tank and then when surplus heat was available to the storage. This type gave promising results where both solar tank and heat storage performed very well. Unfortunately, the simulation model was not able to finish the simulations due to numerical problems.

5. DISCUSSION/CONCLUSION

In this paper, building integrated heat storage of solar energy in the floor of a typical Danish single-family house has been examined. A layout of a floor with two decks has been introduced. In the upper deck, which is of concrete, a floor heating system is installed, and in the lower deck, which is of concrete or sand, a heat storage layer is installed. The heat storage is cheap to install in a new house in which it is already planned to use solar heating for hot water.

In total it was found, that a maximum reduction of the heating demand of up to 100 kWh/m² solar collector can be expected in a 130 m² house with a heating demand of 9000 kWh/year. If the heating demand is lowered to about 5000 kWh, a maximum reduction of 70 kWh/m² solar collector can be expected, if 16 m² solar collector or

less is used. The result for larger area of the solar collector has not been found here. For 16 m² solar collector, the reductions in the energy consumption are 17 % and 22 % respectively for the high and low heating demand.

These results are promising for the need to lower the energy consumption in houses further, especially seen in the light of the new definition of the energy performance of buildings, which has been presented by the European Union. The energy performance is a measure of the amount of energy that is bought from the distribution company. Therefore, the use of solar energy for heating purposes will increase the energy performance.

Seven different types of layout of the floor construction, which the heat storage layer is a part of has been tested. Size and material of storage and pipe distance in the storage had little or no effect on the performance, while the distribution of the insulation between the layers, solar collector area and heating demand of the house had an effect on the performance. For the insulation, it was found that the smaller the thickness of the upper insulation layer towards the room, the larger the reduction in the energy consumption. This did however have the drawback, that the temperature in the summer period in the house could become too high for thermal comfort, both on the floor surface, but also in the room air. This can probably be solved by using a good control strategy.

In addition, the results indicated that through the design of a more advanced control strategy and pipe configuration, the system could be forced to have a more efficient use of the system. Further, the heat storage could be optimized by designing the system in such a way that it has zones, where the heat is only sent to certain parts of the storage during the summer (i.e. under rooms with tiled floors), thereby giving comfort heating to the occupants of the house. Also, the results indicate that the piping in the heat storage could be optimized to more efficiently use the thermal capacity of the storage, thereby saving both installation cost and pump energy to distribute the hot water in the storage. Finally, a more advanced control strategy must also include domestic hot water. The results found here indicate that this can be included without lowering the performance of the heat storage.

NOMENCLATURE

A	Area	m²
C	Thermal capacity	J/K m²
c_p	Specific heat capacity	J/kg K
G	Incident solar radiation	W/m²
$\dot{m}$	Fluid flow	kg/s
η	Solar collector efficiency	-
q	Heat flux	W/m²
ψ	Linear thermal transmittance	W/m K
P	Perimeter	m
R	Heat resistance	m² K/W
ρ	Density	kg/m³
T	Temperature	°C/K
V	Volume	m³

REFERENCES

Athienitis A.K. (1997): Investigation of thermal performance of a passive solar building with floor radiant heating. Solar Energy, Vol. 61, No. 5, pp. 337-345.

Boligministeriet (1995): Bygningsreglement 1995 (Danish Building Code) (In Danish). Bygge- og Boligstyrelsen, København.

Comsol (2002): Femlab User's Guide and Introduction, Comsol.

Duffie J.A. and Beckman W.A. (1991) Solar Engineering of Thermal Processes, 2nd edn. pp. 54-59. Wiley Interscience, New York.

Dutré W. L. (1991): Simulation of thermal systems. A modular program with an interactive preprocessor (EMGP3), Kluwer Academic Publishers.

European Parliament (2003): Directive 2002/91/EC of the European Parliament and of the Council of the 16 December 2002 on the Energy Performance of Buildings. Official Journal of the European Communities. L 1/65.

Lee T., Hawes D. W., Banu D., Feldman D. (2000): Control aspects of latent heat storage and recovery in concrete. Solar Energy Materials & Solar Cells, Vol. 62, pp. 217-237.

Heller A. (2000): 15 years of R&D in central solar heating in Denmark, Solar Energy, Vol. 69, No. 6, pp. 437-447

CEN (2000): EN ISO 13370 Thermal performance of buildings - Heat transfer via the ground - Calculation methods

Lund P. D., Ostman M. B. (1985): A numerical model for seasonal storage of solar heat in the ground by vertical pipes. Solar Energy, Vol. 34, Issue 4-5, pp. 351-366.

Mathworks (2002): Using Matlab, Mathworks

Munch-Andersen J., Svendsen S., Tommerup H.M.: Exterior Walls to Meet Future Danish Requirements. In: Detailing design. Towards a joined-up industry. Proceedings of the Third international conference on Detail Design in Architecture, September 12 and 13, 2000, University of Brighton, Sussex, UK. Emmitt, S. (Ed.). Leeds. Metropolitan University. Centre for the Built Environment, CeBE. 2001. pp. 95-108.

Nielsen TR, Duer K., Svendsen S. (2001).: Energy performance of glazings and windows, Solar Energy, Vol. 69, pp. 137-143.

Olesen B.W. (1977): Thermal comfort requirements for floors occupied by people with bare feet. ASHRAE Transactions, 83, Pt. 2, 41-57, 1977

ACKNOWLEDGEMENT

The results in this paper are based on work that has been financed by the Danish Energy Agency by the Energy Research Program.